UNIVERZITA PALACKÉHO V OLOMOUCI

Přírodovědecká fakulta

Katedra biochemie

Charakterizace nových inhibitorů kinas v modelových systémech *in vitro*

DISERTAČNÍ PRÁCE

Autor:	**Mgr. Eva Řezníčková**
Studijní program:	P1416 Biochemie
Studijní obor:	Biochemie
Forma studia:	Prezenční
Vedoucí práce:	**doc. RNDr. Vladimír Kryštof, Ph.D.**
Rok:	2016

„Prohlašuji, že jsem předloženou disertační práci vypracovala samostatně za použití citované literatury.“

V Olomouci …….. ……..

„Na tomto místě bych ráda poděkovala svému školiteli doc. RNDr. Vladimíru Kryštofovi, Ph.D. za odborné vedení mé disertační práce, všechny konzultace, cenné rady, trpělivost a vstřícnost a také Mgr. Radku Jordovi, Ph.D. za odbornou pomoc, rady a připomínky. Dále děkuji celému kolektivu Laboratoře růstových regulátorů za vstřícnost a příjemné pracovní prostředí a zejména pak Janě Hudcové, Olze Hustákové a Bc. Ditě Parobkové za jejich ochotu a praktickou pomoc. V neposlední řadě pak patří můj dík mé rodině a přátelům za velkou podporu.“

Bibliografická identifikace

Jméno a příjmení autora	Eva Řezníčková
Název práce	Charakterizace nových inhibitorů kinas v modelových systémech *in vitro*
Typ práce	disertační
Pracoviště	Laboratoř růstových regulátorů Centrum regionu Haná pro biotechnologický a zemědělský výzkum, Přírodovědecká fakulta Univerzity Palackého & Ústav experimentální botaniky AV ČR, v.v.i.
Vedoucí práce	doc. RNDr. Vladimír Kryštof, Ph.D.
Rok obhajoby práce	2016

Abstrakt

Zapojení cyklin-dependentních kinas (CDK) do regulace esenciálních buněčných pochodů je staví do pozice vhodných terapeutických cílů pro léčbu celé řady onemocnění. Tato disertační práce je zaměřena na charakterizaci protinádorových a antiparazitických účinků nových sérií nízkomolekulárních inhibitorů CDK, u kterých bylo na základě cílených modifikací dosaženo zlepšení biologických vlastností oproti výchozímu roskovitinu. V několika nezávislých experimentálních modelech byla prokázána CDK-inhibiční a antiproliferační účinnost nově připravených sloučenin a popsán mechanismus jejich protinádorového působení. Aktivita nejúčinnějších inhibitorů byla navíc ověřena v komplexních modelech hepatocelulárního karcinomu *in vitro* a *in vivo*, kde byl prokázán možný terapeutický potenciál CDK inhibitorů pro léčbu tohoto onemocnění. Závěrečná část práce se zabývá alternativní možností uplatnění 2,6,9-trisubstituovaných purinů s nízkou protinádorovou aktivitou jako potenciálních antiparazitik. Prokázané submikromolární inhibitory leishmaniální CDK (CRK3) redukovaly viabilitu těchto protozoálních parazitů, aniž by ovlivňovaly viabilitu lidských buněk a jeví se tak být zajímavým výchozím strukturním motivem pro vývoj nových antileishmaniálních sloučenin.

Klíčová slova	cyklin-dependentní kinasa, inhibitor, rakovina, hepatocelulární karcinom, leishmanie
Počet stran	81
Počet příloh	5
Jazyk	český

Bibliographical identification

Autor's first name and surname	Eva Řezníčková
Title	Characterization of novel kinase inhibitors in model systems *in vitro*
Type of thesis	Ph.D.
Department	Laboratory of Growth Regulators Centre of the region Hana for biotechnological and agricultural research, Faculty of Science Palacky University & Institute of experimental botany ASCR
Supervisor	doc. RNDr. Vladimír Kryštof, Ph.D.
The year of presentation	2016

Abstract

Involvement of cyclin-dependent kinases (CDKs) in the regulation of essential cellular processes makes them suitable therapeutic targets for the treatment of many diseases. This dissertation thesis is focused on the characterization of antitumor and antiparasitic activities of the novel series of small-molecule CDK inhibitors with improved biological properties in comparison to roscovitine which were obtained via targeted modifications of their molecules. CDK-inhibitory and antiproliferative activities as well as mechanisms of anticancer action of these newly synthesized compounds were evaluated in several independent experimental models. The activity of the most effective inhibitors was moreover verified in complex models of hepatocellular carcinoma *in vitro* and *in vivo* in which the therapeutical potential of CDK inhibitors for the treatment of this disease was demonstrated. The last part of this thesis deals with the alternative possibility of application of 2,6,9-trisubstituted purines as potential antiparasitic drugs. Submicromolar inhibitors of leishmanial CDK (CRK3) reduced viability of these protozoan parasites without affecting the human cell viability and seem to be interesting lead structure motif for the development of new antileishmanial compounds.

Keywords	cyclin-dependent kinase, inhibitor, cancer, hepatocellular carcinoma, leishmania
Number of pages	81
Number of appendices	5
Language	Czech

OBSAH

1 ÚVOD A CÍLE PRÁCE

Fosforylace proteinů, zprostředkované enzymy z rodiny proteinkinas, hrají nenahraditelnou úlohu v regulaci celé řady signálních drah a buněčných procesů zahrnujících transkripci, buněčný růst, proliferaci, diferenciaci, buněčný cyklus nebo apoptózu (Johnson, 2009; Rask-Andersen *et al.*, 2014). Mechanismus působení proteinkinas je založen na přenosu γ-fosfátové skupiny z molekuly ATP na hydroxylovou skupinu serinu, threoninu nebo tyrosinu cílového proteinu, kdy přenosem fosfátové skupiny dochází ke konformačním změnám substrátu a změnám jeho aktivity (Johnson, 2009; Rask-Andersen *et al.*, 2014).

Soubory všech genů kódujících kinasy jsou označovány jako kinomy. Jejich velikost se s fylogenetickým vývojem eukaryotických organismů paralelně zvětšovala, a zatímco pro jednobuněčné organismy, jako jsou kvasinky nebo prvoci, je dostačující kinom čítající do dvou set genů *(Saccharomyces cerevisiae* 113, *Trypanosoma brucei* 176, *Leismania major* 199) (Hunter *et* Plowman, 1997; Parsons *et al.*, 2005), obratlovci disponují kinomem více než dvakrát větším (např. *Mus musculus* 540) (Caenepeel *et al.*, 2004). Mezi nejprostudovanější kinomy patří bezesporu ten lidský, který byl charakterizován v roce 2002 a čítá 518 genů (Manning *et al.*, 2002). Během jeho studia bylo prokázáno, že proteinkinasy neplní svou úlohu jen ve fyziologických procesech, ale hrají klíčovou roli i v rozvoji celé řady onemocnění. Popsán je vliv proteinkinas na rozvoj neurodegenerativních chorob jako je Alzheimerova nebo Parkinsonova choroba, zánětlivých onemocnění, metabolických poruch, ale nejvýznamnější a nejstudovanější je jejich dopad na rozvoj nádorových onemocnění. Ve všech těchto odvětvích probíhá intenzivní výzkum a proteinkinasy jsou v centru zájmu jako atraktivní terapeutické cíle (Johnson, 2009; Rask-Andersen *et al.*, 2014).

Většina proteinkinas sdílí podobné charakteristické znaky ve struktuře. Katalytická doména proteinkinas je tvořena dvěma laloky, větším C-terminálním tvořeným převážně strukturou α-helixů a menším N-terminálním tvořeným β-skládanými listy. Mezi nimi se nachází ATP-vazebné místo kinasy. Avšak i přes velkou podobnost v sekundární a terciární struktuře proteinu se jednotlivé kinasy odlišují sekvencí (Ubersax *et* Ferrell, 2007), která tak determinuje jejich citlivost k nízkomolekulárním inhibitorům.

V současné době je známo několik desítek inhibitorů proteinkinas schválených pro léčbu celé řady zejména maligních onemocnění a velké množství dalších látek prochází preklinickým a klinickým zkoušením (Fabbro *et al.*, 2015).

Cílem této disertační práce bylo pochopit vztahy mezi strukturou a aktivitou zcela nových nízkomolekulárních inhibitorů proteinkinas na bázi trisubstituovaných purinů a pyrazolo[4,3-*d*]pyrimidinů (připravených kolegy v Laboratoři růstových regulátorů) se zaměřením na cyklin-dependentní kinasy lidské a leishmaniální, charakterizace mechanismu jejich účinku v modelových systémech *in vitro* a prokázání účinnosti *in vivo*.

2 CYKLIN-DEPENDENTNÍ KINASY (CDK) A JEJICH KLÍČOVÉ FUNKCE

Cyklin-dependentní kinasy (CDK) patří do skupiny serin/threonin-specifických proteinkinas, které se v buňce podílí zejména na regulaci buněčného cyklu, ale účastní se rovněž regulace transkripce, apoptózy a celé řady dalších buněčných pochodů (Lim *et* Kaldis, 2013; Malumbres, 2014; Malumbres *et al.*, 2009). Na základě strukturní podobnosti spadají do skupiny CMGC kinomu spolu s mitogenně-aktivovanými proteinkinasami (MAPK), glykogen-synthasou kinasou 3β (GSK3β), CDK-like kinasami a kinasou DYRK (Malumbres, 2014; Manning *et al.*, 2002).

Pro svou enzymatickou aktivitu vyžadují CDK vazbu regulační podjednotky, kterou je nejčastěji cyklin. Kromě ní se na regulaci aktivity CDK podílí rovněž řada aktivačních kinas a fosfatas (CDK-aktivační kinasa, kinasa Wee1, fosfatasy Cdc25) a přirozených inhibitorů CDK rodiny Cip/Kip a INK4 (Carnero, 2002).

Stejně jako se během fylogenetického vývoje zvětšovala velikost kinomu, rostl paralelně i počet CDK nezbytných pro zajištění správného chodu všech procesů regulovaných CDK. Například pro zajištění bezchybné regulace buněčného cyklu je u kvasinek *S. cerevisie* potřebná pouze jedna CDK (označovaná jako Cdc28), u prvoků rodu *Leishmania* se jedná již o enzymy 2 (CRK1 a CRK3) a u člověka je pro bezchyný průchod buněčným cyklem všech typů buněk nezbytná aktivita nejméně 4 hlavních CDK (CDK1/2/4/6) (Hassan *et al.*, 2001; Malumbres *et* Barbacid, 2009).

U člověka je známo 20 enzymů patřících do rodiny CDK (CDK1-20) a 5 patřících do vzdálenější skupiny tzv. CDK-like enzymů (Malumbres *et al.*, 2009). Funkce jednotlivých lidských CDK shrnuje Tabulka 1.

Tab. 1: Funkce lidských cyklin-dependentních kinas.

CDK	Vazebný partner	Funkce
CDK1 *Cdc2*	cyklin A, cyklin B	regulace buněčného cyklu (S-G2, G2-M), dokončení mitózy
CDK2	cyklin E, cyklin A	regulace buněčného cyklu (G1-S)
CDK3	cyklin C	vstup do buněčného cyklu a jeho regulace (G1-S)
CDK4	cyklin D	regulace buněčného cyklu (G1)
CDK5	p35, p39	vývoj nervové soustavy a její správná funkce, angiogeneze, migrace, senescence, buněčná adheze a motilita
CDK6	cyklin D	regulace buněčného cyklu (G1)
CDK7	cyklin H	CDK-aktivační kinasa (CAK), regulace transkripce
CDK8	cyklin C	regulace transkripce
CDK9	cyklin T	regulace transkripce
CDK10	cyklin M	regulace buněčného cyklu (G2-M), kontrola transkripčního faktoru Ets2
CDK11 *PITSLRE*	cyklin L	mRNA sestřih, regulace transkripce, mitóza
CDK12	cyklin K cyklin L	regulace transkripce, mRNA sestřih, elongace axonů, regulace exprese genů zapojených v opravě DNA
CDK13 *CDC2L5*	cyklin K cyklin L	sestřih mRNA, regulace transkripce, elongace axonů
CDK14 *PFTK1*	cyklin D3 cyklin Y	regulace buněčného cyklu (G1-S) a proliferace, buněčná migrace a invazivita
CDK15 *ALS2CR7*		regulace apoptózy (fosforylace survivinu)
CDK16 *PCTK1*, *PCTAIRE1*	cyklin Y	zapojení v procesu spermatogeneze, vezikulární transport, migrace neuronů, rozvoj neuritů, vývoj kosterního svalstva
CDK17 *PCTK2* *PCTAIRE2*	cyklin Y	správné fungování nervové soustavy (exprimována v terminálně diferencovaných neuronech)
CDK18 *PCTK3*	cyklin A2	organizace aktinového cytoskeletu
CDK19 *CDC2L6*	cyklin C	regulace transkripce
CDK20 *CCRK*	cyklin H	regulace transkripce, CAK pro CDK2

Reference k Tab. 1: Arif, 2012; Blazek *et al.*, 2011; Bösken *et al.*, 2014; Galbraith *et al.*, 2010; Guen *et al.*, 2013; Hirose *et al.*, 2000; Hu *et al.*, 2003; Hu *et al.*, 2007; Chen *et al.*, 2006; Chen *et al.*, 2007; Chen *et al.*, 2014; Cheng *et al.*, 2012; Jiang *et al.*, 2009; Kohoutek *et* Blazek, 2012; Leung *et al.*, 2011; Liebl *et al.*, 2010; Malumbres; 2014; Malumbres *et* Barbacid, 2009; Matsuda *et al.*, 2014; Mikolcevic *et al.*, 2011; Mikolcevic *et al.*, 2012; Park *et al.*, 2014; Ren *et* Rollins, 2004; Shimizu *et al.*, 2014; Shu *et al.*, 2007; Tian *et al.*, 2012; Trakala *et* Malumbres, 2014; Yanagi *et* Matsuzawa, 2015.

Klíčovou úlohu hrají CDK bezesporu v regulaci buněčného cyklu, které se účastní zejména CDK2/4/6 zapojené v regulaci interfázních pochodů a dále mitotická CDK1. CDK jsou aktivovány na základě fázově-specifické exprese jejich vazebných partnerů cyklinů rodin D, E, A a B. V odpovědi na mitogenní signalizaci je zahájena nejprve exprese cyklinů rodiny D, které jsou aktivačními podjednotkami CDK4 a CDK6. Jejich aktivní komplexy zahájí fosforylaci retinoblastomového proteinu (Rb), který v buňce plní roli represoru transkripčních faktorů rodiny E2F. Fosforylací proteinu Rb na specifických místech dochází k částečnému rozvolnění komplexu Rb-E2F a může dojít k zahájení exprese cílových genů zahrnujících i cykliny typu E. Ty vytváří aktivní komplexy s CDK2 a dokončují fosforylaci proteinu Rb a úplnou inaktivaci jeho komplexu, čímž dochází k průchodu tzv. restrikčním bodem, kdy buňky přestávají být závislé na mitogenních faktorech, dokončují G1 fázi a spouští expresi genů nezbytných pro další fáze buněčného cyklu (Lapenna *et* Giordano, 2009; Malumbres *et* Barbacid, 2009; Malumbres *et* Barbacid, 2005). Kromě toho se komplex CDK2/cyklin E účastní i regulace replikace DNA a fosforylace proteinů zapojených v opravách DNA, modifikacích histonů nebo v duplikaci a maturaci centrosomů (Malumbres *et* Barbacid, 2005). Jakmile je replikace DNA zahájena, je aktivita komplexu CDK2/cyklin E utlumena proteolytickou degradací cyklinu E a CDK2 interaguje s cykliny typu A, které následně aktivují na konci S fáze i CDK1 (Malumbres *et* Barbacid, 2005). Funkce CDK2 a CDK1 se značně překrývají a jsou nezbytné pro správný průběh všech procesů nutných pro dokončení S a vstup do G2 fáze buněčného cyklu (Lapenna *et* Giordano, 2009). Během G2 fáze jsou cykliny A degradovány a funkci aktivační podjednotky přebírají cykliny B. Komplex CDK1/cyklin B je klíčový pro zahájení a řádný průchod mitózou. Účastní se regulace pochodů zahrnujících separaci centrosomů, kondenzaci chromosomů, fragmentaci Golgiho aparátu či rozpad jaderné laminy. Úplné dokončení mitózy je pak závislé na proteolytické degradaci cyklinu B a tím inaktivaci CDK1 (Malumbres *et* Barbacid, 2005).

Dalším důležitým pochodem regulovaným aktivitou CDK je transkripce. Jedním z ústředních enzymů tohoto procesu je RNA polymerasa II zodpovědná jak za zahájení přepisu sekvence DNA do RNA, tak také za prodlužování vznikajících transkriptů. Na iniciaci transkripce se podílí multiproteinový iniciační komplex TFIIH, jehož složkou je CDK7 spolu s cyklinem H a proteinem Mat1. Ten je odpovědný za fosforylaci C-terminální domény (CTD) RNA polymerasy II na Ser5, která je

nezbytná pro zahájení celého procesu. Pro prodlužování nově vznikajících transkriptů je poté potřebná fosforylace CTD RNA polymerasy II na Ser2 zprostředkovaná pozitivním transkripčním elongačním faktorem P-TEFb, jehož součastí je CDK9 s cyklinem T. CDK8 se spolu s cyklinem C a proteiny Med12 a Med13 jako složka mediátorového komplexu poté podílí jak na pozitivní tak negativní regulaci transkripce (fosforylace CTD RNA polymerasy II, regulace hladiny transkripčních faktorů, ovlivnění funkce aktivátorů a represorů transkripce) (Canavese *et al.*, 2012; Galbraith *et al.*, 2010; Knuesel *et al.*, 2009; Larochelle *et al.*, 2012; Nemet *et al.*, 2014).

Unikátní postavení mezi CDK má CDK5, která na rozdíl od ostatních není aktivována cyklinem ale regulačními proteiny p35 a p39 a nevyžaduje aktivační fosforylaci. I co se týká známých funkcí, odlišuje se CDK5 od ostatních. CDK5 je nezbytná pro správný vývoj a funkci mozku a nervové soustavy. Účastní se migrace neuronů, prodlužování axonů, kontroluje uvolňování neurotransmiterů při přenosu nervového vzruchu a řady dalších nezbytných procesů (Kawauchi, 2014). S objevem, že exprese CDK5 a jejích aktivátorů není spjata pouze s nervovou soustavou, ale je významná i v dalších typech tkání, byly známé úlohy CDK5 podstatně rozšířeny a bylo prokázáno, že aktivita CDK5 se podílí např. na regulaci apoptózy, regeneraci tkání, senescenci, angiogenezi nebo buněčné adhezi a migraci (Arif, 2012).

3 MOŽNOSTI VYUŽITÍ CÍLENÉ INHIBICE CDK

Ačkoli zapojení CDK do centrálních buněčných pochodů tyto enzymy předurčuje jako ideální terapeutický cíl pro léčbu nádorových onemocnění, možnosti využití jejich inhibice jsou daleko širší (Knockaert *et al.*, 2002).

Velký potenciál má zejména farmakologická inhibice CDK9, jejíž účinnost byla prokázána již v řadě experimentálních modelů (Wang *et* Fisher, 2008). Některá kardiovaskulární onemocnění jsou provázena hypertrofií srdce v důsledku zvětšování diferencovaných srdečních myocytů vlivem nadměrné transkripce a translace. Ačkoli se fyziologicky jedná o adaptaci srdce v odpovědi na stresové podmínky, z dlouhodobého hlediska může jejím vlivem docházet k narušení správné funkce tohoto orgánu a k jeho selhání. Prokázaná korelace mezi zvýšenou aktivitou CDK9, deregulací transkripce a hypertrofií srdce učinila z CDK9 možný molekulární cíl pro terapii kardiovaskulárních onemocnění (Kryštof *et al.*, 2010; Wang *et* Fisher, 2008). Popsaná souvislost mezi inhibicí CDK9 a aktivací apoptózy u neutrofilů skrz snížení hladiny antiapoptotického proteinu Mcl-1 činí z inhibice CDK9 zajímavý terapeutický přístup i pro léčbu chronických zánětlivých onemocnění (Wang *et al.*, 2012). Zánět je klíčovým obranným mechanismem organismu při infekci nejrůznějšími patogeny. Klíčovými hráči tohoto procesu jsou právě neutrofily, nejpočetnější skupina leukocytů, která se vyznačuje velmi krátkou životností, kdy po zhruba 5 dnech je eliminována z krevního oběhu procesem apoptózy. Avšak v případě některých zánětlivých onemocnění, jako je například revmatoidní artritida, je vstup neutrofilů do apoptózy inhibován zvýšenou expresí antiapoptotických proteinů, což přispívá k jejich akumulaci v organismu a tvorbě zánětlivých ložisek (Wang *et al.*, 2012).

Inhibice CDK je také jedním z potenciálních způsobů, jak zablokovat šíření virových infekcí. Enzymatická aktivita CDK napadených hostitelských buněk je totiž nezbytná pro celou řada virů (Schang, 2002; Wang *et* Fisher, 2008). Příkladem může být závislost viru HIV na aktivitě komplexu CDK9/cyklin T hostitelské buňky, která umožňuje aktivaci HIV proteinu Tat, regulátoru virové transkripce (Németh *et al.*, 2011; Wang *et al.*, 2009). Cytomegalovirus (CMV) zase pro svou replikaci vyžaduje aktivitu CDK2 hostitelské buňky. Po infekci CMV dochází k translokaci CDK2 do jádra, ke snížení hladiny přirozených inhibitorů CDK2, k výraznému nárůstu hladiny cyklinu E

a tím ke zvýšení enzymatické aktivity CDK2 (Bresnahan *et al.*, 1997; Knockaert *et al.*, 2002).

CDK5 je zase studována v souvislosti s možnou terapií neurodegenerativních chorob (López-Tobón *et al.*, 2011). Jedním z průvodních znaků Alzheimerovy choroby je hyperfosforylace proteinu Tau. Tento protein se za fyziologických podmínek podílí na regulaci stability a polymerace mikrotubulů a účastní se vnitrobuněčného transportu nezbytného pro správný chod nervové soustavy. V případě jeho nadměrné fosforylace však dochází k jeho disociaci z mikrotubulů, jeho intracelulární akumulaci a tvorbě tzv. neurofibrilárních klubek (neurofibrillary tangles). Fosforylace Tau se účastní celá řada nadřazených kinas, z nichž jednou je právě CDK5, jejíž abnormální kontinuální aktivace v důsledku vazby proteolyticky štěpené aktivační podjednotky p25 byla u pacientů s Alzheimerovou chorobou prokázána (Knockaert *et al.*, 2002; López-Tobón *et al.*, 2011; Tell *et* Hilgeroth, 2013).

Výše uvedené příklady naznačují, že je potenciál využití cílené inhibice CDK v terapii lidských onemocnění skutečně široký. V dalších kapitolách budou proto blíže popsány pouze možnosti využití inhibitorů CDK jako látek s protinádorovými a antiprotozoálními účinky, jak bylo zmíněno v cílech této disertační práce.

3.1 Protinádorová terapie

Neomezený proliferační potenciál nádorových buněk je úzce spjat s abnormální enzymatickou aktivitou CDK zapojených v regulaci buněčného cyklu, ke které dochází u většiny lidských malignit. Nejčastěji je způsobena změnami exprese, mutacemi nebo epigenetickými alteracemi genů pozitivních a negativních regulátorů CDK, ať už cyklinů, přirozených CDK inhibitorů z rodin INK4 a Cip/Kip nebo fosfatas Cdc25, případně některých ze substrátů CDK. Mutace v genech samotných CDK jsou poměrně vzácné (Malumbres *et* Barbacid, 2005).

Téměř všechny nádorové buňky se vyznačují alteracemi v regulačních mechanismech, které kontrolují vstup do buněčného cyklu případně jeho rané fáze G1 a S. Vůbec nejčastější je narušení dráhy cyklin D – CDK4/6 – protein Rb – p16. Vzhledem k tomu, že protein Rb za normálních podmínek plní úlohu transkripčního represoru a brání přepisu genů nezbytných pro zahájení replikace DNA a mitózy,

jakékoli narušení jeho fyziologické funkce poskytuje buňce možnost neomezené proliferace. K inaktivaci proteinu Rb může docházet řadou mechamismů jako jsou genové mutace, vazba onkoproteinu E7 nebo velmi častá abnormální fosforylace, která je způsobena deregulací nadřazených kinas např. v důsledku amplifikace a/nebo zvýšené exprese cyklinu D, delece nebo epigenetického umlčení genu p16 případně amplifikace nebo zvýšené exprese CDK4 a CDK6. V případě CDK4 a CDK6 jsou rovněž známy bodové mutace (Arg24Cys resp. Asp32Tyr), které mají za následek ztrátu vazebného místa pro inhibitor p16 (Asghar *et al.*, 2015; Giacinti *et* Giordano, 2006; Knudsen *et* Knudsen, 2008; Peyressatre *et al.*, 2015). Obvyklá je rovněž deregulace aktivity CDK2, ke které dochází díky zvýšené expresi samotné kinasy, cyklinu E, případně snížené hladině inhibitoru p27 u řady lidských malignit a naznačuje tak její vliv v procesu tumorogeneze (Malumbres *et* Barbacid, 2009; Peyressatre *et al.*, 2015). Naopak méně časté jsou alterace ovlivňující aktivitu CDK1 (Peyressatre *et al.*, 2015), která je schopná zastoupit aktivitu interfázních CDK a je zároveň jako jediná mitotická CDK pro buněčný cyklus esenciální (Santamaría *et al.*, 2007). I přesto byla u některých maligních onemocnění například u rakoviny hrtanu (Bednarek *et al.*, 2016) nebo melanomu (Abdullah *et al.*, 2011) zaznamenána zvýšená exprese CDK1 a její aktivita může být rovněž ovlivněna v důsledku zvýšené hladiny cyklinů A a B.

V souvislosti s možnou protinádorovou terapií stojí za zmínku i CDK5, která je známá především díky své nepostradatelné úloze pro rozvoj a správnou funkci nervové soustavy. Její bližší studium totiž prokázalo její významnou roli i v procesech provázejících progresi některých nádorových onemocnění. Genetická i farmakologická inhibice CDK5 například odhalila snížení motility, invazivity a metastazování některých typů nádorových buněk (Bisht *et al.*, 2015; Liang *et al.*, 2013; Strock *et al.*, 2006). CDK5 byla rovněž prokázána jako regulátor adheze a migrace epiteliálních buněk (Tripathi *et* Zelenka, 2010) i samotné angiogeneze (Liebl *et al.*, 2010). Angiogeneze neboli proces tvorby krevního řečiště je fyziologickým pochodem nezbytným pro normální vývoj organismu, avšak její abnormální indukce rovněž provází řadu maligních onemocnění, kdy přispívá k růstu nádorů a umožňuje metastazování nádorových buněk do okolních tkání (Potente *et al.*, 2011).

Častá zvýšená hladina antiapoptotických proteinů poskytuje nádorovým buňkám u řady onkologických onemocnění výhodu v podobě rezistence vůči apoptóze (Hanahan *et* Weinberg, 2011). Fakt, že inhibice transkripce má dopad především na proteiny s krátkou životností, mezi které se řadí právě i proteiny s antiapoptototickou funkcí

např. Mcl-1, Bcl-2, XIAP nebo survivin, staví zejména transkripční CDK7 a CDK9 do pozice atraktivního terapeutického cíle (Kryštof *et* Uldrijan, 2010). Za zmínku rovněž stojí korelace mezi aktivitou CDK9 a expresí proteinu ICAM-1, který ovlivňuje buněčnou adhezi, invazivitu a angiogenezi (Kryštof *et al.*, 2011).

Podle Hanahana a Weinberga sdílí nádory společné charakteristické rysy, mezi které patří například neomezený replikační a proliferační potenciál, rezistence vůči programované buněčné smrti, schopnost indukovat angiogenezi a možnost invazivity a metastazování do okolních tkání (Hanahan *et* Weinberg, 2011). Z výše uvedeného tedy vyplývá, že cílenou inhibicí enzymatické aktivity CDK je možné do jisté míry tyto vlastnosti společné pro většinu typů nádorů zasáhnout (Obr. 1).

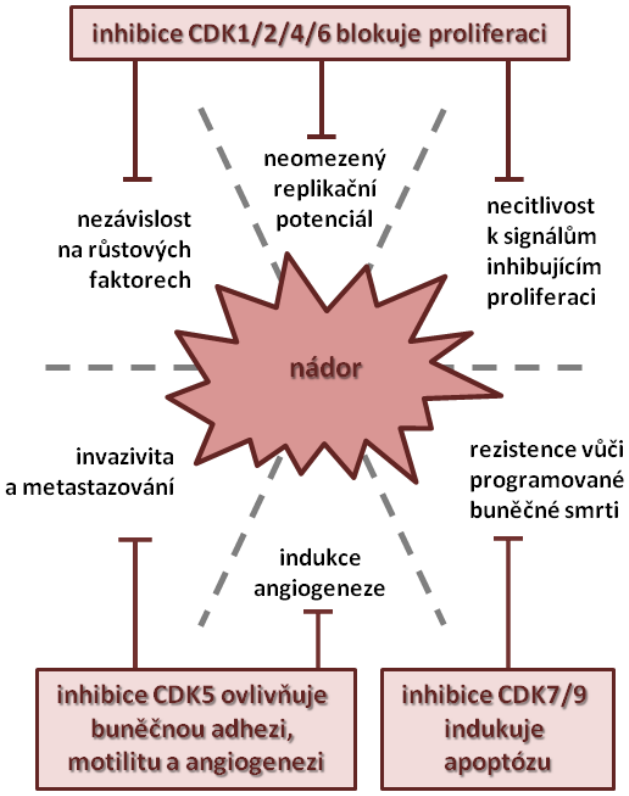

Obr. 1: Vlastnosti nádorů a možnosti jejich ovlivnění cílenou inhibicí CDK (podle Arif, 2012; Hanahan *et* Weinberg, 2011; Liebl *et al.*, 2011; Malumbres, 2014).

3.1.1 Inhibitory CDK s protinádorovými vlastnostmi

Většina známých CDK inhibitorů patří do skupiny látek vážících se do ATP-vazebného místa kinasy. Typicky se jedná o nízkomolekulární sloučeniny s různě substituovaným heterocyklickým skeletem, které se váží do aktivního místa pomocí hydrofobních interakcí a vodíkových můstků (Knockaert *et al.*, 2002; Zhang *et al.*, 2009). Na základě jejich selektivity rozlišujeme skupinu pan-selektivních inhibitorů, které jsou relativně nespecifické a inhibují široké spektrum CDK. Jedněmi z prvních zástupců této skupiny jsou CDK inhibitory tzv. první generace flavopiridol a roskovitin. Strukturně obě látky vycházejí z přírodních sloučenin. Flavopiridol (Obr. 2A) je semi-syntetický flavonový analog přírodního alkaloidu rohitukinu, který již v nanomolárních koncentracích inhibuje CDK1/2/4/6/7 a 9 a patří k nejstudovanějším CDK inhibitorům (Blagosklonny, 2004; Sedlacek, 2001), roskovitin (Obr. 2B) patří do skupiny trisubstituovaných purinů, je derivátem rostlinných hormonů cytokininů a submikromolárním inhibitorem CDK1/2/5/7 a 9 (Meijer *et al.*, 2006; Vermeulen *et al.*, 2002). Obě zmiňované látky vstoupily do klinických studií, ale slibné výsledky získané experimentálně *in vitro*, se v těchto studiích příliš nepotvrdily (Asghar *et al.*, 2015; Meijer *et al.*, 2006).

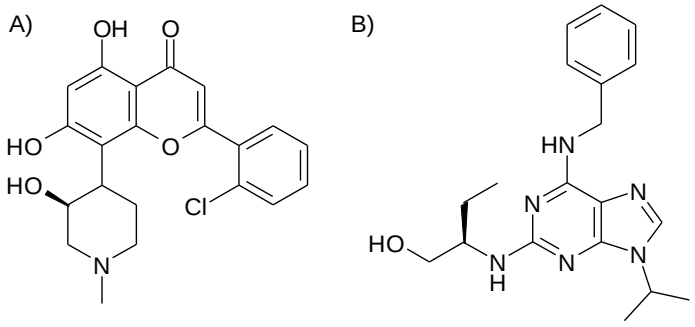

Obr. 2: Chemická struktura A) flavopiridolu a B) roskovitinu.

Na základě znalostí získaných studiem těchto inhibitorů však byla vytvořena celá řada nových sloučenin označovaných jako CDK inhibitory druhé generace (Asghar *et al.*, 2015; Kryštof *et* Uldrijan, 2010; Lapenna *et* Giordano, 2009; Peyressatre *et al.*, 2015). Do této kategorie můžeme zahrnout celou řadu sloučenin, které i přes výraznou strukturní variabilitu (Obr. 3) sdílí řadu společných vlastností. Výrazně převyšují inhibitory první generace v otázce CDK-inhibiční i antiproliferační aktivity. Účinné inhibice na enzymatické úrovni je docíleno působením již nízkých nanomolárních

koncentrací a srovnatelná účinnost byla prokázána i na buněčné úrovni za použití širokého panelu nádorových buněčných linií různého histologického původu. Inhibice CDK zapojených v regulaci buněčného cyklu v závislosti na inhibičním profilu indukuje zablokování buněčného cyklu v některé z jeho fází. Díky inhibici transkripčních CDK pak dochází k inhibici fosforylace RNA polymerasy II a tím celého procesu transkripce, což má dopad na snížení hladiny antiapoptotických proteinů a indukci programované buněčné smrti. Tyto látky tudíž mají jak cytostatické, tak i cytotoxické vlastnosti. Nejznámnějšími zástupci CDK inhibitorů druhé generace je například dinaciclib (SCH727965) (Desai *et al.*, 2013; Feldmann *et al.*, 2011; Fu *et al.*, 2011; Parry *et al.*, 2010), AT7519 (Santo *et al.*, 2010; Squires *et al.*, 2009; Squires *et al.*, 2010), BAY-1000394 (Siemeister *et al.*, 2012) a celá řada dalších. Účinnost těchto látek byla prokázána i v řadě *in vivo* modelů nejčastěji s využitím xenograftů lidských nádorových buněk a řada z nich se nachází v různých fázích klinického testování jako potenciální léčiva nejrůznějších onkologických onemocnění.

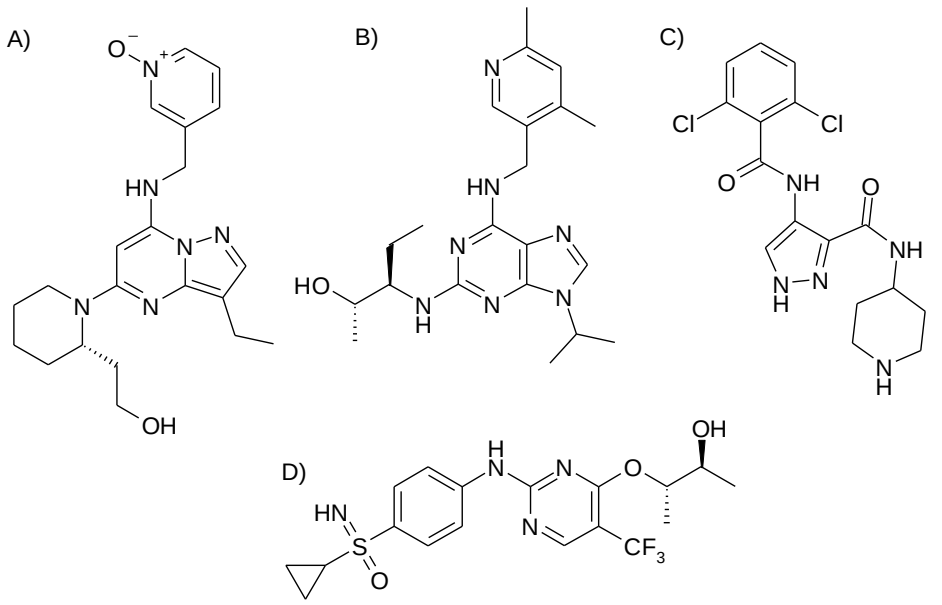

Obr. 3.: Chemická struktura vybraných pan-selektivních CDK inhibitorů druhé generace. A) dinaciclib, B) CYC065, C) AT7519, D) BAY-1000394.

Speciální kategorii představují pan-selektivní CDK inhibitory, které díky nižší selektivitě dosahují zajímavé protinádorové účinnosti skrz inhibici dalších molekulárních cílů. Mezi tyto látky se řadí například TG02 (Goh *et al.*, 2012; Obr. 4A), který kromě inhibice širokého spektra CDK inhibuje se srovnatelnou účinností

i receptorové tyrosinkinasy FLT3 a JAK2, které hrají významnou úlohu v rozvoji hematologických malignit. Účinnost TG02 byla prokázána na panelu leukemických linií, kdy díky kombinované inhibici zmiňovaných molekulárních cílů dosahovala výrazné antiproliferační a proapoptotické aktivity a je tak slibnou látkou pro možnou léčbu pacientů s leukémií (Goh *et al.*, 2012; Pallis *et al.*, 2012). Dalším příkladem může být duální inhibitor CDK-TRK, látka PHA-848125 (Albanese *et al.*, 2010; Obr. 4B). Deregulace TRK (Tropomyosin receptor kinase) v podobě konstitutivní aktivace provází řadu nádorových onemocnění, kdy podporuje proliferaci a metazování nádorových buněk a je tak negativním prognostickým markerem. Jeho inhibice tudíž může zvyšovat terapeutický potenciál této látky u některých agresivních typů malignit (Albanese *et al.*, 2010; Brasca *et al.*, 2009). Jedinečným kinasovým inhibičním profilem se vyznačuje i ZK 304709 (Siemeister *et al.*, 2006; Obr. 4C), která kromě inhibice CDK blokuje aktivitu i VEGFR a PDGFR, dvou receptorových tyrosinkinas, které hrají významnou úlohu v procesu angiogeneze. Díky tomu nejen že blokuje proliferaci nádorových buněk a aktivuje proces apoptózy, ale zároveň dosahuje silných antiangiogenních účinků a blokuje tvorbu nových cév, čímž významnou měrou limituje možnost dalšího růstu nádorů (Siemeister *et al.*, 2006; Scholz *et al.*, 2009).

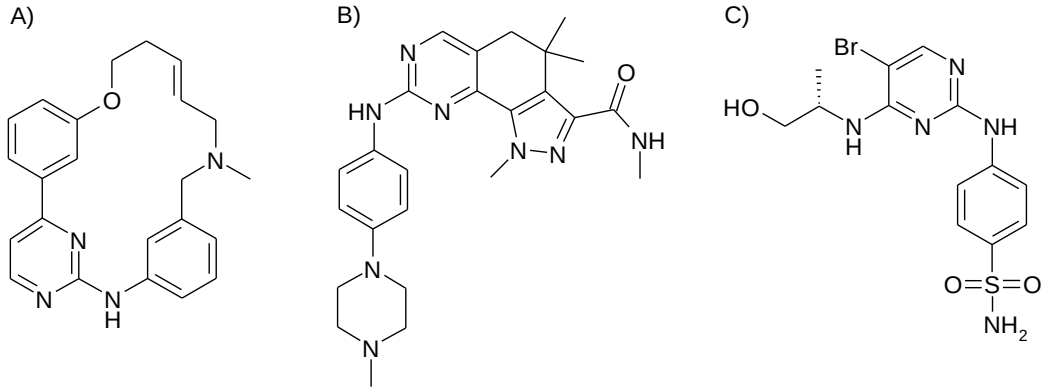

Obr. 4: Chemická struktura A) TG02, B) PHA-848125 a C) ZK 304709.

Všechny výše zmiňované látky vykazují nižší selektivitu v důsledku poměrně vysoké míry homologie v aminokyselinové sekvenci ATP-vazebných míst napříč kinomem, ale i přesto je možné vytvoření selektivních ATP-kompetitivních CDK inhibitorů. Významnou skupinu tvoří zejména CDK4/6 selektivní inhibitory. Vzhledem k časté deregulaci dráhy cyklin D – CDK4/6 – protein Rb – p16 prokázáné v celé řadě nádorů se právě tyto inhibitory jeví být vhodným potenciálním terapeutikem. CDK4/6

inhibitory fungují na bázi cytostatického působení, kdy skrz inhibici enzymatické aktivity CDK4/6 dochází k zablokování fosforylace proteinu Rb a tím k zabránění rozpadu jeho komplexu s transkripčními faktory rodiny E2F. Výsledkem je zablokování buněčného cyklu v G1 fázi a zastavení proliferace (Dickson, 2014; Fry *et al.*, 2004). Nejvýznamnějším zástupcem této skupiny inhibitorů je pyridopyrimidin palbociclib (PD-0332991) (Obr. 5A), který byl popsán jako první nanomolární selektivní inhibitor CDK4/6. Již v nízkých nanomolárních koncentracích indukoval zablokování buněčného cyklu v G1 fázi a dosahoval tak silných antiproliferačních účinků u Rb-pozitivních buněk *in vitro* i *in vivo* (Fry *et al.*, 2004; Toogood *et al.*, 2005). Významným zástupcem je i jeho strukturní analog ribociclib (LEE011) nebo abemaciclib (LY2835219) (Vidula *et* Rugo, 2015) (Obr. 5).

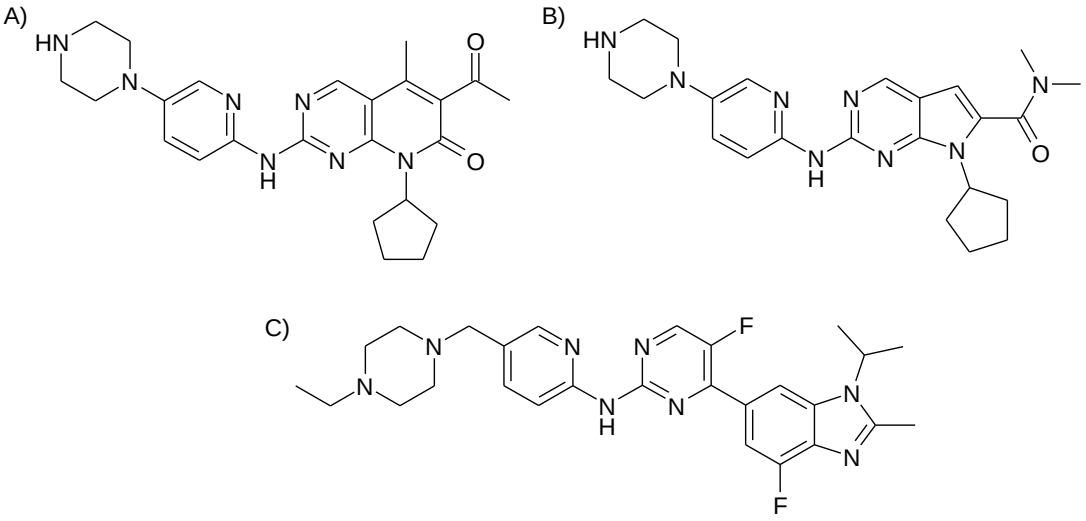

Obr. 5: Chemická struktura CDK4/6 selektivních inhibitorů: A) palbociclib, B) ribociclib, C) abemaciclib

Další vysoce specifické ATP-kompetitivní inhibitory byly nalezeny vůči transkripčním CDK. Inhibice CDK7, která jako klíčová transkripční CDK zároveň plní i funkci CAK a stojí tak na pomezí hned dvou esenciálních buněčných pochodů, regulace buněčného cyklu a transkripce, se jeví být zajímavým molekulárním cílem. Pyrazolo[1,5-*a*]pyrimidinový nanomolární inhibitor CDK7 BS-181 (Obr. 6A) účinně snižuje v nízkých mikromolárních koncentracích proliferaci řady lidských nádorových buněčných linií, inhibuje transkripci, aktivuje apoptózu a zároveň také indukuje blok buněčného cyklu (Ali *et al.*, 2009). Antiproliferační a proapoptotické účinky dosažené přes inhibici transkripce vykazují i nanomolární inhibitory CDK9 EXEL-8647 (Heuer *et al.*, 2008), LDC000067 (Albert *et al.*, 2014; Obr. 6B) nebo subnanomolární i-CDK9 (Lu

et al., 2015; Obr. 6C). Selektivní ATP-kompetitivní inhibitory byly nalezeny rovněž vůči CDK8 a jeho isoformě CDK19. Jedná se o senexin A (Porter *et al.*, 2012; Obr. 6D) a inhibitor 109 (Mallinger *et al.*, 2016; Obr. 6E), a vzhledem k prokázané roli deregulace CDK8 v progresi nádorových onemocnění (Xu *et* Ji, 2011), mají tyto látky zajímavý terapeutický potenciál. Otázkou však zůstává, zda-li při dalším studiu těchto selektivních CDK inhibitorů nebude odhalen jejich další molekulární cíl ať už mezi dalšími CDK nebo jinými kinasami.

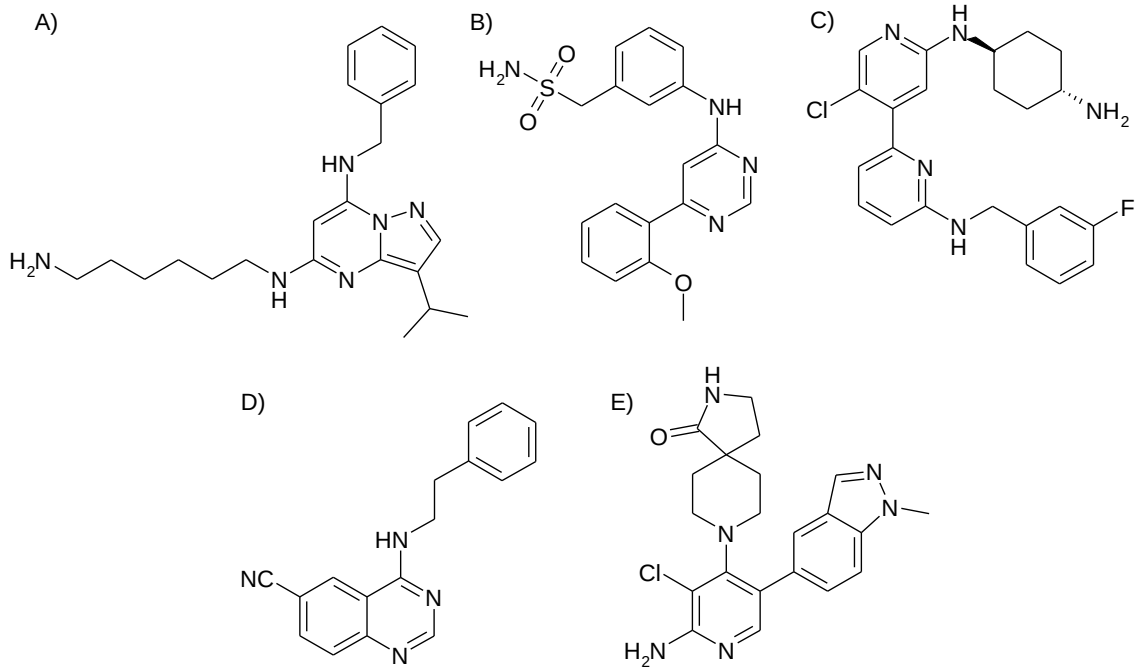

Obr. 6: Chemická struktura A) BS-181, B) LDC000067 , C) i-CDK9, D) senexinu A a E) inhibitoru 109.

Velký potenciál mají také sloučeniny, které se na molekulu enzymu váží pevnou kovalentní vazbou. Tyto látky interagují s postranními řetězci aminokyselin cysteinu nebo lysinu v oblasti ATP vazebného místa. Prvním zástupcem této kategorie byl fenylaminopyrimidin THZ1 (Kwiatkowski *et al.*, 2014; Obr. 7A), který je vysoce účinným inhibitorem CDK7. Látka interaguje s postranním řetězcem aminokyseliny cysteinu (Cys312) v blízkosti aktivního místa. Již v nízkých nanomolárních koncentracích způsobuje zablokování fosforylace CTD RNA polymerasy II a následnou inhibici transkripce, v jejíž návaznosti dochází k indukci apoptózy v nádorových buněčných liniích (Kwiatkowski *et al.*, 2014). Z důvodu nízké stability, která omezuje jeho použití *in vivo*, byla struktura THZ1 modifikována záměnou 4-akrylamidbenzamidu na 3-akrylamidbenzamid za vzniku nového analogu THZ2

(Wang *et al.*, 2015; Obr. 7B). THZ2 si stále díky inhibici CDK7 udržuje významnou protinádorovou aktivitu a navíc vykazuje výrazně lepší farmakokinetické vlastnosti. Obdobný mechanismus účinku stojí za aktivitou NU6300 (Obr. 7C), prvního ireverzibilního inhibitoru CDK2, který interaguje s postranním řetězcem Lys89 za tvorby pevné kovalentní vazby a inhibuje aktivitu CDK2 v submikromolárních koncentracích (Anscombe *et al.*, 2015).

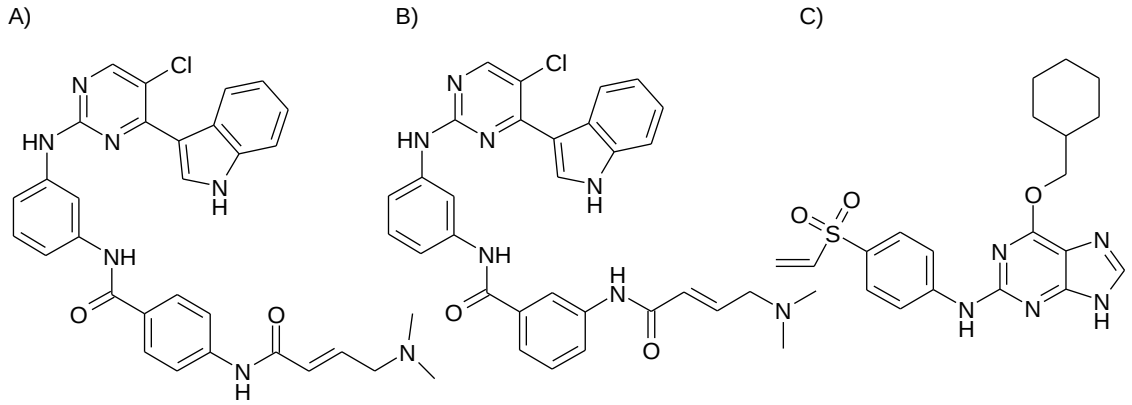

Obr. 7: Chemická struktura A) THZ1, B) THZ2 a C) NU6300.

Problém selektivity ATP-kompetitivních sloučenin způsobený konzervativní sekvencí a strukturou aktivního místa kinas lze vyřešit také nalezením látek, jejichž mechanismus účinku bude založený na vazbě mimo toto aktivní místo. Vyvíjeny jsou tak ATP-nekompetitivní inhibitory, kterých ovšem není mnoho. Jedná se převážně o malé molekuly nebo častěji krátké peptidy, mimikující přirozené CDK inhibitory nebo některý ze substrátů CDK (např. protein Rb nebo p53), které způsobí zablokování buněčných pochodů jimi regulovaných (Abate *et al.*, 2013; Orzaez *et al.*, 2009).

Další významnou skupinu tvoří tzv. alosterické inhibitory, u kterých se předpokládá velmi vysoká míra selektivity (Mariaule *et* Belmont, 2014; Zhang *et al.*, 2009). Jedinečnou vlastností CDK je jejich aktivace vazbou regulační podjednotky. Narušením této interakce by byla možná jejich selektivní inaktivace. V případě CDK2 bylo popsáno alosterické místo v blízkosti αC (PSTAIRE) helixu, jehož interakce s nízkomolekulární sloučeninou způsobí významnou konformační změnu, která zabrání ustavení komplexu CDK/cyklin a dochází tak k zablokování kinasové aktivity (Betzi *et al.*, 2011; Palmieri *et* Rastelli, 2013). V současné době je již známo několik látek, u nichž byla prokázána inhibice CDK2 alosterickým mechanismem (Rastelli *et al.*, 2014).

Vývojem nových sloučenin fungujících na bázi inhibice CDK se stále zabývá řada výzkumných týmů usilujících o zlepšení biologických, fyzikálně-chemických a farmakologických vlastností těchto látek (Galons *et al.*, 2013; Malínková *et al.*, 2015).

3.1.2 Inhibitory CDK v terapii lidských nádorových onemocnění

V současné době se několik sloučenin z kategorie CDK inhibitorů nachází v různých fázích klinického testování proti řadě nádorových onemocnění (Tab. 2).

Tab. 2: Přehled CDK inhibitorů procházejících v současnosti klinickým testováním jako potenciální léčiva onkologických onemocnění.

	Inhibitor	Molekulární cíl	Onemocnění	Fáze
Pan-selektivní CDK inhibitory	**Alvocidib** (flavopiridol)	CDK1/2/4/6/7/9	CLL, lymfom, mnohočetný myelom, AML	I/II
	Dinaciclib (SCH727965)	CDK1/2/5/7/9	rakovina pankreatu, solidní tumory, mnohočetný myelom, karcinom prsu, CLL, melanom	I/II
	CYC065	CDK2/5/9	pokročilá maligní onemocnění	I
	AT7519	CDK1/2/4/5/9	solidní tumory	I
	Roniciclib (BAY1000394)	CDK1/2/3/4/7/9	pokročilá maligní onemocnění, karcinom plic	I/II
	TG02	CDK1/2/3/5/7/9, JAK2, FLT3	AML, ALL, CLL	I
	Milciclib (PHA-848125)	CDK1/2/4/5/7, TRKA	karcinom thymu	II
CDK4/6-selektivní inhibitory	**Palbociclib** (PD-0332991)	CDK4/6	karcinom prsu, plic, prostaty, trávicího traktu, hlavy a krku, jater, sarkom, liposarkom	I/II/III
	Ribociclib (LEE011)	CDK4/6	karcinom prsu, plic, hlavy a krku, jater, prostaty, melanom, neuroblastom, lymfom, liposarkom	I/II/III
	Abemaciclib (LY2835219)	CDK4/6	karcinom prsu, plic, lymfom, lymfom z plášťových buněk, melanom	I/II/III
	G1T28	CDK4/6	karcinom plic	I/II

AML – akutní myeloidní leukémie, ALL – akutní lymfoblastická leukémie, CLL – chronická lymfatická leukémie

Reference k Tab. 2: clinicaltrials.gov; Bisi *et al.*, 2015; Brasca *et al.*, 2009; Fry *et al.*, 2004; Goh *et al.*, 2012; Parry *et al.*, 2010; Saladino *et al.*, 2015; Squires *et al.*, 2010; Siemeister *et al.*, 2012; Vidula *et* Rugo, 2015.

Z dosavadních výsledků klinických studií vyplývá, že pan-selektivní CDK inhibitory dosahují slibných výsledků zejména u pacientů s chronickou lymfocytickou leukémií (CLL), jejímž charakteristickým znakem je přítomnost velkého množství nereplikujících se CLL buněk, které jsou často rezistentní vůči apoptóze kvůli mutacím v genech ATM a p53 (Abrisqueta *et al.*, 2011) a také díky expresi antiapoptotických proteinů (Blachly *et* Byrd, 2013; Desai *et al.*, 2014). I přes neproliferující charakter CLL buněk byla u flavopiridolu prokázána schopnost indukovat v těchto buňkách programovanou buněčnou smrt. Flavopiridol skrz inhibici CDK9 blokuje fosforylaci RNA polymerasy II a tím proces transkripční elongace. Výsledkem je výrazné snížení hladiny proteinů s krátkou životností, mezi něž právě patří i antiapoptotické proteiny např. Mcl-1, které chrání buňky CLL před indukcí apoptózy (Chen *et al.,* 2005). Účinnost flavopiridolu byla prokázána v řadě klinických studií u pacientů v pokročilých stádiích CLL, u nichž došlo ke stabilizaci onemocnění a zpomalení její progrese (Byrd *et al.*, 2007; Lin *et al.*, 2009; Phelps *et al.*, 2009). Stejný mechanismus účinku byl prokázán i v případě dinaciclibu, selektivnějšího a účinnějšího zástupce druhé generace pan-selektivních CDK inhibitorů (Johnson *et al.*, 2012), a jeho účinnost byla rovněž potvrzena v klinických studiích (Flynn *et al.*, 2015).

Avšak na rozdíl od slibných výsledků, kterých pan-selektivní CDK inhibitory dosahují v případě hematologických malignit, které se jeví být k inhibici buněčného cyklu a indukci apoptózy nejcitlivější (Bose *et al.*, 2013), v případě klinických studií u pacientů se solidními tumory účinnost těchto látek často selhává a nedosahuje efektivity standardně používaných chemoterapeutik (Mita *et al.*, 2014; Stephenson *et al.*, 2014). Vysvětlením nízké účinnosti CDK inhibitorů může být samotná molekulární podstata onemocnění, kdy zasažený molekulární cíl nemusí být pro viabilitu některých nádorových buněk nezbytný. Absence vhodných tumorových markerů navíc omezuje možnosti výběru vhodných pacientů pro klinické studie a tím do jisté míry limituje i jejich možnou úspěšnost (Asghar *et al.*, 2015; Guha, 2012). Problematické může být rovněž dosažení efektivní koncentrace CDK inhibitoru v místě tumoru, případně nedostačující délka jeho působení a pro terapeutický účinek je rovněž zásadní zvolení správného dávkování (Dickson *et* Schwartz, 2009; Malumbres *et al.*, 2008). Limitujícím faktorem použití pan-selektivních CDK inhibitorů je zejména poměrně úzké terapeutické okno, kdy příliš nízká koncentrace látky nezpůsobí požadovanou odezvu a naopak příliš vysoká často zasáhne další buněčné cíle a dochází k rozvoji nežádoucích vedlejších účinků (Asghar *et al.*, 2015; Guha, 2012).

Z těchto důvodů se trendem posledních let stalo testování účinnosti CDK inhibitorů v kombinaci s dalším léčivem (Cicenas *et al.*, 2014). Výhodou tohoto přístupu je možnost vystavení nádoru působení dvou látek s odlišným mechanismem účinku umožňující zasažení více buněčných cílů najednou. To výrazně snižuje pravděpodobnost rozvoje rezistence nádoru, umožňuje redukovat výsledné dávky a také může omezit rozvoj nežádoucích účinků. V ideálním případě je cílem najít kombinaci takových látek, u kterých dojde k jejich synergickému působení, kdy i přes snížení jejich dávek dojde k výraznému zesílení jejich účinku *in vivo* (Kummar *et al.*, 2010).

Terapii onkologických onemocnění využívající konvenčních chemoterapeutik, jejichž mechanismus účinku je založen na narušení procesu replikace v nádorových buňkách, v jehož důsledku dochází k poškození DNA, inhibici buněčné proliferace a indukci apoptózy, často komplikuje rozvoj rezistence nádorových buněk vůči těmto látkám. Důvodem je často aktivace kontrolního bodu reagujícího na poškození DNA, který indukuje zablokování buněčného cyklu a iniciaci DNA-reparačních mechanismů. Vzhledem k prokázané úloze CDK v aktivaci zmiňovaného kontrolního bodu a následných oprav DNA (Trovesi *et al.*, 2013; Xu *et al.*, 2012) bylo v řadě preklinických studií zjištěno, že pan-selektivní CDK inhibitory mohou výrazně zesilovat účinek chemoterapeutik a zároveň omezovat možnost vzniku rezistence (Johnson *et* Shapiro, 2010), což bylo potvrzeno i v rámci klinických studií. Terapeutický účinek kombinace cisplatiny s flavopiridolem byl prokázán například u pacientek s karcinomem vaječníků rezistentním vůči platině (Bible *et al.*, 2012), zesílení účinku doxorubicinu působením flavopiridolu bylo prokázáno u pacientů s pokročilým stádiem sarkomu (Luke *et al.*, 2012) a řada dalších klinických studií kombinujících působení chemoterapeutik s CDK inhibitory i nadále probíhá (clinicaltrials.gov).

Intenzivní výzkum probíhá i v případě testování kombinací CDK inhibitorů s další látkou se specifickým buněčným cílem. V rámci preklinického zkoušení dosáhly slibných výsledků v mnoha experimentálních modelech například kombinace s inhibitory Bcl-2, kdy snížení hladiny Mcl-1 vlivem CDK inhibitorů synergicky potencuje jejich účinek a kombinací těchto látek dochází k výraznému nárůstu proapoptotického působení u řady nádorových buněk odvozených například od lidského mnohočetného myelomu nebo gliomu (Chen *et al.*, 2007; Chen *et al.*, 2012; Jane *et al.*, 2015). Synergické působení bylo prokázáno i v případě kombinace flavopiridolu s inhibitorem proteasomu bortezomibem (Dai *et al.*, 2004) a značný terapeutický

potenciál má rovněž zasažení více kinasových cílů najednou. Popsáno je například zvýšení protinádorového působení multikinasového inhibitoru sorafenibu (Nagaria *et al.*, 2013) nebo inhibitoru Bcr/Abl imatinibu (Yu *et al.*, 2002) působením flavopiridolu. Účinnost CDK inhibitorů v kombinacích s dalším cíleným léčivem je ověřován i v rámci klinických studií (Bose *et al.*, 2012; Holkova *et al.*, 2014).

Výběru vhodných látek pro kombinační terapii často napomáhají také znalosti tzv. syntetické letality popisující vztahy mezi mutacemi dvěma (nebo více) genů, které samy o sobě nenarušují viabilitu buňky, ale v kombinaci působí letálně (Kaelin, 2005). Taková interakce byla odhalena například pro CDK5, jejíž umlčenní výrazně zvyšuje citlivost nádorových buněk k inhibitoru PARP-1 (Bolin *et al.*, 2012; Turner *et al.*, 2008). Použití dinaciclibu v kombinaci s inhibitorem PARP-1 ABT-888 v modelu mnohočetného myelomu vedlo ke specifické letalitě nádorových buněk a k inhibici růstu xenograftu (Alagpulinsa *et al.*, 2016), což potvrzuje významný léčebný potenciál této kombinace sloučenin.

Další skupinou látek, u kterých probíhá intenzivní klinické testování, jsou CDK4/6-selektivní inhibitory a rovněž u nich často pokračuje trend jejich testování v kombinaci s další látkou. Díky jedinečným výsledkům získaným v rámci preklinického zkoušení vstoupil do klinického testování palbociclib. Jeho výjimečnost zde byla potvrzena a stal se historicky prvním schváleným léčivem ze skupiny CDK inhibitorů. Palbociclib (obchodní název Ibrance®) našel v kombinace s letrozolem uplatnění v léčbě žen s estrogenovým receptorem-pozitivním, HER2-negativním metastazujícím karcinomem prsu (Dhillon, 2015; Lu, 2015; Morikawa *et* Henry, 2015). Estrogen je jedním z faktorů, který přispívá k progresi karcinomu prsu, a inhibice aromatasy, enzymu katalyzujícího jeho poslední biosyntetický krok, je jedním z možných terapeutických přístupů. Letrozol, selektivní a vysoce účinný inhibitor aromatasy, blokuje syntézu estrogenu a tím inhibuje růst tumoru. Tato látka prošla intenzivním klinickým zkoušením a stala se schváleným léčivem pro terapii různých forem karcinomu prsu (Bhatnagar, 2007). Jeho účinnost však byla výrazně zesílena právě kombinovanou léčbou s palbociclibem, kdy oproti letrozolu samotnému došlo u pacientek k výrazně dlouhodobější stabilizaci onemocnění bez její další progrese (Finn *et al.*, 2015).

Po úspěchu palbociclibu i další CDK4/6 inhibitory ribociclib, abemaciclib a G1T28 vstoupili do klinického testování (Tab. 2) proti nejrůznějším typům malignit (Johnston, 2015; clinicaltrials.gov).

Kromě samotné protinádorové účinnosti CDK4/6 inhibitorů, která je omezena na Rb-pozitivní nádorové buňky, jsou studovány i alternativní možnosti jejich využití. Jedním z nejzávažnějších vedlejších účinků při používání konvenčních chemoterapeutik je zasažení normální krvetvorby a navození tzv. myelosuprese. U palbociclibu (Roberts *et al.*, 2012) a G1T28 (Bisi *et al.*, 2015; Sorrentino *et al.*, 2015) bylo prokázáno, že přechodné navození G1 bloku buněčného cyklu u hematopoetických buněk může významně snížit citlivost těchto buněk k cytostatikům a výrazně omezit rozvoj chemoterapií-indukované myelosuprese, která je významným limitujícím faktorem léčby (Bisi *et al.*, 2015; Roberts *et al.*, 2012; Sorrentino *et al.*, 2015).

Ačkoli účinnost CDK inhibitorů je testována na celé řadě nejrůznějších onkologických onemocnění, stále zůstává mnoho typů malignit, kde jsou znalosti o působení těchto typů látek poměrně omezené a jejichž léčba je zároveň z různých důvodů problematická (rozvoj rezistence, nedostatečná cílená terapie). Jedním z nich je například hepatocelulární karcinom.

3.1.3 Hepatocelulární karcinom (HCC)

HCC je nejčastějším typem jaterních malignit. Celosvětově se řadí na první příčky v četnosti nádorových onemocnění a vzhledem ke špatné prognóze a omezeným možnostem léčby se jedná o třetí nejčastější příčinu úmrtí související s rakovinou (Bupathi *et al.*, 2015; Germano *et* Daniele, 2014). Na rozdíl od jiných nádorových onemocnění jsou v případě HCC dobře známy rizikové faktory vzniku nemoci. U většiny nových případů HCC předchází rozvoji malignity chronické onemocnění jater nejčastěji virová hepatitida B nebo C (Venook *et al.*, 2010; Whittaker *et al.*, 2010), jaterní cirhóza nebo nealkoholová jaterní steatóza. Rizikovým faktorem je rovněž působení aflatoxinů (Bupathi *et al.*, 2015).

3.1.3.1 Současné možnosti léčby

Na základě diagnostikovaného stádia onemocnění se přistupuje k odlišným způsobům léčby. V nejranějším stádiu se jedná zejména o léčbu chirurgickou resekcí, kdy je odstraněna přímo část jater s maligním ložiskem. Pokud je tato možnost léčby

vyloučena, je pacientům indikována transplantace jater. Ta přináší velmi dobré výsledky, co se týká délky přežití pacientů a rovněž u nich ve velmi nízkém procentu dochází k opětovnému rozvoji onemocnění. Problémem je ovšem nalezení vhodných dárců (El-Serag, 2011). Vzhledem k asymptomatickému průběhu nemoci však často nedochází k včasné diagnostice a onemocnění progreduje do pokročilejších stádií, kdy je již často chirurgická léčba vyloučena. Možností je poté využití radiofrekvenční ablace a perkutánních injekcí ethanolu, jejichž cílem je vlivem tepla nebo koncentrovaného roztoku ethanolu způsobit přímo nekrózu nádorové tkáně (Crissien *et* Frenette, 2014). Dalším možným přístupem léčby je také transarteriální chemoembolizace, která zahrnuje intraarteriální injekci vysoké dávky chemoterapeutika (např. doxorubicinu) rozpuštěného v nosném médiu (nejčastěji lipiodolu) přímo do jaterní arterie, která je následně zablokována embolizačními částicemi. Tím je docíleno dlouhodobějšího působení chemoterapeutika v místě nádorového ložiska a zároveň navození hypoxie a nekrózy nádorové tkáně (Mazzoccoli *et al.*, 2015; Schlachterman *et al.*, 2015).

Co se týká využití cílených chemoterapeutik pro léčbu HCC je jedinou používanou látkou multikinasový inhibitor sorafenib (Nexavar®, BAY 43-9006, Obr. 8) (Cervello *et al.*, 2012).

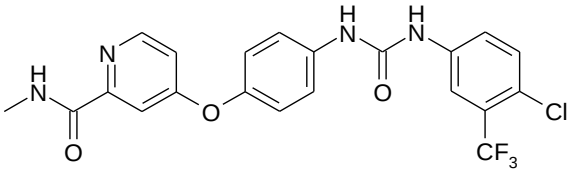

Obr. 8: Chemická struktura sorafenibu.

Molekulární podstata jeho působení spočívá v inhibici několika receptorových tyrosinkinas konkrétně VEGFR2, VEGFR3, PDGFR, FLT3, Ret a c-kit a serin-threoninové kinasy Raf (Cervello *et al.*, 2012; Liu *et al.*, 2006). Inhibicí kinasy Raf, klíčového hráče MAPK kinasové dráhy, dochází k zablokování MEK/ERK signalizace a k redukci hladiny cyklinu D, což má za následek inhibici proliferace. Sorafenib rovněž snižuje hladinu antiapoptotických proteinů Mcl-1 a survivinu, čímž účinně indukuje apoptózu. Nezanedbatelným benefitem je rovněž antiangiogenní působení sorafenibu díky inhibici receptorových tyrosinkinas VEGFR a PDGFR, neboť pro progresi HCC je bohaté krevní zásobení nádorové tkáně zcela nezbytné (Cervello *et al.*, 2012; Liu *et al.*, 2006). Účinnost sorafenibu byla prokázána v řadě preklinických modelů *in vitro* a *in*

vivo, úspěšně prošel všemi fázemi klinického testování a v současné době je jediným léčivem schváleným Úřadem pro kontrolu potravin a léčiv (FDA) a Evropskou lékovou agenturou (EMEA) pro léčbu pacientů v pokročilých stádiích HCC, kdy jeho působením dochází k signifikantnímu zpomalení postupu onemocnění (Cervello *et al.*, 2012; McNamara *et* Knox, 2014).

3.1.3.2 Deregulace aktivity CDK u HCC

Stejně jako u jiných typů nádorových onemocnění, je i progrese hepatocelulárního karcinomu provázena změnami v expresi důležitých regulátorů buněčného cyklu. Při porovnávání tkáně hepatocelulárního karcinomu a odpovídající nenádorové tkáně byla sledována zvýšená hladina CDK zapojených přímo v regulaci buněčného cyklu, konkrétně CDK1, CDK2 a CDK4, které provázejí zvýšenou proliferaci HCC buněk (Kohzato *et al.*, 2001; Li *et al.*, 2002; Masaki *et al.*, 2003). Zvýšená hladina byla popsána rovněž u CDK5, CDK13 a CDK14 a má vliv především na progresi HCC (Ehrlich *et al.*, 2015; Kim *et al.*, 2012; Pang *et al.*, 2007). Zvýšená exprese CDK5 koreluje se zvýšenou proliferací HCC buněk a podporuje progresi HCC *in vitro* a *in vivo* (Ehrlich *et al.*, 2015). Amplifikace genu pro CDK13 má souvislost s ranějším rozvojem HCC, podporuje proliferaci HCC buněk a jejich migrační potenciál (Kim *et al.*, 2012). U CDK14 byla prokázána korelace mezi hladinou proteinu a agresivitou a metastazováním nádorů, kdy CDK14 skrz fosforylaci transgelinu 2 ovlivňuje polymeraci aktinu a přispívá ke zvýšenému migračnímu potenciálu a invazivitě HCC buněk (Pang *et al.*, 2007; Leung *et al.*, 2011). Podobný dopad na HCC buňky má rovněž pozměněná exprese CDK10, která je považována za regulátor přechodu mezi fázemi G2 a M buněčného cyklu. V tomto případě je ale progrese HCC provázena sníženou hladinou CDK10 v porovnání s nenádorovou jaterní tkání a přispívá ke zvýšené proliferaci HCC buněk, snížené chemosensitivitě k cytostatikům a agresivitě tumorů (Zhong *et al.*, 2012).

Změny v hladinách byly prokázány i v případě aktivačních regulátorů CDK. Zvýšená hladina proteinu byla popsána u všech hlavních typů cyklinů (A, B, E a D) regulujících aktivitu CDK zapojených v kontrole buněčného cyklu (Bisteau *et al.*, 2014; Kohzato *et al.*, 2001; Masaki *et al.*, 2003), u aktivátoru CDK5 (p35) (Ehrlich *et al.*,

2015) i v případě CDK-aktivační kinasy Wee1 (Masaki *et al.*, 2003). Ve všech případech tak může docházet vlivem zvýšené hladiny těchto proteinů k abnormální aktivaci CDK a tím ke zvýšené proliferaci HCC buněk a rozvoji hepatokarcinogeneze. Chronická infekce virovou hepatitidou B, zmiňovaná jako jeden z nejčastějších rizikových faktorů rozvoje HCC, může přímo ovlivňovat i regulaci buněčného cyklu a tím samotný proces tumorogeneze skrz inzerci virové DNA do intronové oblasti genu pro cyklin A. Výsledkem je přepis hybridních transkriptů HBV/cyklin a vzniklý cyklin A vyznačující se zvýšenou stabilitou (Benhenda *et al.*, 2009; Wang *et al.*, 1992).

Dalším prokázaným mechanismem, který může způsobit deregulaci kinasové aktivity CDK je umlčení přirozených inhibitorů těchto enzymů. U HCC je popsána řada těchto proteinů z rodiny Cip/Kip (p27) i INK4 (p16, p18), u kterých dochází k zablokování jejich přirozené aktivity a to nejčastěji prostřednictvím epigenetického umlčení promotorové oblasti daného genu nebo zvýšené proteolytické degradace proteinu (Matsuda *et al.*, 2013; Morishita *et al.*, 2004).

3.1.3.3 Inhibice CDK jako potenciální terapie HCC

I přes známé abnormality v regulaci aktivit CDK u HCC, nejsou příliš popsány účinky farmakologických inhibitorů CDK jako potenciálních kandidátů pro léčbu. Jednou z komplexnějších prací zabývajících se studiem účinků CDK inhibitorů na lidský HCC je práce od Cho a spolupracovníků z roku 2010, která popisuje biologické účinky xylocidinu, méně známého inhibitoru CDK1/2/7 a 9 (Obr. 9A). Látka má prokazatelné proapoptotické účinky na lidské nádorové buněčné linie odvozené od HCC. Působením mikromolárních koncentrací xylocydinu dochází ke snížení hladiny antiapoptotických proteinů Bcl-2, XIAP a survivinu a ke stabilizaci proteinu p53 a Bax. Účinnost xylocydinu byla prokázána i na úrovni *in vivo* v modelu xenograftu lidských HCC buněk SNU-354, kde intraperitoneální injekce látky v dávkách 50 a 100 mg/kg účinně snižovaly rychlost růstu tumoru a v nádorových buňkách indukovaly apoptózu, aniž by došlo k ovlivnění normální zdravé tkáně (Cho *et al.*, 2010). Na tuto práci navazuje další publikace od stejného kolektivu autorů Cho *et al.*, 2011, popisující účinky nového derivátu ibulocydinu (Obr. 9B). Rovněž tato látka má na buňky HCC antiproliferační a proapoptotické účinky a v *in vivo* modelu HCC xenograftu zpomaluje růst tumorů

a indukuje buněčnou smrt nádorových buněk, avšak ibulocydin dosahuje v porovnání s xylocydinem vyšší účinnosti (Cho *et al.*, 2011). I přes toto zlepšení jsou však efektivní koncentrace obou látek příliš vysoké a není pravděpodobné jejich další terapeutické využití.

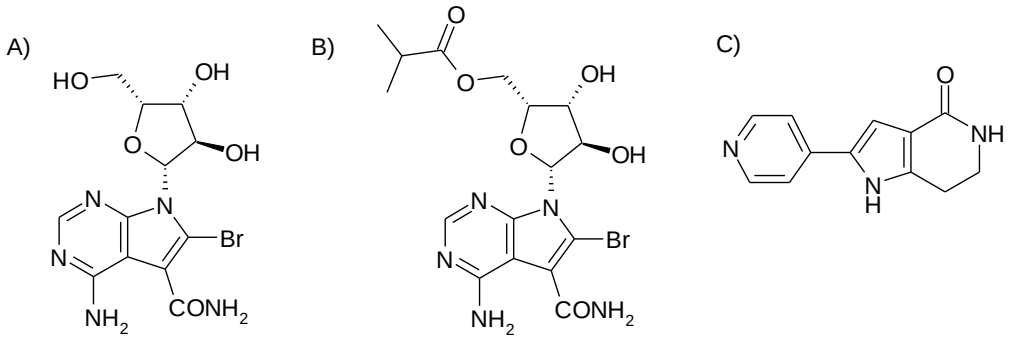

Obr. 9.: Chemická struktura A) xylocydinu, B) ibulocydinu a C) PHA-767491.

Častým jevem u pacientů s HCC je rozvoj chemorezistence v důsledku aktivace kinasy Chk1. Možnou strategií řešící tento problém se jeví být inhibice jeho nadřazené kinasy Cdc7. V modelu HCC byla studována účinnost látky PHA-767491, duálního inhibitoru Cdc7/CDK9 (Li *et al.*, 2015; Natoni *et al.*, 2011; Obr. 9C), která díky inhibici Cdc7 redukuje fosforylaci Chk1 a zároveň v důsledku inhibice CDK9 snižuje hladinu Mcl-1. Spojením PHA-767491 s 5-fluorouracilem pak bylo prokázáno synergické působení obou látek a výrazný nárůst jejich cytotoxicity v modelu HCC *in vitro* a *in vivo* (Li *et al.*, 2015).

Průvodním znakem HCC je i častá Rb-deficience případně narušení funkčnosti dráhy cyklin D – CDK4/6 – protein Rb – p16 (Azechi *et al.*, 2001; Mayhew *et al.*, 2007). I přesto byl studován vliv cílené inhibice CDK4/6 na nádorové linie odvozené od HCC (Rivadeneira *et al.*, 2010), kde bylo prokázáno, že palbociclib inhibuje replikaci Rb-pozitivních HCC buněk a blokuje jejich buněčný cyklus v G1 fázi. Zajímavé bylo ovšem zjištění, že podobného účinku je dosaženo i v případě HCC buněk s geneticky inaktivovaným Rb, u kterých palbociclib indukoval G1 blok patrně díky kompenzaci ztráty proteinu Rb proteinem p107, jehož stabilita a tím i celková hladina byla v těchto buňkách výrazně zvýšená. Obdobné výsledky byly získány i v rámci *in vivo* experimentů (Rivadeneira *et al.*, 2010) a účinnost palbociclibu byla ověřována i v rámci klinické studie na pacientech s pokročilým HCC (Littman *et al.*, 2013; clinicaltrials.gov, NCT01356628).

Vhodným terapeutickým cílem se zdá být rovněž CDK5 zapojená v procesu angiogeneze (Liebl *et al.*, 2010), protože HCC je často provázen abnormální vaskularizací, která umožňuje růst tumoru a jeho metastazovaní do okolních tkání (Patel *et* Sun, 2014; Zhu *et al.*, 2011). Genetické umlčení CDK5 v nádorových buněčných liniích odvozených od HCC snížilo proliferaci u všech studovaných linií a stejného výsledku bylo dosaženo i farmakologicky s využitím pan-selektivního inhibitoru roskovitinu, který je účinným inhibitorem i CDK5. Tyto výsledky byly prokázány i na úrovni *in vivo* experimentů v modelu HCC xenograftu (Ehrlich *et al.*, 2015).

3.2 Antiprotozoální terapie

Onemocnění vyvolávaná jednobuněčnými parazity patří k nejrozšířenějším a nejzávažnějším medicínským problémům ve světě. Jedním z nich je i leishmanióza, onemocnění způsobené parazitickými prvoky rodu *Leishmania*, které ohrožuje více než 350 miliónů lidí zejména v tropických oblastech světa a vzhledem k nedostatku vhodných léčiv je obrovským globálním problémem (den Boer *et al.*, 2011; Knockaert *et al.*, 2002; Singh *et al.*, 2012). Různé druhy leishmanií jsou původci odlišných forem leishmaniózy s odlišnými klinickými projevy. Nejmírnější formou je kožní leishmanióza. Jejími původci jsou například *L. major* nebo *L. mexicana* a projevuje se vznikem kožních lézí a jizev. Pokud je však původcem onemocnění například *L. braziliensis*, může tato kožní forma onemocnění progredovat do závažnější mukokutánní formy, která napadá sliznice dutiny ústní, nosu nebo krku. Nejzávažnější formou onemocnění je ale Kala-Azar, viscerální forma. Jejími původci jsou například druhy *L. infantum* nebo *L. donovani*. Tato forma onemocnění má fatální dopad na lidský organismus. Dochází při ní k zasažení vnitřních orgánů jako je kostní dřeň, slezina nebo játra, narušuje krvetvorbu a imunitní systém a pokud není včas zahájena léčba, ve většině případů končí smrtí (McGwire *et* Satoskar, 2014; Sharlow *et al.*, 2010). Současné možnosti léčby leishmaniózy nejsou dostačující. Používanými terapeutiky jsou často látky, které nebyly primárně připraveny za účelem léčby leishmaniózy (například soli antimonu, amphotericin B, miltefosin nebo paromomycin), jejich aplikace je mnohdy provázena závažnými vedlejšími účinky a velkým problémem je i rozvoj rezistence k těmto léčivům zejména v oblastech s velkým výskytem leishmaniózy (Singh *et al.*, 2012). Z těchto důvodů se hledají nové možnosti léčby. Pro zajištění dobré účinnosti a zároveň snížení pravděpodobnosti rozvoje vedlejších účinků, by měl být nový terapeutický cíl specifický pro parazita anebo alespoň strukturně a funkčně odlišný od homologu jeho hostitele (Chawla *et* Madhubala, 2010). Z toho důvodu je výzkum zaměřen například na studium jedinečných metabolických drah esenciálních pro viabilitu parazita nebo na mechanismy interakce mezi parazitem a hostitelem (Singh *et al.*, 2012). Velký terapeutický potenciál mají rovněž proteinkinasy regulující proliferaci leishmanií. Jednou z nich je i homolog lidských CDK, proteinkinasa CRK3 (Cdc2-related protein kinase 3) (Chawla *et* Madhubala,

2010; Singh *et al.*, 2012), která je nezbytná pro viabilitu těchto parazitů (Hassan *et al.*, 2001).

Vzhledem k určité míře homologie s lidskými enzymy rodiny CDK byla pro řadu známých CDK inhibitorů prokázána účinnost i vůči CRK3 (Grant *et al.*, 2004; Hassan *et al.*, 2001; Jorda *et al.*, 2011; Reichwald *et al.*, 2008; Xingi *et al.*, 2009). Odlišnosti v sekvenci těchto enzymů (Obr. 10) by však mohly být dostačující pro nalezení takových látek, které budou specificky inhibovat parazitární CRK3, aniž by docházelo k ovlivnění hostitelských buněk. S ohledem na výraznou převahu známých inhibitorů kinas s ATP-kompetitivním mechasnimem účinku patří mezi nejzajímavější sekvenční odlišnosti ty v aminokyselinách formujících ATP-vazebné místo. Při porovnání sekvence lidské CDK2 (HsCDK2) a leishmaniální CRK3 (LmCRK3) se jedná hlavně o záměnu Phe82^{HsCDK2} za Tyr101^{LmCRK3} a dále Leu83^{HsCDK2} za Val102^{LmCRK3}. Další změny v ATP-vazebné oblasti, konkrétně nahrazení His84^{HsCDK2} za Glu103^{LmCRK3} a Gln85^{HsCDK2} za Ala104^{LmCRK3}, nejsou vzhledem k orientaci jejich postranních řetězců vně ATP-vazebné kavity a tudíž minoritní úloze při interakci kinasy s inhibitorem příliš významné (Cleghorn *et al.*, 2011). 75% míra sekvenční homologie mezi HsCDK2 a LmCRK3 navíc naznačuje možnost nalezení inhibitorů s ATP-nekompetitvním charakterem, které budou výrazně specifičtější vůči parazitární CRK3.

```
HsCDK2          ------------------MENFQKVEKIGEGTYGVVYKARNKLTGEVVALKKIRLDTET
LmCRK3          MSSFGRVTARSGDAGTRDSLDRYNRLDVLGEGTYGVVYRAVDKITGQYVALKKVRLDRTE
                                  ::.:::::: :**********:* :*:**: *****:***

HsCDK2          EGVPSTAIREISLLKELNHPNIVKLLDVIHTENKLYLVFEFLHQDLKKFMDASALTGIPL
LmCRK3          EGIPQTALREVSILQEFDHPNIVNLLDVICSDGKLYLVFEYVEADLKKAIEK-QEGGYSG
                **:*.**:**:*:*:*::*****:***** ::.*******::. **** ::     * .

HsCDK2          PLIKSYLFQLLQGLAFCHSHRVLHRDLKPQNLLINTEGAIKLADFGLARAFGVPVRTYTH
LmCRK3          MDLKRLIYQLLDGLYFCHRHRIIHRDLKPANILLTSGNVLKLADFGLARAFQVPMHTYTH
                  :*  ::***:** *** **::****** *:*:.: ..:*********** **::****

HsCDK2          EVVTLWYRAPEILLGCKYYSTAVDIWSLGCIFAEMVTRRALFPGDSEIDQLFRIFRTLGT
LmCRK3          EVVTLWYRAPEILLGEKHYTPAVDMWSVGCIFAELTRRKVLFRGDSEIGQLFEIFQVLGT
                *************** *:*:.***:**:******:. *:.** *****.***.**:.***

HsCDK2          P--DEVVWPGVTSMPDYKPSFPKWARQDFSKVVPPLDEDGRSLLSQMLHYDPNKRISAKA
LmCRK3          PTDTEGSWPGVSRLPDYRDVFPKWTAKRLGQVLPELHPDAIDLLSKMLKYDPRERISAKE
                *   *  ****: :***:  ****: : :.:*:* *. *. .***:**:***.:*****

HsCDK2          ALAHPFFQDVTKPVPHLRL
LmCRK3          ALQHPWFSDLRW-------
                ** **:*.*:
```

Obr. 10: Odlišnosti v sekvencích lidské CDK2 (HsCDK2: P24941) a leishmaniální CRK3 (*L. major*, LmCRK3: O96526) s vyznačením aminokyselin formujících ATP-vazebné místo (červeně). Srovnání sekvencí provedeno s využitím programu ClustalW. Shoda aminokyselin označena „*“, konzervativní substituce označena „**:**“, semi-konzervativní substituce označena „**.**“

4 METODIKA

4.1 Buněčné kultury a analýzy viability

Lidské nádorové buněčné linie byly kultivovány v kultivačním médiu DMEM nebo RPMI-1640 doplněném o fetální sérum (10 – 20 %), glutamin (2 mM), penicilin (100 IU/ml) a streptomycin (100 μg/ml) v CO_2 inkubátoru při teplotě 37 °C. Pro určení antiproliferačních vlastností testovaných látek byly využívány metody Calcein AM a MTT test. V obou případech byly požadované buňky vysazeny do 96-jamkové mikrotitrační desky a následující den ovlivněny požadovanými koncentracemi testovaných látek. Po 72 hodinové inkubaci byl k buňkám přidán roztok Calceinu AM (výsledná koncentrace 1 μg/ml) a po hodině změřena fluorescence (485/538 nm ex/em) pomocí destičkového fluorimetru Fluoroskan Ascent (Labsystems). V případě MTT testu byl k buňkám po skončení inkubace přidán roztok MTT (výsledná koncentrace 1 mg/ml), po 4 hodinách byl vzniklý formazan rozpuštěn v DMSO a stanovena absorbance při 570 nm pomocí destičkového spektrofotometru Infinite M200 PRO (Tecan).

Antileishmaniální účinky byly testovány na druhu *L. turanica* (MRHO/MN/08/BZ18) v životním stádiu promastigotů. Leishmanie byly kultivovány v kultivačním médiu RPMI-1640 v přítomnosti 10% fetálního séra, glutaminu (2 mM) a gentamicinu (80 μg/ml) při teplotě 25 °C. Pro potřeby analýz byly vysazeny do 96-jamkové mikrotitrační desky v počtu 150000 na jamku a následující den ovlivněny testovanými látkami v požadované koncentraci. Po 72 hodinách byl do desek přidán roztok AlamarBlue® (Invitrogen) a po dalších 6 hodinách změřena fluorescence (544/590 nm ex/em) pomocí destičkového fluorimetru Fluoroskan Ascent (Labsystems).

4.2 SDS-PAGE a imunodetekce

Po sklizení buněk ovlivněných testovanými látkami byly vzorky po dobu 25 minut lyzovány v extrakčním pufru (20 mM TRIS pH 7,4, 100 mM NaCl, 2 mM EGTA, 5 mM EDTA, 2 mM NaF, 0,2 % Nonidet P40, 1 mM DTT, 1 mM PMSF, 0,5 μg/ml leupeptin, 2 μg/ml aprotinin) a následně centrifugovány po dobu 25 minut při 14000 rpm a teplotě 4 °C. Bradfordovou metodou (Bradford, 1976) byla změřena

koncentrace proteinů v lyzátu, byl k nim přidán vzorkovací pufr (0,3 M TRIS pH 6,8, 10 % SDS, 50% glycerol, 0,05% bromfenolová modř, 5% 2-merkaptoethanol) a poté byly denaturovány 5 minut při teplotě 95 °C.

Vzorky byly separovány za denaturujících podmínek v polyakrylamidovém gelu v diskontinuálním uspořádání a následně přeneseny na nitrocelulózovou membránu metodou western blotting. Po vyblokování membrán následovala jejich inkubace s primárními a odpovídajícími sekundárními protilátkami značenými křenovou peroxidasou (informace o použitých protilátkách jsou uvedeny v přiložených publikačních výstupech). Vizualizace byla provedena za použití chemiluminiscenčního kitu ECL (Thermo Fisher Scientific).

4.3 Fluorimetrické stanovení aktivity caspasy 3/7 a 9

Nádorové buňky ovlivněné testovanou látkou byly zlyzovány v extrakčním pufru (20 mM TRIS pH 7,4, 100 mM NaCl, 5 mM EDTA, 2 mM EGTA, 2 mM NaF, 0,2% Nonidet P40, inhibitory proteas) a buněčné lyzáty napipetovány do 96-jamkové desky v množství 15 μg celkových proteinů na jamku. K lyzátům byl přidán reakční pufr (pro caspasu 3/7: 25 mM PIPES, 2 mM EGTA, 2 mM $MgCl_2$, 5 mM DTT, pH 7,3; pro caspasu 9: 100 mM HEPES, 0,5 mM EDTA, 20% glycerol, 5 mM DTT, pH 7,5) obsahující 100 μM fluorescenčně značený peptidový substrát Ac-DEVD-AMC (pro caspasu 3/7) nebo Ac-LEHD-AMC (pro caspasu 9). Vzorky byly inkubovány při laboratorní teplotě ve tmě a následně byla změřena fluorescence na destičkovém fluorimetru Fluoroskan Ascent (Labsystems) při 346/442 nm (ex/em).

4.4 Analýza buněčného cyklu

Po sklizení buněk ovlivněných testovanými látkami byly vzorky zafixovány ledově vychlazeným 70% ethanolem, promyty a následně nabarveny propidium jodidem (10 μg/ml). Po půlhodinové inkubaci ve tmě byl analyzován relativní obsah DNA pomocí průtokového cytometru Cell Lab Quanta^{TM} SC MPL (Beckman Coulter). Naměřená data byla následně analyzována pomocí programu Multicycle AV for Windows.

4.5 Analýza replikace DNA

30 minut před ukončením inkubace s testovanými látkami byly buňky naznačeny 10 μM 5-bromo-2´-deoxyuridinem (BrdU) a poté sklizeny a zafixovány 70% ethanolem. Po promytí byly vzorky inkubovány 30 min s 2 M HCl s 0,5% tritonem X-100 a následně promyty 0,1 M $Na_2B_4O_7.10H_2O$ (pH 8,5). Poté byly buňky inkubovány s fluorescenčně značenou protilátkou anti-BrdU-FITC po dobu 1 hodiny ve tmě, promyty, nabarveny propidium jodidem (10 μg/ml) a analyzovány pomocí průtokového cytometru Cell Lab Quanta^{TM} SC MPL (Beckman Coulter).

4.6 Detekce proteinů průtokovou cytometrií

Buňky ovlivněné testovanými látkami byly sklizeny a zafixovány ledově vychlazeným 90% methanolem. Následně byly promyty a 1 hodinu inkubovány buď přímo s fluorescenčně značenou primární protilátkou, nebo s nekonjugovanou primární protilátkou a následně s odpovídající fluorescenčně značenou protilátkou sekundární. Poté byly vzorky opět promyty, nabarveny propidium jodidem (10 μg/ml) a analyzovány na průtokovém cytometru Cell Lab Quanta^{TM} SC MPL (Beckman Coulter).

4.7 Analýza transkripce

Buňky byly kultivovány v médiu obsahujícím [^{14}C] thymidin (62,5 Bq/ml), aby došlo k radioaktivnímu naznačení DNA. Po 36 hodinách bylo toto médium nahrazeno kompletním kultivačním médiem obsahujícím požadovanou koncentraci testované látky na dobu 24 hodin a pro radioaktivní naznačení RNA byl půl hodiny před koncem inkubace do média přidán [^{3}H] uridin (0,75 MBq/ml). Podíl buněk pro izolaci celkové DNA a RNA byl zlyzován v 1% SDS, tepelně zdenaturován a následně doplněn 10% trichloroctovou kyselinou (TCA). Vzorky byly naneseny na filtr, promyty 5% TCA a DNA a RNA byla vyeluována 1M NaOH. Pro izolaci mRNA byl použit Oligotex® Direct mRNA Mini Kit (Qiagen). Radioaktivní signál byl změřen pomocí scintilačního počítače LS6500 (Beckman Coulter).

4.8 *In vivo* experimenty

HCC xenograft: 5 milionů nádorových buněk linie HepG2 nebo PLC/PRF/5 bylo resuspendováno v Ringerově roztoku a subkutánně injikováno do imunodeficientních SCID myší. Po vytvoření tumorů byly myši rozděleny do experimentálních skupin a bylo zahájeno podávání testovaných inhibitorů pomocí intraperitoneálních injekcí v dávkách 5 mg/kg BA-12 a 1 mg/kg BP-14 jedenkrát denně po dobu 17 dní. Kontrolní skupině bylo aplikováno pouze samotné vehikulum.

Diethynitrosaminem-indukovaný hepatom: Ve stáří 14 dní byla samcům myší C57BL/6J intraperitoneálně podána jedna dávka diethylnitrosaminu (25 mg/kg). Po 8 měsících bylo zahájeno podávání experimentálních inhibitorů ve 3 desetidenních cyklech s týdenními pauzami intraperitoneálně v dávkách 5 mg/kg BA-12 a 1 mg/kg BP-14. Kontrolní skupině bylo aplikováno pouze samotné vehikulum.

Po dokončení *in vivo* experimentů byly sesbírány biologické vzorky, které byly následně analyzovány.

In vivo experimenty byly prováděny pod vedením prof. W. Mikulitse na pracovišti Department of Medicine I, Institute of Cancer Research, Medical University of Vienna v souladu s rakouskými právními normami.

5 KOMENTOVANÉ VÝSLEDKY A DISKUSE

5.1 Biologická aktivita nových derivátů roskovitinu

Heterocyklický skelet tvořený 2,6,9-trisubstituovaným purinem je patrně jedním z nejstudovanějších výchozích strukturních motivů CDK inhibitorů vůbec. Nejvýznamnějším zástupcem této skupiny látek je roskovitin, CDK inhibitor první generace a zároveň jeden z nejdetailněji popsaných CDK inhibitorů (McClue *et al.*, 2002; Meijer *et al.*, 2006; Whittaker *et al.*, 2007), který se stal inspirací při navrhování celé řady nových derivátů. Účinnost a biologické vlastnosti jeho strukturních analogů mohou být do značné míry ovlivněny charakterem substituentů v pozicích 2, 6 a 9 purinového skeletu. Tímto přístupem byla připravena celá řada sloučenin, u které došlo ke zlepšení účinnosti. Příkladem může být například olomoucin II (Kryštof *et al.*, 2005), purvalanol A/B (Gray *et al.*, 1998, Chang *et al.*, 1999), CYC065 (Saladino *et al.*, 2015; Skead *et al.*, 2011) a celá řada dalších.

Součástí této práce byla charakterizace biologických účinků série nových roskovitinových derivátů, u které byl kladen důraz jednak na zlepšení CDK-inhibičních a antiproliferačních vlastností, ale rovněž na zdokonalení jejich metabolické stability (**Zatloukal *et al.*, 2013, Příloha I**). Kromě nepříliš vysoké biologické aktivity roskovitinu v porovnání s jinými známými sloučeninami z této kategorie, je jednou z jeho známých nežádoucích vlastností rychlá metabolická přeměna. Jako jeho majoritní metabolit byla identifikována kyselina roskovitinová, která vzniká oxidací primární hydroxyskupiny na postranním řetězci v pozici 2 purinového skeletu a oproti mateřské molekule se vyznačuje výrazným snížením biologické aktivity (Nutley *et al.*, 2005). Proto byly v případě některých nových sloučenin voleny substituenty pro pozici 2 se snahou omezit jejich možnou oxidovatelnost a primární hydroxyskupina byla nahrazena aminoskupinou případně sekundárním nebo terciárním alkoholem. Obdobným přístupem modifikace roskovitinových derivátů se zabývali i Wilson se spolupracovníky, kteří prokázali zlepšení stability a farmakokinetických vlastností záměnou primárního alkoholu v pozici 2 za alkohol sekundární (Wilson *et al.*, 2011).

Dalších strukturních změn bylo u této série dosaženo modifikacemi benzylového kruhu v pozici 6, který je klíčovou částí molekuly ovlivňující selektivitu vůči CDK a biologickou účinnost (De Azevedo *et al.*, 1997). Jako substituent v pozici 9 u všech

sloučenin figuroval isopropyl, který byl v řadě studií prokázán jako optimální varianta pro inhibici CDK (Gray *et al.*, 1998; Chang *et al.*, 1999).

U všech nově připravených sloučenin byla studována CDK-inhibiční aktivita s využitím purifikované rekombinantní CDK2 v komplexu s cyklinem E a dále jejich antiproliferační aktivita na panelu 6 buněčných linií s různým histologickým původem (přehled modifikací a jednotlivé výsledky shrnuje tabulka 1 v příloze I). Z výsledků vyplývá, že v porovnání s roskovitinem u zhruba poloviny sloučenin došlo ke zlepšení jejich cytotoxických vlastností a u většiny nově připravených sloučenin se zvýšila inhibiční aktivita vůči CDK2. Výjimku tvoří sloučeniny s deriváty piperazinu v pozici 2 purinového skeletu, které i přes snížení CDK2-inhibiční aktivity vykazovaly silné cytotoxické účinky patrně díky inhibici jiných molekulárních cílů.

Pro detailnější stanovení biologické účinnosti byl z připravené série vybrán nejúčinnější derivát **3r** (Obr. 11), který oproti roskovitinu dosáhl výrazného zvýšení inhibice CDK2 a zároveň snížení průměrné hodnoty IC_{50} na panelu nádorových linií.

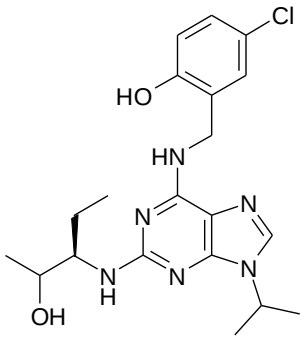

Obr. 11: Chemická struktura látky **3r**.

Jeho vlastnosti byly testovány na nádorových buňkách odvozených od karcinomu tlustého střeva HCT-116 a od chronické myeloidní leukémie K562. Díky inhibici CDK zapojených v regulaci buněčného cyklu došlo působením inhibitoru **3r** v nízkých mikromolárních koncentracích u obou linií k zablokování buněčného cyklu ve fázích S a G2/M a zároveň k zablokování replikace DNA (Příloha I, Obr. 1). Inhibice transkripčních CDK7 a CDK9 odhalená pomocí kinasových inhibičních testů byla potvrzena studiem hladin fosforylovaných forem RNA polymerasy II na Ser2 a Ser5, které jsou substrátem těchto kinas (Příloha I, Obr. 2A, B). V souladu s dříve publikovanými výsledky (Ljungman *et* Paulsen, 2001) došlo v důsledku zablokování transkripce inhibitorem **3r** rovněž k poklesu hladiny negativního regulátoru p53,

proteinu MDM-2, což vedlo k výrazné akumulaci p53 i p53-regulovaného proteinu p21 (Příloha I, Obr. 2C).

Souvislost mezi cytotoxicitou testovaných látek a mechanismem buněčné smrti byla studována pomocí analýzy proteinových apoptotických markerů. U obou testovaných linií došlo po ovlivnění inhibitorem **3r** díky inhibici transkripčních CDK, v souladu s dříve publikovanými výsledky (Gojo *et al.*, 2002; Chen *et al.*, 2009; MacCallum *et al.*, 2005), k výraznému poklesu hladiny antiapoptického proteinu Mcl-1 a zároveň k výraznému nárůstu štěpného fragmentu proteinu PARP-1, který je substrátem hlavního efektoru apoptotické kaskády, proteolytického enzymu caspasy 3, a je tedy hojně využívaným markerem apoptózy. Proapoptotické účinky **3r** byly ověřeny za pomoci fluorescenčně značeného peptidového substrátu caspasy 3/7 (Příloha I, Obr. 3).

Ačkoli strukturní změny v molekulách nově připravených roskovitinových derivátů vedly ke zlepšení jejich biologických a patrně i farmakokinetických vlastností, jejich účinnost stále nedosahovala hodnot klinicky zkoušených CDK inhibitorů. Proto bylo při navrhování a přípravě další knihovny CDK inhibitorů využito poznatků o významném zesílení biologické účinnosti záměnou benzylového substituentu v pozici 6 za biarylový systém (Bettayeb *et al.*, 2008; Oumata *et al.*, 2008; Trova *et al.*, 2009). Kromě extenze benzylového kruhu v pozici 6 se nové roskovitinové deriváty (**Gucký *et al.*, 2013, Příloha II)** vyznačují rovněž záměnou isopropylu v pozici 9 za cyklopentyl a v pozici 2 u většiny připravených molekul figuruje 4-aminocyklohexylamin. Tato kombinace substituentů u řady látek výrazně zlepšila CDK2-inhibiční i cytotoxické vlastnosti a v otázce účinnosti tak překonala známé strukturně příbuzné sloučeniny CR8 (Bettayeb *et al.*, 2008) a H717 (Dreyer *et al.*, 2001) (Obr. 12; Příloha II, Tab. 1). Pro potvrzení cytotoxického působení připravených inhibitorů byla melanomová buněčná linie G361 ovlivněna připravenými deriváty o koncentraci 300 nM na dobu 24 hodin. Následné analýzy (Příloha II, Obr. 2A, B) odhalily, že v buňkách došlo působením nejúčinnějších derivátů k aktivaci caspasy 3, 7 a 9 a zároveň k výrazným změnám v hladinách apoptotických markerů (detekce štěpného fragmentu PARP-1 a snížení exprese antiapoptotického proteinu Mcl-1), což potvrzuje jejich proapoptotické působení. Jako nejúčinnější molekula připravené série byla i v těchto experimentech potvrzena látka **6b** kombinující cyklopentyl v pozici 9 purinového skeletu s 4-aminocyklohexylaminovou skupinou v pozici 2 a (2-hydroxyfenyl)-pyridin-3-ylmethylamin v pozici 6 (Obr. 12C), která dosahovala CDK-inhibiční i antiproliferační

aktivity na řadě nádorových linií již v nízkých nanomolárních koncentracích a svou účinností se tak vyrovnala i klinicky zkoušenému dinaciclibu (Parry *et al.*, 2010).

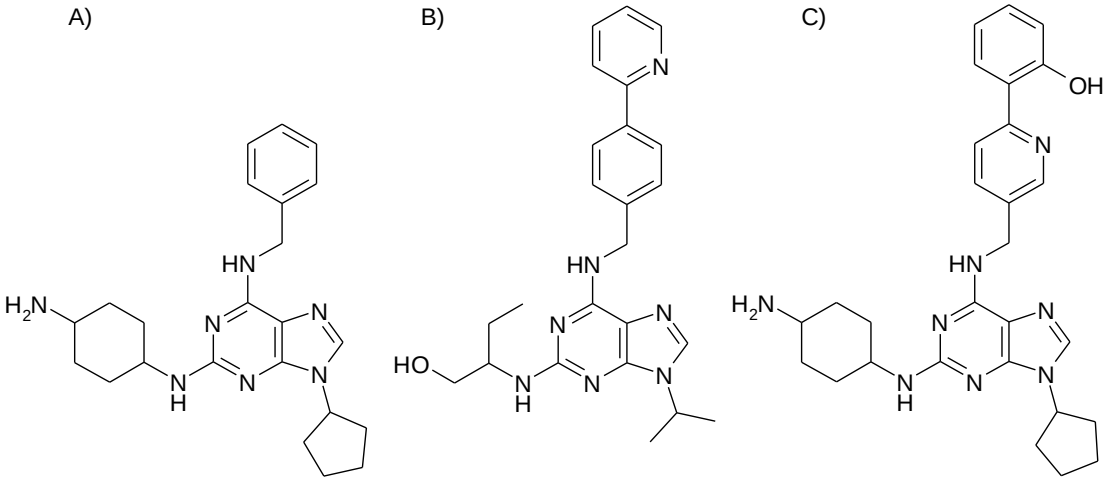

Obr. 12: Chemická struktura A) H717, B) CR8 a C) námi studované **6b**.

Při detailnějším studiu mechanismu působení **6b** bylo zjištěno, že kromě aktivace apoptózy, ke které dochází u buněčné linie G361 působením 80 nM koncentrace, která indukuje aktivaci caspas, štěpení PARP-1 (Příloha II, Obr. 4A) a nárůst populace sub-G1, dochází působením **6b** i k zablokování replikace DNA.

Pro studium kinetiky buněčných procesů byly buňky G361 ovlivněny látkou **6b** v koncentraci 640 nM na dobu 1-24 hodin a bylo zjištěno, že samotné aktivaci apoptózy předchází defosforylace substrátů CDK. To naznačuje, že k indukci apoptózy by mohlo docházet vlivem transkripční represe. Pokles fosforylace Ser2 a Ser5 RNA polymerasy II byl patrný již po 1 hodině od ovlivnění, což potvrzuje inhibici CDK7 a CDK9 a s tím související zablokování transkripce, v jejímž důsledku poté došlo k poklesu hladiny antiapoptotického proteinu Mcl-1 a k aktivaci apoptotické kaskády (Příloha II, Obr. 4B).

Nejaktivnější deriváty této série jsou zároveň nejúčinnějšími známými CDK inhibitory s purinovým skeletem a vzhledem k výrazným protinádorovým účinkům mají velký terapeutický potenciál.

5.2 *In vitro* a *in vivo* aktivita inhibitorů CDK v modelech HCC

Vzhledem ke slibným protinádorovým účinkům prokázaným při studiu biarylových derivátů roskovitinu (**Gucký *et al.*, 2013, příloha II**) diskutovaných v předchozí kapitole byly tyto látky detailně studovány i v dalších experimentálních modelech. Z důvodu absence cílených terapeutik pro léčbu maligních onemocnění jater a zároveň nedostatečné znalosti o účincích CDK inhibitorů na nádorové buňky odvozené od lidského hepatomu, byly tyto experimenty voleny právě se zaměřením na HCC. Některé výsledky experimentů byly předloženy v patentové přihlášce (Gucký *et al.*, 2014) a na jejich základě byly vybrány dva inhibitory pro detailní studii v modelech HCC (**Haider *et al.*, 2013, příloha III**).

V první fázi byla tedy ověřena antiproliferační aktivita dvou sloučenin označených jako BA-12 a BP-14 (Obr. 13) *in vitro* na lidských nádorových liniích odvozených od HCC.

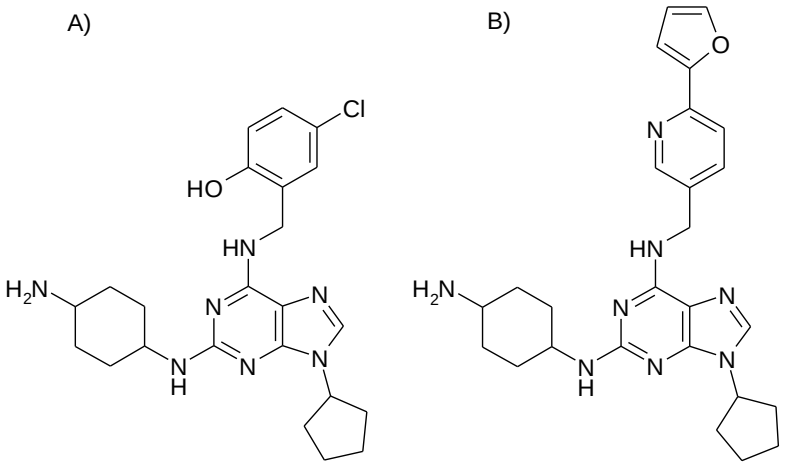

Obr. 13.: Chemická struktura látky A) BA-12 a B) BP-14.

Působením obou látek došlo k inhibici proliferace HCC linií již v submikromolárních koncentracích a na buněčné úrovni byla rovněž prokázána schopnost těchto látek indukovat apoptózu a blokovat buněčný cyklus. Velmi pozitivní bylo rovněž zjištění, že ačkoli u nádorových buněk HepG2 a PLC/PRF/5 látky vykazovaly silné proapoptotické účinky (detekce štěpného fragmentu proteinu PARP-1 a aktivace caspasy 7) již v nízkých mikromolárních koncentracích, stejné dávky neovlivnily viabilitu primárních lidských hepatocytů (Příloha III, Obr. 3) a i hodnoty IC_{50} pro obě testované látky byly v případě těchto normálních buněk 40x resp. 140x

vyšší (hodnota IC_{50} pro látku BA-12 byla 26 μM a pro látku BP-14 20 μM). Dlouhodobá kultivace HCC buněk v přítomnosti nízkých koncentrací BA-12 a BP-14 navíc neovlivnila citlivost buněk k těmto látkám a neindukovala u nich rozvoj chemorezistence (Příloha III, Tab. 1).

Vzhledem ke slibným výsledkům dosaženým *in vitro* byly látky dále testovány ve dvou nezávislých modelech HCC *in vivo*. První experimenty byly provedeny na imunodeficientních SCID myších s xenografty lidských HCC buněk HepG2 a PLC/PRF/5. Intraperitoneální podávání látek BA-12 v dávce 5 mg/kg a BP-14 v dávce 1 mg/kg výrazně snížilo růst tumorů v porovnání s kontrolní skupinou a s využitím imunohistochemických metod byla na tkáňových řezech xenograftů prokázána snížená proliferace nádorových buněk a indukce apoptózy (Příloha III, Obr. 4). V dalším experimentálním modelu byla ověřována schopnost testovaných inhibitorů ovlivnit chemicky-indukovaný karcinom jater. Experiment byl zahájen intraperitoneální injekcí diethylnitrosaminu v dávce 25 mg/kg myším ve stáří 14 dnů, čímž byla specificky indukována hepatokarcinogeneze (Heindryckx *et al.*, 2009). Po 8 měsících bylo započato podávání testovaných látek pomocí intraperitoneálních injekcí ve třech desetidenních cyklech se sedmidenními pauzami v dávkách 5 mg/kg pro BA-12 a 1 mg/kg pro BP-14. Působením obou látek došlo k signifikantnímu snížení velikosti nádorových ložisek na povrchu jater v porovnání s kontrolní skupinou (Příloha III, Obr. 5).

Provedené experimenty potvrdily výraznou protinádorovou účinnost testovaných látek v modelech HCC *in vitro* a *in vivo* a naznačily terapeutický potenciál CDK inhibitorů pro léčbu tohoto maligního onemocnění.

5.3 Biologická aktivita pyrazolo[4,3-*d*]pyrimidinových inhibitorů CDK

Kromě jednotlivých substituentů může účinnost CDK inhibitorů ovlivňovat podstatně i sám heterocyklický skelet, kdy cílenou modifikací počtu a/nebo umístění atomů dusíku může dojít k významným změnám jejich vlastností jako je metabolická aktivita, biologická stabilita a dostupnost, farmakokinetika a další (Lima *et* Bareiro, 2005; Popowycz *et al.*, 2009). Tato tzv. bioisosterická strategie byla využita i při hledání nových derivátů roskovitinu (Jorda *et al.*, 2012), kdy byly nalezeny látky dosahující oproti výchozí molekule vyšší účinnosti. Jedná se zejména o látky s pyrazolo[1,5-*a*]-1,3,5-triazinovým (Popowycz *et al.*, 2009), pyrazolo[1,5-*a*]pyrimidinovým (Paruch *et al.*, 2010) a pyrazolo[4,3-*d*]pyrimidinovým (Jorda *et al.*, 2011) skeletem (Obr. 14). Právě posledně jmenovaný heterocyklický skelet se stal inspirací pro vytvoření nové série pyrazolo[4,3-*d*]pyrimidinových sloučenin (**Řezníčková *et al.*, 2015, příloha IV**).

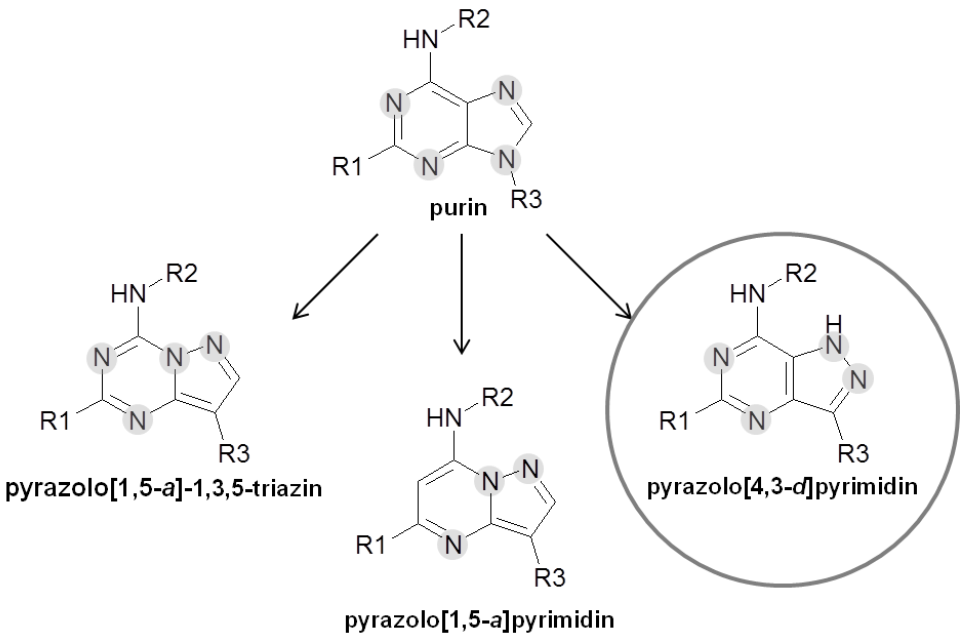

Obr. 14: Obecná struktura vybraných heterocyklických skeletů CDK inhibitorů.

Všechny nově připravené sloučeniny sdílely isopropyl v pozici 3, který byl prokázán jako optimální substituce u purinových CDK inhibitorů (Gray *et al.*, 1998; Chang *et al.*, 1999) a rovněž substituenty v pozicích 5 a 7 byly voleny s ohledem na známé vlastnosti purinových analogů. V pozici 7 heterocyklického skeletu se konkrétně jednalo o benzylaminovou skupinu, pozice 5 pak byla modifikována nejčastěji alkyl- případně cykloalkyl- aminy. Pro všechny připravené sloučeniny byla

stanovena CDK-inhibiční aktivita s využitím rekombinantní CDK2 v komplexu s cyklinem E a antiproliferační aktivita na nádorových buněčných liniích odvozených od adenokarcinomu prsu MCF-7 a chronické myeloidní leukémie K562. Výsledky a přehled strukturních modifikací shrnuje tabulka 1 přílohy IV. Ze všech 7-benzylamino derivátů dosahovaly nejmenší účinnosti látky s lineárním postranním řetězcem v pozici 5 (**1b-d, 1f**), jejich záměnou za rozvětvený alkyl (**1e, 1g, 1i**) došlo ke zlepšení zejména CDK-inhibiční účinnosti a nejlepších antiproliferačních účinků dosahovaly látky nesoucí v pozici 5 2-aminocyklohexylamin (**1k, 1l**). V podstatě stejný trend byl pozorován i v případě skupiny sloučenin nesoucích 2-aminobenzylamin v pozici 7. Protože bylo u purinových inhibitorů dříve opakovaně potvrzeno, že lepší účinnosti dosahují *R*-isomery (2-hydroxypropyl)aminu a [1-(hydroxymethyl)propyl]aminu v pozici 5 (**Zatloukal *et al.*, 2013, příloha I**; Bach *et al.*, 2005; Oumata *et al.*, 2008), byly i v případě pyrazolo[4,3-*d*]pyrimidinové série připraveny obě opticky aktivní isoformy (**2g** a **2h**, **2i** a **2j**). Ačkoli všechny tyto sloučeniny patřily k nejúčinnějším látkam této série, účinnost *R*-isomerů v porovnání s *S*-isomery byla dle předpokladů vždy lepší (Příloha IV, Tab. 1). Mechanismus působení nejúčinnějšího CDK inhibitoru této série, látky **2i** (Obr. 15), byl studován detailněji.

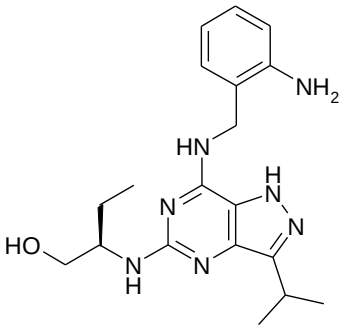

Obr. 15: Chemická struktura látky **2i.**

Testování antiproliferačního působení látky **2i** bylo oproti prvotnímu screeningu rozšířeno o dalších 9 nádorových linií různého histologického původu (Příloha IV, Tab. 2). Stanovená průměrná hodnota IC_{50} = 5 μM výrazně převyšuje účinnost roskovitinu, jehož hodnota IC_{50} se v závislosti na nádorové linii pohybuje v rozsahu 15 až 28 μM (Kryštof *et al.*, 2005; McClue *et al.*, 2002; Meijer *et al.*, 2006). Ačkoli antiproliferační účinky byly zaznamenány i u normálních lidských buněk linie HMEC-1 (IC_{50} = 5,4 μM), viabilita těchto buněk nebyla zasažena a ani v testech

na neproliferujících lidských fibroblastech nebyla zaznamenána redukce viability až do koncentrace 100 μM.

Vzhledem ke strukturní podobnosti s roskovitinem byla účinnost látky **2i** testována na panelu CDK a dalších kinas, kdy bylo zjištěno, že látka **2i** účinně inhibuje v submikromolárních koncentracích CDK2 a CDK5 (IC_{50} = 70 resp. 260 nM) a v mikromolárních koncentracích CDK9 a CDK1 (IC_{50} = 1,91 resp. 3,13 μM). Jedinou další inhibovanou kinasou z celkem 97 testovaných byla Aurora A (IC_{50} = 0,40 μM) (Příloha IV, Tab. 3). Účinnost zejména vůči CDK2 velmi výrazně převýšila aktivitu roskovitinu. Rozdíl v účinnosti byl prokázán pomocí metod molekulárního modelování, které potvrdilo, že i přes velkou strukturní podobnost obou látek, je vazba **2i** do aktivního místa kinasy výrazně silnější.

Abychom prokázali kinasovou inhibici i na buněčné úrovni, zaměřili jsme se na studium fosforylačního statusu substrátů CDK2 a Aurory A. Jako substrát CDK2 byl sledován Ser807/811 proteinu Rb, pro studium inhibice Aurory A pak Thr210 Polo-like kinasy 1 (Plk1) a Ser10 histonu H3 (Crosio *et al.*, 2002; Macůrek *et al.*, 2008; Seki *et al.*, 2008). Buňky nádorové linie HCT-116 byly ovlivněny zvyšujícími se koncentracemi látky **2i**, které způsobily výraznou redukci fosforylace studovaných kinasových substrátů (Příloha IV, Obr. 2).

Z důvodu prokázané inhibice kinas zapojených do regulace buněčného cyklu, byl dopad **2i** na tento proces studován pomocí vybraných cytometrických technik (Příloha IV, Obr. 3). Analýzy prokázaly u buněk HCT-116 po ovlivnění **2i** redukci populace buněk v G1 fázi a jejich přesun do pozdních fází buněčného cyklu (G2/M), což souvisí s již dříve prokázanou inhibicí CDK2, CDK1 a aurory A (Emanuel *et al.*, 2005; Payton *et al.*, 2006; Seamon *et al.*, 2006; Shapiro, 2006).

Zajímavé ovšem bylo zjištění, že proapoptotický účinek 10 μM koncentrace **2i** prokázaný nárůstem populace buněk v sub-G1 fázi buněčného cyklu, zvýšenou aktivitou caspasy 3 a změnami v hladinách proteinových apoptotických markerů, působením vyšších koncentrací **2i** (40 μM) téměř vymizel a výrazně převažoval cytostatický účinek látky **2i** nad cytotoxickým (Příloha IV, Obr. 3 a 4). To může být patrně důsledkem odlišného inhibičního profilu cílových kinas při působení různých koncentrací látky **2i**.

Vzhledem k potvrzené úloze CDK5 v angiogenezi (Liebl *et al.*, 2010) byl dále studován vliv látky **2i** na tento proces, který je esenciální pro progresi nádorového

bujení (Hanahan *et* Weinberg, 2011). Experimenty potvrdily vliv mikromolárních koncentrací látky **2i** na inhibici migrace endoteliálních buněk i tvorby tubulů, dvou základních kroků angiogeneze (Příloha IV, Obr. 5 a 6).

Kombinovaný mechanismus účinku látky **2i**, tedy schopnost blokovat proliferaci nádorových buněk, indukovat u nich apoptózu a zároveň blokovat proces angiogeneze, má určitý terapeutický potenciál. Proto byly nedávno připraveny další deriváty pyrazolo[4,3-*d*]pyrimidinových inhibitorů CDK, u kterých bylo prokázáno další zlepšení jejich biologických vlastností (Vymětalová *et al.*, 2016).

5.4 Antileishmaniální aktivita trisubstituovaných purinů

Pro skupinu 2,6,9-trisubstitovaných purinových sloučenin, která vykazovala aktivitu vůči lidské CDK2, avšak její antiproliferační účinnost na lidské nádorové linie byla poměrně nízká, byla zvažována možnost uplatnění v jiném medicínském odvětví. S ohledem na nízkou cytotoxicitu těchto látek vůči lidským buňkám byla testována jejich potenciální antileishmaniální aktivita (**Řezníčková *et al.*, 2015, příloha V**).

Zvolené sloučeniny se lišily substituenty v pozicích 2 a 6 purinového skeletu. Zatímco pozice 2 byla modifikována širokým spektrem substituentů od jednoduchých alifatických řetězců po rozvětvené a cyklické substituenty, většina látek nesla v pozici 6 substituovaný benzylamin a všechny látky sdílely v pozici 9 isopropyl (Příloha V, Schéma 1). Jejich aktivita byla testována jednak vůči rekombinantní CRK3, která je nezbytná pro progresi buněčným cyklem a proliferaci leishmanií (Hassan *et al.*, 2001), a dále byl studován vliv těchto látek na viabilitu promastigotů druhu *Leishmania turanica* a zároveň neproliferujících lidských fibroblastů.

Nejúčinnější inhibitory CRK3 byly modifikovány v pozici 2 rozvětveným [1-(hydroxymethyl)propyl]aminem (**2i**, **5i**, **6i**, **9i**, **10i**, **11i**, **15i**, **16i** a **17i**) a většina nesla na 6-benzylaminu hydroxyskupinu v ortho poloze (**2i**, **5i**, **6i**, **9i**, **10i**, **11i**). Při koncentraci 30 μM tyto látky redukovaly enzymatickou aktivitu CRK3 na méně než 5 % v porovnání s kontrolou a byly pro ně stanoveny hodnoty IC_{50}, které se pohybovaly v rozsahu od 0,1 μM (**16i**) do 1,6 μM (**9i**) (Příloha V, Tab. 1).

Zatímco viabilita neproliferujících lidských fibroblastů při použití 30 μM koncentrace ani u jedné z testovaných látek neklesla pod 75 %, řada sloučenin (**2i**, **9i**, **10i**, **11i**, **19i**) při stejné koncentraci výrazně ovlivňovala viabilitu promastigotů druhu *L. turanica*. Pro nejúčinnější látky byla studována závislost mezi jejich koncentrací a viabilitou leishmanií a stanoveny hodnoty IC_{50} jednak na promastigotech *L. turanica*, ale také na lidských parazitech, konkrétně promastigotech *L. major*, která je původcem kožní formy onemocnění a promatigotech *L. donovani*, která je zodpovědná za rozvoj viscerální formy leishmaniózy (Příloha V, Tab. 1). Nejlepší výsledky z testované série vykazovala látka s označením **10i** (Obr. 16), která účinně redukovala viabilitu lidských parazitů *L. major* a *L. donovani* již v nízkých mikromolárních koncentracích (hodnoty IC_{50} = 2,3 μM resp. 2,2 μM). Vzhledem k její výrazné účinnosti vůči CRK3 (IC_{50} = 0,162 μM) byly pomocí metod molekulárního modelování popsány hlavní interakce

mezi **10i** a aktivním místem CRK3 a potvrzen pozitivní vliv přítomnosti *o*-hydroxyskupiny benzylaminu na stabilizaci celého komplexu (Příloha V, Obr. 1).

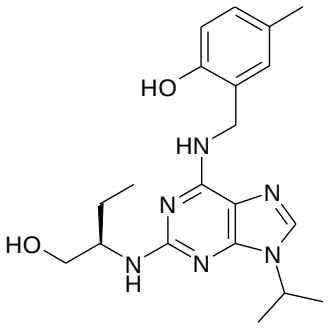

Obr. 16: Chemická struktura látky **10i**.

Vzhledem k nízké cytotoxicitě vůči lidským buňkám by se tyto submikromolární inhibitory CRK3, u kterých byla zároveň prokázána i schopnost redukovat viabilitu tří různých druhů leishmanií, mohly stát výchozím strukturním motivem pro vývoj nových antileishmaniálních sloučenin.

6 ZÁVĚR

Vzhledem k zapojení CDK do centrálních buněčných procesů stojí tyto enzymy v centru zájmu mnoha vědeckých týmů jako zajímavé terapeutické cíle pro léčbu celé řady lidských onemocnění. Jedním z nejstudovanějších strukturních motivů známých CDK inhibitorů je 2,6,9-trisubstituovaný purin s nejznámnějším zástupcem roskovitinem, který patří k nejdetailněji popsaným CDK inhibitorům. Roskovitin vstoupil dokonce do klinického testování, kde však bohužel vzhledem k jeho nižší účinnosti selhal. Podnítil však navazující experimenty, které vedly k vylepšení jeho vlastností.

První část této disertační práce byla věnována charakterizaci biologických účinků nových inhibitorů CDK, které byly připraveny cílenou modifikací substituovatelných pozic 2, 6 a 9 purinového skeletu za účelem zlepšení jejich biologických vlastností v porovnání s roskovitinem. Výsledkem byly dvě nové série roskovitinových derivátů, u kterých došlo k výraznému zlepšení CDK-inhibičních a antiproliferačních vlastností a nejúčinnější deriváty série kombinující biarylový systém v pozici 6 purinového skeletu s cyklopentylem v pozici 9 se dokonce zařadily k nejúčinnějším známým CDK inhibitorům na bázi purinů. Vzhledem k jejich výraznému protinádorovému působení prokázanému v řadě experimentů byly dva vybrané inhibitory testovány v komplexních modelech hepatocelulárního karcinomu, kde byla jejich aktivita potvrzena na úrovni *in vitro* i *in vivo*. Získané výsledky naznačily možný terapeutický potenciál CDK inhibitorů pro léčbu tohoto agresivního typu maligního onemocnění.

Další část práce byla poté věnována charakterizaci knihovny látek příbuzných roskovitinu, která byla vytvořena na základě bioisosterické strategie a vyznačuje se pyrazolo[4,3-*d*]pyrimidinovým skeletem. U této série látek sice došlo oproti výchozímu roskovitinu ke zlepšení CDK-inhibiční i antiproliferační aktivity, ale přesto nedosahovala účinnosti 6-biarylových purinů. Benefitem této práce však bylo odhalení sloučeniny **2i** se zajímavým inhibičním kinasovým profilem s preferencí vůči CDK2, CDK5 a Auroře A. Tato látka se vyznačuje kombinovaným mechanismem protinádorového působení spojujícím antiproliferační a proapoptotické účinky s inhibicí angiogeneze, což může mít určitý terapeutický význam. Tato série látek se tudíž stala inspirací pro přípravu dalších pyrazolo[4,3-*d*]pyrimidinových sloučenin.

Ačkoli je většina známých inhibitorů CDK studována v souvislosti s možnou protinádorovou terapií, potenciál jejich možného použití je daleko širší. Z toho důvodu byla poslední část této disertační práce věnována alternativnímu použití známých CDK inhibitorů s nízkou cytotoxicitou vůči lidským buňkám jako potenciálních antiparazitik. U řady sloučenin byla prokázána inhibice leishmaniálního homologu lidských CDK, enzymu CRK3, již v submikromolárních koncentracích a zároveň redukce viability leishmanií působením nízkých mikromolárních koncentrací těchto látek. Vzhledem k tomu, že tyto látky výrazněji neovlivnily viabilitu lidských fibroblastů, lze uvažovat o možném použití těchto látek jako výchozího strukturního motivu při navrhování nových sloučenin se snahou o dosažení lepších biologických účinků.

7 SEZNAM CITOVANÉ LITERATURY

Abate AA, Pentimalli F, Esposito L, Giordano A (2013) ATP-noncompetitive CDK inhibitors for cancer therapy: an overview. Expert Opin Investig Drugs. 22, 895-906.

Abdullah C, Wang X, Becker D (2011) Expression analysis and molecular targeting of cyclin-dependent kinases in advanced melanoma. Cell Cycle. 10, 977-988.

Abrisqueta P, Crespo M, Bosch F (2011) Personalizing treatment for chronic lymphocytic leukemia. Expert Rev Hematol. 4, 27-35.

Alagpulinsa DA, Ayyadevara S, Yaccoby S, Shmookler Reis RJ (2016) A Cyclin-Dependent Kinase Inhibitor, Dinaciclib, Impairs Homologous Recombination and Sensitizes Multiple Myeloma Cells to PARP Inhibition. Mol Cancer Ther. 15, 241-50.

Albanese C, Alzani R, Amboldi N, Avanzi N, Ballinari D, Brasca MG, Festuccia C, Fiorentini F, Locatelli G, Pastori W, Patton V, Roletto F, Colotta F, Galvani A, Isacchi A, Moll J, Pesenti E, Mercurio C, Ciomei M (2010) Dual targeting of CDK and tropomyosin receptor kinase families by the oral inhibitor PHA-848125, an agent with broad-spectrum antitumor efficacy. Mol Cancer Ther. 9, 2243-2254.

Albert TK, Rigault C, Eickhoff J, Baumgart K, Antrecht C, Klebl B, Mittler G, Meisterernst M (2014) Characterization of molecular and cellular functions of the cyclin-dependent kinase CDK9 using a novel specific inhibitor. Br J Pharmacol. 171, 55-68.

Ali S, Heathcote DA, Kroll SH, Jogalekar AS, Scheiper B, Patel H, Brackow J, Siwicka A, Fuchter MJ, Periyasamy M, Tolhurst RS, Kanneganti SK, Snyder JP, Liotta DC, Aboagye EO, Barrett AG, Coombes RC (2009) The development of a selective cyclin-dependent kinase inhibitor that shows antitumor activity. Cancer Res. 69, 6208-6215.

Anscombe E, Meschini E, Mora-Vidal R, Martin MP, Staunton D, Geitmann M, Danielson UH, Stanley WA, Wang LZ, Reuillon T, Golding BT, Cano C, Newell DR, Noble ME, Wedge SR, Endicott JA, Griffin RJ (2015) Identification and Characterization of an Irreversible Inhibitor of CDK2. Chem Biol. 22, 1159-1164.

Arif A (2012) Extraneuronal activities and regulatory mechanisms of the atypical cyclin-dependent kinase Cdk5. Biochem Pharmacol. 84, 985-993.

Asghar U, Witkiewicz AK, Turner NC, Knudsen ES (2015) The history and future of targeting cyclin-dependent kinases in cancer therapy. Nat Rev Drug Discov. 14, 130-146.

Azechi H, Nishida N, Fukuda Y, Nishimura T, Minata M, Katsuma H, Kuno M, Ito T, Komeda T, Kita R, Takahashi R, Nakao K (2001) Disruption of the p16/cyclin D1/retinoblastoma protein pathway in the majority of human hepatocellular carcinomas. Oncology. 60, 346-354.

Bach S, Knockaert M, Reinhardt J, Lozach O, Schmitt S, Baratte B, Koken M, Coburn SP, Tang L, Jiang T, Liang DC, Galons H, Dierick JF, Pinna LA, Meggio F, Totzke F, Schächtele C, Lerman AS, Carnero A, Wan Y, Gray N, Meijer L (2005) Roscovitine targets, protein kinases and pyridoxal kinase. J Biol Chem. 280, 31208-31219.

Bednarek K, Kiwerska K, Szaumkessel M, Bodnar M, Kostrzewska-Poczekaj M, Marszalek A, Janiszewska J, Bartochowska A, Jackowska J, Wierzbicka M, Grenman R, Szyfter K, Giefing M, Jarmuz-Szymczak M (2016) Recurrent CDK1 overexpression in laryngeal squamous cell carcinoma. Tumour Biol. v tisku: DOI 10.1007/s13277-016-4991-4.

Benhenda S, Cougot D, Neuveut C, Buendia MA (2009) Liver cell transformation in chronic HBV infection. Viruses. 1, 630-646.

Bettayeb K, Oumata N, Echalier A, Ferandin Y, Endicott JA, Galons H, Meijer L (2008) CR8, a potent and selective, roscovitine-derived inhibitor of cyclin-dependent kinases. Oncogene. 27, 5797-5807.

Betzi S, Alam R, Martin M, Lubbers DJ, Han H, Jakkaraj SR, Georg GI, Schönbrunn E (2011) Discovery of a potential allosteric ligand binding site in CDK2. ACS Chem Biol. 6, 492-501.

Bhatnagar AS (2007) The discovery and mechanism of action of letrozole. Breast Cancer Res Treat. 105 supplement 1, 7-17.

Bible KC, Peethambaram PP, Oberg AL, Maples W, Groteluschen DL, Boente M, Burton JK, Gomez Dahl LC, Tibodeau JD, Isham CR, Maguire JL, Shridhar V, Kukla AK, Voll KJ, Mauer MJ, Colevas AD, Wright J, Doyle LA, Erlichman C (2012) A phase 2 trial of flavopiridol (Alvocidib) and cisplatin in platin-resistant ovarian and primary peritoneal carcinoma: MC0261. Gynecol Oncol. 127, 55-62.

Bisht S, Nolting J, Schütte U, Haarmann J, Jain P, Shah D, Brossart P, Flaherty P, Feldmann G (2015) Cyclin-Dependent Kinase 5 (CDK5) Controls Melanoma Cell

Motility, Invasiveness, and Metastatic Spread-Identification of a Promising Novel therapeutic target. Transl Oncol. 8, 295-307.

Bisi JE, White HS, Sorrentino JA, Roberts RP, Strum JC (2015) Pre-clinical characterization of G1T28-1, a novel CDK 4/6 inhibitor for protection of bone marrow from cytotoxic chemotherapies [abstract]. AACR 106th Annual Meeting 2015 Apr 18-22, Philadelphia, PA.

Bisteau X, Caldez MJ, Kaldis P (2014) The Complex Relationship between Liver Cancer and the Cell Cycle: A Story of Multiple Regulations. Cancers. 13, 79-111.

Blagosklonny MV (2005) Flavopiridol, an inhibitor of transcription: implications, problems and solutions. Cell Cycle. 3, 1537-1542.

Blachly JS, Byrd JC (2013) Emerging drug profile: cyclin-dependent kinase inhibitors. Leuk Lymphoma. 54, 2133-2143.

Blazek D, Kohoutek J, Bartholomeeusen K, Johansen E, Hulinkova P, Luo Z, Cimermancic P, Ule J, Peterlin BM (2011) The Cyclin K/Cdk12 complex maintains genomic stability via regulation of expression of DNA damage response genes. Genes Dev. 25, 2158-2172.

Bolin C, Boudra MT, Fernet M, Vaslin L, Pennaneach V, Zaremba T, Biard D, Cordelières FP, Favaudon V, Mégnin-Chanet F, Hall J (2012) The impact of cyclin-dependent kinase 5 depletion on poly(ADP-ribose) polymerase activity and responses to radiation. Cell Mol Life Sci. 69, 951-962.

Bose P, Perkins EB, Honeycut C, Wellons MD, Stefan T, Jacobberger JW, Kontopodis E, Beumer JH, Egorin MJ, Imamura CK, Douglas Figg W Sr, Karp JE, Koc ON, Cooper BW, Luger SM, Colevas AD, Roberts JD, Grant S (2012) Phase I trial of the combination of flavopiridol and imatinib mesylate in patients with Bcr-Abl+ hematological malignancies. Cancer Chemother Pharmacol. 69, 1657-1667.

Bose P, Simmons GL, Grant S (2013) Cyclin-dependent kinase inhibitor therapy for hematologic malignancies. Expert Opin Investig Drugs. 22,723-738.

Bösken CA, Farnung L, Hintermair C, Merzel Schachter M, Vogel-Bachmayr K, Blazek D, Anand K, Fisher RP, Eick D, Geyer M (2014) The structure and substrate specificity of human Cdk12/Cyclin K. Nat Commun. 5, 3505.

Bradford MM (1976) A rapid and sensitive method for the quantitation of microgram quantities of protein utilizing the principle of protein-dye binding. Anal Biochem. 72, 248-54.

Brasca MG, Amboldi N, Ballinari D, Cameron A, Casale E, Cervi G, Colombo M, Colotta F, Croci V, D'Alessio R, Fiorentini F, Isacchi A, Mercurio C, Moretti W, Panzeri A, Pastori W, Pevarello P, Quartieri F, Roletto F, Traquandi G, Vianello P, Vulpetti A, Ciomei M (2009) Identification of N,1,4,4-tetramethyl-8-{[4-(4-methylpiperazin-1-yl)phenyl]amino}-4,5-dihydro-1H-pyrazolo[4,3-h]quinazoline-3-carboxamide (PHA-848125), a potent, orally available cyclin dependent kinase inhibitor. J Med Chem. 52, 5152-5163.

Bresnahan WA, Boldogh I, Chi P, Thompson EA, Albrecht T (1997) Inhibition of cellular Cdk2 activity blocks human cytomegalovirus replication. Virology. 231, 239-247.

Bupathi M, Kaseb A, Meric-Bernstam F, Naing A (2015) Hepatocellular carcinoma: Where there is unmet need. Mol Oncol. 9, 1501-1509.

Byrd JC, Lin TS, Dalton JT, Wu D, Phelps MA, Fischer B, Moran M, Blum KA, Rovin B, Brooker-McEldowney M, Broering S, Schaaf LJ, Johnson AJ, Lucas DM, Heerema NA, Lozanski G, Young DC, Suarez JR, Colevas AD, Grever MR (2007) Flavopiridol administered using a pharmacologically derived schedule is associated with marked clinical efficacy in refractory, genetically high-risk chronic lymphocytic leukemia. Blood. 109, 399-404.

Caenepeel S, Charydczak G, Sudarsanam S, Hunter T, Manning G (2004) The mouse kinome: discovery and comparative genomics of all mouse protein kinases. Proc Natl Acad Sci U S A. 101, 11707-11712.

Canavese M, Santo L, Raje N (2012) Cyclin dependent kinases in cancer: potential for therapeutic intervention. Cancer Biol Ther. 13, 451-457.

Carnero A (2002) Targeting the cell cycle for cancer therapy. Br J Cancer. 87, 129-133.

Cervello M, Bachvarov D, Lampiasi N, Cusimano A, Azzolina A, McCubrey JA, Montalto G (2012) Molecular mechanisms of sorafenib action in liver cancer cells. Cell Cycle. 11, 2843-2855.

Cicenas J, Kalyan K, Sorokinas A, Jatulyte A, Valiunas D, Kaupinis A, Valius M (2014) Highlights of the Latest Advances in Research on CDK Inhibitors. Cancers. 6, 2224-2242.

Cleghorn LA, Woodland A, Collie IT, Torrie LS, Norcross N, Luksch T, Mpamhanga C, Walker RG, Mottram JC, Brenk R, Frearson JA, Gilbert IH, Wyatt PG (2011) Identification of inhibitors of the Leishmania cdc2-related protein kinase CRK3. ChemMedChem. 6, 2214-2224.

Crissien AM, Frenette C (2014) Current management of hepatocellular carcinoma. Gastroenterol Hepatol. 10, 153-161.

Crosio C, Fimia GM, Loury R, Kimura M, Okano Y, Zhou H, Sen S, Allis CD, Sassone-Corsi P (2002) Mitotic phosphorylation of histone H3: spatio-temporal regulation by mammalian Aurora kinases. Mol Cell Biol. 22, 874-885.

Dai Y, Rahmani M, Pei XY, Dent P, Grant S (2004) Bortezomib and flavopiridol interact synergistically to induce apoptosis in chronic myeloid leukemia cells resistant to imatinib mesylate through both Bcr/Abl-dependent and -independent mechanisms. Blood. 104, 509-518.

De Azevedo WF, Leclerc S, Meijer L, Havlicek L, Strnad M, Kim SH (1997) Inhibition of cyclin-dependent kinases by purine analogues: crystal structure of human cdk2 complexed with roscovitine. Eur J Biochem. 243, 518-526.

den Boer M, Argaw D, Jannin J, Alvar J (2011) Leishmaniasis impact and treatment access. Clin Microbiol Infect. 17, 1471-1477.

Desai AV, El-Bakkar H, Abdul-Hay M (2014) Novel agents in the treatment of chronic lymphocytic leukemia: a review about the future. Clin Lymphoma Myeloma Leuk. 15, 314-322.

Desai BM, Villanueva J, Nguyen TT, Lioni M, Xiao M, Kong J, Krepler C, Vultur A, Flaherty KT, Nathanson KL, Smalley KS, Herlyn M (2013) The anti-melanoma activity of dinaciclib, a cyclin-dependent kinase inhibitor, is dependent on p53 signaling. PLoS One. 8, e59588.

Dhillon S (2015) Palbociclib: first global approval. Drugs. 75, 543-551.

Dickson MA (2014) Molecular pathways: CDK4 inhibitors for cancer therapy. Clin Cancer Res. 20, 3379-3383.

Dickson MA, Schwartz GK (2009) Development of cell-cycle inhibitors for cancer therapy. Curr Oncol. 16, 36-43.

Dreyer MK, Borcherding DR, Dumont JA, Peet NP, Tsay JT, Wright PS, Bitonti AJ, Shen J, Kim SH (2001) Crystal structure of human cyclin-dependent kinase 2 in complex with the adenine-derived inhibitor H717. J Med Chem. 44, 524-530.

Ehrlich SM, Liebl J, Ardelt MA, Lehr T, De Toni EN, Mayr D, Brandl L, Kirchner T, Zahler S, Gerbes AL, Vollmar AM (2015) Targeting cyclin dependent kinase 5 in hepatocellular carcinoma - A novel therapeutic approach. J Hepatol. 63, 102-113.

El-Serag HB (2011) Hepatocellular carcinoma. N Engl J Med. 365, 1118-1127.

Emanuel S, Rugg CA, Gruninger RH, Lin R, Fuentes-Pesquera A, Connolly PJ, Wetter SK, Hollister B, Kruger WW, Napier C, Jolliffe L, Middleton SA (2005) The in vitro and in vivo effects of JNJ-7706621: a dual inhibitor of cyclin-dependent kinases and aurora kinases. Cancer Res. 65, 9038-9046.

Fabbro D, Cowan-Jacob SW, Moebitz H (2015) Ten things you should know about protein kinases: IUPHAR Review 14. Br J Pharmacol. 172, 2675-2700.

Feldmann G, Mishra A, Bisht S, Karikari C, Garrido-Laguna I, Rasheed Z, Ottenhof NA, Dadon T, Alvarez H, Fendrich V, Rajeshkumar NV, Matsui W, Brossart P, Hidalgo M, Bannerji R, Maitra A, Nelkin BD (2011) Cyclin-dependent kinase inhibitor Dinaciclib (SCH727965) inhibits pancreatic cancer growth and progression in murine xenograft models. Cancer Biol Ther. 12, 598-609.

Finn RS, Crown JP, Lang I, Boer K, Bondarenko IM, Kulyk SO, Ettl J, Patel R, Pinter T, Schmidt M, Shparyk Y, Thummala AR, Voytko NL, Fowst C, Huang X, Kim ST, Randolph S, Slamon DJ (2015) The cyclin-dependent kinase 4/6 inhibitor palbociclib in combination with letrozole versus letrozole alone as first-line treatment of oestrogen receptor-positive, HER2-negative, advanced breast cancer (PALOMA-1/TRIO-18): a randomised phase 2 study. Lancet Oncol. 16, 25-35.

Flynn J, Jones J, Johnson AJ, Andritsos L, Maddocks K, Jaglowski S, Hessler J, Grever MR, Im E, Zhou H, Zhu Y, Zhang D, Small K, Bannerji R, Byrd JC (2015) Dinaciclib is a novel cyclin-dependent kinase inhibitor with significant clinical activity in relapsed and refractory chronic lymphocytic leukemia. Leukemia. 29, 1524-1529.

Fry DW, Harvey PJ, Keller PR, Elliott WL, Meade M, Trachet E, Albassam M, Zheng X, Leopold WR, Pryer NK, Toogood PL (2004) Specific inhibition of cyclin-dependent kinase 4/6 by PD 0332991 and associated antitumor activity in human tumor xenografts. Mol Cancer Ther. 3, 1427-1438.

Fu W, Ma L, Chu B, Wang X, Bui MM, Gemmer J, Altiok S, Pledger WJ (2011) The cyclin-dependent kinase inhibitor SCH 727965 (dinacliclib) induces the apoptosis of osteosarcoma cells. Mol Cancer Ther. 10, 1018-1027.

Galbraith MD, Donner AJ, Espinosa JM (2010) CDK8: a positive regulator of transcription. Transcription. 1, 4-12.

Galons H, Oumata N, Gloulou O, Meijer L (2013) Cyclin-dependent kinase inhibitors closer to market launch? Expert Opin Ther Pat. 23, 945-963.

Germano D, Daniele B (2014) Systemic therapy of hepatocellular carcinoma: current status and future perspectives. World J Gastroenterol. 20, 3087-3099.

Giacinti C, Giordano A (2006) RB and cell cycle progression. Oncogene. 25, 5220-5227.

Goh KC, Novotny-Diermayr V, Hart S, Ong LC, Loh YK, Cheong A, Tan YC, Hu C, Jayaraman R, William AD, Sun ET, Dymock BW, Ong KH, Ethirajulu K, Burrows F, Wood JM (2012) TG02, a novel oral multi-kinase inhibitor of CDKs, JAK2 and FLT3 with potent anti-leukemic properties. Leukemia. 26, 236-243.

Gojo I, Zhang B, Fenton R (2002) The cyclin-dependent kinase inhibitor flavopiridol induces apoptosis in multiple myeloma cells through transcriptional repression and down-regulation of Mcl-1. Clin Cancer Res. 8, 3527-3538.

Grant KM, Dunion MH, Yardley V, Skaltsounis AL, Marko D, Eisenbrand G, Croft SL, Meijer L, Mottram JC (2004) Inhibitors of Leishmania mexicana CRK3 cyclin-dependent kinase: chemical library screen and antileishmanial activity. Antimicrob Agents Chemother. 48, 3033-3042.

Gray NS, Wodicka L, Thunnissen AM, Norman TC, Kwon S, Espinoza FH, Morgan DO, Barnes G, LeClerc S, Meijer L, Kim SH, Lockhart DJ, Schultz PG (1998) Exploiting chemical libraries, structure, and genomics in the search for kinase inhibitors. Science. 281, 533-538.

Gucký T, Jorda R, Zatloukal M, Kryštof V, Rárová L, Řezníčková E, Mikulits W, Strnad M (2014) 2-substituted-6-biarylmethylamino-9-cyclopentyl-9h-purine derivatives, use thereof as medicaments, and pharmaceutical compositions. WO2014121764 A2.

Guen VJ, Gamble C, Flajolet M, Unger S, Thollet A, Ferandin Y, Superti-Furga A, Cohen PA, Meijer L, Colas P (2013) CDK10/cyclin M is a protein kinase that controls ETS2 degradation and is deficient in STAR syndrome. Proc Natl Acad Sci U S A. 110, 19525-19530.

Guha M (2012) Cyclin-dependent kinase inhibitors move into Phase III. Nat Rev Drug Discov. 11, 892-894.

Hanahan D, Weinberg RA (2011) Hallmarks of cancer: the next generation. Cell. 144, 646-674.

Hassan P, Fergusson D, Grant KM, Mottram JC (2001) The CRK3 protein kinase is essential for cell cycle progression of Leishmania mexicana. Mol Biochem Parasitol. 113, 189-198.

Heindryckx F, Colle I, Van Vlierberghe H (2009) Experimental mouse models for hepatocellular carcinoma research. Int J Exp Pathol. 90, 367-386.

Heuer TS (2008) Discovery of selective CDK9 small molecule inhibitors: CDK9 inhibition in tumor cells is associated with inhibition of proliferation and induction of apoptosis [abstract]. AACR-NCI-EORTC International Conference on Molecular Targets and Cancer Therapeutics 2008 Oct 21–24, Geneva, Switzerland.

Hirose T, Kawabuchi M, Tamaru T, Okumura N, Nagai K, Okada M (2000) Identification of tudor repeat associator with PCTAIRE 2 (Trap). A novel protein that interacts with the N-terminal domain of PCTAIRE 2 in rat brain. Eur J Biochem. 267, 2113-2121.

Holkova B, Kmieciak M, Perkins EB, Bose P, Baz RC, Roodman GD, Stuart RK, Ramakrishnan V, Wan W, Peer CJ, Dawson J, Kang L, Honeycutt C, Tombes MB, Shrader E, Weir-Wiggins C, Wellons M, Sankala H, Hogan KT, Colevas AD, Doyle LA, Figg WD, Coppola D, Roberts JD, Sullivan D, Grant S (2014) Phase I trial of bortezomib (PS-341; NSC 681239) and "nonhybrid" (bolus) infusion schedule of alvocidib (flavopiridol; NSC 649890) in patients with recurrent or refractory indolent B-cell neoplasms. Clin Cancer Res. 20, 5652-5662.

Hu D, Mayeda A, Trembley JH, Lahti JM, Kidd VJ (2003) CDK11 complexes promote pre-mRNA splicing. J Biol Chem. 278, 8623-8629.

Hu D, Valentine M, Kidd VJ, Lahti JM (2007) CDK11(p58) is required for the maintenance of sister chromatid cohesion. J Cell Sci. 120, 2424-2434.

Hunter T, Plowman GD (1997) The protein kinases of budding yeast: six score and more. Trends Biochem Sci. 22, 18-22.

Chang YT, Gray NS, Rosania GR, Sutherlin DP, Kwon S, Norman TC, Sarohia R, Leost M, Meijer L, Schultz PG (1999) Synthesis and application of functionally diverse 2,6,9-trisubstituted purine libraries as CDK inhibitors. Chem Biol. 6, 361-375.

Chawla B, Madhubala R (2010) Drug targets in Leishmania. J Parasit Dis. 34, 1-13.

Chen HH, Wang YC, Fann MJ. (2006) Identification and characterization of the CDK12/cyclin L1 complex involved in alternative splicing regulation. Mol Cell Biol. 26, 2736-2745.

Chen HH, Wong YH, Geneviere AM, Fann MJ (2007) CDK13/CDC2L5 interacts with L-type cyclins and regulates alternative splicing. Biochem Biophys Res Commun. 354, 735-740.

Chen HR, Lin GT, Huang CK, Fann MJ (2014) Cdk12 and Cdk13 regulate axonal elongation through a common signaling pathway that modulates Cdk5 expression. Exp Neurol. 261, 10-21.

Chen R, Keating MJ, Gandhi V, Plunkett W (2005) Transcription inhibition by flavopiridol: mechanism of chronic lymphocytic leukemia cell death. Blood. 106, 2513-2519.

Chen R, Wierda WG, Chubb S, Hawtin RE, Fox JA, Keating MJ, Gandhi V, Plunkett W (2009) Mechanism of action of SNS-032, a novel cyclin-dependent kinase inhibitor, in chronic lymphocytic leukemia. Blood. 113, 4637-4645.

Chen S, Dai Y, Harada H, Dent P, Grant S (2007) Mcl-1 down-regulation potentiates ABT-737 lethality by cooperatively inducing Bak activation and Bax translocation. Cancer Res. 67, 782-791.

Chen S, Dai Y, Pei XY, Myers J, Wang L, Kramer LB, Garnett M, Schwartz DM, Su F, Simmons GL, Richey JD, Larsen DG, Dent P, Orlowski RZ, Grant S (2012) CDK inhibitors upregulate BH3-only proteins to sensitize human myeloma cells to BH3 mimetic therapies. Cancer Res.72, 4225-4237.

Cheng SW, Kuzyk MA, Moradian A, Ichu TA, Chang VC, Tien JF, Vollett SE, Griffith M, Marra MA, Morin GB (2012) Interaction of cyclin-dependent kinase 12/CrkRS with cyclin K1 is required for the phosphorylation of the C-terminal domain of RNA polymerase II. Mol Cell Biol. 32, 4691-4704.

Cho SJ, Lee SS, Kim YJ, Park BD, Choi JS, Liu L, Ham YM, Moon Kim B, Lee SK (2010) Xylocydine, a novel Cdk inhibitor, is an effective inducer of apoptosis in hepatocellular carcinoma cells in vitro and in vivo. Cancer Lett. 287, 196-206.

Cho SJ, Kim YJ, Surh YJ, Kim BM, Lee SK (2011) Ibulocydine is a novel prodrug Cdk inhibitor that effectively induces apoptosis in hepatocellular carcinoma cells. J Biol Chem. 286, 19662-19671.

Jane EP, Premkumar DR, Cavaleri JM, Sutera PA, Rajasekar T, Pollack IF (2016) Dinaciclib, a Cyclin-Dependent Kinase Inhibitor Promotes Proteasomal Degradation of Mcl-1 and Enhances ABT-737-Mediated Cell Death in Malignant Human Glioma Cell Lines. J Pharmacol Exp Ther. 356, 354-365.

Jiang M, Gao Y, Yang T, Zhu X, Chen J (2009) Cyclin Y, a novel membrane-associated cyclin, interacts with PFTK1. FEBS Lett. 583, 2171-2178.

Johnson AJ, Yeh YY, Smith LL, Wagner AJ, Hessler J, Gupta S, Flynn J, Jones J, Zhang X, Bannerji R, Grever MR, Byrd JC (2012) The novel cyclin-dependent

kinase inhibitor dinaciclib (SCH727965) promotes apoptosis and abrogates microenvironmental cytokine protection in chronic lymphocytic leukemia cells. Leukemia. 26, 2554-2557.

Johnson LN (2009) The regulation of protein phosphorylation. Biochem. Soc. Trans. 37, 627-641.

Johnson N, Shapiro GI (2010) Cyclin-dependent kinases (cdks) and the DNA damage response: rationale for cdk inhibitor-chemotherapy combinations as an anticancer strategy for solid tumors. Expert Opin Ther Targets. 14, 1199-1212.

Johnston SR (2015) Enhancing Endocrine Therapy for Hormone Receptor-Positive Advanced Breast Cancer: Cotargeting Signaling Pathways. J Natl Cancer Inst. 107. djv212.

Jorda R, Havlícek L, McNae IW, Walkinshaw MD, Voller J, Sturc A, Navrátilová J, Kuzma M, Mistrík M, Bártek J, Strnad M, Kryštof V (2011) Pyrazolo[4,3-d]pyrimidine bioisostere of roscovitine: evaluation of a novel selective inhibitor of cyclin-dependent kinases with antiproliferative activity. J Med Chem. 54, 2980-2993.

Jorda R, Paruch K, Kryštof V (2012) Cyclin-dependent kinase inhibitors inspired by roscovitine: purine bioisosteres. Curr Pharm Des. 18, 2974-2980.

Jorda R, Sacerdoti-Sierra N, Voller J, Havlíček L, Kráčalíková K, Nowicki MW, Nasereddin A, Kryštof V, Strnad M, Walkinshaw MD, Jaffe CL (2011) Anti-leishmanial activity of disubstituted purines and related pyrazolo[4,3-*d*]pyrimidines. Bioorg Med Chem Lett. 21, 4233-4237.

Kaelin WG Jr (2005) The concept of synthetic lethality in the context of anticancer therapy. Nat Rev Cancer. 5, 689-698.

Kawauchi T (2014) Cdk5 regulates multiple cellular events in neural development, function and disease. Dev Growth Differ. 56, 335-348.

Kim HE, Kim DG, Lee KJ, Son JG, Song MY, Park YM, Kim JJ, Cho SW, Chi SG, Cheong HS, Shin HD, Lee SW, Lee JK (2012) Frequent amplification of CENPF, GMNN and CDK13 genes in hepatocellular carcinomas. PLoS One. 7, e43223.

Knockaert M, Greengard P, Meijer L (2002) Pharmacological inhibitors of cyclin-dependent kinases. Trends Pharmacol Sci. 9, 266-269.

Knudsen ES, Knudsen KE (2008) Tailoring to RB: tumour suppressor status and therapeutic response. Nat Rev Cancer. 8, 714-724.

Knuesel MT, Meyer KD, Bernecky C, Taatjes DJ (2009) The human CDK8 subcomplex is a molecular switch that controls Mediator coactivator function. Genes Dev. 23, 439-451.

Kohoutek J, Blazek D (2012) Cyclin K goes with Cdk12 and Cdk13. Cell Div. 7, 12.

Kohzato N, Dong Y, Sui L, Masaki T, Nagahata S, Nishioka M, Konishi R, Tokuda M (2001) Overexpression of cyclin E and cyclin-dependent kinase 2 is correlated with development of hepatocellular carcinomas. Hepatol Res. 21, 27-39.

Kryštof V, Chamrád I, Jorda R, Kohoutek J (2010) Pharmacological targeting of CDK9 in cardiac hypertrophy. Med Res Rev. 30, 646-666.

Kryštof V, McNae IW, Walkinshaw MD, Fischer PM, Müller P, Vojtesek B, Orság M, Havlícek L, Strnad M (2005) Antiproliferative activity of olomoucine II, a novel 2,6,9-trisubstituted purine cyclin-dependent kinase inhibitor. Cell Mol Life Sci. 62, 1763-1771.

Kryštof V, Rárová L, Liebl J, Zahler S, Jorda R, Voller J, Cankař P (2011) The selective P-TEFb inhibitor CAN508 targets angiogenesis. Eur J Med Chem. 46, 4289-4294.

Kryštof V, Uldrijan S (2010) Cyclin-dependent kinase inhibitors as anticancer drugs. Curr Drug Targets. 11, 291-302.

Kummar S, Chen HX, Wright J, Holbeck S, Millin MD, Tomaszewski J, Zweibel J, Collins J, Doroshow JH (2010) Utilizing targeted cancer therapeutic agents in combination: novel approaches and urgent requirements. Nat Rev Drug Discov. 9, 843-56.

Kwiatkowski N, Zhang T, Rahl PB, Abraham BJ, Reddy J, Ficarro SB, Dastur A, Amzallag A, Ramaswamy S, Tesar B, Jenkins CE, Hannett NM, McMillin D, Sanda T, Sim T, Kim ND, Look T, Mitsiades CS, Weng AP, Brown JR, Benes CH, Marto JA, Young RA, Gray NS (2014) Targeting transcription regulation in cancer with a covalent CDK7 inhibitor. Nature. 511, 616-620.

Lapenna S, Giordano A (2009) Cell cycle kinases as therapeutic targets for cancer. Nat Rev Drug Discov. 8, 547-566.

Larochelle S, Amat R, Glover-Cutter K, Sansó M, Zhang C, Allen JJ, Shokat KM, Bentley DL, Fisher RP (2012) Cyclin-dependent kinase control of the initiation-to-elongation switch of RNA polymerase II. Nat Struct Mol Biol. 19, 1108-1115.

Leung WK, Ching AK, Chan AW, Poon TC, Mian H, Wong AS, To KF, Wong N (2011) A novel interplay between oncogenic PFTK1 protein kinase and tumor

suppressor TAGLN2 in the control of liver cancer cell motility. Oncogene. 30, 4464-4475.

Li KK, Ng IO, Fan ST, Albrecht JH, Yamashita K, Poon RY (2002) Activation of cyclin-dependent kinases CDC2 and CDK2 in hepatocellular carcinoma. Liver. 22, 259-268.

Li W, Zhao XL, Shang SQ, Shen HQ, Chen X (2015) Dual Inhibition of Cdc7 and Cdk9 by PHA-767491 Suppresses Hepatocarcinoma Synergistically with 5-Fluorouracil. Curr Cancer Drug Targets. 15, 196-204.

Liang Q, Li L, Zhang J, Lei Y, Wang L, Liu DX, Feng J, Hou P, Yao R, Zhang Y, Huang B, Lu J (2013) CDK5 is essential for TGF-β1-induced epithelial-mesenchymal transition and breast cancer progression. Sci Rep. 3, 2932.

Liebl J, Weitensteiner SB, Vereb G, Takács L, Fürst R, Vollmar AM, Zahler S (2010) Cyclin-dependent kinase 5 regulates endothelial cell migration and angiogenesis. J Biol Chem. 285, 35932-35943.

Lim S, Kaldis P (2013) Cdks, cyclins and CKIs: roles beyond cell cycle regulation. Development. 140, 3079-3093.

Lima LM, Barreiro EJ (2005) Bioisosterism: a useful strategy for molecular modification and drug design. Curr Med Chem. 12, 23-49.

Lin TS, Ruppert AS, Johnson AJ, Fischer B, Heerema NA, Andritsos LA, Blum KA, Flynn JM, Jones JA, Hu W, Moran ME, Mitchell SM, Smith LL, Wagner AJ, Raymond CA, Schaaf LJ, Phelps MA, Villalona-Calero MA, Grever MR, Byrd JC (2009) Phase II study of flavopiridol in relapsed chronic lymphocytic leukemia demonstrating high response rates in genetically high-risk disease. J Clin Oncol. 27:6012-6018.

Littman SJ, Knudsen ES, Witkiewicz A, Hyslop T, Lewis N, Pillai MV, Brus C, Mitchell EP (2013) A phase II study of PD-0332991 in patients with advanced hepatocellular cancer [abstract]. Gastrointestinal Cancers Symposium 2013 Jan 24-26, San Francisco, California.

Liu L, Cao Y, Chen C, Zhang X, McNabola A, Wilkie D, Wilhelm S, Lynch M, Carter C (2006) Sorafenib blocks the RAF/MEK/ERK pathway, inhibits tumor angiogenesis, and induces tumor cell apoptosis in hepatocellular carcinoma model PLC/PRF/5. Cancer Res. 66, 11851-11858.

Ljungman M, Paulsen MT (2001) The cyclin-dependent kinase inhibitor roscovitine inhibits RNA synthesis and triggers nuclear accumulation of p53 that is unmodified at Ser15 and Lys382. Mol Pharmacol. 60, 785-789.

López-Tobón A, Castro-Álvarez JF, Piedrahita D, Boudreau RL, Gallego-Gómez JC, Cardona-Gómez GP (2011) Silencing of CDK5 as potential therapy for Alzheimer's disease. Rev Neurosci. 22, 143-152.

Lu H, Xue Y, Yu GK, Arias C, Lin J, Fong S, Faure M, Weisburd B, Ji X, Mercier A, Sutton J, Luo K, Gao Z, Zhou Q (2015) Compensatory induction of MYC expression by sustained CDK9 inhibition via a BRD4-dependent mechanism. Elife. 4, e06535.

Lu J (2015) Palbociclib: a first-in-class CDK4/CDK6 inhibitor for the treatment of hormone-receptor positive advanced breast cancer. J Hematol Oncol. 8, 98.

Luke JJ, D'Adamo DR, Dickson MA, Keohan ML, Carvajal RD, Maki RG, de Stanchina E, Musi E, Singer S, Schwartz GK (2012) The cyclin-dependent kinase inhibitor flavopiridol potentiates doxorubicin efficacy in advanced sarcomas: preclinical investigations and results of a phase I dose-escalation clinical trial. Clin Cancer Res. 18, 2638-2647.

MacCallum DE, Melville J, Frame S, Watt K, Anderson S, Gianella-Borradori A, Lane DP, Green SR (2005) Seliciclib (CYC202, R-Roscovitine) induces cell death in multiple myeloma cells by inhibition of RNA polymerase II-dependent transcription and down-regulation of Mcl-1. Cancer Res. 65, 5399-5407.

Macůrek L, Lindqvist A, Lim D, Lampson MA, Klompmaker R, Freire R, Clouin C, Taylor SS, Yaffe MB, Medema RH (2008) Polo-like kinase-1 is activated by aurora A to promote checkpoint recovery. Nature. 455, 119-123.

Mallinger A, Schiemann K, Rink C, Stieber F, Calderini M, Crumpler S, Stubbs M, Adeniji-Popoola O, Poeschke O, Busch M, Czodrowski P, Musil D, Schwarz D, Ortiz-Ruiz MJ, Schneider R, Thai C, Valenti M, de Haven Brandon A, Burke R, Workman P, Dale T, Wienke D, Clarke PA, Esdar C, Raynaud FI, Eccles SA, Rohdich F, Blagg J (2016) Discovery of Potent, Selective, and Orally Bioavailable Small-Molecule Modulators of the Mediator Complex-Associated Kinases CDK8 and CDK19. J Med Chem. 59, 1078-1101.

Malínková V, Vylíčil J, Kryštof V (2015) Cyclin-dependent kinase inhibitors for cancer therapy: a patent review (2009 - 2014). Expert Opin Ther Pat. 25, 953-970.

Malumbres M (2014) Cyclin-dependent kinases. Genome Biol. 15, 122.

Malumbres M, Barbacid M (2005) Mammalian cyclin-dependent kinases. Trends Biochem Sci. 30, 630-641.

Malumbres M, Barbacid M (2009) Cell cycle, CDKs and cancer: a changing paradigm. Nat Rev Cancer. 9, 153-166.

Malumbres M, Harlow E, Hunt T, Hunter T, Lahti JM, Manning G, Morgan DO, Tsai LH, Wolgemuth DJ (2009) Cyclin-dependent kinases: a family portrait. Nat Cell Biol. 11, 1275-1276.

Malumbres M, Pevarello P, Barbacid M, Bischoff JR (2008) CDK inhibitors in cancer therapy: what is next? Trends Pharmacol Sci. 29, 16-21.

Manning G, Whyte DB, Martinez R, Hunter T, Sudarsanam S (2002) The protein kinase complement of the human genome. Science. 298, 1912-1934.

Mariaule G, Belmont P (2014) Cyclin-dependent kinase inhibitors as marketed anticancer drugs: where are we now? A short survey. Molecules. 19, 14366-14382.

Masaki T, Shiratori Y, Rengifo W, Igarashi K, Yamagata M, Kurokohchi K, Uchida N, Miyauchi Y, Yoshiji H, Watanabe S, Omata M, Kuriyama S (2003) Cyclins and cyclin-dependent kinases: comparative study of hepatocellular carcinoma versus cirrhosis. Hepatology. 37, 534-543.

Matsuda S, Kominato K, Koide-Yoshida S, Miyamoto K, Isshiki K, Tsuji A, Yuasa K (2014) PCTAIRE kinase 3/cyclin-dependent kinase 18 is activated through association with cyclin A and/or phosphorylation by protein kinase A. J Biol Chem. 289, 18387-18400.

Matsuda Y, Wakai T, Kubota M, Takamura M, Yamagiwa S, Aoyagi Y, Osawa M, Fujimaki S, Sanpei A, Genda T, Ichida T (2013) Clinical significance of cell cycle inhibitors in hepatocellular carcinoma. Med Mol Morphol. 46, 185-192.

Mayhew CN, Carter SL, Fox SR, Sexton CR, Reed CA, Srinivasan SV, Liu X, Wikenheiser-Brokamp K, Boivin GP, Lee JS, Aronow BJ, Thorgeirsson SS, Knudsen ES (2007) RB loss abrogates cell cycle control and genome integrity to promote liver tumorigenesis. Gastroenterology. 133, 976-984.

Mazzoccoli G, Tarquini R, Valoriani A, Oben J, Vinciguerra M, Marra F (2015) Management strategies for hepatocellular carcinoma: old certainties and new realities. Clin Exp Med. v tisku: DOI 10.1007/s10238-015-0368-z.

McClue SJ, Blake D, Clarke R, Cowan A, Cummings L, Fischer PM, MacKenzie M, Melville J, Stewart K, Wang S, Zhelev N, Zheleva D, Lane DP (2002) In vitro and in

vivo antitumor properties of the cyclin dependent kinase inhibitor CYC202 (R-roscovitine). Int J Cancer. 102, 463-468.

Meijer L, Bettayeb K, Galons H (2006) (R)-Roscovitine (CYC202, Seliciclib). In: Smith PJ, Yue EW eds. Inhibitors of cyclin-dependent kinases as anti-tumor agents. Boca Raton, FL, CRC Press, 187-226.

McClue SJ, Blake D, Clarke R, Cowan A, Cummings L, Fischer PM, MacKenzie M, Melville J, Stewart K, Wang S, Zhelev N, Zheleva D, Lane DP (2002) In vitro and in vivo antitumor properties of the cyclin dependent kinase inhibitor CYC202 (R-roscovitine). Int J Cancer. 102, 463-468.

McGwire BS, Satoskar AR (2014) Leishmaniasis: clinical syndromes and treatment. QJM. 107, 7-14.

McNamara MG, Knox JJ (2014) Systemic therapy for hepatocellular carcinoma. Hepatic Oncol. 1, 23-38.

Mikolcevic P, Sigl R, Rauch V, Hess MW, Pfaller K, Barisic M, Pelliniemi LJ, Boesl M, Geley S (2011) Cyclin-dependent kinase 16/PCTAIRE kinase 1 is activated by cyclin Y and is essential for spermatogenesis. Mol Cell Biol. 32, 868-879.

Mikolcevic P, Rainer J, Geley S (2012) Orphan kinases turn eccentric: a new class of cyclin Y-activated, membrane-targeted CDKs. Cell Cycle. 11, 3758-3768.

Mita MM, Joy AA, Mita A, Sankhala K, Jou YM, Zhang D, Statkevich P, Zhu Y, Yao SL, Small K, Bannerji R, Shapiro CL (2014) Randomized phase II trial of the cyclin-dependent kinase inhibitor dinaciclib (MK-7965) versus capecitabine in patients with advanced breast cancer. Clin Breast Cancer. 14, 169-176.

Morikawa A, Henry NL (2015) Palbociclib for the Treatment of Estrogen Receptor-Positive, HER2-Negative Metastatic Breast Cancer. Clin Cancer Res. 21, 3591-3596.

Morishita A, Masaki T, Yoshiji H, Nakai S, Ogi T, Miyauchi Y, Yoshida S, Funaki T, Uchida N, Kita Y, Funakoshi F, Usuki H, Okada S, Izuishi K, Watanabe S, Kurokohchi K, Kuriyama S (2004) Reduced expression of cell cycle regulator p18(INK4C) in human hepatocellular carcinoma. Hepatology. 40, 677-686.

Nagaria TS, Williams JL, Leduc C, Squire JA, Greer PA, Sangrar W (2013) Flavopiridol synergizes with sorafenib to induce cytotoxicity and potentiate antitumorigenic activity in EGFR/HER-2 and mutant RAS/RAF breast cancer model systems. Neoplasia. 15, 939-951.

Natoni A, Murillo LS, Kliszczak AE, Catherwood MA, Montagnoli A, Samali A, O'Dwyer M, Santocanale C (2011) Mechanisms of action of a dual Cdc7/Cdk9

kinase inhibitor against quiescent and proliferating CLL cells. Mol Cancer Ther. 10, 1624-1634.

Nemet J, Jelicic B, Rubelj I, Sopta M (2014) The two faces of Cdk8, a positive/negative regulator of transcription. Biochimie. 97, 22-27.

Németh G, Varga Z, Greff Z, Bencze G, Sipos A, Szántai-Kis C, Baska F, Gyuris A, Kelemenics K, Szathmáry Z, Minárovits J, Kéri G, Orfi L (2011) Novel, selective CDK9 inhibitors for the treatment of HIV infection. Curr Med Chem. 18, 342-358.

Nutley BP, Raynaud FI, Wilson SC, Fischer PM, Hayes A, Goddard PM, McClue SJ, Jarman M, Lane DP, Workman P (2005) Metabolism and pharmacokinetics of the cyclin-dependent kinase inhibitor R-roscovitine in the mouse. Mol Cancer Ther. 4, 125-139.

Orzáez M, Gortat A, Mondragón L, Bachs O, Pérez-Payá E (2009) ATP-noncompetitive inhibitors of CDK-cyclin complexes. ChemMedChem. 4, 19-24.

Oumata N, Bettayeb K, Ferandin Y, Demange L, Lopez-Giral A, Goddard ML, Myrianthopoulos V, Mikros E, Flajolet M, Greengard P, Meijer L, Galons H (2008) Roscovitine-derived, dual-specificity inhibitors of cyclin-dependent kinases and casein kinases 1. J Med Chem. 51, 5229-5242.

Pallis M, Abdul-Aziz A, Burrows F, Seedhouse C, Grundy M, Russell N (2012) The multi-kinase inhibitor TG02 overcomes signalling activation by survival factors to deplete MCL1 and XIAP and induce cell death in primary acute myeloid leukaemia cells. Br J Haematol. 159, 191-203.

Palmieri L, Rastelli G (2013) αC helix displacement as a general approach for allosteric modulation of protein kinases. Drug Discov Today. 18, 407-414.

Pang EY, Bai AH, To KF, Sy SM, Wong NL, Lai PB, Squire JA, Wong N (2007) Identification of PFTAIRE protein kinase 1, a novel cell division cycle-2 related gene, in the motile phenotype of hepatocellular carcinoma cells. Hepatology. 46, 436-445.

Park MH, Kim SY, Kim YJ, Chung YH (2014) ALS2CR7 (CDK15) attenuates TRAIL induced apoptosis by inducing phosphorylation of survivin Thr34. Biochem Biophys Res Commun. 450, 129-134.

Parsons M, Worthey EA, Ward PN, Mottram JC (2005) Comparative analysis of the kinomes of three pathogenic trypanosomatids: Leishmania major, Trypanosoma brucei and Trypanosoma cruzi. BMC Genomics. 6, 127.

Parry D, Guzi T, Shanahan F, Davis N, Prabhavalkar D, Wiswell D, Seghezzi W, Paruch K, Dwyer MP, Doll R, Nomeir A, Windsor W, Fischmann T, Wang Y, Oft M, Chen T, Kirschmeier P, Lees EM (2010) Dinaciclib (SCH 727965), a novel and potent cyclin-dependent kinase inhibitor. Mol Cancer Ther. 9, 2344-2353.

Paruch K, Dwyer MP, Alvarez C, Brown C, Chan TY, Doll RJ, Keertikar K, Knutson C, McKittrick B, Rivera J, Rossman R, Tucker G, Fischmann T, Hruza A, Madison V, Nomeir AA, Wang Y, Kirschmeier P, Lees E, Parry D, Sgambellone N, Seghezzi W, Schultz L, Shanahan F, Wiswell D, Xu X, Zhou Q, James RA, Paradkar VM, Park H, Rokosz LR, Stauffer TM, Guzi TJ (2010) Discovery of Dinaciclib (SCH 727965): A Potent and Selective Inhibitor of Cyclin-Dependent Kinases. ACS Med Chem Lett. 1, 204-208.

Patel A, Sun W (2014) Molecular targeted therapy in hepatocellular carcinoma: from biology to clinical practice and future. Curr Treat Options Oncol. 15, 380-394.

Payton M, Chung G, Yakowec P, Wong A, Powers D, Xiong L, Zhang N, Leal J, Bush TL, Santora V, Askew B, Tasker A, Radinsky R, Kendall R, Coats S (2006) Discovery and evaluation of dual CDK1 and CDK2 inhibitors. Cancer Res. 66, 4299-4308.

Peyressatre M, Prével C, Pellerano M, Morris MC (2015) Targeting cyclin-dependent kinases in human cancers: from small molecules to Peptide inhibitors. Cancers. 7, 179-237.

Phelps MA, Lin TS, Johnson AJ, Hurh E, Rozewski DM, Farley KL, Wu D, Blum KA, Fischer B, Mitchell SM, Moran ME, Brooker-McEldowney M, Heerema NA, Jarjoura D, Schaaf LJ, Byrd JC, Grever MR, Dalton JT (2009) Clinical response and pharmacokinetics from a phase 1 study of an active dosing schedule of flavopiridol in relapsed chronic lymphocytic leukemia. Blood. 113, 2637-2645.

Popowycz F, Fournet G, Schneider C, Bettayeb K, Ferandin Y, Lamigeon C, Tirado OM, Mateo-Lozano S, Notario V, Colas P, Bernard P, Meijer L, Joseph B (2009) Pyrazolo[1,5-a]-1,3,5-triazine as a purine bioisostere: access to potent cyclin-dependent kinase inhibitor (R)-roscovitine analogue. J Med Chem. 52, 655-663.

Porter DC, Farmaki E, Altilia S, Schools GP, West DK, Chen M, Chang BD, Puzyrev AT, Lim CU, Rokow-Kittell R, Friedhoff LT, Papavassiliou AG, Kalurupalle S, Hurteau G, Shi J, Baran PS, Gyorffy B, Wentland MP, Broude EV, Kiaris H, Roninson IB (2012) Cyclin-dependent kinase 8 mediates chemotherapy-induced tumor-promoting paracrine activities. Proc Natl Acad Sci U S A. 109, 13799-13804.

Potente M, Gerhardt H, Carmeliet P (2011) Basic and therapeutic aspects of angiogenesis. Cell. 146, 873-887.

Rask-Andersen M, Zhang J, Fabbro D, Schiöth HB (2014) Advances in kinase targeting: current clinical use and clinical trials. Trends pharmacol Sci. 35, 604-620.

Rastelli G, Anighoro A, Chripkova M, Carrassa L, Broggini M (2014) Structure-based discovery of the first allosteric inhibitors of cyclin-dependent kinase 2. Cell Cycle. 13, 2296-2305.

Reichwald C, Shimony O, Dunkel U, Sacerdoti-Sierra N, Jaffe CL, Kunick C (2008) 2-(3-aryl-3-oxopropen-1-yl)-9-tert-butyl-paullones: a new antileishmanial chemotype. J Med Chem. 51, 659-665.

Ren S, Rollins BJ (2004) Cyclin C/cdk3 promotes Rb-dependent G0 exit. Cell. 117, 239-251.

Rivadeneira DB, Mayhew CN, Thangavel C, Sotillo E, Reed CA, Graña X, Knudsen ES (2010) Proliferative suppression by CDK4/6 inhibition: complex function of the retinoblastoma pathway in liver tissue and hepatoma cells. Gastroenterology. 138, 1920-1930.

Roberts PJ, Bisi JE, Strum JC, Combest AJ, Darr DB, Usary JE, Zamboni WC, Wong KK, Perou CM, Sharpless NE (2012) Multiple roles of cyclin-dependent kinase 4/6 inhibitors in cancer therapy. J Natl Cancer Inst. 104, 476-487.

Saladino C, Frame S, Davis S, Blake D, Zheleva D (2015) CYC065, a novel CDK2/5/9 inhibitor: detailed mechanistic studies, determinants of sensitivity and synergistic combinations [abstract]. AACR 106th Annual Meeting 2015 Apr 18-22, Philadelphia, PA.

Santamaría D, Barrière C, Cerqueira A, Hunt S, Tardy C, Newton K, Cáceres JF, Dubus P, Malumbres M, Barbacid M (2007) Cdk1 is sufficient to drive the mammalian cell cycle. Nature. 448, 811-815.

Santo L, Vallet S, Hideshima T, Cirstea D, Ikeda H, Pozzi S, Patel K, Okawa Y, Gorgun G, Perrone G, Calabrese E, Yule M, Squires M, Ladetto M, Boccadoro M, Richardson PG, Munshi NC, Anderson KC, Raje N (2010) AT7519, A novel small molecule multi-cyclin-dependent kinase inhibitor, induces apoptosis in multiple myeloma via GSK-3beta activation and RNA polymerase II inhibition. Mol Cancer Ther. 9, 920-928.

Seamon JA, Rugg CA, Emanuel S, Calcagno AM, Ambudkar SV, Middleton SA, Butler J, Borowski V, Greenberger LM (2006) Role of the ABCG2 drug transporter in the

resistance and oral bioavailability of a potent cyclin-dependent kinase/Aurora kinase inhibitor. Mol Cancer Ther. 5, 2459-2467.

Sedlacek HH (2001) Mechanisms of action of flavopiridol. Crit Rev Oncol Hematol. 38, 139-170.

Seki A, Coppinger JA, Jang CY, Yates JR, Fang G (2008) Bora and the kinase Aurora a cooperatively activate the kinase Plk1 and control mitotic entry. Science. 320, 1655-1658.

Shapiro GI (2006) Cyclin-dependent kinase pathways as targets for cancer treatment. J Clin Oncol. 24, 1770-1783.

Sharlow ER, Grögl M, Johnson J, Lazo JS (2010) Anti-leishmanial drug discovery: rising to the challenges of a highly neglected disease. Mol Interv. 10, 72-75.

Shimizu K, Uematsu A, Imai Y, Sawasaki T (2014) Pctaire1/Cdk16 promotes skeletal myogenesis by inducing myoblast migration and fusion. FEBS Lett. 588, 3030-3037.

Shu F, Lv S, Qin Y, Ma X, Wang X, Peng X, Luo Y, Xu BE, Sun X, Wu J (2007) Functional characterization of human PFTK1 as a cyclin-dependent kinase. 104, 9248-9253.

Schang LM (2002) Cyclin-dependent kinases as cellular targets for antiviral drugs. J Antimicrob Chemother. 50, 779-792.

Schlachterman A, Craft WW Jr, Hilgenfeldt E, Mitra A, Cabrera R (2015) Current and future treatments for hepatocellular carcinoma. World J Gastroenterol. 21, 8478-8491.

Scholz A, Wagner K, Welzel M, Remlinger F, Wiedenmann B, Siemeister G, Rosewicz S, Detjen KM (2009) The oral multitarget tumour growth inhibitor, ZK 304709, inhibits growth of pancreatic neuroendocrine tumours in an orthotopic mouse model. Gut. 58, 261-270.

Siemeister G, Luecking U, Wagner C, Detjen K, Mc Coy C, Bosslet K (2006) Molecular and pharmacodynamic characteristics of the novel multi-target tumor growth inhibitor ZK 304709. Biomed Pharmacother. 60, 269-272.

Siemeister G, Lücking U, Wengner AM, Lienau P, Steinke W, Schatz C, Mumberg D, Ziegelbauer K (2012) BAY 1000394, a novel cyclin-dependent kinase inhibitor, with potent antitumor activity in mono- and in combination treatment upon oral application. Mol Cancer Ther. 11, 2265-2273.

Singh N, Kumar M, Singh RK (2012) Leishmaniasis: current status of available drugs and new potential drug targets. Asian Pac J Trop Med. 5, 485-497.

Skead BM, Worrall CP, Atherton JCC, Northen JS, Fernandes P (2011) Crystalline forms of a purine derivative. WO2011089401 A1.

Sorrentino JA, He S, Bisi JE, Roberts PJ, Strum JC, Sharpless NE (2015) G1T28-1, a novel CDK4/6 inhibitor, protects murine hematopoietic stem and progenitor cells from cytotoxic chemotherapy [abstract]. AACR 106th Annual Meeting 2015 Apr 18-22, Philadelphia, PA.

Squires MS, Feltell RE, Wallis NG, Lewis EJ, Smith DM, Cross DM, Lyons JF, Thompson NT (2009) Biological characterization of AT7519, a small-molecule inhibitor of cyclin-dependent kinases, in human tumor cell lines. Mol Cancer Ther. 8, 324-332.

Squires MS, Cooke L, Lock V, Qi W, Lewis EJ, Thompson NT, Lyons JF, Mahadevan D (2010) AT7519, a cyclin-dependent kinase inhibitor, exerts its effects by transcriptional inhibition in leukemia cell lines and patient samples. Mol Cancer Ther. 9, 920-928.

Stephenson JJ, Nemunaitis J, Joy AA, Martin JC, Jou YM, Zhang D, Statkevich P, Yao SL, Zhu Y, Zhou H, Small K, Bannerji R, Edelman MJ (2014) Randomized phase 2 study of the cyclin-dependent kinase inhibitor dinaciclib (MK-7965) versus erlotinib in patients with non-small cell lung cancer. Lung Cancer. 83, 219-223.

Strock CJ, Park JI, Nakakura EK, Bova GS, Isaacs JT, Ball DW, Nelkin BD (2006) Cyclin-dependent kinase 5 activity controls cell motility and metastatic potential of prostate cancer cells. Cancer Res. 66, 7509-7515.

Tell V, Hilgeroth A (2013) Recent developments of protein kinase inhibitors as potential AD therapeutics. Front Cell Neurosci. 7, 189.

Tian Y, Wan H, Tan G (2012) Cell cycle-related kinase in carcinogenesis. Oncol Lett. 4, 601-606.

Toogood PL, Harvey PJ, Repine JT, Sheehan DJ, VanderWel SN, Zhou H, Keller PR, McNamara DJ, Sherry D, Zhu T, Brodfuehrer J, Choi C, Barvian MR, Fry DW (2005) Discovery of a potent and selective inhibitor of cyclin-dependent kinase 4/6. J Med Chem. 48, 2388-2406.

Trakala M, Malumbres M (2014) Cyclin C surprises in tumour suppression. Nat Cell Biol. 16, 1031-1033.

Tripathi BK, Zelenka PS (2010) Cdk5: A regulator of epithelial cell adhesion and migration. Cell Adh Migr. 4, 333-336.

Trova MP, Barnes KD, Barford C, Benanti T, Bielaska M, Burry L, Lehman JM, Murphy C, O'Grady H, Peace D, Salamone S, Smith J, Snider P, Toporowski J, Tregay S, Wilson A, Wyle M, Zheng X, Friedrich TD (2009) Biaryl purine derivatives as potent antiproliferative agents: inhibitors of cyclin dependent kinases. Part I. Bioorg Med Chem Lett. 19, 6608-6612.

Trovesi C, Manfrini N, Falcettoni M, Longhese MP (2013) Regulation of the DNA damage response by cyclin-dependent kinases. J Mol Biol. 425, 4756-4766.

Turner NC, Lord CJ, Iorns E, Brough R, Swift S, Elliott R, Rayter S, Tutt AN, Ashworth A (2008) A synthetic lethal siRNA screen identifying genes mediating sensitivity to a PARP inhibitor. EMBO J. 27, 1368-1377.

Ubersax JA, Ferrell JE Jr (2007) Mechanisms of specificity in protein phosphorylation. Nat Rev Mol Cell Biol. 8, 530-541.

Venook AP, Papandreou C, Furuse J, de Guevara LL (2010) The incidence and epidemiology of hepatocellular carcinoma: a global and regional perspective. Oncologist. 15 supplement 4, 5-13.

Vermeulen K, Strnad M, Kryštof V, Havlícek L, Van der Aa A, Lenjou M, Nijs G, Rodrigus I, Stockman B, van Onckelen H, Van Bockstaele DR, Berneman ZN (2002) Antiproliferative effect of plant cytokinin analogues with an inhibitory activity on cyclin-dependent kinases. Oncogene. 16, 299-305.

Vidula N, Rugo HS (2015) Cyclin-Dependent Kinase 4/6 Inhibitors for the Treatment of Breast Cancer: A Review of Preclinical and Clinical Data. Clin Breast Cancer. 16,8-17.

Vymětalová L, Havlíček L, Šturc A, Skrášková Z, Jorda R, Pospíšil T, Strnad M, Kryštof V (2016) 5-Substituted 3-isopropyl-7-[4-(2-pyridyl)benzyl]amino-1(2)H-pyrazolo[4,3-d]pyrimidines with anti-proliferative activity as potent and selective inhibitors of cyclin-dependent kinases. Eur J Med Chem. 110, 291-301.

Wang J, Zindy F, Chenivesse X, Lamas E, Henglein B, Bréchot C (1992) Modification of cyclin A expression by hepatitis B virus DNA integration in a hepatocellular carcinoma. Oncogene. 7, 1653-1656.

Wang K, Hampson P, Hazeldine J, Kryštof V, Strnad M, Pechan P, Lord JM (2012) Cyclin-dependent kinase 9 activity regulates neutrophil spontaneous apoptosis. PLoS One. 7, e30128.

Wang S, Fischer PM (2008) Cyclin-dependent kinase 9: a key transcriptional regulator and potential drug target in oncology, virology and cardiology. Trends Pharmacol Sci. 29, 302-313.

Wang Y, Liu XY, De Clercq E (2009) Role of the HIV-1 positive elongation factor P-TEFb and inhibitors thereof. Mini Rev Med Chem. 9, 379-385.

Wang Y, Zhang T, Kwiatkowski N, Abraham BJ, Lee TI, Xie S, Yuzugullu H, Von T, Li H, Lin Z, Stover DG, Lim E, Wang ZC, Iglehart JD, Young RA, Gray NS, Zhao JJ (2015) CDK7-dependent transcriptional addiction in triple-negative breast cancer. Cell. 163, 174-186.

Whittaker SR, Te Poele RH, Chan F, Linardopoulos S, Walton MI, Garrett MD, Workman P (2007) The cyclin-dependent kinase inhibitor seliciclib (R-roscovitine; CYC202) decreases the expression of mitotic control genes and prevents entry into mitosis. Cell Cycle. 6, 3114-3131.

Whittaker S, Marais R, Zhu AX (2010) The role of signaling pathways in the development and treatment of hepatocellular carcinoma. Oncogene. 29, 4989-5005.

Wilson SC, Atrash B, Barlow C, Eccles S, Fischer PM, Hayes A, Kelland L, Jackson W, Jarman M, Mirza A, Moreno J, Nutley BP, Raynaud FI, Sheldrake P, Walton M, Westwood R, Whittaker S, Workman P, McDonald E (2011) Design, synthesis and biological evaluation of 6-pyridylmethylaminopurines as CDK inhibitors. Bioorg Med Chem. 19, 6949-6965.

Xingi E, Smirlis D, Myrianthopoulos V, Magiatis P, Grant KM, Meijer L, Mikros E, Skaltsounis AL, Soteriadou K (2009) 6-Br-5methylindirubin-3'oxime (5-Me-6-BIO) targeting the leishmanial glycogen synthase kinase-3 (GSK-3) short form affects cell-cycle progression and induces apoptosis-like death: exploitation of GSK-3 for treating leishmaniasis. Int J Parasitol. 39, 1289-1303.

Xu N, Libertini S, Black EJ, Lao Y, Hegarat N, Walker M, Gillespie DA (2012) Cdk-mediated phosphorylation of Chk1 is required for efficient activation and full checkpoint proficiency in response to DNA damage. Oncogene. 31, 1086-1094.

Xu W, Ji JY (2011) Dysregulation of CDK8 and Cyclin C in tumorigenesis. J Genet Genomics. 38, 439-452.

Yanagi T, Matsuzawa S (2015) PCTAIRE1/PCTK1/CDK16: a new oncotarget? Cell Cycle. 14, 463-464.

Yu C, Krystal G, Dent P, Grant S (2002) Flavopiridol potentiates STI571-induced mitochondrial damage and apoptosis in BCR-ABL-positive human leukemia cells. Clin Cancer Res. 8, 2976-2984.

Zhang J, Yang PL, Gray NS (2009) Targeting cancer with small molecule kinase inhibitors. Nat Rev Cancer. 9, 28-39.

Zhong XY, Xu XX, Yu JH, Jiang GX, Yu Y, Tai S, Wang ZD, Cui YF. (2012) Clinical and biological significance of Cdk10 in hepatocellular carcinoma. Gene. 498, 68-74.

Zhu AX, Duda DG, Sahani DV, Jain RK (2011) HCC and angiogenesis: possible targets and future directions. Nat Rev Clin Oncol. 8, 292-301.

8 SEZNAM POUŽITÝCH ZKRATEK

ALL	Acute lymphoblastic leukemia
AMC	7-amido-4-methylcoumarin
AML	Acute myeloid leukemia
ATM	Ataxia telangiectasia mutated
ATP	Adenosine triphosphate
Bax	Bcl-2-associated X protein
Bcl-2	B-cell CLL/lymphoma 2
Bcr/Abl	Breakpoint cluster region/abelson kinase
CAK	CDK-activating kinase
Cdc	Cell division cycle
CDK	Cyclin-dependent kinase
Chk1	Checkpoint kinase 1
Cip/Kip	CDK interacting protein/ kinase inhibitory protein
CLL	Chronic lymphocytic leukemia
CMV	Cytomegalovirus
CRK	Cdc2-related kinase
CTD	C-terminal domain
DMEM	Dulbecco's Modified Eagle Medium
DMSO	Dimethylsulfoxide
DNA	Deoxyribonucleic acid
DTT	Dithiothreitol
DYRK	Dual specificity tyrosine-phosphorylation-regulated kinase
EGTA	Ethylene glycol tetraacetic acid
EDTA	Ethylenediaminetetraacetic acid
EMEA	European Medicines Agency
ERK	Extracellular-signal-regulated kinase
FDA	Food and Drug Administration
FITC	Fluorescein isothiocyanate
FLT3	Fms-like tyrosine kinase 3
GSK3β	Glykogen synthase kinase 3β
HBV	Hepatitis B virus

HCC	Hepatocellular carcinoma
HEPES	2-[4-(2-hydroxyethyl)piperazin-1-yl]ethanesulfonic acid
HER2	Human epidermal growth factor receptor 2
HIV	Human immunodeficiency virus type 1
IC_{50}	Half maximal inhibitory concentration
ICAM-1	Intercellular adhesion molecule 1
INK4	Inhibitor of cyclin-dependent kinase 4
JAK2	Janus kinase 2
MAPK	Mitogen-activated protein kinase
Mat1	Ménage-à-trois 1
Mcl-1	Myeloid-cell leukemia 1
Mdm-2	Murine double minute 2
Med	Mediator complex subunit
MEK	Mitogen-activated protein kinase kinase
MTT	3-(4,5-dimethylthiazol-2-yl)-2,5-diphenyltetrazolium bromide
mRNA	Messenger ribonucleic acid
PAGE	Polyacrylamide gel electrophoresis
PARP-1	Poly(ADP-ribose)polymerase 1
PDGFR	Platelet-derived growth factor receptor
PIPES	1,4-Piperazinediethanesulfonic acid
Plk1	Polo-like kinase 1
PMSF	Phenylmethanesulfonyl fluoride
P-TEFb	Positive transcription elongation factor
Rb	Retinoblastoma protein
RNA	Ribonucleic acid
RPMI	Roswell Park Memorial Institute
SCID	Severe combined immunodeficiency diseases
SDS	Sodium dodecyl sulfate
TCA	Trichloroacetic acid
TFIIH	Transcription factor IIH
TRIS	Tris(hydroxymethyl) aminomethane
TRK	Tropomyosin receptor kinase
VEGFR	Vascular endothelial growth factor receptor
XIAP	X-linked inhibitor of apoptosis

9 CURRICULUM VITAE

Jméno: Eva Řezníčková

Narozena: 20. 8. 1985 v Olomouci

Bydliště: Foerstrova 13, 779 00 Olomouc

Vzdělání:

2005 – 2008 bakalářský studijní obor Molekulární a buněčná biologie
Přírodovědecká fakulta, Univerzita Palackého v Olomouci

2008 – 2010 magisterský studijní obor Molekulární a buněčná biologie
Přírodovědecká fakulta, Univerzita Palackého v Olomouci

od 2010 doktorské studium Biochemie
Přírodovědecká fakulta, Univerzita Palackého v Olomouci

Pedagogická činnost:

Cvičení z buněčné biologie (LRR/BUBCV), od roku 2010 dosud

Vedení bakalářských prací (Marta Zbožínková, obor Experimentální biologie, obhájeno 2013; Marie Kulatá, obor Experimentální biologie, obhájeno 2016)

Zahraniční stáže:

2010 (1 měsíc) Department of Medicine I, Div.: Institute of Cancer Research, Medical University of Vienna (prof. W. Mikulits)

2012 (3 měsíce) Department of Medicine I, Div.: Institute of Cancer Research, Medical University of Vienna (prof. W. Mikulits)

Seznam publikovaných prací:

Řezníčková E, Weitensteiner S, Havlíček L, Jorda R, Gucký T, Berka K, Bazgier V, Zahler S, Kryštof V, Strnad M (2015) Characterization of a Pyrazolo[4,3-d]pyrimidine Inhibitor of Cyclin-Dependent Kinases 2 and 5 and Aurora A With Pro-Apoptotic and Anti-Angiogenic Activity In Vitro. Chem Biol Drug Des. 86, 1528-1540.

Řezníčková E, Popa A, Gucký T, Zatloukal M, Havlíček L, Bazgier V, Berka K, Jorda R, Popa I, Nasereddin A, Jaffe CL, Kryštof V, Strnad M (2015) 2,6,9-

Trisubstituted purines as CRK3 kinase inhibitors with antileishmanial activity in vitro. Bioorg Med Chem Lett. 25, 2298-2301.

Haider C, Grubinger M, **Řezníčková E**, Weiss TS, Rotheneder H, Miklos W, Berger W, Jorda R, Zatloukal M, Gucky T, Strnad M, Kryštof V, Mikulits W (2013) Novel inhibitors of cyclin-dependent kinases combat hepatocellular carcinoma without inducing chemoresistance. Mol Cancer Ther. 12, 1947-1957.

Gucký T, Jorda R, Zatloukal M, Bazgier V, Berka K, **Řezníčková E**, Béres T, Strnad M, Kryštof V (2013) A novel series of highly potent 2,6,9-trisubstituted purine cyclin-dependent kinase inhibitors. J Med Chem. 56, 6234-6247.

Zatloukal M, Jorda R, Gucký T, **Řezníčková E**, Voller J, Pospíšil T, Malínková V, Adamcová H, Kryštof V, Strnad M (2013) Synthesis and in vitro biological evaluation of 2,6,9-trisubstituted purines targeting multiple cyclin-dependent kinases. Eur J Med Chem. 61, 61-72.

Imramovský A, Jorda R, Pauk K, **Řezníčková E**, Dušek J, Hanusek J, Kryštof V (2013) Substituted 2-hydroxy-N-(arylalkyl)benzamides induce apoptosis in cancer cell lines. Eur J Med Chem. 68, 253-259.

Gucký T, **Řezníčková E**, Džubák P, Hajdúch M, Kryštof V (2010) Synthesis and anticancer activity of some 1,5-diaryl-3-(3,4,5-trihydroxyphenyl)-1H-pyrazolo[4,3-e][1,2,4]triazines. Monatsh Chem. 141, 709-714.

Patentová přihláška:

Gucký T, Jorda R, Zatloukal M, Kryštof V, Rárová L, Řezníčková E, Mikulits W, Strnad M (2014) 2-substituted-6-biarylmethylamino-9-cyclopentyl-9H-purine derivatives, use thereof as medicaments, and pharmaceutical compositions. WO2014121764 A2.

Konferenční příspěvky:

Jorda R, Skrášková Z, **Řezníčková E**, Kryštof V: Phosphorylation of androgen receptor at serine 81 by cyclin-dependent kinases. 11th World Congress on Urological Research (ESUR-SBUR15), 10.-12. září 2015, Nijmegen, Nizozemí; poster

Gucký T, Jorda R, Zatloukal M, **Řezníčková E**, Kryštof V, Strnad M: A novel series of highly potent 2,6,9-trisubstituted purine cyclin-dependent kinase inhibitors. Drug Discovery and Selection: When Chemical Biology meets Drug Design, 3.-5. červenec 2013, Nice, Francie; poster.

Jorda R, Imramovský A, Pauk K, **Řezníčková E**, Dušek J, Hanusek J, Kryštof V: Substituted 2-hydroxy-N-(arylalkyl)benzamides induce apoptosis in cancer cell lines. Drug Discovery and Selection: When Chemical Biology meets Drug Design, 3.-5. červenec 2013, Nice, Francie; poster.

Řezníčková E, Jorda R, Gucký T, Kryštof V: Pharmacological inhibitors of protein kinases: An example of screening and development. VIIIth Joint Meeting on Medicinal Chemistry, 30. červen-4. červenec 2013, Lublin, Polsko; poster.

Řezníčková E, Jorda R, Kryštof V, Havlíček L, Strnad M: Antiproliferative and proapoptotic effects of a new pyrazolo[4,3-*d*]pyrimidine inhibitor of cyclin-dependent kinases. The Student Scientific Conference on Cancer Research, 7.-8. duben 2011, Brno, Česká republika; poster.

Jorda R, Zatloukal M, **Řezníčková E**, Vymětalová L, Kryštof V, Strnad M: Novel derivatives of cyclin-dependent kinase inhibitor roscovitine. Cell Cycle Regulators/Inhibitors and Cancer, 5.-8. únor 2011, Vídeň, Rakousko; poster.

Jorda R, **Řezníčková E**, Kryštof V, Havlíček L, Strnad M. A novel pyrazolo[4,3-*d*]pyrimidine inhibitor of cyclin-dependent kinases: antiproliferative and proapoptotic effects. 22nd EORTC-NCI-AACR Symposium on Molecular Targets and Cancer Therapeutics, 16.-19. listopad 2010. Berlin, Germany; poster.

Vědecká ocenění:

Prix Sanofi de Pharmacie 2015 (1. místo), soutěž pro studenty doktorských studií pořádaná společně Francouzským velvyslanectví v České republice a společností Sanofi

10 SEZNAM PŘÍLOH

Příloha I

Zatloukal M, Jorda R, Gucký T, **Řezníčková E**, Voller J, Pospíšil T, Malínková V, Adamcová H, Kryštof V, Strnad M (2013) Synthesis and in vitro biological evaluation of 2,6,9-trisubstituted purines targeting multiple cyclin-dependent kinases. Eur J Med Chem. 61, 61-72.

Příloha II

Gucký T, Jorda R, Zatloukal M, Bazgier V, Berka K, **Řezníčková E**, Béres T, Kryštof V, Strnad M (2013) A novel series of highly potent 2,6,9-trisubstituted purine cyclin-dependent kinase inhibitors. J Med Chem. 56, 6234-6247.

Příloha III

Haider C, Grubinger M, **Řezníčková E**, Weiss TS, Rotheneder H, Miklos W, Berger W, Jorda R, Zatloukal M, Gucký T, Strnad M, Kryštof V, Mikulits W (2013) Novel inhibitors of cyclin-dependent kinases combat hepatocellular carcinoma without inducing chemoresistance. Mol Cancer Ther. 12, 1947-1957.

Příloha IV

Řezníčková E, Weitensteiner S, Havlíček L, Jorda R, Gucký T, Berka K, Bazgier V, Zahler S, Kryštof V, Strnad M (2015) Characterization of a Pyrazolo[4,3-d]pyrimidine Inhibitor of Cyclin-Dependent Kinases 2 and 5 and Aurora A With Pro-Apoptotic and Anti-Angiogenic Activity In Vitro. Chem Biol Drug Des. 86, 1528-1540.

Příloha V

Řezníčková E, Popa A, Gucký T, Zatloukal M, Havlíček L, Bazgier V, Berka K, Jorda R, Popa I, Nasereddin A, Jaffe CL, Kryštof V, Strnad M (2015) 2,6,9-Trisubstituted purines as CRK3 kinase inhibitors with antileishmanial activity in vitro. Bioorg Med Chem Lett. 25, 2298-2301.

PŘÍLOHA I

Zatloukal M, Jorda R, Gucký T, Řezníčková E, Voller J, Pospíšil T, Malínková V, Adamcová H, Kryštof V, Strnad M (2013) Synthesis and in vitro biological evaluation of 2,6,9-trisubstituted purines targeting multiple cyclin-dependent kinases. Eur J Med Chem. 61, 61-72.

European Journal of Medicinal Chemistry 61 (2013) 61–72

Contents lists available at SciVerse ScienceDirect

European Journal of Medicinal Chemistry

journal homepage: http://www.elsevier.com/locate/ejmech

Original article

Synthesis and in vitro biological evaluation of 2,6,9-trisubstituted purines targeting multiple cyclin-dependent kinases

Marek Zatloukal [a,*], Radek Jorda [b], Tomáš Gucký [a], Eva Řezníčková [b], Jiří Voller [a,b], Tomáš Pospíšil [a], Veronika Malínková [a], Helena Adamcová [c], Vladimír Kryštof [b], Miroslav Strnad [a,b]

[a] Centre of the Region Haná for Biotechnological and Agricultural Research, Department of Growth Regulators, Faculty of Science, Palacký University, Šlechtitelů 11, 783 71 Olomouc, Czech Republic
[b] Laboratory of Growth Regulators, Faculty of Science, Palacký University & Institute of Experimental Botany, Šlechtitelů 11, 78371 Olomouc, Czech Republic
[c] BioPatterns s.r.o., Šlechtitelů 21, 78371 Olomouc, Czech Republic

ARTICLE INFO

Article history:
Received 19 January 2012
Received in revised form
7 June 2012
Accepted 16 June 2012
Available online 23 June 2012

Keywords:
Cyclin-dependent kinase
Inhibitor
Roscovitine
Cancer
Apoptosis
Cell cycle

ABSTRACT

Several inhibitors of cyclin-dependent kinases (CDKs), including the 2,6,9-trisubstituted purine derivative roscovitine, are currently being evaluated in clinical trials as potential anticancer drugs. Here, we describe a new series of roscovitine derivatives that show increased potency in vitro. The series was tested for cytotoxicity against six cancer cell lines and for inhibition of CDKs. For series bearing 2-(hydroxyalkylamino) moiety, cytotoxic potency strongly correlated with anti-CDK2 activity. Importantly, structural changes that increase biochemical and anticancer activities of these compounds also increase elimination half-life. The most potent compounds were investigated further to assess their ability to influence cell cycle progression, p53-regulated transcription and apoptosis. All the observed biological effects were consistent with inhibition of CDKs involved in the regulation of cell cycle and transcription.

1. Introduction

The cell division cycle is driven by sequential activation of cyclin-dependent kinases (CDKs), enzymes activated primarily by binding to phase-specific protein cyclins. When complexed with cyclins, CDKs are involved in, e.g., changes in the expression of cell cycle-specific genes in the G1 phase required for cell cycle entry, duplication of chromosomes and centrosomes during the S phase, mitotic spindle formation, nuclear membrane breakout, and chromatin condensation in the M phase [1]. CDKs and cyclins, as well as many other proteins that interact with them, are frequently deregulated in cancer cells, causing the cell cycle control mechanisms to be dismantled and hyperactivation of CDKs [1]. These observations have provided a basis for the development of CDK inhibitors as novel anticancer drugs.

To date, more than 20 of the most potent inhibitors have been registered for clinical trials in cancer patients [2]. These compounds are often classified according to their selectivity towards CDKs. The majority of known inhibitors exhibit activity towards a broad range of CDKs, which may be therapeutically advantageous as genetic studies have shown that CDK 2, 4 and 6 are dispensable for the cycling of most cell types, whereas CDK1 has been shown to be absolutely essential for cell proliferation, at least in mice [3–6].

One of the clinically evaluated compounds is the trisubstituted purine derivative roscovitine, which inhibits CDK 1, 2, 5, 7, and 9 [7,8]. By targeting CDK1 and CDK2, roscovitine arrests the cell cycle, while inhibition of transcriptional CDK7 and CDK9 induces apoptosis in cancer cells [9,10]. Roscovitine is currently being evaluated in patients diagnosed with non-small cell lung cancer and nasopharyngeal cancer [11].

Roscovitine is orally bioavailable but displays a strong first-pass effect and rapid clearance [12]. Moreover, it is a relatively low potency drug in comparison with other clinically evaluated CDK inhibitors, such as AT7519 or dinaciclib [13,14]. Clinical studies suggest that b.i.d. dosing is necessary to maintain therapeutically effective concentrations [15]. The aim of the present work was to prepare novel derivatives of roscovitine that possessed enhanced

Abbreviations: CDK, cyclin-dependent kinase; DIAD, diisopropyldiazadicarboxylate; NMP, *N*-methylpyrrolidone; PARP, poly(ADP-ribose)polymerase; TLC, thin layer chromatography.

* Corresponding author. Tel.: +420 585634953; fax: +420 585634870.
E-mail address: marek.zatloukal@upol.cz (M. Zatloukal).

0223-5234/$ – see front matter © 2012 Elsevier Masson SAS. All rights reserved.
http://dx.doi.org/10.1016/j.ejmech.2012.06.036

anti-kinase and cytotoxic activities as well as structural features that could increase their elimination half-lives. Replacement of the primary hydroxy group in the side-chain with an amino group, or a secondary or tertiary hydroxy moiety was conducted to prevent formation of the carboxylate, which is a dominant and relatively inactive roscovitine metabolite [16,17]. Furthermore, introduction of a basic moiety was expected to increase the affinity of the compounds for tissues [18–20].

2. Results and discussion

2.1. Synthesis

In this paper, a series of novel 2,6,9-trisubstituted purine CDK inhibitors was successfully synthesized through an improved procedure (see Experimental section 4.3., Scheme 1). The identity of all final compounds was confirmed by ^{1}H NMR, ^{1}H–^{1}H COSY, ^{13}C NMR and ^{1}H–^{13}C HSQC spectrometry, mass spectrometry (ESI-MS) and elemental analysis.

The straightforward three-step synthesis of 2,6,9-trisubstituted purines started from commercially available 2,6-dichloropurine, which was in the first step alkylated by isopropyl alcohol via Mitsunobu alkylation [21] at N9 to give 2,6-dichloro-9-isopropylpurine (**1**). A former conventional method for the preparation of this key intermediate used an isopropyl halide as an alkylating agent [22–24], but the disadvantage of this method was a poor regioselectivity as a considerable amount of by-product, which is N7 − isomer, was also formed. The crude product has to be purified by multiple crystallizations or by column chromatography. Moreover, the method uses a toxic and cancerogenic isopropyl halogenide. For this reason we decided to use the Mitsunobu alkylation reaction, which employs isopropanol as an alkylating agent [21]. The reaction temperature was kept within the range of 20–25 °C to minimize the formation of undesired N7 − isomer, on the contrast to Weibing Lu et al. [21], who carried out the alkylation at 70 °C. We have found that the regioselectivity of the alkylation decreased with an increase of the reaction temperature. This method proceeded very smoothly and was much more regioselective in comparison with the halide method. We also employed a lower excess of DIAD (1.2 eq.) and triphenyl phosphine (1.2 eq.), and shorter reaction time (1–2 h) than Weibing Lu, who used 2.1 eq. of both reactants and longer reaction time (6 h). The crude alkyl derivative was purified from contaminating by-products (triphenyl phosphine oxide and traces of N7 − isomer) by crystallization from lower alcohol or flash chromatography.

The second step, preparation of 2-chloro-6-(subst. benzylamino)-9-isopropylpurines (**2a**–**2i**, see Experimental section 4.3.2.) was a nucleophilic substitution at C6 purine position with appropriate substituted benzylamine [22,25,26]. The reaction was carried out in *n*-propanol and triethylamine, or *N*,*N*-diisopropyl-*N*-ethyl amine (Hunig's base) was used as an auxiliary base. The reaction temperature was kept within the range of 80–100 °C. The reaction time varied from 3 to 6 h, depending on the reaction temperature and amine reactivity. Crude intermediates were purified by crystallization from isopropanol, if necessary. The yields were satisfactory (70–85%) in all cases.

The final step was accomplished by previously described method [7,22,25,26]. The appropriate aminoalcohol or diamine for the S_N2 substitution at C2 was used in excess (5–20 equiv.) and Hunig's base was employed as an auxiliary base in several cases. When a C2 substituent was a rare sterically hindered amine (4-amino-2-methylbutan-2-ol, 1-amino-2-methylpropan-2-ol, (2*RS*,3*R*)-3-aminopentan-2-ol, (*S*)-3-amino-2-methylbutan-2-ol), only a small excess of amine (5–7 equiv.) was used, in the presence of an auxiliary base (DIPEA), and *N*-methylpyrrolidone was used as a solvent. The reaction temperature was kept at 150–160 °C (sealed tube) and the reaction time varied from several hours in case of reactive amines (all C2 − roscovitine amine derivatives, **3f**, **3n**, **3o**, piperazine derivatives) to 72 h in cases of less reactive sterically hindered aminoalcohols (**3b**–**e**, **3q**, **3r**, **3t**). Yields varied from 60 to 80% in cases of usage of reactive roscovitine type aminoalcohols to 20–40% in cases of sterically hindered secondary and tertiary aminoalcohols.

Crude products were purified by crystallization from diethyl ether and finally re-crystallized from mixture of ethyl acetate and hexanes (1:2). The majority of final compounds were crystallized with exception of **3c**, **3e**, **3n**, **3q**, **3r**, **3t**, which had to be purified by flash chromatography. The reaction conditions including yields were optimized in some cases for the future possibility of a large scale production.

2.2. Structure–activity relationships in biological assays

From a structural point of view, the prepared compounds differ from roscovitine by substitutions at positions 2 and 6. As in roscovitine, all compounds bear an isopropyl substitution at position 9, which was previously shown to be optimal for purine CDK inhibitors [7,27,28]. All newly synthesized purines were tested for cytotoxicity against various cancer cell lines (MCF7, K562, HOS, CEM, HCT-116, and G361) and for CDK2/5/7/9 kinase inhibition, according to established protocols [25,29]. The resulting data are presented in Table 1 and clearly show that most of new compounds are significantly more potent CDK2 inhibitors than the reference compound roscovitine, and about half of them also had higher cytotoxicity. These results confirmed previous data with another library of purine inhibitors where correlation between inhibition of CDK and antiproliferative activity was shown [32]. On the other hand, cytotoxic activities for a number of C2-piperazine derivatives (**3g**–**i**, **3m**) that have not shown reliable anti-kinase activity could be probably explained by additional off-targets as documented e.g. for roscovitine with pyridoxalkinase.

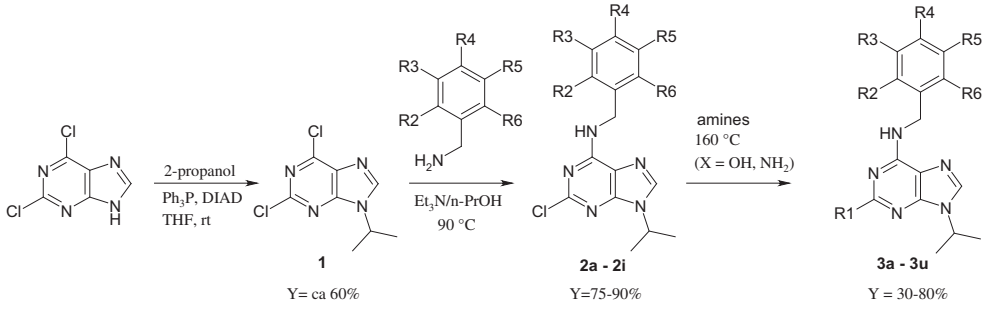

Scheme 1. Synthesis of 2,6,9-trisubstituted purine CDK inhibitors. The numbering of substituents (R1–R6) corresponds to the description of structures given in Table 1.

Table 1
Structures and biological activity of prepared compounds.

General structure	Compound	R1	R2	R3	R4	R5	R6	IC_{50}	
								CDK2 (nM)	Cytotoxicity[a] (μM)
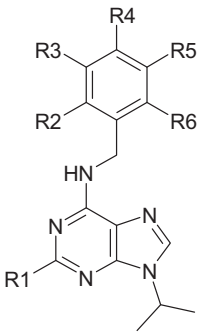	Roscovitine	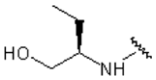	H	H	H	H	H	180	22.5
	Olomoucine II	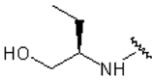	OH	H	H	H	H	50	10.6
	3a	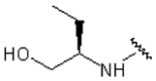	H	H	H_2N	H	H	20	31.9
	3b	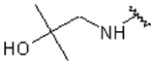	NH_2	H	H	H	H	20	17.1
	3c	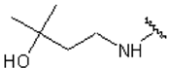	NH_2	H	H	H	H	790	100
	3d	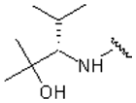	NH_2	H	H	H	H	70	23.2
	3e	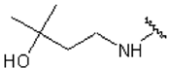	OH	H	H	H	H	260	51.6
	3f	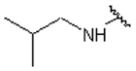	OH	H	H	H	H	220	16.7
	3g	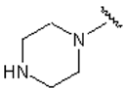	H	H	OH	H	H	340	9.2
	3h	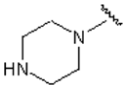	H	H	H_3CO	H	H	890	7.7
	3i	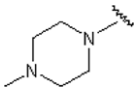	H–	H–	H_3CO–	H–	H–	890	12.6
	3j	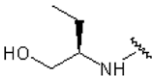	H_3CO–	H_3CO–	H–	H–	H–	31	40.5
	3k	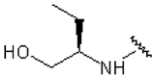	OH–	H_3CO–	H–	H–	H–	60	22.2
	3l	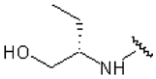	OH–	H_3CO–	H–	H–	H–	59	9.0

(*continued on next page*)

Table 1 (*continued*)

General structure	Compound	R1	R2	R3	R4	R5	R6	IC_{50}	
								CDK2 (nM)	Cytotoxicity[a] (μM)
	3m	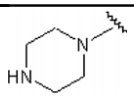	OH–	H_3CO–	H–	H–	H–	630	20.3
	3n	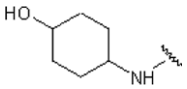	OH–	H–	H–	Cl–	H–	61	6.0
	3o	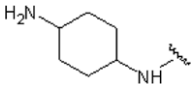	OH–	H–	H–	Cl–	H–	25	2.4
	3p	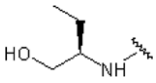	OH–	H–	H–	Cl–	H–	9.4	4.4
	3q	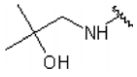	OH–	H–	H–	Cl–	H–	19.0	4.1
	3r	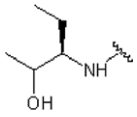	OH––	H–	H–	Cl–	H–	13.1	2.4
	3s	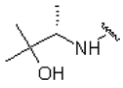	OH–	H–	H–	Cl–	H–	24.3	1.8
	3t	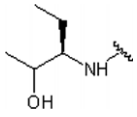	OH–	H–	H–	F–	H–	11.8	2.1
	3u	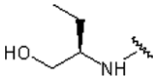	OH–	H–	H–	F–	H–	19.0	4.6

[a] Cytotoxicity averaged from measurements on a panel of 6 cancer cell lines. Full results available in the Supplementary data.

Several reports in the literature have demonstrated that a hydroxy substituent on the benzyl ring enhances CDK inhibitory activity [25,26,30,31]; an example of such a compound is olomoucine II, which has a 2-hydroxybenzyl side chain [25,32]. Except of derivatives bearing hydroxy group on the benzyl ring (**3e**–**g**) we introduced also compounds with amino group (**3a**–**d**) as well as some derivatives with methoxy group (**3h**, **3i**). CDK activity of compounds bearing this type of substituents at position 2 and different at position 6 (**3c** vs **3e**, R2 = NH_2 vs OH; **3g** vs **3h**, R2 = OH vs OCH_3) demonstrates this positive effect of hydroxy substituent (see Table 1). An addition of methoxy group at meta position (**3j**–**3l**) sustained high anti-CDK2 activity of 2-substituted compounds. A positive effect on CDK inhibition has also been shown for halogenated benzyl derivatives [26,27]. Our results indicate that the combination of both structural motives may be advantageous because substitution of hydrogen in the olomoucine II R5 position with a halide group at R5 further improved inhibitory activity (**3p**, **3u**). Overall, the 2-hydroxy-5-chloro derivatives **3o**–**s** and 2-hydroxy-5-fluoro derivatives **3t** and **3u** were the most potent among the synthesized novel compounds, both in terms of their anti-CDK2 and cytotoxic activity.

Next, we explored changes at the purine position 2 in compounds where the position 6 was occupied by substituted benzylamine. We introduced alkylamino (**3f**), aminoalkylamino (**3g**–**i**, **3m**, **3o**) and hydroxyalkylamino group with primary (**3a**, **3j**–**l**, **3p**, **3u**), secondary (including hydroxycycloalkyl) (**3n**, **3r**, **3t**) or tertiary hydroxyls (**3b**–**e**; **3q**; **3s**) at position 2. A high activity against CDK2 was observed for the structurally diverse 2-hydroxyalkylamino derivatives, which clearly correlated with antiproliferative activity (rank correlation $\rho = 0.72$, $p < 0.01$). While branching of hydroxyalkylamino substituents at position 2 did not have a pronounced effect (**3u** vs. **3t**; **3p** vs. **3r** vs. **3q**), an increase in the distance between the N2 nitrogen and the hydroxy group resulted in a loss of the activity for the compound pairs **3b**–**c** and (to lesser extent) **3p**–**n**. The high activity of **3o** in both the kinase and cytotoxicity assays suggests that not only the terminal hydroxyl (**3n**) but also the terminal amino group (**3o**) may take part in favorable binding interactions within the active site of CDKs. In

contrast, introduction of a piperazine-1-yl group at position 2 of the purine ring (**3g**–**i**, **3m**) led to a marked decrease in activity against CDK2. Since the latter compounds were all highly active against the studied cancer cell lines, their effect is probably mediated by interference with targets other than CDKs. Comparable activities of **3h** and its *N*-methylated derivative **3i** suggest that the terminal amino group acts as a basic center rather than a hydrogen bond donor in this interaction.

We, and others, have previously found that oxidation of the terminal hydroxyl at the purine position 2 to carboxylate is a major route of metabolic inactivation of roscovitine and related inhibitors in vivo [8,16,33], and protection against oxidation contributes to lower metabolic clearance [17]. Overall, the observed structure–activity relationships demonstrate that compounds in which this oxidizable group is replaced by a secondary or tertiary hydroxy or even an amino group, which do not readily convert to carboxylate, retain strong anti-CDK activity. This is in agreement with findings published recently by Wilson et al. [17], who studied similar CDK inhibitors with oxidizable group at position and showed increased stability towards mouse microsomes and promising in vivo PK properties and efficacy in vivo following oral administration for candidate compound αSβR-21 [17] 2. The analogous compounds in our study, **3b** and **3q**–**t**, belong to the most active in the described series of compounds, with IC_{50} values below 20 nM.

Several recent reports have suggested that CDK inhibition in cells causes accumulation of tumor suppressor p53 in an active form [34,35]. A positive relationship between inhibition of CDK and p53-regulated transcription is clear also for this series of compounds; rank correlation between IC_{50} for CDK 2, 5, 9 and concentration inducing p53 in cell reporter system $\rho > 0.71$ ($p < 0.05$). The most potent CDK inhibitors **3o**–**r**, **3u** and **3t** induced p53-regulated transcription at low micromolar concentrations, as assessed by a cellular reporter assay. Molecular mechanisms of induced p53-dependent transcription are not yet fully understood, but our recent studies suggest that inhibition of CDK9 (an essential transcriptional activator) leads to down-regulation of HDM2 (a negative regulator of p53), which in turn stabilizes p53 [36,37]. Therefore, in the present study we investigated the inhibitory activity of the most potent compounds towards CDKs other than CDK2, including CDK5, CDK7 and CDK9. As shown in Table 2, all compounds that potently inhibited CDK2 also exhibited a strong activity towards CDK5 and CDK9, as expected based on the high sequence and structural similarities of their active sites [38]. Interestingly, comparison of the selectivity profiles and effects on p53-regulated transcription (Table 2) suggest that activation of p53 may not be caused only by inhibition of CDK9, but also CDK2, and perhaps other kinases that were not screened. This can be seen by comparing **3r** and **3t** with **3o**, which shows that the latter produces 2-fold lower and 2-fold higher CDK2 and CDK9 inhibition, respectively. Increased potency and selectivity of **3o** towards CDK9 was however not reflected by an increased ability to activate p53.

2.3. Cellular effects of selected compounds

Compound **3r** was selected for this study as the most potent inhibitor among the series of compounds showing over 13-fold higher activity versus roscovitine in terms of CDK inhibition that corresponds with over 9-fold increase in cytotoxicity on a panel of six cancer cell lines (see Table 1). The antiproliferative activity of **3r**, was measured in an asynchronously growing colon carcinoma cell line, HCT-116, and a chronic myeloid leukemia cell line, K562. As shown in Fig. 1, inhibitor **3r** potently arrested cells in late S and G2/M phases. This effect was particularly evident in HCT-116 cells, where about 15% more cells were in the G2/M phase of the cell cycle compared to control cells after the treatment with 5 μM **3r**. Staining treated HCT-116 and K562 cells with 5-bromo-2′-deoxyuridine (BrdU) also revealed a decrease in DNA replication (Fig. 1C) in a dose-dependent manner.

Table 2
Biochemical and cellular activities of selected compounds. CDK inhibitory selectivity was determined in biochemical kinase assays; maximum activation of p53 was determined in a cellular reporter system.

Compound	IC_{50} (nM)				Maximum p53 activation (μM)
	CDK2	CDK5	CDK7	CDK9	
Roscovitine	180	1080	793	2694	24.5
Olomoucine II	51	270	n.a.	815	11.4
3b	20	740	1200	1240	16.8
3c	790	>5000	n.a.	>5000	>100
3d	70	675	290	845	24.0
3e	260	4485	n.a.	>5000	50.0
3f	220	2360	n.a.	3130	>100
3n	61	550	540	910	14.6
3o	25	125	160	39	3.4
3p	9	150	n.a.	285	10.0
3q	19	69	435	n.a.	4.1
3r	13	71	97	165	2.1
3s	24	n.a.	n.a.	n.a.	1.8
3t	11	67	180	100	2.5
3u	19	240	n.a.	106	6.6

n.a. – not available.

We next monitored levels of phosphorylation of RNA polymerase II, which is a substrate of CDK7 and CDK9, in cells treated with **3r**. Immunoblotting analysis revealed a rapid decrease in phosphorylation at serines 2 and 5 (Fig. 2A, B), confirming cellular inhibition of these two kinases. Several recent reports have suggested that inhibition of CDK9 (and inhibition of transcription in general) in cells leads to accumulation of the tumor suppressor p53 in an active form [34,35]. Therefore, we investigated the effect of treating colorectal carcinoma HCT-116 cells with **3r**. We found that **3r** rapidly increased the expression of p53 and p53-regulated $p21^{WAF1}$ at concentrations of 1 μM and higher (Fig. 2C). Accumulation of p53 was accompanied by decreased expression of Mdm-2, which is a negative regulator of p53. We also observed the same effect in a reporter assay using cell line Arn-8. **3r** exerted a dose-dependent effect on p53 transcriptional activation, with the maximum effect obtained at a concentration of 2 μM (Fig. 2D).

The strong cytotoxicity of many of the observed potent CDK inhibitors towards different cancer cell lines prompted us to analyze the mechanism of cell death induced by **3r** in HCT116 and K562 cells. The results of an immunoblotting analysis of several proteins involved in apoptotic cell death are shown in Fig. 3A and B. While expression of PUMA, Bcl-2 and caspase-3 remained largely unchanged in both cell lines treated with **3r**, the level of anti-apoptotic protein Mcl-1 showed a large dose-dependent decrease. Another typical apoptotic marker, an 89 kDa fragment of poly(ADP-ribose)polymerase (PARP), was detected in treated cells. A fluorimetry-based caspase-3/7 activity assay of lysates of HCT-116 and K562 cells treated with **3r** revealed potent dose-dependent activation of the caspase in K562 but only weak activation in HCT-116 cells (Fig. 3C).

3. Conclusions

This study involved the synthesis and modification of the biological activity of novel purine CDK inhibitors derived from roscovitine by changing the moieties at positions 2 and 6. Many of the prepared compounds proved to be more potent at limiting the proliferation of the tested cancer cell lines than roscovitine and olomoucine II. For the 2-hydroxyalkylamino derivatives studied,

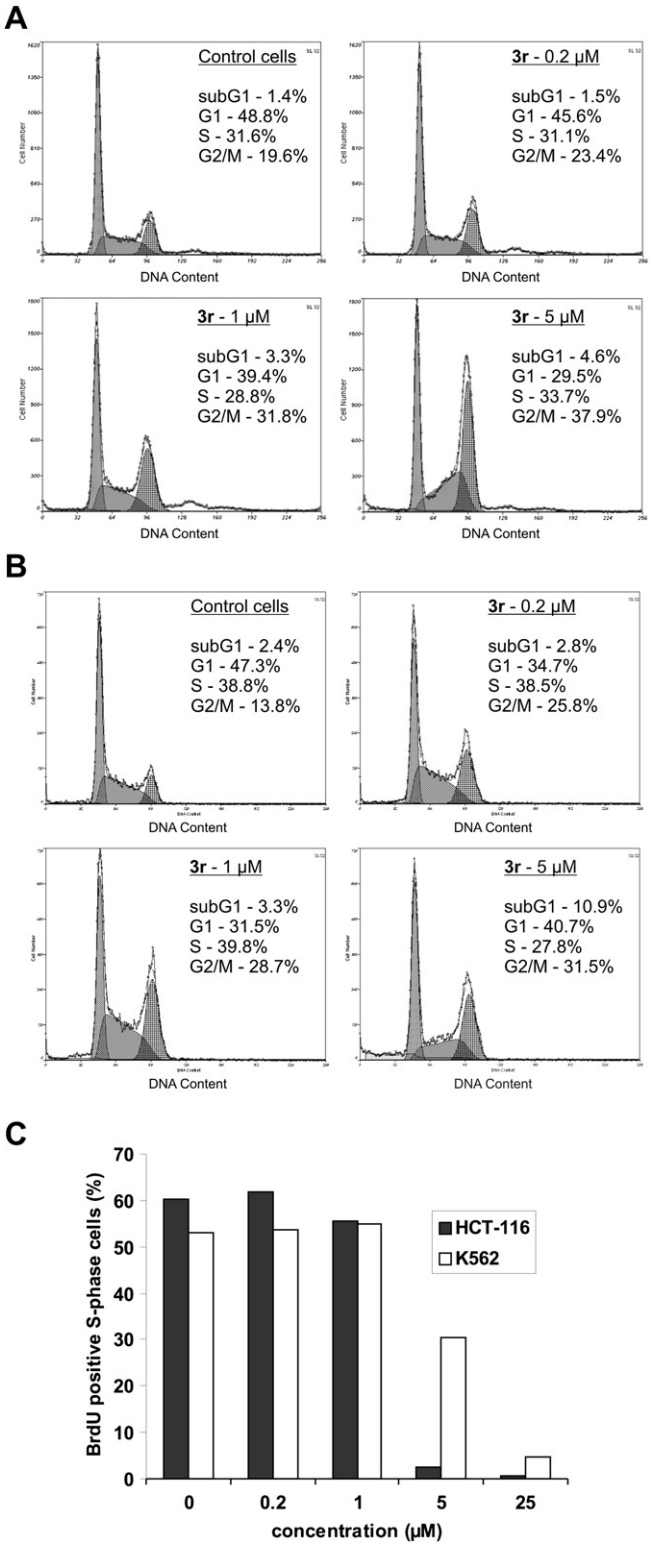

Fig. 1. Effect of **3r** on the cell cycle of HCT-116 and K562 cancer cell lines following 24 h treatment. Flow cytometric analysis of cell cycle after propidium iodide staining in (A) HCT-116 and (B) K562 cell lines, and (C) quantification of actively-replicating BrdU positive S phase cells in both cell lines.

cytotoxic potency strongly correlated with anti-CDK2 activity. However, highly cytotoxic compounds with piperazin-1-yl group at position 2 were only weak CDK2 inhibitors. Importantly, structural changes that were expected to increase the elimination half-life did not abolish biological activity. Example compound **3r** blocked cell cycle progression and induced apoptosis in cells as a result of transcriptional perturbations due to reduced phosphorylation of Ser-2 and Ser-5 in the C-terminal domain of RNAP-II, caused by inhibition of CDK9 and CDK7. Pharmacokinetic studies of selected derivatives are currently underway.

4. Experimental

4.1. General procedures

The elemental contents of the prepared compounds were determined using an EA1108 CHN analyzer (Thermo Finnigan). Their melting points were determined using a Büchi Melting Point B-540 apparatus. Thin layer chromatography (TLC) was performed using silica gel 60 WF_{254} plates (Merck) with a mobile phase ($CHCl_3$:MEOH:conc. NH_4OH, 8:2:0.2, v/v/v). Flash chromatography was performed using a VersaFlash purification station (Supelco) coupled to a 2110 Fraction Collector (Bio-Rad). Compounds were separated on VersaPak Cartridges (25 × 100 mm, Supelco) containing 23 g of spherical silica and eluted with a mobile phase ($CHCl_3$:MeOH, 90:10, v/v). To determine their HPLC purity, samples were dissolved in HPLC mobile phase (initial conditions), applied to an RP-column (150 mm × 4.6 mm, 5 μm, Microsorb C18; Varian) and the separated constituents were eluted with a linear methanolic gradient (10–90% over 30 min, pH adjusted to 4 using ammonium formate) at a flow rate of 0.6 ml/min. Eluting compounds were detected by scanning the UV absorbance of the eluate between 240 and 300 nm. CI+ and EI+ mass spectra were recorded using a Polaris Q (Finnigan) mass spectrometer equipped with a Direct Insertion Probe (DIP). The compounds were heated in an ion source with a 40–450 °C temperature gradient, the mass monitoring interval was 50–1000 am, and spectra were collected using 1.0 s cyclical scans, applying 70 eV electron energy. In the CI+ ionization mode, isobutane was used as a reagent gas at a flow rate of 2 l/h. The mass spectrometer was directly coupled to an Xcalibur data system. NMR spectra were acquired using a Bruker Avance AV 300 spectrometer operating at a temperature of 300 K and a frequency of 300.13 MHz (^1H). Samples were prepared by dissolving compounds in DMSO-d_6 and tetramethylsilane (TMS) was used as the internal standard.

4.2. Chemicals

2,6-Dichloropurine and 4-aminomethylphenol were obtained from OlChemim. Triphenylphosphine, diisopropyldiazadicarboxylate (DIAD), 2-aminobenzylamine, 4-aminobenzylamine, 4-methoxybenzylamine, *R*,*S*-2-amino-1-butanol, *S*-valinol, 1,4-*trans*-diaminocyclohexane, azacycloheptane, piperazine, *N*-methylpiperazine were purchased from Sigma–Aldrich. Variously substituted benzylamines were prepared via reduction of oximes of corresponding substituted benzaldehydes [39]. Secondary and tertiary aminoalcohols, as (2*RS*, 3*R*)-3-aminopentan-2-ol, (*S*)-3-amino-2-methylbutan-2-ol, 1-amino-2-methylpropan-2-ol, 4-amino-2-methylbutan-2-ol and 2,4-dimethyl-3-aminopentan-2-ol were synthesized according the described procedure [40]. Lach-Ner supplied methanol, 2-propanol, chloroform, diethyl ether, dimethylformamide, ethyl acetate, anhydrous magnesium sulfate. Milli-Q water was used throughout. Solvents and chemicals used were all of standard p.a. quality.

4.3. Synthesis of 2,6,9-trisubstituted purines

4.3.1. 2,6-Dichloro-9-isopropylpurine (*1*)

2,6-Dichloropurine (1.89 g; 0.01 mol) was dissolved under a nitrogen atmosphere in a mixture of tetrahydrofuran (40 ml) and

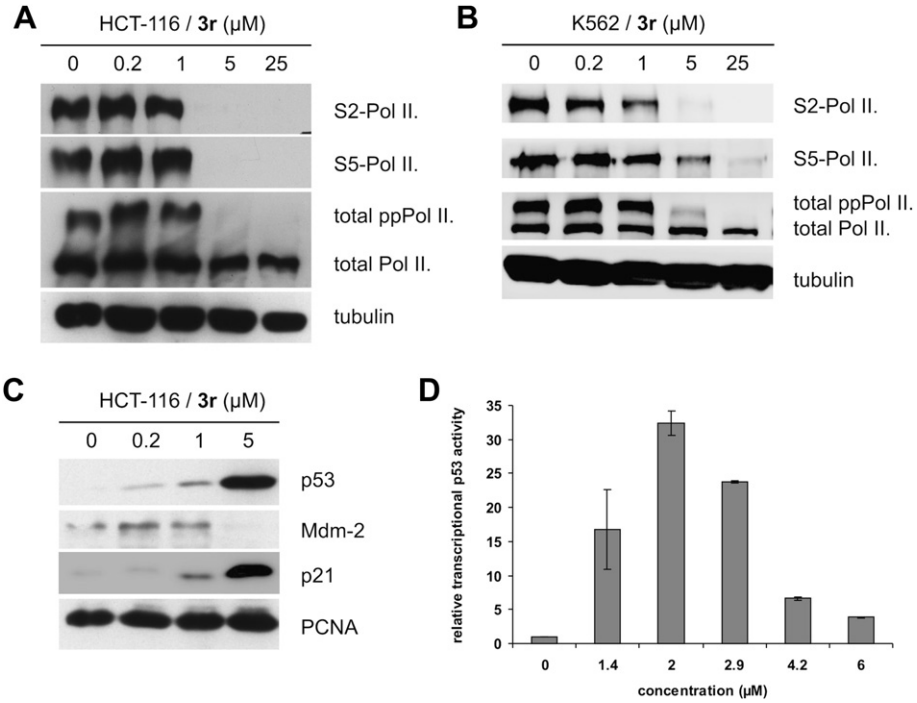

Fig. 2. Effect of **3r** on transcription and activation of p53 in HCT-116 and K562 cell lines following 24 h treatment. (A, B) Immunoblotting analysis of phosphorylation of RNA polymerase II at serines 2 and 5. Tubulin levels were detected to verify equal protein loading. (C) Immunoblotting of p53, $p21^{WAF1}$ and Mdm-2 in HCT-116 cells; PCNA levels were detected to verify equal protein loading. (D) Analysis of relative p53-dependent transcriptional activity by β-galactosidase reporter assay of Arn-8 cell line.

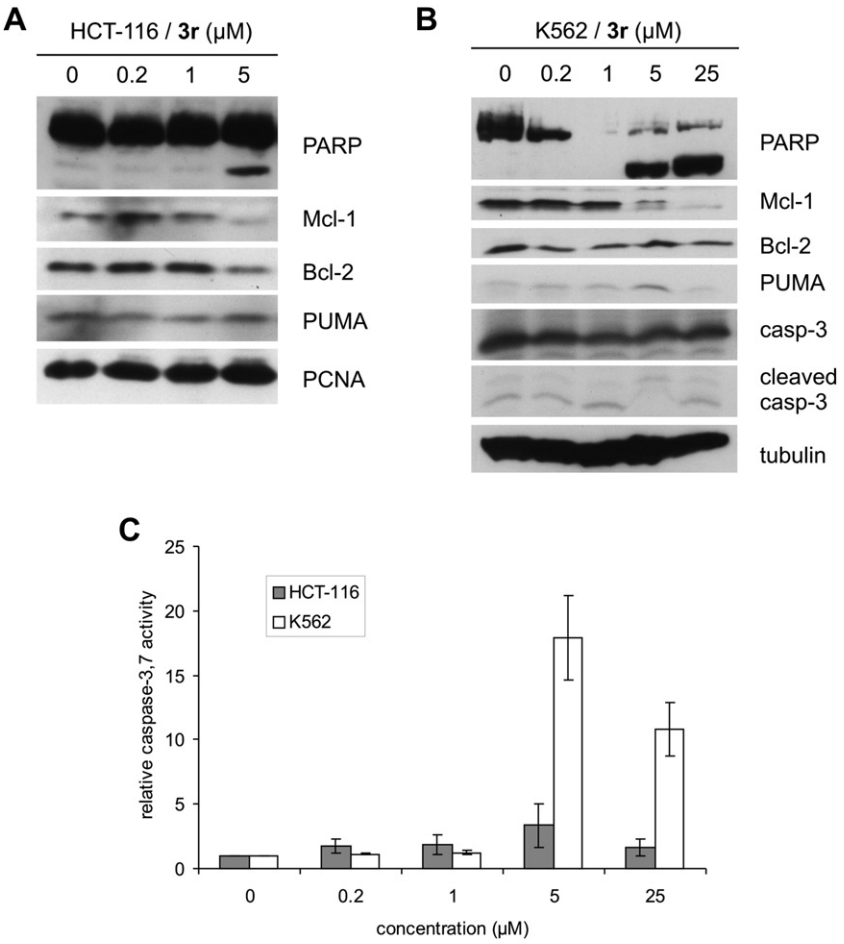

Fig. 3. Effect of **3r** on induction of apoptosis in HCT-116 and K562 cell lines following 24 h treatment. (A, B) Immunoblotting analysis of selected apoptotic markers. PCNA and tubulin levels were detected to verify equal protein loading. (C) Fluorimetric caspase-3,7 activity assay based on the cleavage of a specific Ac-DEVD-AMC peptide substrate.

isopropanol (4 ml; 0.06 mol), and then triphenyl phosphine (3.14 g; 0.012 mol) and DIAD (2.4 ml; 0.012 mol; dropwise) were added. The temperature of reaction mixture was maintained at 20–25 °C during addition of DIAD. The reaction mixture was the stirred for 2 h at 20–25 °C. TLC (mobile phase: ethyl acetate – toluene; 1:1) after 2 h indicated that the reaction had gone to completion. The reaction mixture was then evaporated to a thick yellow residue, which was dissolved in hot (60 °C) methanol (30 ml). After crystallization in a refrigerator (−18 °C) overnight, the crystalline mass was collected by filtration, washed with cold (−10 °C) methanol (2 × 5 ml) and dried in the vacuum drying oven (60 °C) to constant weight. Yield: 1.20 g of almost white crystalline powder (52%). The purity (HPLC): >98%.

M.p. = 149–152 °C. Physico-chemical data including ^{1}H NMR were in accordance with those published [21–24]. The second crop (up to 10%) of product of lower purity could be obtained from mother liquor.

*4.3.2. 2-Chloro-6-(subst. benzylamino)-9-isopropylpurines (**2a**–**2i**)*

2,6-Dichloro-9-isopropylpurine (0.05 mol), appropriate substituted benzylamine (0.05 mol), *n*-propanol (230 ml) and triethylamine (0.15 mol) were placed into a reaction bulb, under nitrogen. The reaction mixture was warmed up to 90 °C, and stirred for a period of 4 h. The contents of the bulb were then evaporated on rotary vacuum evaporator to give a semisolid residue, which was then treated with water (200 ml) for 20 min. The precipitate was filtered off, washed with water (3 × 20 ml) and dried in the vacuum oven to constant weight. Yield: 75–90%, according to the type of benzylamine used. The purity (HPLC): min. 97%. The crude product can be purified by crystallization from isopropyl alcohol if required.

According to this procedure the following compounds were prepared:

*4.3.2.1. (4-Aminobenzyl)-(2-chloro-9-isopropyl-9H-purin-6-yl)-amine (**2a**).* ^{1}H NMR (DMSO-d_6): 1.49 (d, J = 6.6, 6H, CH_3), 4.44 (d, J = 6.7, 2H, CH_2), 4.66 (sep, J = 6.6, 1H, CH), 5.21 (s(br), 2H, NH_2), 6.49 (t, J = 7.0, 1H, ArH), 6.62 (d, J = 7.8, 1H, ArH), 6.94 (t, J = 7.0, 1H, ArH), 7.08 (d, J = 7.8, 1H, ArH), 8.28 (s, 1H, CH), 8.67 (t, J = 6.7, 1H, NH).

*4.3.2.2. (2-Aminobenzyl)-(2-chloro-9-isopropyl-9H-purin-6-yl)-amine (**2b**).* ^{1}H NMR (DMSO-d_6): 1.49 (d, J = 6.6, 6H, CH_3), 4.44 (d, J = 6.7, 2H, CH_2), 4.66 (sep, J = 6.6, 1H, CH), 5.21 (s(br), 2H, NH_2), 6.49 (t, J = 7.0, 1H, ArH), 6.62 (d, J = 7.8, 1H, ArH), 6.94 (t, J = 7.0, 1H, ArH), 7.08 (d, J = 7.8, 1H, ArH), 8.28 (s, 1H, CH), 8.67 (t, J = 6.7, 1H, NH).

*4.3.2.3. 2-[(2-Chloro-9-isopropyl-9H-purin-6-ylamino)-methyl]-phenol (**2c**).* ^{1}H NMR (DMSO-d_6): 1.64 (d, J = 6.8, 6H, CH_3), 4.68 (d, J = 5.3, 2H, CH_2), 4.92 (sep, J = 6.8, 1H, CH), 6.86 (t, J = 7.5, 1H, ArH), 6.97 (d, J = 8.2, 1H, ArH), 7.20 (t, J = 8.2, 1H, ArH), 7.28 (d, J = 7.5, 1H, ArH), 8.44 (t, J = 5.3, 1H, NH), 8.59 (s, 1H, CH), 9.92 (s, 1H, OH).

*4.3.2.4. 4-[(2-Chloro-9-isopropyl-9H-purin-6-ylamino)-methyl]-phenol (**2d**).* ^{1}H NMR (DMSO-d_6): 1.46 (d, J = 6.0, 6H, CH_3), 4.49 (d, J = 5.4, 2H, CH_2), 4.57 (sep, J = 6.0, 1H CH), 6.69 (d, J = 7.50, 2H, ArH), 7.13 (d, J = 7.50, 2H, ArH), 7.85 (t, J = 5.4, 1H, NH), 8.15 (s, 1H, CH), 10.15 (s(br), 1H, OH).

*4.3.2.5. (2-Chloro-9-isopropyl-9H-purin-6-yl)-(4-methoxybenzyl)-amine (**2e**).* ^{1}H NMR (DMSO-d_6): 1.49 (d, J = 6.2, 6H, CH_3), 3.72 (s, 3H, CH_3), 4.50 (s(br), 2H, CH_2), 4.65 (sep, J = 6.2, 1H, CH), 6.83 (d, J = 7.75, 2H, ArH), 7.29 (d, J = 7.75, 2H, ArH), 7.80 (s(br), 1H, NH), 7.95 (s, 1H, CH).

*4.3.2.6. (2-Chloro-9-isopropyl-9H-purin-6-yl)-(2,3-dimethoxybenzyl)-amine (**2f**).* ^{1}H NMR (DMSO-d_6): 1.46 (d, J = 6.0, 6H, CH_3), 3.75–3.77 (m, 6H, 2 × CH_3), 4.50 (s(br), 2H, CH_2), 4.58 (sep, J = 6.0, 1H, CH), 6.67 (t, J = 8.2, 1H, ArH), 6.75–6.88 (m, 2H, ArH), 7.50 (s(br), 1H, NH), 7.78 (s, 1H, CH).

*4.3.2.7. 2-[(2-Chloro-9-isopropyl-9H-purin-6-ylamino)-methyl]-6-methoxyphenol (**2g**).* ^{1}H NMR (DMSO-d_6): 1.49 (d, J = 6.6, 6H, CH_3), 3.77 (s, 3H, CH_3), 4.44 (d, J = 6.7, 2H, CH_2), 4.68 (sep, J = 6.6, 1H, CH), 6.68–6.88 (m, 3H, ArH), 8.28 (s, 1H, CH), 8.67 (t, J = 6.7, 1H, NH), 9.32 (s, 1H, OH).

*4.3.2.8. 4-Chloro-2-[(2-chloro-9-isopropyl-9H-purin-6-ylamino)-methyl]-phenol (**2h**).* ^{1}H NMR (DMSO-d_6): 1.47 (d, J = 6.6, 6H, CH_3), 4.53 (d, J = 5.6, 2H, CH_2), 4.62 (sep, J = 6.8, 1H, CH), 6.79 (d, J = 8.5, 1H, ArH), 7.02–7.09 (m, 2H, ArH), 8.28 (s, 1H, CH), 8.61 (t, J = 5.6, 1H, NH), 9.92 (s, 1H, OH).

*4.3.2.9. 2-[(2-Chloro-9-isopropyl-9H-purin-6-ylamino)-methyl]-4-fluorophenol (**2i**).* ^{1}H NMR (DMSO-d_6): 1.50 (d, J = 6.5, 6H, CH_3), 4.56 (d, J = 4.7, 2H, CH_2), 4.68 (sep, J = 6.3, 1H, CH), 6.75–6.92 (m, 3H, ArH), 8.31 (s, 1H, CH), 8.61 (t, J = 4.7, 1H, NH), 9.63 (s, 1H, OH).

*4.3.3. Substitution at C2 (**3a**–**3u**; final compounds)*

2-Chloro-6-(subst. benzyl)amino-9-isopropylpurine (0.01 mol) and appropriate aminoalcohol or diamine (0.1–0.2 mol) were stirred under nitrogen at 160 °C for 3–12 h, the time depending on the reactivity of amine used and on the character of substituent at C6. The course of the reaction was monitored by TLC (mobile phase: chloroform–methanol 85:15 + trace of ammonia). After the reaction had gone to completion, the reaction mixture was evaporated on a rotary vacuum evaporator. The residue was partitioned between water (100 ml) and ethyl acetate (100 ml). The organic layer was separated and the water phase was extracted with ethyl acetate (2 × 50 ml). The combined organic layers were washed with water (30 ml), dried with anhydrous magnesium sulfate, and evaporated to dryness. The sticky residue was treated with diethyl ether (75 ml). The product gradually crystallized. The crude substance was purified by crystallization from ethyl acetate–hexane (1:1). In some cases a purification by flash chromatography of products was necessary. Yield: 30–80%, according to the type of amine used; purity (HPLC: >98%). When an expensive aminoalcohol or diamine were employed, the reaction conditions could be modified by adding a suitable solvent (e.g. NMP) and an auxiliary base (e.g. *N*,*N*-diisopropyl-*N*-ethyl amine).

*4.3.4. (R)-2-[6-(4-Aminobenzylamino)-9-isopropyl-9H-purin-2-ylamino]-butan-1-ol (**3a**)*

The compound was prepared from the intermediate ***2a*** and (*R*)-2-amino-butan-1-ol by heating at 160 °C for 3 h. Yield: 72%; white solid. M.p. = 126–128 °C. ^{1}H NMR (DMSO-d_6): 0.86 (t, J = 6.5, 3H, CH_3), 1.46 (d, J = 6.0, 6H, CH_3), 1.54–1.69 (m, 2H, CH_2), 3.42–3.55 (m, 2H, CH_2), 3.85 (sex, J = 6.2, 1H, CH), 4.40 (s(br), 2H, CH_2), 4.49 (sep, J = 6.0, 1H, CH), 4.57 (t, J = 6.0, 1H, OH), 4.92 (s(br), 2H, NH_2), 5.83 (d, J = 6.2, 1H, NH), 6.47 (d, J = 7.4, 2H, ArH), 7.11 (d, J = 7.4, 2H, ArH), 7.48 (s(br), 1H, NH), 7.78 (s, 1H, CH). ^{13}C NMR (DMSO-d_6): 11.50, 22.35, 23.04, 24.43, 48.01, 54.00, 61.13, 111.05, 117.22, 120.37, 128.64, 135.91, 151.37, 154.34, 154.99, 159.39. MS *m*/*z* (ESI) 370.2 $(M + H)^+$. Anal.: Calcd for $C_{19}H_{27}N_7O$: C, 61.77; H, 7.37; N, 26.54. Found: C, 61.39; H, 7.38; N, 26.25.

*4.3.5. 1-[6-(2-Aminobenzylamino)-9-isopropyl-9H-purin-2-ylamino]-2-methylpropan-2-ol (**3b**)*

The compound was prepared from the intermediate ***2b*** and 1-amino-2-methylpropan-2-ol by heating at 160 °C in the presence of *N*,*N*-diisopropyl ethyl amine for 48 h. Yield: 80%; white solid. M.p. = 181–183 °C. ^{1}H NMR (DMSO-d_6): 1.10 (s, 6H, CH_3), 1.45

(d, J = 6.4, 6H, CH_3), 3.27 (d, J = 5.6, 2H, CH_2), 4.46 (s(br), 2H, CH_2), 4.54 (sep, J = 6.4, 1H, CH), 4.84 (s(br), 1H, OH), 5.21 (s(br), 2H, NH_2), 6.09 (t, J = 5.6, 1H, NH), 6.45 (t, J = 7.1, 1H, ArH), 6.58 (d, J = 7.1, 1H, ArH), 6.91 (t, J = 6.9, 1H, ArH), 7.12 (d, J = 7.1, 1H, ArH), 7.66 (s(br), 1H, NH), 7.80 (s, 1H, CH). ^{13}C NMR (DMSO-d_6): 22.07, 27.53, 42.10, 45.63, 52.41, 69.99, 113.61, 114.42, 115.45, 122.86, 127.46, 129.53, 135.04, 146.25, 154.41, 159.47. MS m/z (ESI) 370.2 $(M + H)^+$. Anal.: Calcd. for $C_{19}H_{27}N_7O$: C, 61.77; H, 7.37; N, 26.54. Found: C, 61.83; H, 7.59; N, 27.02.

4.3.6. 4-[6-(2-Aminobenzylamino)-9-isopropyl-9H-purin-2-ylamino]-2-methylbutan-2-ol (**3c**)

The compound was prepared from **2b** and 1-amino-3-methylbutan-3-ol by heating at 160 °C in NMP in the presence of *N*,*N*-diisopropyl ethyl amine for 72 h. The crude product was purified by flash chromatography. Yield: 27%; off white amorphous solid. ^{1}H NMR (DMSO-d_6): 1.11 (s, 6H, CH_3), 1.51 (d, J = 6.5, 6H, CH_3), 3.35 (q, J = 6.9, 2H, CH_2), 4.61 (sep, J = 6.5, 1H, CH), 4.68 (s(br), 2H, CH_2), 4.86 (s(br), 1H, OH), 5.21 (s(br), 2H, NH_2), 6.11 (t, J = 6.9, 1H, NH), 7.18–7.43 (m, 4H, ArH), 7.67 (s(br), 1H, NH), 7.80 (s, 1H, CH). ^{13}C NMR (DMSO-d_6): 22.07, 26.30, 27.53, 42.20, 44.92, 52.50, 70.03, 113.61, 114.42, 115.45, 122.86, 127.46, 129.53, 135.04, 146.25, 154.41, 159.47. MS m/z (ESI) 384.2 $(M + H)^+$. The compound was transferred into its corresponding dihydrochloride salt. M.p. = 196–199 °C; white solid. Anal.: Calcd for $C_{20}H_{29}N_7O$. 2 HCl: C, 52.63; H, 6.85; N, 21.48. Found: C, 52.41; H, 6.92; N, 21.14.

4.3.7. (S)-3-[6-(2-Aminobenzylamino)-9-isopropyl-9H-purin-2-ylamino]-2,4-dimethylpentan-2-ol (**3d**)

The compound was prepared from **2b** and 1-amino-2,4-dimethylpentan-2-ol by heating at 160 °C in NMP in the presence of *N*,*N*-diisopropyl ethyl amine for 72 h. Yield: 28%; white solid. M.p. = 198–200 °C. ^{1}H NMR (DMSO-d_6): 0.87–0.90 (d, J = 6.90, 6H, CH_3), 1.04 (s, 3H, CH_3), 1.18 (s, 3H, CH_3), 1.45 (d, J = 6.6, 6H, CH_3), 2.11 (sep, J = 6.9, 1H, CH), 3.93–3.97 (d, J = 6.9, 1H, CH), 4.33 (s(br), 1H, OH), 4.47 (s(br), 2H, CH_2), 4.53 (sep, J = 6.6, 1H, CH), 5.21 (s(br), 2H, NH_2), 5.56 (d, J = 6.9, 1H, NH), 6.44 (t, J = 7.4, 1H, ArH), 6.59 (d, J = 7.4, 1H, ArH), 6.91 (t, J = 7.4, 1H, ArH), 7.14 (d, J = 7.4, 1H, ArH), 7.57 (s(br), 1H, NH), 7.76 (s, 1H, CH). ^{13}C NMR (DMSO-d_6): 17.64, 21.89, 22.79, 28.01, 28.44, 61.27, 67.65, 72.57, 114.35, 115.34, 127.42, 129.73, 134.90, 146.22, 150.60, 154.35, 160.17. MS m/z (ESI) 412.2 $(M + H)^+$. Anal.: Calcd. for $C_{22}H_{33}N_7O$: C, 64.21; H, 8.08; N, 23.82. Found: C, 63.98; H, 8.11; N, 23.55.

4.3.8. 2-{[2-(3-Hydroxy-3-methylbutylamino)-9-isopropyl-9H-purin-6-ylamino]-methyl}-phenol (**3e**)

The compound was prepared from the intermediate **2c** and 1-amino-3-methylbutan-3-ol by heating at 160 °C for 72 h. The crude product was purified by flash chromatography. Yield: 43%; white solid. M.p. = 72–75 °C. ^{1}H NMR (DMSO-d_6): 1.11 (s, 6H, CH_3), 1.46 (d, J = 6.7, 6H, CH_3), 1.65 (t, J = 6.5, 2H, CH_2), 3.29 (q, J = 6.5, 2H, CH_2), 4.28 (s, 1H, OH), 4.50–4.57 (m, 3H, CH, CH_2), 6.30 (t, J = 6.5, 1H, NH), 6.69–6.78 (m, 2H, ArH), 7.05 (t, J = 7.3, ArH), 7.14 (d, J = 7.3, 1H, ArH), 7.56 (s(br), 1H, NH), 7.79 (s, 1H, CH), 9.99 (s(br), 1H, OH). ^{13}C NMR (DMSO-d_6): 22.02, 29.47, 37.56, 42.53, 45.74, 68.57, 84.60, 115.35, 118.73, 122.30, 126.27, 127.82, 128.85, 135.22, 139.85, 150.47, 155.03, 158.81. MS m/z (ESI) 385.3 $(M + H)^+$. Anal.: Calcd. for $C_{20}H_{28}N_6O_2$: C, 62.48; H, 7.34; N, 21.86. Found: C, 62.20; H, 7.31; N, 21.55.

4.3.9. 2-[(2-Isobutylamino-9-isopropyl-9H-purin-6-ylamino)-methyl]-phenol (**3f**)

The compound was prepared from **2c** and isobutyl amine by heating at 160 °C in NMP in the presence of *N*,*N*-diisopropyl ethyl amine for 12 h. Yield: 45%; white solid. M.p. = 83–85 °C. ^{1}H NMR (DMSO-d_6): 0.85 (d, J = 6.6, 6H, CH_3), 1.46 (d, J = 6.7, 6H, CH_3), 1.84 (sep, J = 6.6, 1H, CH), 3.05 (t, J = 6.3, 2H, CH_2), 4.47–4.60 (m, 3H, CH_2, CH), 6.39 (t, J = 6.3, 1H, NH), 6.71 (t, J = 7.4, 1H, ArH), 6.75 (d, J = 7.4, 1H, ArH), 7.04 (t, J = 7.4, 1H, ArH), 7.14 (d, J = 7.4, 1H, ArH), 7.55 (s(br), 1H, NH), 7.79 (s, 1H, CH), 9.94 (s(br), 1H, OH). ^{13}C NMR (DMSO-d_6): 20.26, 21.90, 27.75, 45.62, 48.78, 52.5, 113.41, 114.1, 115.17, 118.60, 126.10, 127.65, 128.66, 135.10, 154.90, 158.92. MS m/z (ESI) 355.4 $(M + H)^+$. Anal.: Calcd. for $C_{19}H_{26}N_6O$: C, 64.38; H, 7.39; N, 23.71. Found: C, 64.23; H, 7.41; N, 23.55.

4.3.10. 4-[(9-Isopropyl-2-piperazin-1-yl-9H-purin-6-ylamino)-methyl]-phenol (**3g**)

The compound was prepared from the intermediate **2d** and piperazine by heating at 160 °C for 20 h. Yield: 51%; white solid. M.p. = 156–158 °C. ^{1}H NMR (DMSO-d_6): 1.46 (d, J = 6.0, 6H, CH_3), 2.84–2.95 (m, 4H, CH_2), 3.69–3.80 (m, 4H, CH_2), 4.49 (s(br), 2H, CH_2), 4.57 (sep, J = 6.0, 1H, CH), 6.70 (d, J = 7.5, 2H, ArH), 7.16 (d, J = 7.5, 2H, ArH), 7.85 (s, 1H, CH), 8.15 (s, 1H, NH), 9.50 (s(br), 1H, NH), 10.15 (s(br), 1H, OH). ^{13}C NMR (DMSO-d_6): 21.97, 43.40, 44.07, 45.70, 54.93, 113.41, 114.74, 128.67, 130.76, 132.58, 135.81, 150.37, 154.00, 155.97, 157.91. MS m/z (ESI) 368.0 $(M + H)^+$. Anal.: Calcd. for $C_{19}H_{25}N_7O$: C, 62.11; H, 6.86; N, 26.68. Found: C, 62.23; H, 6.90; N, 26.55.

4.3.11. (9-Isopropyl-2-piperazin-1-yl-9H-purin-6-yl)-(4-methoxybenzyl)-amine (**3h**)

The compound was prepared from the intermediate **2e** and piperazine by heating at 160 °C for 20 h. Yield: 45%; white solid. M.p. = 132–134 °C. ^{1}H NMR (DMSO-d_6): 1.49 (d, J = 6.2, 6H, CH_3), 2.64–2.72 (m, 4H, CH_2), 3.56–3.65 (m, 4H, CH_2), 3.72 (s, 3H, OCH_3), 4.50 (s(br), 2H, CH_2), 4.65 (sep, J = 6.2, 1H, CH), 6.83 (d, J = 7.6, 2H, ArH), 7.29 (d, J = 7.6, 2H, ArH), 7.80 (1H, s, CH), 7.95 (s(br), 1H, NH), 10.15 (s(br), 1H, NH). ^{13}C NMR (DMSO-d_6): 21.95, 44.85, 45.25, 45.61, 54.47, 59.65, 64.81, 113.38, 128.66, 132.68, 135.52, 150.54, 156.00, 157.94, 158.33. MS m/z (ESI) 382.1 $(M + H)^+$. Anal.: Calcd. for $C_{20}H_{27}N_7O$: C, 62.97; H, 7.13; N, 25.70. Found: C, 62.43; H, 7.13; N, 25.11.

4.3.12. [9-Isopropyl-2-(4-methylpiperazin-1-yl)-9H-purin-6-yl]-(4-methoxybenzyl)-amine (**3i**)

The compound was prepared from **2e** and *N*-methylpiperazine by heating at 135 °C for 4 h. Yield: 56%; almost white solid. M.p. = 129–130 °C. ^{1}H NMR (DMSO-d_6): 1.46 (d, J = 6.0, 6H, CH_3), 2.17 (s, 3H, OCH_3), 2.26–2.37 (m, 4H, CH_2), 3.63–3.72 (m, 6H, CH_2), 4.57 (sep, J = 6.0, 1H, CH), 6.85 (d, J = 7.5, 2H, ArH), 7.30 (d, J = 7.5, 2H, ArH), 7.82 (s, 1H, CH), 7.95 (s(br), 1H, NH), 10.25 (s(br), 1H, H19). ^{13}C NMR (DMSO-d_6): 21.67, 42.45, 43.95, 45.61, 54.84, 64.81, 133.36, 128.64, 132.62, 135.54, 150.48, 153.99, 157.95, 158.20. MS m/z (ESI) 396.2 $(M + H)^+$. Anal.: Calcd. for $C_{21}H_{29}N_7O$: C, 63.77; H, 7.39; N, 24.79. Found: C, 63.63; H, 7.40; N, 24.55.

4.3.13. (R)-2-[6-(2,3-Dimethoxybenzylamino)-9-isopropyl-9H-purin-2-ylamino]-butan-1-ol (**3j**)

The compound was prepared by heating of **2f** in (*R*)-2-amino-butan-1-ol at 160 °C for 3 h. Yield: 65%; white solid. M.p. = 102–105 °C. ^{1}H NMR (DMSO-d_6): 0.81 (t, J = 7.0, 3H, CH_3), 1.42–1.45 (m, 1H, CH_2a), 1.46 (d, 6H, J = 7.0), 1.47–1.49 (m, 1H, CH_2b), 3.35–3.45 (m, 2H, CH_2), 3.77 (s, 3H, OCH_3), 3.79 (s, 3H, OCH_3), 4.45–4.54 (m, 2H, 2 × CH), 4.57 (s(br), 2H, CH_2), 5.79 (d, J = 6.2, 1H, NH), 6.82 (d, J = 6.9, 1H, ArH), 6.85–6.97 (m, 2H, ArH), 7.45 (s(br), 1H, NH), 7.78 (s, 1H, CH). ^{13}C NMR (DMSO-d_6): 10.63, 22.00, 22.10, 23.86, 45.65, 54.00, 55.63, 55.68, 62.95, 111.26, 119.64, 124.15, 133.85, 146.00, 152.14, 154.61, 158.99. MS m/z (ESI) 415.1 $(M + H)^+$. Anal.: Calcd. for $C_{21}H_{30}N_6O_3$: C, 60.85; H, 7.30; N, 20.27. Found: C, 60.61; H, 7.32; N, 20.09.

*4.3.14. 2-{[2-((R)-1-Hydroxymethylpropylamino)-9-isopropyl-9H-purin-6-ylamino]-methyl}-6-methoxyphenol (**3k**)*

The compound was prepared by heating of **2g** in (*R*)-2-amino-butan-1-ol (excess) at 160 °C for 3 h. Yield: 43%; almost white solid. M.p. = 100–103 °C. ^{1}H NMR (DMSO-d_6): 0.86 (t, J = 6.9, 3H, CH_3), 1.46 (d, J = 6.5, 6H, CH_3), 1.63 (sex, J = 6.2, 1H, CH), 2.54 (s(br), 1H, OH), 3.39–3.54 (m, 2H, CH_2), 3.77 (s, 3H, OCH_3), 3.83 (sep, J = 6.9, 1H, CH), 4.48–4.58 (m, 2H, CH_2), 4.63 (s(br), 2H, CH_2), 5.85 (d, 1H, J = 6.2, NH), 6.68–6.88 (m, 3H, ArH), 7.50 (s(br), 1H, NH), 7.78 (s, 1H, CH), 9.32(s(br), 1H, OH). ^{13}C NMR (DMSO-d_6): 10.56, 15.07, 21.86, 21.95, 45.76, 54.01, 55.75, 62.92, 64.83, 110.73, 113.55, 118.43, 120.65, 126.78, 135.21, 144.01, 147.57, 150.55, 154.42, 158.74. MS m/z (ESI) 401.2 $(M + H)^+$. Anal.: Calcd. for $C_{20}H_{28}N_6O_3$: C, 59.98; H, 7.05; N, 20.98. Found: C, 59.63; H, 7.05; N, 20.59.

*4.3.15. 2-{[2-((S)-1-Hydroxymethylpropylamino)-9-isopropyl-9H-purin-6-ylamino]-methyl}-6-methoxyphenol (**3l**)*

The compound was prepared by heating of **2g** in (*S*)-2-amino-butan-1-ol (excess) at 160 °C for 3 h. Yield: 40%; almost white solid. M.p. = 100–102 °C. ^{1}H NMR (DMSO-d_6): 0.86 (t, J = 6.9, 3H, CH_3), 1.46 (d, J = 6.5, 6H, CH_3), 1.63 (sex, J = 6.2, 1H, CH), 2.54 (s(br), 1H, OH), 3.39–3.54 (m, 2H, CH_2), 3.77 (s, 3H, OCH_3), 3.83 (sep, 1H, J = 6.9, CH), 4.48–4.58 (m, 2H, CH_2), 4.63 (s(br), 2H, CH_2), 5.85 (d, J = 6.2, 1H, NH), 6.68–6.88 (m, 3H, ArH), 7.50 (s(br), 1H, NH), 7.78 (s, 1H, CH), 9.32 (s(br), 1H, OH). ^{13}C NMR (DMSO-d_6): 10.56, 15.07, 21.86, 21.95, 45.76, 54.01, 55.75, 62.92, 64.83, 110.73, 113.55, 118.43, 120.65, 126.78, 135.21, 144.01, 147.57, 150.55, 154.42, 158.74. MS m/z (ESI) 401.2 $(M + H)^+$. Anal.: Calcd. for $C_{20}H_{28}N_6O_3$: C, 59.98; H, 7.05; N, 20.98. Found: C, 59.63; H, 7.05; N, 20.59.

*4.3.16. 2-[(9-Isopropyl-2-piperazin-1-yl-9H-purin-6-ylamino)-methyl]-6-methoxyphenol (**3m**)*

The compound was prepared by heating of **2g** in molten piperazine (excess) at 160 °C for 3 h. Yield: 65%; almost white solid. M.p. = 158–160 °C. ^{1}H NMR (DMSO-d_6): 1.45 (d, J = 6.90, 6H, CH_3), 2.55–2.73 (m, 4H), 3.45–3.59 (m, 4H), 3.76 (s, 3H, $-OCH_3$), 4.54 (sep, J = 6.90, 1H, CH), 4.61 (s(br), 2H, CH_2), 6.66 (t, J = 7.7, 1H, ArH), 6.75–6.83 (m, 2H, ArH), 7.55 (s(br), 1H, NH), 7.83 (s, 1H, CH). ^{13}C NMR (DMSO-d_6): 21.29, 22.58, 45.87, 46.06, 46.27, 56.31, 60.30, 110.96, 114.07, 118.94, 121.03, 127.34, 136.35, 144.38, 147.92, 151.01, 154.76, 158.94. MS m/z (ESI) 398.1 $(M + H)^+$. Anal.: Calcd. for $C_{20}H_{27}N_7O_2$: C, 60.44; H, 6.85; N, 24.67. Found: C, 60.25; H, 6.87; N, 24.73.

*4.3.17. 4-Chloro-2-{[2-(4-hydroxycyclohexylamino)-9-isopropyl-9H-purin-6-ylamino]-methyl}-phenol (**3n**)*

The compound was prepared by heating of **2h** in excess of 4-aminocyclohexanol at 160 °C for 12 h. The crude product was purified by flash chromatography. Yield: 70%; white solid. M.p. = 201–204 °C. ^{1}H NMR (DMSO-d_6): 1.11–1.18 (m, 4H), 1.24 (d, J = 6.6, 6H, CH_3), 1.46–1.84 (m, 4H), 3.39 (qui, J = 7.0, CH), 3.57 (s(br), 1H, OH), 4.44 (sex, J = 7.7, 1H, CH), 4.48–4.57 (m, 3H, CH_2, CH), 6.06 (d, J = 7.7, 1H, NH), 6.79 (d, J = 8.4, 1H, ArH), 7.04–7.08 (m, 2H, ArH), 7.58 (s(br), 1H, NH), 7.80 (s, 1H, CH), 10.01 (s(br), 1H, OH). ^{13}C NMR (DMSO-d_6): 22.51, 30.93, 34.81, 42.03, 46.13, 49.91, 69.04, 111.12, 114.10, 117.88, 120.60, 126.71, 135.21, 139.82, 147.57, 150.55, 154.42, 158.74. MS m/z (ESI) 431.3 $(M + H)^+$. Anal.: Calcd. for $C_{21}H_{27}ClN_6O_2$: C, 58.53; H, 6.32; N, 19.50. Found: C, 58.22; H, 6.31; N, 19.55.

*4.3.18. 2-{[2-(4-Aminocyclohexylamino)-9-isopropyl-9H-purin-6-ylamino]-methyl}-4-chlorophenol (**3o**)*

The compound was prepared from **2h** and 1,4-*trans*-diaminocyclohexane (excess) by heating at 160 °C for 4 h. Yield: 38%; white solid. M.p. = 100–103 °C. ^{1}H NMR (DMSO-d_6): 0.97–1.21 (m, 4H), 1.46 (d, J = 6.6, 6H, CH_3), 1.70–1.86 (m, 4H), 2.40 (qui, J = 5.7, 1H, CH), 3.55 (sex, J = 7.1, 1H, CH), 4.05 (s(br), 2H, NH_2), 4.45–4.61 (m, 3H, CH_2, CH), 6.08 (d, J = 7.1, 1H, NH), 6.79 (d, J = 8.5, 1H, ArH), 7.02–7.08 (m, 2H, ArH), 7.62 (s(br), 1H, NH), 7.80 (s, 1H, CH), 10.12(s(br), 1H, OH). ^{13}C NMR (DMSO-d_6): 15.71, 22.60, 31.84, 35.82, 46.26, 50.18, 50.52, 65.46, 117.14, 122.34, 127.50, 127.93, 129.38, 135.80, 154.70, 155.00, 158.84. MS m/z (ESI) 430.3 $(M + H)^+$. Anal.: Calcd. $C_{21}H_{28}ClN_7O$: C, 58.67; H, 6.56; N, 22.80. Found: C, 58.29; H, 6.61; N, 22.53.

*4.3.19. 4-Chloro-2-{[2-((R)-1-hydroxymethylpropylamino)-9-isopropyl-9H-purin-6-ylamino]-methyl}-phenol (**3p**)*

The compound was prepared from **2h** and (*R*)-2-amino-butan-1-ol (excess) by heating at 160 °C for 3 h. Yield: 65%; white solid. M.p. = 180–183 °C. ^{1}H NMR (DMSO-d_6): 0.82 (t, J = 7.2, 3H, CH_3), 1.46 (d, J = 6.6, 6H, CH_3), 3.34–3.48 (m, 2H, CH_2), 3.79 (sex, J = 7.3, 1H, CH), 4.46–4.60 (m, 4H, CH, CH_2, OH), 5.89 (d, J = 7.3, 1H, NH), 6.79 (d, J = 8.4, 1H, ArH), 7.05 (d, J = 8.4, 1H, ArH), 7.10 (s, 1H, ArH), 7.65 (s(br), 1H, NH), 7.81 (s, 1H, CH), 10.11 (s(br), 1H, OH). ^{13}C NMR (DMSO-d_6): 11.14, 22.51, 22.61, 24.43, 46.35, 54.62, 63.49, 114.13, 117.22, 122.78, 127.67, 128.21, 129.27, 135.91, 151.37, 154.34, 154.99, 159.39. MS m/z (ESI) 405.1 $(M + H)^+$. Anal.: Calcd for $C_{19}H_{25}ClN_6O_2$: C, 56.36; H, 6.22; N, 20.76. Found: C, 56.29; H, 6.31; N, 20.53.

*4.3.20. 4-Chloro-2-{[2-(2-hydroxy-2-methylpropylamino)-9-isopropyl-9H-purin-6-ylamino]-methyl}-phenol (**3q**)*

The compound was prepared from **2h** and 1-amino-2-methylpropan-2-ol by heating at 160 °C in NMP in the presence of *N*,*N*-diisopropyl ethyl amine for 24 h. The crude product was purified by flash chromatography. Yield: 40%; white solid. M.p. = 183–186 °C ^{1}H NMR (DMSO-d_6): 1.06 (s, 6H, CH_3), 1.46 (d, J = 6.6, 6H, CH_3), 3.23 (d, J = 5.7, 2H, CH_2), 4.47–4.58 (m, 3H, CH_2, CH), 4.75 (s(br), 1H, OH), 6.07 (t, J = 5.7, 1H, NH), 6.79 (d, J = 8.3, 1H, ArH), 7.06–7.12 (m, 2H, ArH), 7.75 (s(br), 1H, NH), 7.84 (s, 1H, CH), 10.17 (s(br), 1H, OH). ^{13}C NMR (DMSO-d_6): 17.76, 22.59, 26.88, 28.03, 46.30, 52.91, 70.51, 115.26, 117.25, 122.75, 127.70, 128.20, 136.03, 154.33, 154.37, 159.89. MS m/z (ESI) 405.2 $(M + H)^+$. Anal.: Calcd for $C_{19}H_{25}ClN_6O_2$: C, 56.36; H, 6.22; N, 20.76. Found: C, 56.10; H, 6.28; N, 20.49.

*4.3.21. 4-Chloro-2-{[2-((R)-1-ethyl-2-hydroxypropylamino)-9-isopropyl-9H-purin-6-ylamino]-methyl}-phenol (**3r**)*

The compound was prepared from **2h** and (2*RS*, 3*R*)-3-aminopentan-2-ol by heating at 160 °C in NMP in the presence of *N*,*N*-diisopropyl ethyl amine for 72 h. The crude product was purified by flash chromatography. Yield: 29.5%; off white solid. The product is a mixture of diastereoisomers. M.p. = 86–91 °C. ^{1}H NMR (DMSO-d_6): 0.78 (t, J = 6.9, 3H, CH_3), 0.97 (t, J = 5.5, 3H, CH_3), 1.43 (d, J = 6.7, 6H, CH_3), 3.69 (qui, J = 6.9, 2H, CH_2), 4.41–4.72 (m, 4H, CH_2, CH, CH), 5.92 (d, J = 6.6, 1H, NH), 6.76 (d, J = 8.5, 1H, ArH), 7.02–7.08 (m, 2H, ArH), 7.62 (s(br), 1H, NH), 7.77 (s, 1H, CH), 10.12 (s(br), 1H, OH). ^{13}C NMR (DMSO-d_6): 10.78, 20.30, 21.88, 22.53, 45.63, 57.82, 66.94, 68.77, 113.19, 116.53, 122.09, 127.00, 127.57, 128.58, 135.21, 151.25, 153.66, 154.29, 159.22. MS m/z (ESI) 419.2 $(M + H)^+$. Anal.: Calcd for $C_{20}H_{27}ClN_6O_2$: C, 57.34; H, 6.50; N, 20.06. Found: C, 57.31; H, 6.52; N, 19.89.

*4.3.22. 4-Chloro-2-{[2-((S)-2-hydroxy-1,2-dimethyl-propylamino)-9-isopropyl-9H-purin-6-ylamino]-methyl}-phenol (**3s**)*

The compound was prepared from **2h** and (*S*)-3-amino-2-methylbutan-2-ol by heating at 160 °C in NMP in the presence of *N*,*N*-diisopropyl ethyl amine for 24 h. The crude product was purified by flash chromatography. Yield: 47%; white amorphous solid (foam). ^{1}H NMR (DMSO-d_6): 1.25–1.31 (m, 9H, CH_3), 1.53 (d, J = 6.6, 6H, CH_3), 4.02 (qui, J = 7.0, 1H, CH), 4.50–4.55 (s(br), 2H,

CH_2), 4.59 (sep, $J = 6.9$, 1H, CH), 5.01 (s, 1H, OH), 6.84 (d, $J = 8.4$, 1H, ArH), 6.99 (s(br), 1H, NH), 7.13–7.15 (m, 2H, ArH), 7.52 (s, 1H, CH). ^{13}C NMR (DMSO-d_6): 17.02, 22.53, 24.58, 28.30, 40.91, 46.96, 56.72, 74.10, 114.22, 119.47, 124.25, 126.93, 129.56, 130.62, 135.28, 150.11, 154.24, 154.81, 158.70. MS *m/z* (ESI) 419.3 $(M + H)^+$. Anal.: Calcd for $C_{20}H_{27}ClN_6O_2$: C, 57.34; H, 6.50; N, 20.06. Found: C, 57.10; H, 6.43; N, 19.91.

4.3.23. 2-{[2-((R)-1-Ethyl-2-hydroxypropylamino)-9-isopropyl-9H-purin-6-ylamino]-methyl}-4-fluorophenol (**3t**)

The compound was prepared from ***2i*** and (2*RS*, 3*R*)-3-aminopentan-2-ol by heating at 160 °C in NMP in the presence of *N*,*N*-diisopropyl ethyl amine for 72 h. The crude product was purified by flash chromatography. Yield: 26%; an off white amorphous solid. The product is a mixture of diastereoisomers. The free base was transferred into hydrochloride salt; m.p. = 100–106 °C; yellowish solid. ^{1}H NMR (DMSO-d_6): 0.81 (t, $J = 6.9$, 3H, CH_3), 0.99 (t, $J = 5.5$, 3H, CH_3), 1.46 (d, $J = 6.7$, 6H, CH_3), 3.60–3.72 (m, 2H, CH_2), 4.41–4.65 (m, 4H, CH_2, CH, CH), 5.94 (d, $J = 6.6$, 1H, NH), 6.76 (m, 1H, ArH), 6.83–6.88 (m, 2H, ArH), 7.62 (s(br), 1H, NH), 7.79 (s, 1H, CH), 9.88 (s(br), 1H, OH). ^{13}C NMR (DMSO-d_6): 10.81, 20.00, 22.12, 22.53, 45.63, 55.58, 66.94, 65.25, 112.58, 113.25, 115.00, 115.17, 116.38, 116.48, 122.69, 128.70, 129.12, 129.01, 129.82, 136.00, 151.27, 152.50, 154.42, 155.03, 157.52, 160.00. MS *m/z* (ESI) 403.4 $(M + H)^+$. Anal. Calcd. for $C_{20}H_{27}FN_6O_2$: C, 59.69; H, 6.76; N, 20.88. Found: C, 59.38; H, 6.82; N, 20.63.

4.3.24. 4-Fluoro-2-{[2-((R)-1-hydroxymethylpropylamino)-9-isopropyl-9H-purin-6-ylamino]-methyl}-phenol (**3u**)

The compound was prepared from ***2i*** and (*R*)-2-amino-butan-1-ol (excess) by heating at 160 °C for 3 h. Yield: 82%; white solid. Recrystallized from ethyl acetate. M.p. = 165–167 °C. ^{1}H NMR (DMSO-d_6): 0.84 (t, $J = 6.9$, 3H, CH_3), 1.46 (d, $J = 6.0$, 6H, CH_3), 3.40–3.46 (m, 2H, CH_2), 3.76 (sex, $J = 6.9$, 1H, CH), 4.49–4.58 (m, 4H, CH, CH_2, OH), 5.79 (d, $J = 6.9$, 1H, NH), 6.75–6.93 (m, 3H, ArH), 7.51 (s(br), 1H, NH), 7.79 (s, 1H, CH), 9.75 (s(br), 1H, OH). ^{13}C NMR (DMSO-d_6): 11.13, 22.49, 22.59, 24.43, 46.36, 54.62, 63.50, 113.90, 114.19, 114.85, 115.15, 116.38, 116.48, 122.69, 128.53, 128.73, 128.77, 128.82, 135.90, 151.27, 151.57, 154.42, 155.03, 157.52, 159.40. MS *m/z* (ESI) 389.5 $(M + H)^+$. Anal.: Calcd for $C_{19}H_{25}FN_6O_2$: C, 58.75; H, 6.49; N, 21.63. Found: C, 58.62; H, 6.51; N, 21.44.

4.4. Biological assays

4.4.1. Antibodies

Specific antibodies were purchased from Sigma–Aldrich (anti-α-tubulin, clone DM1A, peroxidase-labeled secondary antibodies), Santa Cruz Biotechnology (anti-Mcl-1, clone S-19; anti-PARP, clone F-2; anti-Mdm-2, clone SMP14; anti-Bcl-2), DAKO Cytomation (anti-caspase-3), Roche Applied Science (anti-5-bromo-2′-deoxyuridine-fluorescein, clone BMC 9318), Jackson ImmunoResearch Laboratory (fluorescein-conjugated Goat Anti-Mouse IgG), Bethyl Laboratories (anti-phospho RNA polymerase II (S5); anti-phospho RNA polymerase II (S2)), Millipore (anti-RNA polymerase II, clone ARNA-3), Cell Signaling (anti-PUMA) or were a generous gift from Dr. B. Vojtěšek (anti-p53, clone DO-1; anti-p21^{waf1}, clone 118; anti-PCNA).

4.4.2. Cell maintenance and cytotoxicity assays

The cytotoxicity of the studied compounds was determined using cell lines of different histological origin as described earlier [29,36]. Briefly, the cells were assayed with compounds using three-fold dilutions in triplicate. Treatment lasted for 72 h, followed by addition of Calcein AM solution, and measurement of the fluorescence of live cells at 485 nm/538 nm (ex/em) with a Fluoroskan Ascent microplate reader (Labsystems). IC_{50} (the drug concentration that reduced the number of viable cells to 50%) values were determined from the dose–response curves.

4.4.3. Kinase inhibition assays

CDK2/Cyclin E kinase was produced in Sf9 insect cells via baculoviral infection and purified on a NiNTA column (Qiagen). CDK5/p35, CDK7Cyclin H/MAT1 and CDK9/Cyclin T1 were purchased from ProQinase GmbH. The kinase reactions were assayed with 1 mg/ml histone H1 (for CDK2 and CDK5) or $(YSPTSPS)_2$KK peptide (for CDK7 and CDK9) in the presence of 15/0.15/1.5/1.5 μM ATP (for CDK2/CDK5/CDK7CDK9), 0.05 μCi [γ-^{33}P] ATP and of the test compound in a final volume of 10 μl, all in a reaction buffer (60 mM HEPES-NaOH, pH 7.5, 3 mM $MgCl_2$, 3 mM $MnCl_2$, 3 μM Na-orthovanadate, 1.2 mM DTT, 2.5 μg/50 μl $PEG_{20.000}$). The reactions were stopped by adding 5 μl of 3% aq. H_3PO_4. Aliquots were spotted onto P-81 phosphocellulose (Whatman), washed 3× with 0.5% aq. H_3PO_4 and finally air-dried. Kinase inhibition was quantified using a FLA-7000 digital image analyzer (Fujifilm). The concentration of the test compounds required to decrease the CDK activity by 50% was determined from dose–response curves and designated as IC_{50} [29,36].

4.4.4. Immunoblotting

Immunoblotting analysis was performed as described earlier [29,36]. Briefly, cellular lysates were prepared by harvesting cells in Laemmli sample buffer. Proteins were separated on SDS-polyacrylamide gels and electroblotted onto nitrocellulose membranes. After blocking, the membranes were incubated with specific primary antibodies overnight, washed and then incubated with peroxidase-conjugated secondary antibodies. Finally, peroxidase activity was detected with ECL+ reagents (AP Biotech) using a CCD camera LAS-4000 (Fujifilm).

4.4.5. Cell cycle analysis

Sub-confluent cells were treated with test compounds at different concentrations for 24 h. The cultures were pulse-labeled with 10 μM 5-bromo-2′-deoxyuridine (BrdU) for 30 min at 37 °C prior to harvesting. The cells were then washed in PBS, fixed with 70% ethanol, and denatured in 2 M HCl. Following neutralization, the cells were stained with anti-BrdU fluorescein-labeled antibodies, washed, stained with propidium iodide and analyzed by flow cytometry using a 488 nm laser (Cell Lab Quanta SC, Beckman Coulter) as described previously [29,36].

4.4.6. p53-Dependent transcriptional activity

To measure p53-dependent transcriptional activity, β-galactosidase activity was determined in the human melanoma cell line Arn-8, stably transfected with a p53-responsive reporter construct pRGCΔfoslacZ as described before [29,36]. After 24 h incubation with the inhibitors, the cells were permeabilized with 0.3% Triton X-100 for 15 min, and then 4-methylumbelliferon-ß-D-galactopyranoside was added as a substrate to a final concentration of 80 μM. After 1 h, the fluorescence was measured at 355/460 nm (ex/em) with a Fluoroskan Ascent microplate reader (Labsystems).

4.4.7. Caspase-3/7 assay

The cells were homogenized in an extraction buffer (10 mM KCl, 5 mM HEPES, 1 mM EDTA, 1 mM EGTA, 0.2% CHAPS, inhibitors of proteases, pH 7.4) on ice for 20 min. The homogenates were clarified by centrifugation at 10,000 × *g* for 30 min at 4 °C, and then the proteins were quantified and diluted to equal concentrations. Lysates were then incubated for 1 h with 100 μM Ac-DEVD-AMC as a substrate in the assay buffer (25 mM PIPES, 2 mM EGTA, 2 mM $MgCl_2$, 5 mM DTT, pH 7.3). To serve as negative

controls, the lysates were supplemented with 100 μM Ac-DEVD-CHO, which is a caspase-3/7 inhibitor. The fluorescence of the product was measured using a Fluoroskan Ascent microplate reader (Labsystems) at 355/460 nm (ex/em) as described previously [29].

4.4.8. Statistics

Rank correlation coefficients were calculated in *R*.

Acknowledgment

This work was supported by the Czech Science Foundation (GACR 305/12/0783, GACR 301/08/1649) and Ministry of Education, Youth and Sports, Czech Republic (ED0007/01/01 – Centre of the Region Haná for Biotechnological and Agricultural Research).

Appendix A. Supplementary data

Supplementary data related to this article can be found online at http://dx.doi.org/10.1016/j.ejmech.2012.06.036.

References

[1] M. Malumbres, M. Barbacid, Cell cycle, CDKs and cancer: a changing paradigm, Nat. Rev. Cancer 9 (2009) 153–166.
[2] V. Krystof, S. Uldrijan, Cyclin-dependent kinase inhibitors as anticancer drugs, Curr. Drug Targets 11 (2010) 291–302.
[3] C. Berthet, E. Aleem, V. Coppola, L. Tessarollo, P. Kaldis, Cdk2 knockout mice are viable, Curr. Biol. 13 (2003) 1775–1785.
[4] M. Malumbres, R. Sotillo, D. Santamaria, J. Galan, A. Cerezo, S. Ortega, P. Dubus, M. Barbacid, Mammalian cells cycle without the D-type cyclin-dependent kinases Cdk4 and Cdk6, Cell 118 (2004) 493–504.
[5] S. Ortega, M. Malumbres, M. Barbacid, Cyclin D-dependent kinases, INK4 inhibitors and cancer, Biochim. Biophys. Acta 1602 (2002) 73–87.
[6] D. Santamaria, C. Barriere, A. Cerqueira, S. Hunt, C. Tardy, K. Newton, J.F. Caceres, P. Dubus, M. Malumbres, M. Barbacid, Cdk1 is sufficient to drive the mammalian cell cycle, Nature 448 (2007) 811–815.
[7] L. Havlicek, J. Hanus, J. Vesely, S. LeClerc, L. Meijer, G. Shaw, M. Strnad, Cytokinin-derived cyclin-dependent kinase inhibitors: synthesis and cdc2 inhibitory activity of olomoucine and related compounds, J. Med. Chem. 40 (1997) 408–412.
[8] S.J. McClue, D. Blake, R. Clarke, A. Cowan, L. Cummings, P.M. Fischer, M. MacKenzie, J. Melville, K. Stewart, S. Wang, N. Zhelev, D. Zheleva, D.P. Lane, In vitro and in vivo antitumor properties of the cyclin dependent kinase inhibitor CYC202 (R-roscovitine), Int. J. Cancer 102 (2002) 463–468.
[9] D.E. MacCallum, J. Melville, S. Frame, K. Watt, S. Anderson, A. Gianella-Borradori, D.P. Lane, S.R. Green, Seliciclib (CYC202, R-Roscovitine) induces cell death in multiple myeloma cells by inhibition of RNA polymerase II-dependent transcription and down-regulation of Mcl-1, Cancer Res. 65 (2005) 5399–5407.
[10] S.R. Whittaker, R.H. Te Poele, F. Chan, S. Linardopoulos, M.I. Walton, M.D. Garrett, P. Workman, The cyclin-dependent kinase inhibitor seliciclib (R-roscovitine; CYC202) decreases the expression of mitotic control genes and prevents entry into mitosis, Cell Cycle 6 (2007) 3114–3131.
[11] W.S. Hsieh, R. Soo, B.K. Peh, T. Loh, D. Dong, D. Soh, L.S. Wong, S. Green, J. Chiao, C.Y. Cui, Y.F. Lai, S.C. Lee, B. Mow, R. Soong, M. Salto-Tellez, B.C. Goh, Pharmacodynamic effects of seliciclib, an orally administered cell cycle modulator, in undifferentiated nasopharyngeal cancer, Clin. Cancer Res. 15 (2009) 1435–1442.
[12] T.C. Le, S. Faivre, V. Laurence, C. Delbaldo, K. Vera, V. Girre, J. Chiao, S. Armour, S. Frame, S.R. Green, A. Gianella-Borradori, V. Dieras, E. Raymond, Phase I evaluation of seliciclib (R-roscovitine), a novel oral cyclin-dependent kinase inhibitor, in patients with advanced malignancies, Eur. J. Cancer 46 (2010) 3243–3250.
[13] D. Mahadevan, R. Plummer, M.S. Squires, D. Rensvold, S. Kurtin, C. Pretzinger, T. Dragovich, J. Adams, V. Lock, D.M. Smith, H.D. Von, H. Calvert, A phase I pharmacokinetic and pharmacodynamic study of AT7519, a cyclin-dependent kinase inhibitor in patients with refractory solid tumors, Ann. Oncol. 22 (2011) 2137–2143.
[14] D. Parry, T. Guzi, F. Shanahan, N. Davis, D. Prabhavalkar, D. Wiswell, W. Seghezzi, K. Paruch, M.P. Dwyer, R. Doll, A. Nomeir, W. Windsor, T. Fischmann, Y. Wang, M. Oft, T. Chen, P. Kirschmeier, E.M. Lees, Dinaciclib (SCH 727965), a novel and potent cyclin-dependent kinase inhibitor, Mol. Cancer Ther. 9 (2010) 2344–2353.
[15] S.J. McClue, I. Stuart, Metabolism of the trisubstituted purine cyclin-dependent kinase inhibitor seliciclib (R-roscovitine) in vitro and in vivo, Drug Metab. Dispos. 36 (2008) 561–570.
[16] B.P. Nutley, F.I. Raynaud, S.C. Wilson, P.M. Fischer, A. Hayes, P.M. Goddard, S.J. McClue, M. Jarman, D.P. Lane, P. Workman, Metabolism and pharmacokinetics of the cyclin-dependent kinase inhibitor R-roscovitine in the mouse, Mol. Cancer Ther. 4 (2005) 125–139.
[17] S.C. Wilson, B. Atrash, C. Barlow, S. Eccles, P.M. Fischer, A. Hayes, L. Kelland, W. Jackson, M. Jarman, A. Mirza, J. Moreno, B.P. Nutley, F.I. Raynaud, P. Sheldrake, M. Walton, R. Westwood, S. Whittaker, P. Workman, E. McDonald, Design, synthesis and biological evaluation of 6-pyridylmethylaminopurines as CDK inhibitors, Bioorg. Med. Chem. 19 (2011) 6949–6965.
[18] N.J. Lalak, D.L. Morris, Azithromycin clinical pharmacokinetics, Clin. Pharmacokinet. 25 (1993) 370–374.
[19] P.A. Meredith, H.L. Elliott, Clinical pharmacokinetics of amlodipine, Clin. Pharmacokinet. 22 (1992) 22–31.
[20] R.J. O'Brien, M.A. Lyle, D.E. Snider Jr., Rifabutin (ansamycin LM 427): a new rifamycin-S derivative for the treatment of mycobacterial diseases, Rev. Infect. Dis. 9 (1987) 519–530.
[21] W. Lu, S. Sengupta, J.L. Petersen, N.G. Akhmedov, X. Shi, Mitsunobu coupling of nucleobases and alcohols: an efficient, practical synthesis for novel nonsugar carbon nucleosides, J. Org. Chem. 72 (2007) 5012–5015.
[22] P. Imbach, H.G. Capraro, P. Furet, H. Mett, T. Meyer, J. Zimmermann, 2,6,9-Trisubstituted purines: optimization towards highly potent and selective CDK1 inhibitors, Bioorg. Med. Chem. Lett. 9 (1999) 91–96.
[23] M. Otyepka, V. Krystof, L. Havlicek, V. Siglerova, M. Strnad, J. Koca, Docking-based development of purine-like inhibitors of cyclin-dependent kinase-2, J. Med. Chem. 43 (2000) 2506–2513.
[24] M. Rypka, J. Vesely, Z. Chmela, D. Riegrova, K. Cervenkova, L. Havlicek, K. Lemr, J. Hanus, B. Cerny, J. Lukes, K. Michalikova, In vitro biotransformation of 2,6,9-trisubstituted purine-derived cyclin-dependent kinase inhibitor bohemine by mouse liver microsomes, Xenobiotica 32 (2002) 1017–1031.
[25] V. Krystof, R. Lenobel, L. Havlicek, M. Kuzma, M. Strnad, Synthesis and biological activity of olomoucine II, Bioorg. Med. Chem. Lett. 12 (2002) 3283–3286.
[26] M. Legraverend, O. Ludwig, E. Bisagni, S. LeClerc, L. Meijer, N. Giocanti, R. Sadri, V. Favaudon, Synthesis and in vitro evaluation of novel 2,6,9-trisubstituted purines acting as cyclin-dependent kinase inhibitors, Bioorg. Med. Chem. 7 (1999) 1281–1293.
[27] Y.T. Chang, N.S. Gray, G.R. Rosania, D.P. Sutherlin, S. Kwon, T.C. Norman, R. Sarohia, M. Leost, L. Meijer, P.G. Schultz, Synthesis and application of functionally diverse 2,6,9-trisubstituted purine libraries as CDK inhibitors, Chem. Biol. 6 (1999) 361–375.
[28] S.R. Schow, R.L. Mackman, C.L. Blum, E. Brooks, A.G. Horsma, A. Joly, S.S. Kerwar, G. Lee, D. Shiffman, M.G. Nelson, X.B. Wang, M.M. Wick, X.M. Zhang, R.T. Lum, Synthesis and activity of 2,6,9-trisubstituted purines, Bioorg. Med. Chem. Lett. 7 (1997) 2697–2702.
[29] R. Jorda, L. Havlicek, I.W. McNae, M.D. Walkinshaw, J. Voller, A. Sturc, J. Navratilova, M. Kuzma, M. Mistrik, J. Bartek, M. Strnad, V. Krystof, Pyrazolo [4,3-d]pyrimidine bioisostere of roscovitine: evaluation of a novel selective inhibitor of cyclin-dependent kinases with antiproliferative activity, J. Med. Chem. 54 (2011) 2980–2993.
[30] V. Krystof, I.W. McNae, M.D. Walkinshaw, P.M. Fischer, P. Muller, B. Vojtesek, M. Orsag, L. Havlicek, M. Strnad, Antiproliferative activity of olomoucine II, a novel 2,6,9-trisubstituted purine cyclin-dependent kinase inhibitor, Cell Mol. Life Sci. 62 (2005) 1763–1771.
[31] J. Vesely, L. Havlicek, M. Strnad, J.J. Blow, A. Donella-Deana, L. Pinna, D.S. Letham, J. Kato, L. Detivaud, S. LeClerc, Inhibition of cyclin-dependent kinases by purine analogues, Eur. J. Biochem. 224 (1994) 771–786.
[32] K. Vermeulen, M. Strnad, V. Krystof, L. Havlicek, A. Van der Aa, M. Lenjou, G. Nijs, I. Rodrigus, B. Stockman, O.H. Van, D.R. Van Bockstaele, Z.N. Berneman, Antiproliferative effect of plant cytokinin analogues with an inhibitory activity on cyclin-dependent kinases, Leukemia 16 (2002) 299–305.
[33] Z. Chmela, J. Vesely, K. Lemr, M. Rypka, J. Hanus, L. Havlicek, V. Krystof, L. Michnova, K. Fuksova, J. Lukes, In vivo metabolism of 2,6,9-trisubstituted purine-derived cyclin-dependent kinase inhibitor bohemine in mice: glucosidation as the principal metabolic route, Drug Metab. Dispos. 29 (2001) 326–334.
[34] L. Havlicek, K. Fuksova, V. Krystof, M. Orsag, B. Vojtesek, M. Strnad, 8-Azapurines as new inhibitors of cyclin-dependent kinases, Bioorg. Med. Chem. 13 (2005) 5399–5407.
[35] S. Wang, G. Griffiths, C.A. Midgley, A.L. Barnett, M. Cooper, J. Grabarek, L. Ingram, W. Jackson, G. Kontopidis, S.J. McClue, C. McInnes, J. McLachlan, Ch. Meades, M. Mezna, I. Stuart, M.P. Thomas, D.I. Zheleva, D.P. Lane, R.C. Jackson, D.M. Glover, D.G. Blake, P.M. Fischer, Discovery and characterization of 2-anilino-4-(thiazol-5-yl)pyrimidine transcriptional CDK inhibitors as anticancer agents, Chem. Biol. 17 (2010) 1111–1121.
[36] V. Krystof, D. Moravcova, M. Paprskarova, P. Barbier, V. Peyrot, A. Hlobilkova, L. Havlicek, M. Strnad, Synthesis and biological activity of 8-azapurine and pyrazolo[4,3-d]pyrimidine analogues of myoseverin, Eur. J. Med. Chem. 41 (2006) 1405–1411.
[37] M. Paprskarova, V. Krystof, R. Jorda, P. Dzubak, M. Hajduch, J. Wesierska-Gadek, M. Strnad, Functional p53 in cells contributes to the anticancer effect of the cyclin-dependent kinase inhibitor roscovitine, J. Cell Biochem. 107 (2009) 428–437.
[38] V. Krystof, I. Chamrad, R. Jorda, J. Kohoutek, Pharmacological targeting of CDK9 in cardiac hypertrophy, Med. Res. Rev. 30 (2010) 646–666.
[39] R.A. Robinson, A.K. King, Trans. Faraday Soc. 52 (1955) 327–330.
[40] P.M. Fischer, M. Jarman, E. McDonald, B. Nutley, F. Raynaud, S. Wilson, P. Workman, UK Patent Application, GB 2392155 A, 2004.

PŘÍLOHA II

Gucký T, Jorda R, Zatloukal M, Bazgier V, Berka K, **Řezníčková E**, Béres T, Kryštof V, Strnad M (2013) A novel series of highly potent 2,6,9-trisubstituted purine cyclin-dependent kinase inhibitors. J Med Chem. 56, 6234-6247.

Journal of Medicinal Chemistry

Article

pubs.acs.org/jmc

A Novel Series of Highly Potent 2,6,9-Trisubstituted Purine Cyclin-Dependent Kinase Inhibitors

Tomáš Gucký,*[,†] Radek Jorda,[‡] Marek Zatloukal,[†] Václav Bazgier,[†,§] Karel Berka,[§] Eva Řezníčková,[‡] Tibor Béres,[†] Miroslav Strnad,[‡] and Vladimír Kryštof[‡]

[†]Centre of the Region Haná for Biotechnological and Agricultural Research, Department of Growth Regulators, Faculty of Science, Palacký University, Šlechtitelů 11, 78371 Olomouc, Czech Republic

[‡]Laboratory of Growth Regulators, Faculty of Science, Palacký University & Institute of Experimental Botany ASCR, Šlechtitelů 11, 78371 Olomouc, Czech Republic

[§]Regional Centre of Advanced Technologies and Materials, Department of Physical Chemistry, Faculty of Science, Palacký University Olomouc, 17 Listopadu 12, 77146 Olomouc, Czech Republic

Supporting Information

ABSTRACT: The inhibition of overactive CDKs during cancer remains an important strategy in cancer drug development. We synthesized and screened a novel series of 2-substituted-6-biarylmethylamino-9-cyclopentylpurine derivatives for improved CDK inhibitory activity and antiproliferative effects. One of the most potent compounds, **6b**, exhibited strong cytotoxicity in the human melanoma cell line G361 that correlated with robust CDK1 and CDK2 inhibition and caspase activation. In silico modeling of **6b** in the active site of CDK2 revealed a high interaction energy, which we believe is due to the 6-heterobiarylmethylamino substitution of the purine moiety.

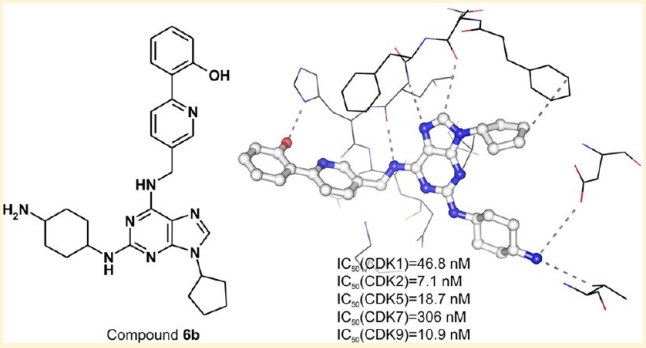

INTRODUCTION

The cyclin-dependent kinases (CDKs) are pivotal regulators of the cell cycle. They are activated in a cell cycle-specific manner by cyclins and phosphorylate targets including the transcriptional regulators that in turn induce phase-specific gene expression, stimulate DNA replication, or initiate mitosis.[1] Because of their frequent deregulation in cancer cells, CDKs have been viewed as valid drug targets and, to this date, more than 20 inhibitors have entered clinical trials in cancer patients.[2,3] The potency of CDK inhibitors designed around a purine heterocycle scaffold is largely determined by the purine's 2,6,9-substitution pattern but can also be affected by the nitrogen atom distribution in the heterocyclic core. Roscovitine (Figure 1), one of the first discovered CDK inhibitors, was identified by optimizing a 2,6,9-trisubstituted purine library.[4] The optically pure *R*-enantiomer of roscovitine is currently being evaluated as an oncology drug candidate in patients diagnosed with nonsmall cell lung cancer and nasopharyngeal cancer[5] or other malignancies.[6] Using structure−activity relationship studies together with a good knowledge of ATP binding sites in various CDKs, the modification of the roscovitine molecule in its substitutable positions has given rise to purine derivatives with increased CDK inhibitory activity and cytotoxicity.[7−13] In particular, derivatives bearing biarylmethylamino or biarylamino substituents in the 6-position of the purine skeleton, such as *R*-CR8 (Figure 1), are among the most active known CDK inhibitors.[11,12]

The modifications of roscovitine-like inhibitors have not been limited to its side chains but have also touched its heterocyclic core [for review, see ref 14]. Related compounds that exhibit anti-CDK activity include trisubstituted pyrazolo[1,5-*a*][1,3,5]triazines,[15,16] pyrazolo[4,3-*d*]pyrimidines,[17] and pyrazolo[1,5-*a*]pyrimidines.[18−20] Notably, the optimization of compounds from the latter of these classes has yielded another drug candidate, dinaciclib (Figure 1).[21,22] Dinaciclib is at a relatively advanced stage of development: it is currently being evaluated in several phase I/II experiments in patients with various solid tumors and leukemias and also in phase III clinical trials in chronic lymphocytic leukemia patients.[23−25]

Although many selective CDK inhibitors have been tested in clinical trials, none have yet been approved, largely due to undesired side effects arising from their unfavorable toxicological properties.[26−29] Therefore the identification of new active compounds and pharmacophores that inhibit CDKs is still a meaningful challenge. The aim of this work was to find new pharmacophores that would increase the desired biological activities of known 2,6,9-trisubstituted purine CDK inhibitors. To this end, we synthesized and performed a SAR study on

Received: May 9, 2013
Published: July 6, 2013

dx.doi.org/10.1021/jm4006884 | *J. Med. Chem.* 2013, 56, 6234−6247

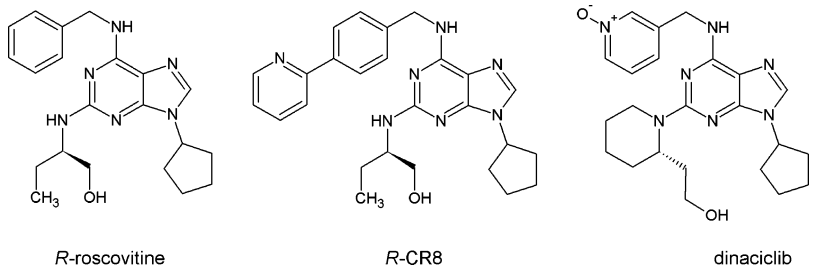

Figure 1. Structures of selected CDK inhibitors with a purine and isosteric pyrazolo[1,5-*a*]pyridine core.

Scheme 1[a]

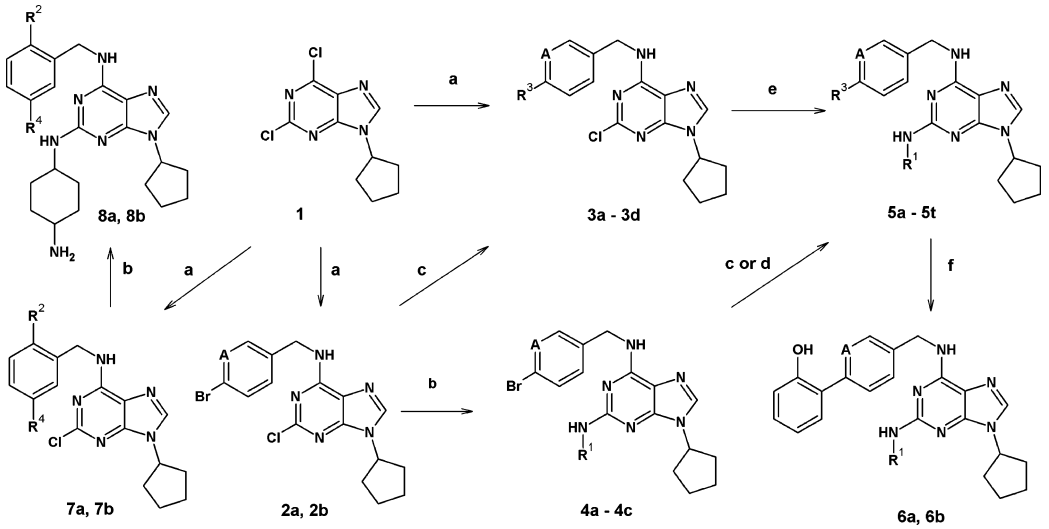

[a]Reagents and conditions: (a) appropriate amine, DIPEA, *n*-propanol, 80−120 °C (sealed tube); (b) appropriate amine, 160 °C (sealed tube); (c) appropriate arylboronic acid, $Pd(OAc)_2$, K_3PO_4, TBAB, DMF, 80−120 °C; (d) appropriate arylboronic acid, $Pd(dba)_2$, PPh_3, Na_2CO_3, DME, water, 80−120 °C; (e) appropriate amine, DIPEA, NMP, 160 °C, 16−36 h; (f) (1) BBr_3, DCM, rt, 18 h, (2) methanol.

novel 2-substituted-6-biarylmethylamino-9-cyclopentyl-9*H*-purine derivatives and found that the combination of a 9-cyclopentyl and 6-heterobiarylmethylamino substitution significantly increased CDK inhibitory activity and cytotoxic effects in cancer cell lines compared to previously described compounds of this class, including the biaryl-substituted derivative CR8.[30]

RESULTS AND DISCUSSION

Chemistry. The target compounds **5**, **6**, and **8** were prepared by conventional chemical procedures which allowed considerable flexibility with respect to the identity of the substituents in the 2- and 6-positions of the purine moiety. The general synthetic approach is outlined in Scheme 1. Supporting Information Table S2 shows the synthesized derivatives **2a**, **2b**, **3a−3d**, **4a−4c**, **5a−5t**, and **6a**, **6b**, **7a**, **7b** and **8a**, **8b**, together with the yields in which they were obtained and the reaction conditions used.

The *C*-(6-bromopyridin-3-yl)methylamine was prepared via a multistep route from 2-bromo-5-methyl-pyridine, which was initially brominated with *N*-bromosuccinimide to give 2-bromo-5-bromomethylpyridine. This was then reacted with urotropine to give a salt, which was hydrolyzed in aqueous ammonia to yield the desired amine.[31]

The synthesis of target compounds **5a−5t**, **6a**, **6b**, and **8a**, **8b** started from commercially available 2,6-dichloropurine, which was alkylated with cyclopentanol under Mitsunobu conditions[32] to obtain 9-cyclopentyl-2,6-dichloro-9*H*-purine (**1**). The alkylation proceeded with over 90% selectivity for the N9 isomer; a small amount of the N7 isomer was formed but could be removed by a single crystallization from ethanol.

The substitution of the 6-position 9-cyclopentyl-2,6-dichloro-9*H*-purine (**1**) with 4-bromobenzylamine or *C*-(6-bromopyridin-3-yl)methylamine gave compounds **2a** and **2b**. In addition, the reactions of (**1**) with commercially available 1-[4-(furan-2-yl)phenyl]methanamine, 1-[6-(furan-2-yl)pyridin-3-yl]-methanamine, 1-[6-(thiophen-2-yl)pyridin-3-yl]methanamine, and 1-[4-(1*H*-pyrazol-1-yl)phenyl]methanamine gave the desired compounds **3a−3d** in high yield and purity. Compound **3a** has previously been synthesized by the Suzuki coupling of **2a** with 2-furanylboronic acid.

The substitution of the purine moiety at position 2 proceeded smoothly to afford compounds **4a**, **4b**, **5i**, **5o**, **5s**, and **5q** with high yields and in good purity. This was achieved by reacting compound **1** with a large excess of *trans*-1,4-diaminocyclohexane (or *trans*-4-aminocyclohexan-1-ol in the case of **5s**) at 160 °C for a few hours. However the preparation of compounds **4c** and **5j** required the use of Hunig's base and a longer reaction time. Compound **5j** was only obtained in a moderate yield (37%), and further heating led to the decomposition of the starting material.

The cross-coupling reactions of compounds **4a−4c** with the appropriate aryl or heteroaryl boronic acids for the synthesis of compounds **5a−5c**, **5e**, **5f**, **5j−5m**, **5o**, and **5p** were performed

dx.doi.org/10.1021/jm4006884 | *J. Med. Chem.* 2013, 56, 6234−6247

Table 1. Inhibition of CDK1 and 2 and in Vitro Antiproliferative Activity of Selected Novel 2-Substituted-6-biarylmethylamino-9-cyclopentyl-9*H*-purines[a]

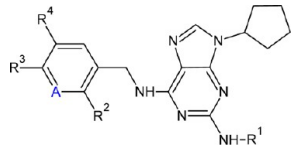

						inhibitory concentration IC_{50} (μM)						enzyme inhibition IC_{50} (nM)	
code	A	R1	R2	R3	R4	K562	MCF-7	G361	HOS	HCT-116	HeLa	CDK2	CDK1
roscovitine	CH					45.5	12.3	22.4	24.3	14.4	28.6	170	2421
CR8	CH					0.175	0.160	0.503	0.170	0.35	0.145	40.7	90
H717	CH											**48**	**52**
4a	CH	4-aminocyclohexyl	−H	−Br	−H	1.168	0.850	1.475	0.995	0.790	1.510		
4b	N	4-aminocyclohexyl	−H	−Br	−H	1.177	0.483	0.640	0.935	0.577	0.633		
5a	CH	4-aminocyclohexyl	−H	phenyl	−H	0.530	0.583	1.020	0.290	0.745	0.240	26	232
5b	CH	4-aminocyclohexyl	−H	2-aminophenyl	−H	1.107	0.977	4.12	1.881	0.930	1.013	20.5	152
5c	CH	4-aminocyclohexyl	−H	2-methoxyphenyl	−H	0.347	0.303	0.545	0.150	0.430	0.333	33	301
5d	CH	4-aminocyclohexyl	−H	3-fluorophenyl	−H	0.290	0.293	0.815	0.211	0.551	0.445	33.5	422
5e	CH	4-aminocyclohexyl	−H	2-furanyl	−H	0.096	0.085	0.164	0.102	0.129	0.071	11.4	148
5f	CH	4-aminocyclohexyl	−H	3-furanyl	−H	0.287	0.247	0.670	0.140	1.035	0.140	13	202
5g	CH	4-aminocyclohexyl	−H	2-thienyl	−H	0.307	0.290	0.655	0.247	0.592	0.358	20	119
5h	CH	4-aminocyclohexyl	−H	3-thienyl	−H	0.150	0.145	0.570	0.120	0.315	0.220	14	183
5i	CH	4-aminocyclohexyl	−H	pyrazol-1-yl	−H	0.119	0.139	0.220	0.103	0.320	0.170	12	58
5j	CH	2-hydroxy-2-methyl-propan-1-yl	−H	2-furanyl	−H	16.847	15.263	17.380	21.410	16.660	14.750	478	>999
5k	N	4-aminocyclohexyl	−H	phenyl	−H	-0.563	0.483	0.895	0.206	0.563	0.114	31	184
5l	N	4-aminocyclohexyl	−H	2-aminophenyl	−H	0.200	0.117	0.730	0.398	0.635	0.535	10	100
5m	N	4-aminocyclohexyl	−H	2-methoxyphenyl	−H	0.066	0.082	0.140	0.122	0.177	0.039	34	118
5n	N	4-aminocyclohexyl	−H	3-fluorophenyl	−H	0.061	0.033	0.049	0.044	0.074	0.036	14	77
5o	N	4-aminocyclohexyl	−H	2-furanyl	−H	0.067	0.033	0.097	0.044	0.086	0.030	10	50
5p	N	4-aminocyclohexyl	−H	3-furanyl	−H	0.056	0.032	0.097	0.024	0.046	0.015	8	66
5q	N	4-aminocyclohexyl	−H	2-thienyl	−H	0.100	0.092	0.150	0.032	0.097	0.040	4	49
5r	N	4-aminocyclohexyl	−H	3-thienyl	−H	0.150	0.100	0.272	0.089	0.145	0.075	18	169
5s	N	4-hydroxycyclohexyl	−H	2-furanyl	−H	0.303	0.390	0.443	0.180	0.617	0.247	23	215
5t	N	2-hydroxy-2-methyl-propan-1-yl	−H	2-furanyl	−H	1.425	1.305	2.095	0.560	1.270	0.667	120	555
6a	CH	4-aminocyclohexyl	−H	2-hydroxyphenyl	−H	2.610	2.910	4.150	1.160	4.350	4.177	68	777
6b	N	4-aminocyclohexyl	−H	2-hydroxyphenyl	−H	0.016	0.018	0.024	0.014	0.035	0.016	7.1	47
8a	CH	4-aminocyclohexyl	−OH	−H	−CL	0.69	0.43	0.39	0.49	0.35	0.75	8.0	23.0
8b	CH	4-aminocyclohexyl	$-NH_2$	−H	−H	4.04	2.33	2.07	2.03	2.30	1.03	18.0	93.0

[a]Bold values are from the literature.

as described elsewhere.[33] We used palladium diacetate as the catalyst in the cross-coupling reactions, potassium phosphate as the base, a tetrabutylammonium bromide phase transfer catalyst, and *N*,*N*-dimethylformamide as the solvent. This method is rapid and simple because the catalyst is not air-sensitive, the reaction time is short, and the products are readily isolated and purified. The yields obtained in these reactions ranged from 75% to 85%, and the method is readily amenable to scaling up.

However, these ligand-free coupling reactions failed for sulfur-containing heteroaryl boronic acids and 3-fluorophenyl boronic acid. In these cases, we adopted a modified procedure that uses a catalyst system consisting of bis-(dibenzylidenacetone)palladium and triphenylphosphine, sodium carbonate as the base, and a mixture of dimethoxyethane and water as the solvent. This method was used to prepare compounds **5d**, **5g**, **5h**, **5n**, and **5r**.

Compounds **5c** and **5m** were efficiently demethylated using boron tribromide in dichloromethane under mild conditions to yield compounds **6a** and **6b**.

The structure of the newly synthesized compounds was verified using ^{1}H NMR spectrometry and for selected compounds also ^{13}C NMR spectrometry and HPLC-MS. The structure of model compound **5m** was further verified using 2D NMR spectrometry (^{1}H−^{1}H COSY, ^{13}C NMR, and ^{1}H−^{13}C HSQC). The purity of all synthesized compounds was checked by HPLC-DAD-MS and elemental analysis. All of the synthesized and compounds were of >95% purity.

SAR of CDK Inhibition. All compounds were tested in kinase inhibition assays for their inhibitory potency toward recombinant human CDK1 and CDK2. Almost all of the derivatives' IC_{50} values were approximately 10 times lower than those for roscovitine (Table 1). The most potent compounds (**5p**, **5q**, and **6b**) had single-digit nanomolar IC_{50} values against CDK2, i.e., they were approximately 20 times more potent inhibitors of this kinase than roscovitine. The compounds were less potent inhibitors of CDK1, yielding IC_{50} values greater than 50 nM against this kinase. However, some of the most potent CDK2 inhibitors in the new series (specifically, compounds **5o**−**q** and **6b**) also had IC_{50} values against

dx.doi.org/10.1021/jm4006884 | J. Med. Chem. 2013, 56, 6234−6247

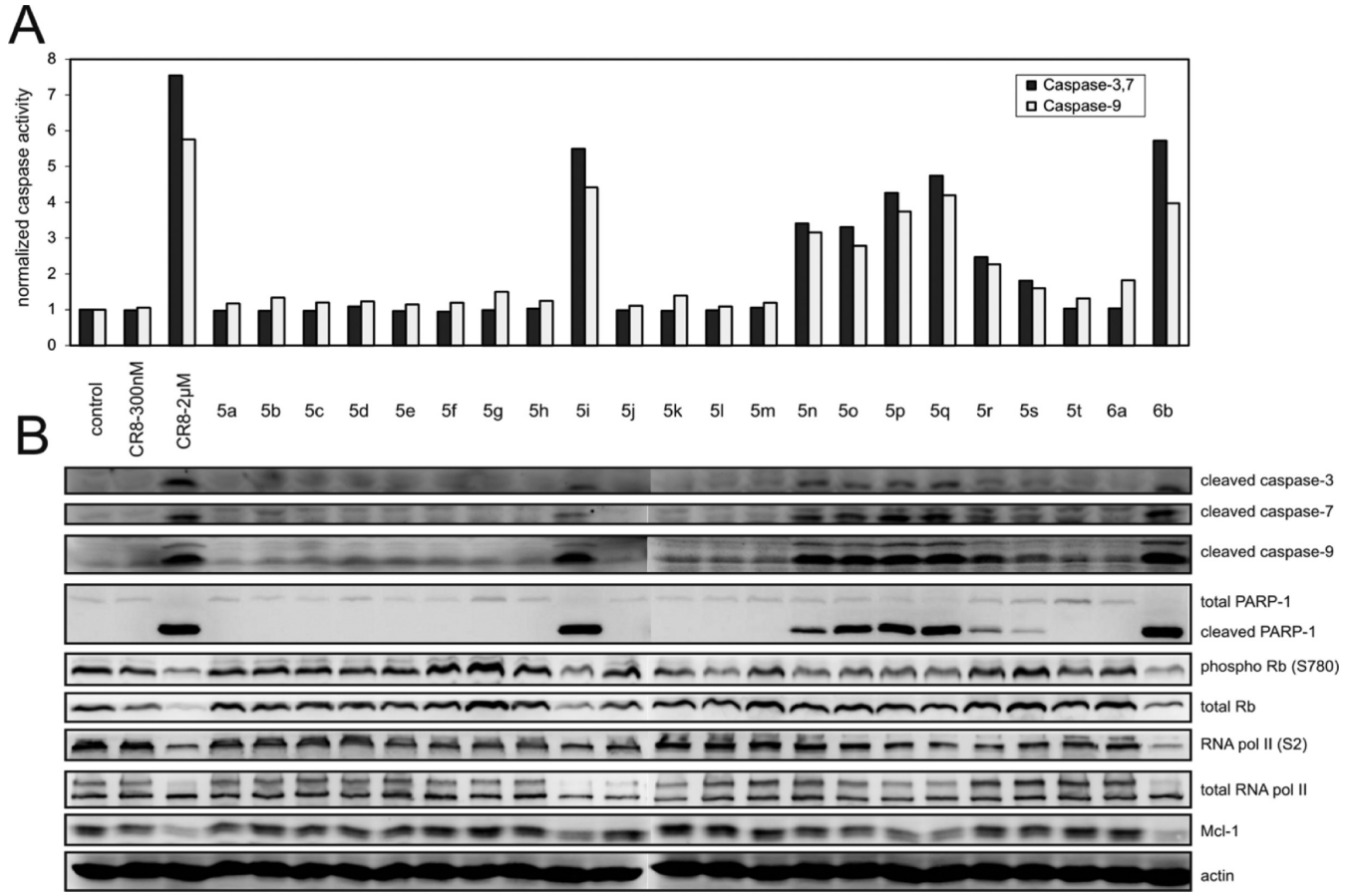

Figure 2. Induction of apoptosis by test compounds after a single 300 nM 24 h dose in G361 melanoma cells. (A) The activities of caspases-3/7/9 were measured in cell lysates using the fluorogenic substrate Ac-DEVD-AMC or Ac-DEVD-AMC (for caspase-9). (B) Immunoblotting analysis of apoptosis proteins and substrates of CDKs. Actin levels are included as controls for equal protein loading. Two concentrations of CR8 were used as an internal control.

CDK1 that were around 40 times lower than that for roscovitine. As with roscovitine, most compounds retained the same ratio between IC_{50} values for CDK1 and CDK2.

The majority of compounds bear the same side groups in positions 2- and 9- of the purine, i.e., 4-aminocyclohexylamino and cyclopentyl, respectively, and a combination of these was found to be advantageous for cancer cell proliferation inhibition. In fact, CDK affinity was reduced when the 4-aminocyclohexylamino side chain at position 2- was replaced with a 4-hydroxycyclohexylamino or hydroxyalkylamino group (compare compound **5o** to **5s** or **5t**). Unexpectedly, **5j** was even less active than roscovitine. This is probably because it adopts a suboptimal position within the active site of CDK2 due to the combined influence of the substituents at the 2- and 6- positions.

Minimizing the diversity of the substituents in the 2- and 9-positions enabled us investigate how varying the substituent at the 6-position of the purine affected activity against CDK1/CDK2. The most potent compounds in this series had substituents with a furanyl (**5e**, **5f**, **5p**, **5o**), thienyl (**5g**, **5h**,**5q**, **5r**), or pyrazolyl (**5i**) ring at the 6-position of the purine. Side chains that incorporated phenyl groups with polar substituents also conferred increased potency against CDK1 and CDK2 (cf. compounds **5l**, **5b**, **6b**). In general, the increased cytotoxicity of the 6-[4-arylpyridin-3-yl] derivatives (A = N) over 6-[4-arylphenyl] derivatives (A = CH) appears to be linked to more effective CDK1/CDK2 inhibition; this is particularly clear when one compares the IC_{50} values for compound pairs such as **5b** and **5l**, **5d** and **5n**, **5g** and **5q**, **5j** and **5t**, and **6a** and **6b**.

The CDK selectivity of the most potent compounds, **5k**−**5t** and **6b**, was further characterized by performing kinase assays with CDK5, CDK7, and CDK9 at two doses. The data in Supporting Information Table S1 clearly show that these compounds were also potent inhibitors of these kinases. A dose−response assay conducted using the most potent derivative from this series (**6b**) with CDK5, CDK7, and CDK9 yielded IC_{50} values of 19, 306, and 11 nM, respectively. These results show that compounds from the new series can inhibit multiple kinases from the CDK family, which may be beneficial because it means they can exert anticancer effects via multiple pathways.

To further explore compound **6b**'s greater affinity for CDK2 relative to roscovitine and CR8, we used our flexible docking procedure in conjunction with the Autodock Vina molecular docking program to model its binding interactions with CDK2 (see the Apparatus and Methods section for details). Our model suggests that all of the tested compounds bind to the ATP-binding site of CDK2 in an orientation similar to that of roscovitine and other purine inhibitors; the predicted binding energies correlated well with the measured IC_{50} values for kinase inhibition (r^2 = 0.73; see Supporting Information Table S3 and Figure S1). Compound **6b** forms conserved hydrogen bonds with the backbone carbonyl and NH moieties of Leu83,

dx.doi.org/10.1021/jm4006884 | J. Med. Chem. 2013, 56, 6234−6247

and an additional conserved hydrogen bond is formed with the backbone carbonyl of Glu81 (Figure 3). The 9-cyclopentyl chain is located in the small hydrophobic patch deep in the active site close to the side chain of Phe80, and the 6-biaryl chain points outward from the active site of CDK2. The model shows that the *trans*-4-amino-cyclohexylamino group in the 2-position forms two hydrogen bonds with Asp145 and Thr 14, which may be why it was the best of the tested substituents at the 2-position; alternatives such as a 4-hydroxycyclohexyl group can only form a single hydrogen bond with Asp145, while the roscovitine-like 2-hydroxy-2-methyl-propan-1-yl substituent forms no such contacts (compare **5o** to **5s** and **5t**). The 2-hydroxyphenyl ring of **6b** may interact with His84. Importantly, the basic nitrogen in the pyridine ring of **6b** helps to stabilize the rigid planar conjugated conformation of both rings by forming an H-bond with the hydroxyl group. Of the tested compounds, **6b** has the highest barrier for the rotation of the second ring, followed by **5o**, **5q**, and **5l**; a high barrier to rotation reduces the thermal motion of this fragment (Supporting Information Figure S1 and S2). Planarity is also promoted by the presence of a functional group on the six-membered ring that can interact with the pyridine nitrogen (compare compounds **5l** and **6b** to **5k** and **5m**). Overall, the interactions described above may significantly contribute to the ability of **6b** to bind more tightly and rigidly to CDK2 than roscovitine can.

Compound Antiproliferative Activity in Cancer Cells Lines. To explore the SAR of our novel compound series, we determined the compounds' cytotoxicity (IC_{50}) in representative cancer cell lines incubated with increasing compound concentrations for 72 h. We found that individual compounds exhibited similar levels of activity across all cell lines tested (Table 1), with IC_{50} values ranging from 14 nM to 4 μM for both series **5** and **6**. In general, the most active CDK inhibitors identified using the kinase inhibition assays (see below and Table 1) had a 4-aminocyclohexylamino chain in the 2-position. Compounds of this type generally had midnanomolar IC_{50} values. To verify the suitability of the 4-amino-cyclohexylamino substitution in position 2- of the purine core, we synthesized derivatives bearing 2-hydroxy-2-methylpropan-1-yl-amino (**5j**, **5t**) and 4-hydroxy-cyclohexyl-amino (**5s**) groups in the 2-position. All of these derivatives proved to be more antiproliferative than the original compounds. The most potent derivatives **5n−p** and **6b** have IC_{50} values of less than 100 nM. The least potent compounds from this series, **5b** and **6a**, both have similar substituents on the 6-position of the second aryl ring (a 2-aminophenyl and a 2-hydroxyphenyl group, respectively), which may be responsible for their comparatively poor activity.

Cells in our cytotoxicity assay displayed morphological signs of apoptosis (data not shown), prompting us to evaluate the ability of the prepared compounds to induce apoptosis at 300 nM in the melanoma cell line G361 (Figure 2). We analyzed caspase 3/7 and 9 activity using a fluorimetry-based assay in cell lysates (Figure 2A). In parallel, levels of known CDK substrates and apoptosis proteins were determined by immunoblotting (Figure 2B). The potent CDK inhibitors **5i**, **5n−5r**, and **6b** induced strong caspase activity (Figure 2A) and caused the cleavage of caspases and their substrate PARP, along with decreases in the abundance of the antiapoptotic protein Mcl-1 (Figure 2B). Importantly, the control compound CR8 induced caspase-dependent cell death in G361 at micromolar (2 μM) but not nanomolar (300 nM) concentrations.

Along with the apoptosis-related markers, we also monitored the phosphorylation of retinoblastoma protein and RNA polymerase II at Ser780 and Ser2, sites known to be phosphorylated by CDK2/4 and CDK9, respectively (Figure 2B). The level of phosphorylation at both sites was reduced in the treated cells, particularly in those exposed to potent compounds such as **5i**, **5n−5q**, and **6b**. For compounds **5i** and **6b**, which strongly activate caspases at the tested doses, this could have been caused by reductions in the total abundance of Rb or RNA polymerase II.

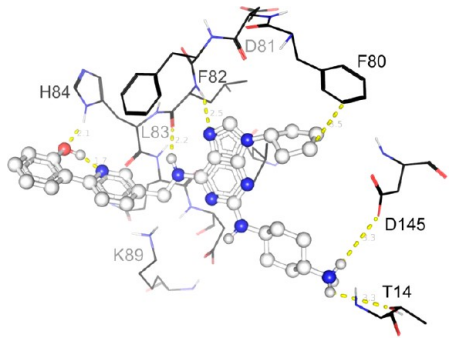

Figure 3. Structure of the binding pose of compound **6b** in CDK2 (template PDB ID: 2A4L). Lines represent important amino acid residues of CDK2. The ligand is shown in a ball and stick representation, with all heteroatoms shown in black. Interactions with K89, T14, D145, E8, and with the backbone of L83 and E81 are illustrated with gray dots.

Interestingly, the potent CDK2 inhibitors **5k** and **5l** blocked the phosphorylation of Rb but not RNA polymerase II. This correlates with their weak inhibition of CDK9 (see Supporting Information Table S1), an RNA polymerase II activator. Neither **5k** nor **5l** induces apoptosis in G361 cells, and because CDK inhibitor cytotoxicity is supposedly based on the inhibition of the RNA polymerase II activators CDK7 and CDK9, **5k** and **5l** should be considered to be cytostatic rather than cytotoxic agents.[34]

Molecular Mechanisms of Activity for Compound 6b. Compound **6b** emerged as one of the most potent CDK inhibitors from this series, being much more potent than the parent compounds roscovitine and CR8 at the same dose. Because of its superior cytotoxicity in the cell lines tested here, its clear cell cycle suppression (Supporting Information Figure S3a), and its significant induction of apoptosis (Supporting Information Figure S3b), we decided to characterize the cellular effects of **6b** in more detail.

We treated G361 cells with increasing doses of **6b** for 24 h and immunoblotted the lysates with antibodies against proteins involved in apoptosis (Figure 4A). Treated cells showed elevated levels of cleaved (activated) caspases 3 and 7 and a concomitant decrease in the levels of the inactive forms of caspases 3 and 7. The presence of an 89 kDa cleavage fragment of PARP, the known substrate of caspase 3, in cells treated with doses as low as 80 nM, correlates well with the activation of caspases. Moreover, treated cells exhibited dose-dependent reductions in the abundance of the antiapoptotic protein Mcl-1, which is consistent with the known mechanisms of action for other CDK inhibitors.[17,35,36] Compound **6b** also causes a dose-dependent increase in the abundance of p53, which is known to be activated and stabilized by CDK inhibitors[35,37,38] and whose induction results in apoptosis via the mitochondrial pathway.

dx.doi.org/10.1021/jm4006884 | J. Med. Chem. 2013, 56, 6234−6247

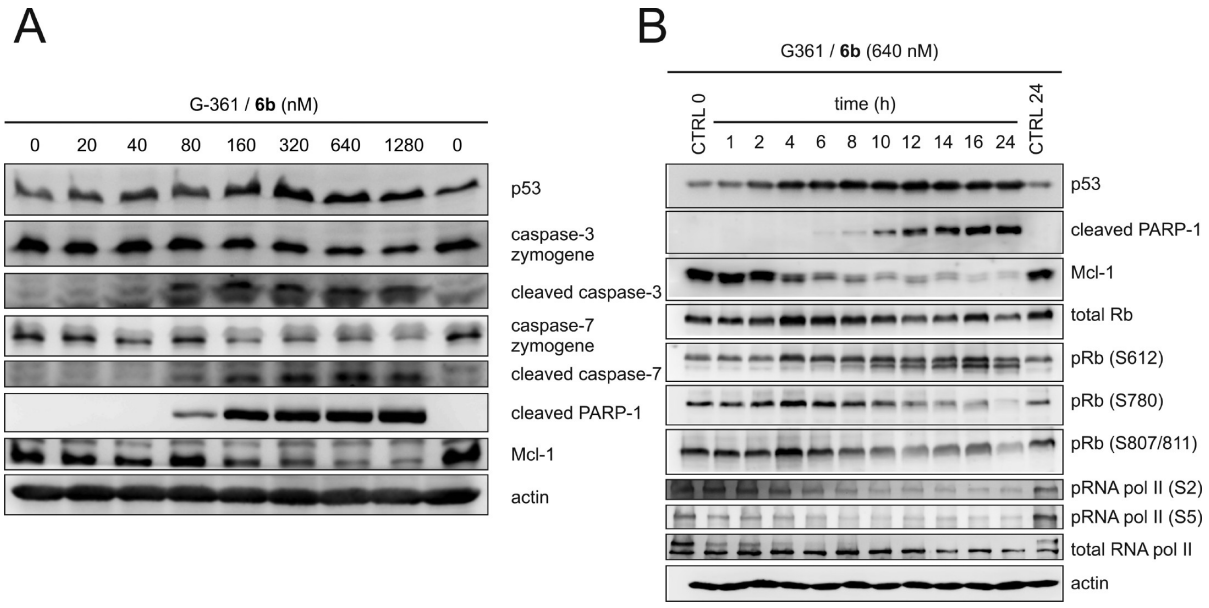

Figure 4. Compound **6b** induces apoptosis and dephosphorylation of Rb protein in G361 cells in a (A) dose and (B) time-dependent manner. (A) The cleavage of caspases, fragmentation of PARP, total p53 protein level, and down-regulation of Mcl-1 were detected by immunoblot analysis. (B) Immunoblotting analysis of selected apoptotic proteins and Rb protein in G361 cells treated with 640 nM of **6b** for the indicated times. Actin was included as a control for equal protein loading.

Our data therefore indicates that in G361 cells, **6b** induces the mitochondrial pathway of apoptosis.

To study the kinetics of its cellular effects, **6b** (640 nM) was added to G361 cells for periods of between 1 and 24 h (Figure 4B). The 640 nM dose was selected because it strongly activated apoptosis within 24 h (Figure 4A), and we therefore anticipated that it would cause pronounced changes in the levels of important cellular markers at earlier time points. Compound **6b** gradually reduced the levels of phosphorylated Rb and RNA polymerase II over 24 h, with the first signs of dephosphorylation appearing within 1 h of treatment. The dephosphorylation of Rb at Ser612 and Ser780 and RNA polymerase II at Ser2 and Ser5 suggests that at least CDK2, CDK7, and CDK9 were effectively inhibited. However, the levels of both substrates started decreasing after 16 h. This was probably due to the initiation of cell death, as evidenced by the strong cleavage of PARP at this time point (Figure 4B) and by the activation of caspase-3,7 observed in the enzymatic assay (Supporting Information Figure S2). In our time-course experiment, CDK substrate dephosphorylation preceded changes in the apoptotic markers. This implies that compound **6b** may also induce cell death by transcriptional repression: an inhibition of transcriptional CDKs would cause a reduced transcription of their target genes and a subsequent down-regulation of proteins with a rapid turnover like Mcl-1, which we note became significantly less abundant within 2 h of exposure to the **6b**.

To determine whether the antiproliferative activity of **6b** may involve mechanisms independent of CDK2 or CDK9, we investigated the phosphorylation of less explored CDK1 and CDK2 substrates: protein phosphatase-1α (PP1α) and nucleophosmin (NPM).[39,40] These proteins are phosphorylated during mitosis, but any changes in their phosphorylation caused by CDK inhibitors are barely detectable in asynchronous cells, where approximately 10% of cells undergo mitosis. We therefore treated G361 cells with nocodazole to block mitosis (94%, data not shown) and visualized the phosphorylation of PP1α and NPM at threonins 320 and 199, respectively (Figure 5, second lane). When these cells were dosed with **6b** for 4 h, the abundance of the phospho-forms of both PP1α and NPM decreased (Figure 5). After 8 h of treatment, NPM phosphorylation returned to asynchronous levels and its dephosphorylation due to **6b** exposure was no longer evident. However, the difference in PP1a phosphorylation remained.

Additionally we observed decreases in the phosphorylation of CDK1 (T161) and CDK2 (T160).[41] These sites are phosphorylated by CDK7, and their lower levels of phosphorylation are consistent with the inhibition of CDK7 by compound **6b** (Supporting Information Table S1).

DISCUSSION AND CONCLUSIONS

There is considerable controversy regarding the suitability of CDKs as targets for anticancer drugs. Experiments in mice have shown that most CDKs are dispensable for the cell cycle,[42] confirming earlier findings that some cancer cells proliferate well even without CDK2.[34,43] However, other studies have suggested that CDK2 might be a good target in the treatment of melanoma,[44,45] which has recently been shown to be sensitive to dinaciclib both in vitro and in vivo.[46] Dinaciclib is a nanomolar CDK inhibitor that was developed as a bioisostere of roscovitine and is currently undergoing phase II and III clinical trials.[19,21−25,47]

The experiments described herein demonstrate that 2-substituted-6-biarylmethylamino-9-cyclopentylpurines are strong CDK inhibitors; the prototype compound **6b** proved to be even more potent than the experimental purine-based inhibitor CR8[30,48] and the pyrazolo[1,5-*a*]pyrimidine drug candidate dinaciclib, which is active in melanoma cell lines at micromolar concentrations.[46] Its remarkable potency was achieved by introducing a cyclopentyl group in the 9-position of the purine unit (as demonstrated by its superior performance compared to compounds **8a** and **8b**, which have 9-isopropyl units instead of the cyclopentyl group[13]), along with a 4-

dx.doi.org/10.1021/jm4006884 | J. Med. Chem. 2013, 56, 6234−6247

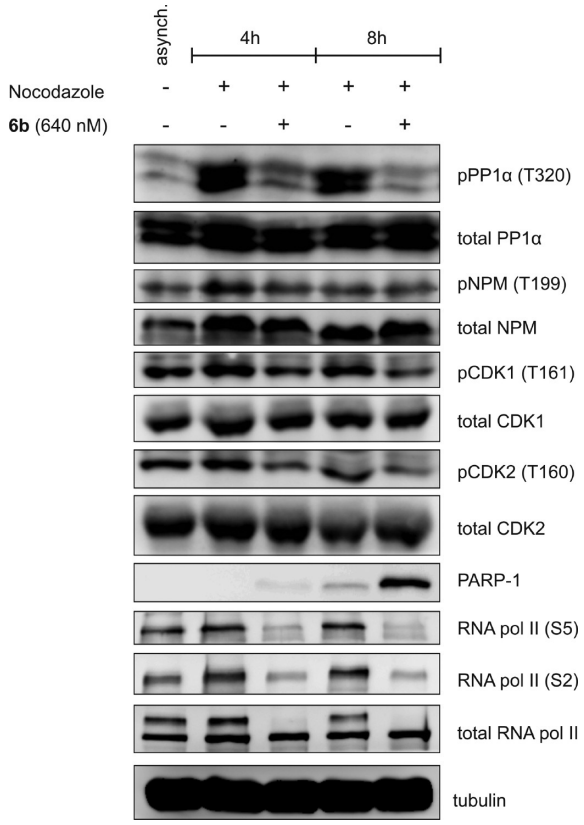

Figure 5. Compound **6b** inhibits the phosphorylation of CDK2- or CDK9-independent substrates. G361 cells were first synchronized with nocodazole (3 ng/mL for 16 h) and then treated with 640 nM **6b** for the indicated times in the presence of nocodazole. Substrates of CDKs and other cell cycle regulatory proteins were detected by immunoblotting analysis. Tubulin was included as a control for equal protein loading.

aminocyclohexyl group in the 2-position, and by modifying the 6-substituent that confers CDK selectivity.[10−12,30,32,49]

A theoretical model of compound **6b** bound to the active site of CDK2 revealed that it has one of the highest interaction energies of the whole series with this active site. This is because its purine unit has an optimal substitution pattern arising from the presence of the (2-hydroxy-phenyl)-pyridin-3-ylmethylamino group in the 6-position, a cyclopentyl group in the 9-position, and a 4-aminocyclohexyl group in the 2-position of the purine. Its increased inhibitory activity is also partly due to the nitrogen in the pyridine ring (**5k**−**5r**, **6b**), which allows the rings of the substituent at position 6 to assume a more planar conformation and imposes a higher barrier to rotation than is present in the analogous phenyl derivatives (**5a**−**5h**), thereby restricting the thermal motion of the two rings. This enforced planarity is especially pronounced when five-membered rings are added on to the pyridine ring (**5o**−**5q**) or when an additional group on the second six-membered ring can interact with the pyridine nitrogen (compare **5l**, **6b** with **5k**, **5m**). Compound **6b**'s second ring has the highest barrier to rotation of the entire series, followed by those of **5o**, **5l**, and **5q**. The 2-thienyl ring (**5q**) has an advantage over the 2-furanyl ring (**5o**) due to the stronger interaction of nitrogen with its sulfur. A similar skeleton-stabilizing N−S interaction has also been found in MAPK and aurora A inhibitors.[50]

The high theoretical and in vitro activity of the novel biaryl purine derivatives described herein is consistent with their in vivo performance. In addition, more recent experiments have demonstrated that **6b** and related compounds have strong antitumorigenic effects in mouse models of hepatocarcinoma (manuscript submitted to *Mol. Cancer Ther.*). The new purine CDK inhibitors impinge on multiple cancer phenotypes: they are not only directly cytotoxic in cancer cells but also block their invasion and migration and, in addition, interfere with angiogenesis, probably via CDK-dependent noncell cycle mechanisms. For example, CDK7 limits the migration of cancer cell lines[51] and CDK5 is critical for endothelial cell migration and angiogenesis.[52] Because the novel inhibitors are pan-selective and act on all of these CDKs, their interference with multiple malignant hallmarks of cancer makes them attractive drug candidates that should be considered for clinical evaluation.

EXPERIMENTAL SECTION

Apparatus and Methods. Melting points were determined on a Boetius stage and are corrected. ^{1}H NMR spectra were measured in DMSO-d_6 or $CDCl_3$ at 300 K on a Bruker Avance 300 spectrometer (300 MHz); chemical shifts are reported in ppm and coupling constants in Hz. Mass spectra were recorded by using an LCQ ion trap mass spectrometer (Finnigan MAT, San Jose, CA, USA). The chromatographic purity of the compounds were determined using HPLC-DAD-MS. An Alliance 2695 separations module (Waters) linked simultaneously to a PDA 996 (Waters) and a Q-Tof micro (Waters) benchtop quadrupole orthogonal acceleration time-of-flight tandem mass spectrometer were used. Samples were dissolved in methanol and diluted to a concentration of 10 $\mu g \cdot mL^{-1}$ in the mobile phase (initial conditions). Then 10 μL of the solution were injected on a RP-column (150 mm × 2.1 mm; 3.5 μm; Symmetry C18, Waters). The column was kept in a thermostat at 25 °C. Solvent (A) consisted of 15 mM formic acid adjusted to pH 4.0 by ammonium hydroxide. Methanol was used as the organic modifier (solvent B). At flow rate of 0.2 $mL \cdot min^{-1}$, the following binary gradient was used: 0 min, 10% B; 0−24 min, a linear gradient to 90% B, followed by 10 min isocratic elution of 90% B. At the end of the gradient, the column was re-equilibrated to initial conditions for 10 min. The effluent was introduced into the DAD (scanning range 210−400 nm, with 1.2 nm resolution) and an electrospray source (source temperature 110 °C, capillary voltage +3.0 kV, cone voltage +20 V, desolvation temperature 250 °C). Nitrogen was used both as desolvation gas (500 $L \cdot h^{-1}$) and as cone gas (50 $L \cdot h^{-1}$). The mass spectrometer was operated in positive (ESI+) ionization mode. The data were acquired in the 50−1000 m/z range. Elemental analyses were performed by using an EA 1108 elemental analyzer (Fison Instruments); their values (C, H, N) agreed with the calculated ones within acceptable limits. Merck silica gel Kieselgel 60 (230−400 mesh) was used for column chromatography. The purity of biologically evaluated compounds was >95% as determined by HPLC-DAD-MS and elemental analysis.

Prepared Compounds. *Preparation of 9-Cyclopentyl-2,6-dichloro-9H-purine.* 2,6-Dichloro-9*H*-purine (30.0 mmol), cyclopentanol (60.0 mmol), and triphenylphosphine (36.0 mmol) were dissolved in dry tetrahydrofuran (120 mL) and cooled to 0 °C. To the stirred solution diisopropyl azodicarboxylate (36.0 mmol) was added dropwise under an argon atmosphere, and the temperature was kept between 0 and 20 °C. The reaction mixture was stirred under an argon atmosphere at 20 °C for a further 2 h. The reaction mixture was then evaporated under reduced pressure, and the residue was dissolved in boiling toluene (100 mL). After cooling to room temperature, the solution was inoculated with a small amount of triphenylphosphine oxide and the solution was kept at 5 °C for 24 h. The triphenylphospine oxide was filtered off, and the filtrate was evaporated under reduced pressure. The residue was crystallized from ethanol to obtain pure 9-cyclopentyl-2,6-dichloro-9*H*-purine. Yield 56%; mp 118−120 °C. Elemental analysis Calcd for $C_{10}H_{10}Cl_2N_4$ (257.12): C, 46.71; H, 3.92; N, 21.79. Found: C, 46.95; H, 3.81; N, 21.70. HPLC-MS (ESI+): 288.10 (99.6%). ^{1}H

dx.doi.org/10.1021/jm4006884 | *J. Med. Chem.* 2013, 56, 6234−6247

NMR (DMSO-d_6): 1.64−1.69 (m, 2H), 1.81−1.96 (m, 4H), 2.09−2.15 (m, 2H), 4.92 (qui, J = 7.53, 1H, CH), 8.82 (s, 1H, CH).

Preparation of C-(6-Bromopyridin-3-yl)methylamine. 2-Bromo-5-methylpyridine (70.0 mmol) and *N*-bromosuccinimide (80.0 mmol) were dissolved in 1,2-dichloroethane (150 mL), and to this mixture 2,2′-azobis(2-ethylpropionitrile) (1.50 mmol) was added. The reaction mixture was heated under reflux at 85 °C for 15 min and the next portion of 2,2′-azobis(2-methylpropionitrile) (1.50 mmol) was added and the reaction mixture was heated at 85 °C for a further 15 min. After cooling to room temperature, the reaction mixture was kept at 5 °C for 2 h and the precipitate was filtered off and washed with a small amount of 1,2-dichloroethane. The filtrate was evaporated under reduced pressure, and the crude product was used for further reaction steps without purification.

The crude 2-bromo-5-bromomethylpyridine was dissolved in chloroform (100 mL), and urotropine (70.0 mmol) was added. The reaction mixture was stirred at room temperature for 16 h. The precipitate was filtered off, washed with a small amount of chloroform, and dried on air. The crude urotropine salt was refluxed in a mixture of concd ammonium hydroxide (12 mL) and water (80 mL) for 90 min, and after cooling to room temperature, 40% formaldehyde (5.0 mL) was added while stirring. The precipitate was filtered off, washed with ice-cold water, and dried in a vacuum desiccator. The crude product was crystallized from ethanol.

Yield 40%; mp 105−106 °C. Elemental analysis Calcd for $C_6H_7BrN_2$ (187.04): C, 38.53; H, 3.77; N, 14.98. Found: C, 38.22; H, 3.72; N, 14.71. HPLC-MS (ESI+): 188.02 (97.2%). ^{1}H NMR (DMSO-d_6): 4.04 (t, J = 5.67, 2H, CH_2), 7.71 (d, J = 8.19, 1H, ArH), 7.95 (dd, J = 8.19, J' = 1.95, 1H, ArH), 8.51 (d, J = 1.95, 1H, ArH), 8.74 (s(br), 2H, NH_2)

General Procedure A for Preparing Compounds 2a, 2b, 3a−3d, 7a and 7b. To the suspension of 9-cyclopentyl-2,6-dichloro-9*H*-purine (7.78 mmol) in a mixture of *n*-propanol (40 mL) and *N*,*N*-diisopropyl-*N*-ethylamine (23.34 mmol), the appropriate amine (8.56 mmol) was added. The suspension was heated with stirring in a sealed tube under an argon atmosphere (for detailed conditions see Table 1). After cooling to room temperature, the reaction mixture was evaporated under reduced pressure and the residue was partitioned between water (50 mL) and dichloromethane (50 mL). In addition, the water phase was extracted twice with dichloromethane. The combined organic phases were washed with water and brine and evaporated under reduced pressure.

*(4-Bromobenzyl)-(2-chloro-9-cyclopentyl-9H-purin-6-yl)-amine (**2a**).* Yield 98%; mp 152−154 °C. Elemental analysis Calcd for $C_{17}H_{17}ClBrN_5$ (406.71): C, 50.20; H, 4.21; N, 17.22. Found: C, 50.00; H, 3.99; N, 16.95. HPLC-MS (ESI+): 408 (99.9%). ^{1}H NMR (DMSO-d_6): 1.64−1.69 (m, 2H), 1.81−1.96 (m, 4H), 2.09−2.15 (m, 2H), 4.59 (d, J = 6.72, 2H, CH_2), 4.77 (qui, J = 7.05, 1H, CH), 7.28 (d, J = 8.22, 2H, ArH), 7.49 (d, J = 8.22, 2H, ArH), 8.26 (s, 1H, CH), 8.83 (t, J = 6.72, 1H, NH).

*(6-Bromopyridin-3-ylmethyl)-(2-chloro-9-cyclopentyl-9H-purin-6-yl)-amine (**2b**).* Yield 71%; mp 178−179 °C. Elemental analysis Calcd for $C_{16}H_{16}ClBrN_6$ (407.70): C, 47.14; H, 3.96; N, 20.61. Found: C, 47.35; H, 3.88; N, 20.48. HPLC-MS (ESI+): 409 (98.5%). ^{1}H NMR (DMSO-d_6): 1.64−1.69 (m, 2H), 1.81−1.96 (m, 4H), 2.09−2.15 (m, 2H), 4.61 (s(br), 2H, CH_2), 4.77 (qui, J = 7.20, 1H, CH), 7.59 (d, J = 8.19, 1H, ArH), 7.70 (d, J = 8.19, 1H, ArH), 8.26 (s, 1H, CH), 8.38 (s, 1H, ArH), 8.82 (s(br), 1H, NH). ^{13}C NMR (DMSO-d_6): 10.25, 23.88, 25.98, 33.00, 56.13, 64.74, 118.34, 128.16, 133.25, 138.39, 141.40, 149.87.

*(2-Chloro-9-cyclopentyl-9H-purin-6-yl)-(4-furan-2-yl-benzyl)-amine (**3a**).* Yield 85%; mp 135−137 °C. Elemental analysis Calcd for $C_{21}H_{20}ClN_5O$ (393.87): C, 64.04; H, 5.12; N, 17.78. Found: C, 64.25; H, 4.98; N, 17.67. HPLC-MS (ESI+): 394 (97.4%). ^{1}H NMR ($CDCl_3$): 1.72−1.93 (m, 6H), 2.22−2.28 (m, 2H), 4.85−4.92 (m, 3H, CH, CH_2), 6.48 (d, J = 3.28, 1H, ArH), 6.55 (s(br), 1H, NH), 6.65 (d, J = 3.33, 1H, ArH), 7.40 (d, J = 8.13, 2H, ArH), 7.48 (t, J = 3.33, 1H, ArH), 7.64−7.69 (m, 3H, ArH, CH).

*(2-Chloro-9-cyclopentyl-9H-purin-6-yl)-(6-furan-2-yl-pyridin-3-yl-methyl)-amine (**3b**).* Yield 96%; mp 119−122 °C. Elemental analysis Calcd for $C_{20}H_{19}ClN_6O$ (394.86): C, 60.84; H, 4.85; N, 21.28. Found: C, 60.56; H, 4.92; N, 21.48. HPLC-MS (ESI+): 396 (97.6%). ^{1}H NMR ($CDCl_3$): 1.76−1.91 (m, 6H), 2.22−2.28 (m, 2H), 4.85−4.92 (m, 3H, CH, CH_2), 6.54 (d, J = 3.42, 1H, ArH), 6.59 (s(br), 1H, NH), 7.05 (d, J = 3.42, 1H, ArH), 7.53 (d, J = 3.42, 1H, ArH), 7.64−7.69 (m, 2H, ArH), 7.75 (d, J = 6.27, 1H, ArH) 8.61 (s, 1H, CH).

*(2-Chloro-9-cyclopentyl-9H-purin-6-yl)-(6-thiophen-2-yl-pyridin-3-ylmethyl)-amine (**3c**).* Yield 92%; mp 111−114 °C. Elemental analysis Calcd for $C_{20}H_{19}ClSN_6$ (410.92): C, 58.46; H, 4.66; N, 20.45; S, 7.80. Found: C, 58.56; H, 4.72; N, 20.37, S, 7.55. HPLC-MS (ESI+): 411.3 (97.3%). ^{1}H NMR (DMSO-d_6):1.61−1.70 (m, 2H), 1.78−1.96 (m, 4H), 2.09−2.16 (m, 2H), 4.64 (d, J = 5.37, 2H, CH_2), 4.77 (qui, J = 7.20, 1H, CH), 7.14 (t, J = 4.52, 1H, ArH), 7.59 (d, J = 5.01, 1H, ArH), 7.74 (d, J = 5.01, 1H, ArH), 7.80 (d, J = 4.52, 1H, ArH), 7.85 (d, J = 4.52, 1H, ArH), 8.27 (s, 1H, CH), 8.51 (s, 1H, ArH), 8.87 (t, J = 5.37, 1H, NH).

*(2-Chloro-9-cyclopentyl-9H-purin-6-yl)-(4-pyrazol-1-yl-benzyl)-amine (**3d**).* Yield 72%; mp 165−167 °C. Elemental analysis Calcd for $C_{20}H_{19}ClN_6O$ (394.86): C, 60.84; H, 4.85; N, 21.28. Found: C, 60.56; H, 4.92; N, 21.48. HPLC-MS (ESI+): 394.3 (97.6%). ^{1}H NMR (DMSO-d_6): 1.61−1.71 (m, 2H), 1.80−1.98 (m, 4H), 2.09−2.18 (m, 2H), 4.66 (d, J = 5.25, 2H, CH_2), 4.77 (qui, J = 7.05, 1H, CH), 6.51 (t, J = 2.16, 1H, ArH), 7.45 (d, J = 8.37, 2H, ArH), 7.71 (d, J = 2.16, 1H, ArH), 7.77 (d, J = 8.37, 2H, ArH), 8.27 (s, 1H, CH), 8.43 (d, J = 2.16, 1H, ArH), 8.86 (t, J = 5.25, 1H, NH).

*4-Chloro-2-[(2-chloro-9-cyclopentyl-9H-purin-6-ylamino)-methyl]-phenol (**7a**).* Yield 96%; mp 121−123 °C. Elemental analysis Calcd for $C_{17}H_{17}Cl_2N_5O$ (378.26): C, 53.98; H, 4.53; N, 18.51. Found: C, 54.09; H, 4.59; N, 18.11. HPLC-MS (ESI+): 379.3 (98.5%). ^{1}H NMR (DMSO-d_6): 1.67−1.71 (m, 2H), 1.75−1.98 (m, 4H), 2.09−2.13 (m, 2H), 4.56 (d, J = 5.19, 2H, CH_2), 4.79 (qui, J = 7.20, 1H, CH), 6.84 (d, J = 8.43, 1H, ArH), 7.05−7.12 (m, 2H, ArH), 8.29 (s, 1H, CH), 8.64 (t, J = 5.19, 1H, NH), 9.97 (s, 1H, OH).

*(2-Aminobenzyl)-(2-chloro-9-cyclopentyl-9H-purin-6-yl)-amine (**7b**).* Yield 97%; mp 128−130 °C. Elemental analysis Calcd for $C_{17}H_{19}ClN_6$ (342.83): C, 59.56; H, 5.59; N, 24.51. Found: C, 59.59; H, 5.32; N, 24.33. HPLC-MS (ESI+): 343.3 (96.6%). ^{1}H NMR (DMSO-d_6): 1.67−1.71 (m, 2H), 1.75−1.98 (m, 4H), 2.09−2.14 (m, 2H), 4.44 (d, J = 5.13, 2H, CH_2), 4.77 (qui, J = 7.44, 1H, CH), 5.21 (s(br), 2H, NH_2), 6.48 (t, J = 7.41, 1H, ArH), 6.64 (d, J = 7.86, 1H, ArH), 6.93 (t, J = 7.23, 1H, ArH), 7.07 (d, J = 7.23, 1H, ArH), 8.26 (s, 1H, CH), 8.67 (t, J = 5.13, 1H, NH).

General Procedure B for Preparing Compounds 4a, 4b, 5i, 5o, 5q, 8a, and 8b. Well powdered bromoderivative **2** or **3** (7.36 mmol) and *trans*-1,4-diaminocyclohexane (110.0 mmol) were mixed and heated with stirring in a sealed tube under an argon atmosphere (for detailed conditions see Table 1). After cooling to 100 °C, water (50 mL) was added to the reaction mixture and the resulting suspension was extracted three times with ethyl acetate (50 mL). Combined organic phases were washed with water and brine, dried over sodium sulfate, and evaporated under reduced pressure. The residue was dissolved in ethyl acetate (10 mL) and triturated with diethyl ether to obtain a white crystalline mass, which was filterd off and dried at 80 °C for 4 h. The crude product was purified by column chromatography, mobile phase chloroform−methanol (19:1, v/v), if necessary.

*N^2-(4-Aminocyclohexyl)-N^6-(4-bromobenzyl)-9-cyclopentyl-9H-purine-2,6-diamine (**4a**).* Yield 91%; mp 123−124 °C. Elemental analysis Calcd for $C_{23}H_{30}BrN_7$ (484.44): C, 57.02; H, 6.24; N, 20.24. Found: C, 56.88; H, 6.19; N, 20.02. HPLC-MS (ESI+): 484.2, 486.1 (100.0%). ^{1}H NMR (DMSO-d_6): 0.85−1.22 (m, 4H), 1.64−2.04 (m, 12H) 3.29−3.37 (m, 3H, CH, NH_2), 3.52 (sex, J = 7.11, 1H, CH), 4.57 (s(br), 2H, CH_2), 4.62 (qui, 1H, J = 7.38, CH), 6.02 (d, J = 7.89, 1H, NH), 7.28 (d, J = 8.31, 2H, ArH), 7.46 (d, J = 8.31, 2H, ArH), 7.73 (s, 1H, CH), 7.84 (s(br), 1H, NH).

*N^2-(4-Aminocyclohexyl)-N^6-(6-bromo-pyridin-3-ylmethyl)-9-cyclopentyl-9H-purine-2,6-diamine (**4b**).* Yield 33%; mp 114−116 °C. Elemental analysis Calcd for $C_{22}H_{29}BrN_8$ (485.42): C, 54.43; H, 6.02; N, 23.08. Found: C, 54.29; H, 6.15; N, 23.00. HPLC-MS (ESI+): 487.2, 488.2 (98.1%). ^{1}H NMR ($CDCl_3$): 1.13−1.29 (m, 4H), 1.50

dx.doi.org/10.1021/jm4006884 | J. Med. Chem. 2013, 56, 6234−6247

(s(br), 2H, NH_2), 1.71−2.22 (m, 12H), 2.75 (sep, J = 7.43, 1H, CH), 3.67 (sex, J = 7.52, 1H, CH), 4.59 (d, J = 7.52, 1H, NH), 4.70 (qui, J = 7.20, 1H, CH), 4.82 (d, J = 7.20, 2H, CH_2), 6.21 (t, J = 5.25, 1H, NH), 7.40 (d, J = 8.16, 1H, ArH), 7.55 (dd, J = 8.16, J' = 2.4, 1H, ArH), 8.34 (s(br), 1H, NH), 8.39 (s, 1H, CH). ^{13}C NMR ($CDCl_3$): 24.25, 31.99, 32.66, 35.21, 41.30, 50.11, 50.27, 55.56, 114.53, 127.91, 134.77, 135.72, 137.96, 140.67, 149.49, 152.52, 154.58, 158.77.

*N^2-(4-Aminocyclohexyl)-9-cyclopentyl-N^6-(4-pyrazol-1-yl-benzyl)-9H-purine-2,6-diamine (**5i**).* Yield 78%; mp 186−187 °C. Elemental analysis Calcd for $C_{26}H_{33}N_9$ (471.60): C, 66.22; H, 7.05; N, 26.73. Found: C, 66.48; H, 7.24; N, 16.51. HPLC-MS (ESI+): 472.4 (99.8%). ^{1}H NMR (DMSO-d_6): 1.02−1.21 (m, 4H), 1.64−2.05 (m, 12H), 2.90−3.15 (m, 3H, CH, NH_2), 3.59 (sex, J = 5.05, 1H, CH), 4.58−4.67 (m, 3H, CH_2, CH), 6.05 (d, J = 7.29, 1H, NH), 6.51 (t, J = 2.28, 1H, ArH), 7.45 (d, J = 8.34, 2H, ArH), 7.70−7.86 (m, 4H, ArH), 7.95 (s(br), 1H, NH), 8.42 (d, J = 7.29, 1H, CH). ^{13}C NMR (DMSO-d_6): 24.26, 31.93, 32.70, 34.83, 50.01, 50.30, 55.47, 107.61, 114.56, 119.35, 126.83, 128.67, 135.45, 137.78, 139.32, 141.08, 154.84, 158.90.

*N^2-(4-Aminocyclohexyl)-9-cyclopentyl-N^6-(6-furan-2-yl-pyridin-3-ylmethyl)-9H-purine-2,6-diamine (**5o**).* Yield 89%; mp 184−186 °C. Elemental analysis Calcd for $C_{26}H_{32}N_8O$ (472.59): C, 66.08; H, 6.83; N, 23.71. Found: C, 66.32; H, 6.59; N, 23.99. HPLC-MS (ESI+): 473.5 (98.6%). ^{1}H NMR ($CDCl_3$): 1.12−1.28 (m, 4H), 1.71−2.15 (m, 12H), 2.60−2.68 (m, 3H, CH, NH_2), 3.68 (sex, J = 7.02, 1H, CH), 4.65−4.73 (m, 4H, CH, CH_2, NH), 6.50 (t, J = 3.42, 1H, ArH), 6.62 (s(br), 1H, NH), 7.00 (s, 1H, ArH), 7.41−7.69 (m, 4H, ArH), 8.57 (s, 1H, CH).

*N^2-(4-Aminocyclohexyl)-9-cyclopentyl-N^6-(6-thiophen-2-yl-pyridin-3-ylmethyl)-9H-purine-2,6-diamine (**5q**).* Yield 88%; mp 151−153 °C. Elemental analysis Calcd for $C_{26}H_{34}N_8S$ (497.64): C, 63.64; H, 6.98; N, 22.84; S, 6.53. Found: C, 63.72; H, 7.08; N, 23.02; S, 6.28. HPLC-MS (ESI+): 489.4 (99.9%). ^{1}H NMR (DMSO-d_6): 1.04−1.17 (m, 4H), 1.64−2.05 (m, 12H), 3.25−3.38 (m, 3H, CH, NH_2), 3.54 (sex, J = 7.83, 1H, CH), 4.59−4.65 (m, 3H, CH_2, CH), 6.09 (d, J = 7.83, 1H, NH), 7.13 (t, J = 4.05, 1H, ArH), 7.58 (d, J = 4.05, 1H, ArH), 7.71−7.84 (m, 4H, ArH), 7.90 (s(br), 1H, NH), 8.51 (s, 1H, CH).

*2-{[2-(4-Aminocyclohexylamino)-9-cyclopentyl-9H-purin-6-ylamino]-methyl}-4-chloro-phenol (**8a**).* Yield 85%; mp 134−136 °C. Elemental analysis Calcd for $C_{23}H_{30}ClN_7O$ (455.99): C, 60.58; H, 6.63; N, 21.50. Found: C, 60.69; H, 6.67; N, 21.34. HPLC-MS (ESI+): 448.4 (99.5%). ^{1}H NMR (DMSO-d_6): 1.05−1.22 (m, 4H), 1.60−2.02 (m, 12H), 3.53 (sex, J = 7.68, 1H, CH), 4.44−4.52 (m, 3H, CH, CH_2), 4.61 (qui, J = 7.17, 1H, CH), 6.07 (d, J = 7.68, 1H, NH), 6.77 (d, J = 8.70, 1H, ArH), 7.00−7.03 (m, 2H, ArH), 7.62 (s(br), 1H, NH), 7.73 (s, 1H, CH).

*N^6-(2-Aminobenzyl)-N^2-(4-amino-cyclohexyl)-9-cyclopentyl-9H-purine-2,6-diamine (**8b**).* Yield 82%; mp 135−136 °C. Elemental analysis Calcd for $C_{23}H_{32}N_8$ (420.57): C, 65.69; H, 7.67; N, 26.64. Found: C, 65.34; H, 7.84; N, 26.42. HPLC-MS (ESI+): 421.4 (99.6%). ^{1}H NMR (DMSO-d_6): 1.04−1.29 (m, 4H), 1.61−2.03 (m, 12H), 3.34 (sep, J = 7.20, 1H, CH), 3.65 (sex, J = 6.96, 1H, CH), 4.45 (s(br), 2H, CH_2), 4.65 (qui, J = 6.63, 1H, CH), 5.21 (s(br), 2H, NH_2), 6.08 (d, J = 7.11, 1H, NH), 6.44 (t, J = 7.05, 1H, ArH), 6.58 (d, J = 7.77, 1H, ArH), 6.91 (t, J = 7.77, 1H, ArH), 7.12 (d, J = 7.05, 1H, ArH), 7.57 (s(br), 1H, NH), 7.71 (s, 1H, CH).

General Procedure C for the Preparation of Compounds 3a, 5a−5c, 5e, 5f, 5j, 5k−5m, 5o, and 5p. To the suspension of bromoderivative **2** or **4** (0.21 mmol), the appropriate arylboronic acid (0.31 mmol), potassium phosphate trihydrate (0.80 mmol) and tetrabutylammonium bromide (0.003 mmol) in *N*,*N*-dimethylformamide (5.0 mL), and palladium diacetate (2.5 μmol) were added under an argon atmosphere. The suspension was heated with stirring in a sealed tube under an argon atmosphere (for detailed conditions see Table 1). After cooling to room temperature, the reaction mixture was diluted with water (20 mL) and the resulting suspension was extracted twice with ethyl acetate (25 mL). Combined organic phases were washed with brine, dried over anhydrous sodium sulfate, and evaporated under reduced pressure. The crude product was purified by column chromatography on silica, mobile phase chloroform−methanol−concd ammonium hydroxide (9:1:0.05).

*(2-Chloro-9-cyclopentyl-9H-purin-6-yl)-(4-furan-2-yl-benzyl)-amine (**3a**).* Yield 55%; mp 135−137 °C.

*N^2-(4-Aminocyclohexyl)-9-cyclopentyl-N^6-biphenyl-4-ylmethyl)-9H-purine-2,6-diamine (**5a**).* Yield 78%; mp 146−148 °C. Elemental analysis Calcd for $C_{29}H_{36}N_8$ (496.65): C, 72.32; H, 7.32; N, 20.36. Found: C, 72.61; H, 7.16; N, 20.19. HPLC-MS (ESI+): 482.4 (99.7%). ^{1}H NMR (DMSO-d_6): 1.06−1.20 (m, 4H), 1.64−2.05 (m, 12H), 3.17−3.30 (m, 3H, NH_2, CH), 3.60 (sex, J = 6.71, 1H, CH), 4.60−4.65 (m, 3H, CH, CH_2), 6.03 (d, J = 7.20, 1H, NH), 7.35 (t, J = 7.29, 1H, ArH), 7.41−7.46 (m, 4H, ArH), 7.56−7.62 (m, 4H, ArH), 7.74 (s, 1H, CH).

*N^6-(2′-Aminobiphenyl-4-ylmethyl)-N^2-(4-aminocyclohexyl)-9-cyclopentyl-9H-purine-2,6-diamine (**5b**).* Yield 85%; mp 168−170 °C. Elemental analysis Calcd for $C_{29}H_{36}N_8$ (496.65): C, 70.13; H, 7.31; N, 22.56. Found: C, 70.32; H, 7.28; N, 22.46. HPLC-MS (ESI+): 497.4 (99.9%). ^{1}H NMR (DMSO-d_6): 1.14−1.26 (m, 4H), 1.72−1.82 (m, 2H), 1.83−1.96 (m, 10H), 1.98−2.22 (m, 4H), 2.71 (sex, J = 6.72, 1H, CH), 3.69−3.80 (m, 3H, NH_2, CH), 4.66 (d, J = 7.71, 1H, NH), 4.74 (qui, J = 7.08, 1H, CH), 4.81 (d, J = 5.43, 2H, CH_2), 6.15 (s(br), 1H, NH), 6.76 (d, J = 7.41, 1H, ArH), 6.82 (t, J = 7.41, 1H, ArH), 7.11 (d, J = 7.41, 1H, ArH), 7.15 (t, J = 7.41, 1H, ArH), 7.38−7.46 (m, 5H, ArH, CH).

*N^2-(4-Aminocyclohexyl)-9-cyclopentyl-N^6-(2′-methoxybiphenyl-4-ylmethyl)-9H-purine-2,6-diamine (**5c**).* Yield 88%; mp 178−180 °C. Elemental analysis Calcd for $C_{30}H_{37}N_7O$ (511.66): C, 70.42; H, 7.29; N, 19.16. Found: C, 70.58; H, 7.10; N, 19.45. HPLC-MS (ESI+): 512.4 (99.8%). ^{1}H NMR ($CDCl_3$): ^{1}H NMR ($CDCl_3$): 1.14−1.34 (m, 4H), 1.71−2.22 (m, 14H), 2.74 (sep, J = 6.33, 1H, CH), 3.78 (sex, J = 7.05, 1H, CH), 4.00 (s, 3H, CH_3), 4.59 (d, J = 5.87, 1H, NH), 4.71 (qui, J = 6.87, 1H, CH), 4.79 (d, J = 7.20, 2H, CH_2), 6.12 (s(br), J = 7.42, 1H, NH), 7.05 (d, J = 8.05, 1H, ArH), 7.09 (t, J = 8.05, 1H, ArH), 7.32 (t, J = 8.05, 1H, ArH), 7.49 (d, J = 8.05, 1H, ArH), 7.38−7.46 (m, 4H, ArH), 8.65 (s, 1H, CH).

*N^2-(4-Aminocyclohexyl)-9-cyclopentyl-N^6-(4-furan-2-yl-benzyl)-9H-purine-2,6-diamine (**5e**).* Yield 87%; mp 157−159 °C. Elemental analysis Calcd for $C_{27}H_{33}N_7O$ (471.60): C, 68.76; H, 7.05; N, 20.79. Found: C, 68.81; H, 7.22 N, 20.51. HPLC-MS (ESI+): 472.4 (99.8%). ^{1}H NMR (DMSO-d_6): 1.04−1.17 (m, 4H), 1.64−2.05 (m, 12H), 2.65−2.72 (m, 3H, CH, NH_2), 3.58 (sex, J = 7.55, 1H, CH), 4.58−4.63 (m, 3H, CH, CH_2), 6.04 (d, J = 7.55, 1H, NH), 7.28 (d, J = 7.89, 2H, ArH), 7.38 (d, J = 5.95, 1H, ArH), 7.46 (d, J = 7.89, 2H, ArH), 7.61 (d, J = 5.95, 1H, ArH), 7.70−7.73 (m, 2H, ArH, NH), 7.95 (s, 1H, CH). ^{13}C NMR (DMSO-d_6): 24.24, 31.93, 32.70, 34.74, 49.97, 50.29, 55.44, 104.90, 111.69, 114.52, 128.01, 129.27, 129.92, 131.60, 135.36, 138.55, 142.03, 151.63, 153.95, 154.78, 158.91.

*N^2-(4-Aminocyclohexyl)-9-cyclopentyl-N^6-(6-furan-3-yl-pyridin-3-ylmethyl)-9H-purine-2,6-diamine (**5f**).* Yield 94%; mp 154−156 °C. Elemental analysis Calcd for $C_{27}H_{33}N_7O$ (471.60): C, 68.76; H, 7.05; N, 20.79. Found: C, 68.52; H, 7.16 N, 20.49. HPLC-MS (ESI+): 472.4 (97.8%). ^{1}H NMR (DMSO-d_6): 1.04−1.17 (m, 4H), 1.64−2.05 (m, 12H), 3.15−3.19 (m, 3H, CH, NH_2), 3.58 (sex, J = 7.32, 1H, CH), 4.58−4.63 (m, 3H, CH, CH_2), 6.05 (d, J = 7.32, 1H, NH), 6.91 (s, 1H, ArH), 7.34 (d, J = 7.92, 2H, ArH), 7.51 (d, J = 7.92, 2H, ArH), 7.70−7.73 (m, 2H, ArH), 7.78 (s(br), 1H, NH), 8.12 (s, 1H, CH). ^{13}C NMR (DMSO-d_6): 24.39, 31.74, 32.28, 35.06, 49.13, 50.13, 50.37, 56.10, 109.24, 125.80, 126.25, 128.32, 130.66, 136.80, 138.31, 139.51, 144.70, 153.10, 158.88.

*1-[9-Cyclopentyl-6-(4-furan-2-yl-benzylamino)-9H-purin-2-ylamino]-2-methyl-propan-2-ol (**5j**).* Yield 80%; mp 121−123 °C. Elemental analysis Calcd for $C_{25}H_{30}N_6O_2$ (446.54): C, 67.24; H, 6.77; N, 18.82. Found: C, 67.59; H, 6.37; N, 18.62. HPLC-MS (ESI+): 447.4 (99.8%). ^{1}H NMR ($CDCl_3$): 1.27 (s, 6H, CH_3), 1.70−1.91 (m, 6H), 2.20−2.35 (m, 2H), 3.40 (d, J = 6.18, 2H, CH_2), 4.70 (qui, J = 5.01, 1H, CH), 4.79 (s(br), 2H, CH_2), 5.29 (s(br), 1H, OH), 5.62 (t, J = 6.21, 1H, NH), 7.21−7.63 (m, 7H, ArH), 7.68 (s(br), 1H, NH), 8.63 (s, 1H, CH).

*N^2-(4-Aminocyclohexyl)-9-cyclopentyl-N^6-(6-phenyl-pyridin-3-ylmethyl)-9H-purine-2,6-diamine (**5k**).* Yield 86%; mp 136−137 °C. Elemental analysis Calcd for $C_{28}H_{34}N_8$ (482.62): C, 69.68; H, 7.10; N,

23.22. Found: C, 69.55; H, 7.16; N, 23.28. HPLC-MS (ESI+): 483.5 (99.9%). ^{1}H NMR (DMSO-d_6): 1.05−1.18 (m, 4H), 1.64−2.05 (m, 12H), 2.65−2.72 (m, 3H, CH, NH_2), 3.58 (sex, J = 7.55, 1H, CH), 4.67−4.78 (m, 3H, CH, CH_2), 7.27−7.72 (m, 6H, ArH), 7.80 (d, J = 7.8, 2H, ArH), 7.70 (s(br), 1H, NH), 7.95 (s, 1H, CH).

*N^2-(4-Aminocyclohexyl)-N^6-[6-(2-aminophenyl)-pyridin-3-yl-methyl]-9-cyclopentyl-9H-purine-2,6-diamine (**5l**).* Yield 56%; mp 173−175 °C. Elemental analysis Calcd for $C_{28}H_{35}N_9$ (497.64): C, 67.58; H, 7.09; N, 25.33. Found: C, 67.69; H, 7.19; N, 25.02. HPLC-MS (ESI+): 498.4 (99.9%). ^{1}H NMR ($CDCl_3$): 1.14−1.34 (m, 4H), 1.71−2.05 (m, 12H), 2.10−2.23 (m, 4H, 2 × NH_2), 2.75 (sep, J = 7.32, 1H, CH), 3.73 (sex, J = 7.52, 1H, CH), 4.59 (d, J = 7.52, 1H, NH), 4.70 (qui, J = 7.20, 1H, CH), 4.82 (d, J = 7.20, 2H, CH_2), 5.92 (t, J = 7.20, 1H, NH), 6.75−6.81 (m, 2H, ArH), 7.20 (t, J = 7.89, 1H, ArH), 7.47−7.51 (m, 2H, ArH), 7.61 (d, J = 8.34, 1H, ArH), 7.79 (d, J = 8.34, 1H, ArH), 8.63 (s, 1H, CH).

*N^2-(4-Aminocyclohexyl)-N^6-[6-(2-methoxyphenyl)-pyridin-3-yl-methyl]-9-cyclopentyl-9H-purine-2,6-diamine (**5m**).* Yield 85%; mp 184−186 °C. Elemental analysis Calcd for $C_{29}H_{36}N_8O$ (512.65): C, 67.94; H, 7.08; N, 21.86. Found: C, 67.78; H, 7.01; N, 21.59. HPLC-MS (ESI+): 513.5 (99.6%). ^{1}H NMR ($CDCl_3$): 1.14−1.34 (m, 4H), 1.71−2.22 (m, 12H), 2.72 (sep, J = 5.87, 1H, CH), 3.75 (sex, J = 6.25, 1H, CH), 3.85 (s, 3H, CH_3), 4.61 (d, J = 5.87, 1H, NH), 4.69 (qui, J = 6.87, 1H, CH), 4.82 (d, J = 7.20, 2H, CH_2), 6.00 (s(br), J = 7.20, 1H, NH), 7.00 (d, J = 8.22, 1H, ArH), 7.09 (t, J = 7.32, 1H, ArH), 7.35 (t, J = 7.32, 1H, ArH), 7.49 (s, 1H, ArH), 7.70−7.74 (m, 3H, ArH), 8.72 (s, 1H, CH). ^{13}C NMR ($CDCl_3$): 24.21, 31.76, 32.71, 33.82, 41.84, 49.81, 55.43, 55.68, 111.42, 114.51, 121.18, 125.01, 128.89, 130.01, 131.13, 133.23, 135.14, 135.44, 148.64, 152.50, 154.71, 155.03, 156.95, 158.79.

*N^2-(4-Aminocyclohexyl)-9-cyclopentyl-N^6-(6-furan-2-yl-pyridin-3-ylmethyl)-9H-purine-2,6-diamine (**5o**).* Yield 81%; mp 180−183 °C. Elemental analysis Calcd for $C_{26}H_{32}N_8O$ (472.59): C, 66.08; H, 6.83; N, 23.71. Found: C, 66.18; H, 6.59; N, 23.88. HPLC-MS (ESI+): 473.5 (99.8%).

*N^2-(4-Aminocyclohexyl)-9-cyclopentyl-N^6-(6-furan-3-yl-pyridin-3-ylmethyl)-9H-purine-2,6-diamine (**5p**).* Yield 76%; mp 165−167 °C. Calcd for $C_{26}H_{32}N_8O$ (472.59): C, 66.08; H, 6.83; N, 23.71. Found: C, 66.01; H, 6.93; N, 23.51. HPLC-MS (ESI+): 473.26 (98.6%). ^{1}H NMR ($CDCl_3$): 1.12−1.28 (m, 4H), 1.71−2.15 (m, 12H), 2.60−2.68 (m, 3H, CH, NH_2), 3.68 (sex, J = 10.00, 1H, CH), 4.65−4.73 (m, 4H, CH, CH_2, NH), 6.50 (t, J = 3.42, 1H, ArH), 6.62 (s(br), 1H, NH), 6.91 (s, 1H, ArH), 7.00 (s, 1H, ArH), 7.61−7.73 (m, 3H, ArH), 8.57 (s, 1H, CH).

General Procedure D for the Preparation of Compounds 5d, 5g, 5h, 5n, 5r, and 5o. To the suspension of bromoderivative **4** (0.50 mmol), the appropriate arylboronic acid (1.50 mmol), triphenylphosphine (0.25 mmol), and sodium carbonate (2.0 mmol) in a mixture of 1,2-dimethoxyethane (3.0 mL) and water (2.0 mL), and bis(dibenzylideneacetone)palladium (15.0 μmol) were added under an argon atmosphere. The suspension was heated with stirring in a sealed tube at 120 °C for 65 h under an argon atmosphere. After cooling to room temperature, the reaction mixture was diluted with water (25 mL) and the suspension was extracted twice with ethyl acetate (25 mL). Combined organic phases were washed with brine, dried over anhydrous sodium sulfate, and evaporated under reduced pressure. The residue was purified by column chromatography on silica, mobile phase chloroform−methanol−concd ammonium hydroxide (9:1:0.05).

*N^2-(4-Aminocyclohexyl)-9-cyclopentyl-N^6-(3′-fluorobiphenyl-4-yl-methyl)-9H-purine-2,6-diamine (**5d**).* Yield 75%; mp 146−148 °C. Elemental analysis Calcd for $C_{29}H_{34}FN_7$ (499.63): C, 69.71; H, 6.86; N, 19.62. Found: C, 69.95; H, 7.12; N, 19.45. HPLC-MS (ESI+): 500.4 (99.9%). ^{1}H NMR (DMSO-d_6): 1.02−1.21 (m, 4H), 1.61−2.06 (m, 12H), 2.65−2.72 (m, 3H, CH, NH_2), 3.59 (sex, J = 7.19, 1H, CH), 4.60−4.66 (m, 3H, CH_2, CH), 6.01 (d, J = 6.60, 1H, NH), 7.12−7.18 (s, 1H, ArH), 7.42−7.48 (m, 5H, ArH), 7.61 (d, J = 8.01, 2H, ArH), 7.73 (s, 1H, CH), 7.86 (s(br), 1H, NH). ^{13}C NMR (DMSO-d_6): 24.35, 31.89, 32.28, 35.83, 43.11, 50.24, 50.53, 55.44, 113.57, 113.85, 114.27, 114.55, 123.08, 123.12, 127.05, 128.44, 129.36, 131.26, 131.38, 131.95, 132.09, 136.32, 137.46, 137.49, 141.43, 143.09, 143.19, 152.40, 155.01, 158.92, 161.62, 164.85.

*N^2-(4-Aminocyclohexyl)-9-cyclopentyl-N^6-(4-thiophen-2-yl-benzyl)-9H-purine-2,6-diamine (**5g**).* Yield 71%; mp 225−226 °C. Elemental analysis Calcd for $C_{27}H_{33}N_7S$ (487.66): C, 66.50; H, 6.82; N, 20.11; S, 6.58. Found: C, 66.58; H, 6.51; N, 20.35; S, 6.41. HPLC-MS (ESI+): 488.5 (99.8%). ^{1}H NMR ($CDCl_3$): 1.20−1.28 (m, 4H), 1.61−2.22 (m, 14H), 2.71 (sep, J = 5.52, 1H, CH), 3.72 (sex, J = 7.44, 1H, CH), 4.61 (d, J = 7.44, 1H, NH), 4.71 (qui, J = 6.36, 1H, CH), 4.78 (d, J = 5.25, 2H, CH_2), 5.93 (s(br), 1H, NH), 7.08 (t, J = 4.50, 1H, ArH), 7.30 (d, J = 4.50, 1H, ArH), 7.38 (d, J = 7.95, 2H, ArH), 7.47 (d, J = 4.50, 1H, ArH), 7.57 (d, J = 7.95, 2H, ArH), 8.63 (s, 1H, CH).

*N^2-(4-Aminocyclohexyl)-9-cyclopentyl-N^6-(6-thiophen-3-yl-benzyl)-9H-purine-2,6-diamine (**5h**).* Yield 71%; mp 114−118 °C. Elemental analysis Calcd for $C_{27}H_{33}N_7S$ (487.66): C, 66.50; H, 6.82; N, 20.11; S, 6.58. Found: C, 66.49; H, 7.06 N, 20.39; S, 6.32. HPLC-MS (ESI+): 488.4 (99.9%). ^{1}H NMR (DMSO-d_6): 1.07−1.22 (m, 4H), 1.64−2.04 (m, 12H), 2.62−2.75 (m), 3H, CH, NH_2), 3.58 (sex, J = 7.25, 1H, CH), 4.60−4.65 (m, 3H, CH, CH_2), 6.02 (d, J = 7.20, 1H, NH), 7.37 (d, J = 7.71, 2H, ArH), 7.50 (d, J = 4.83, 1H, ArH), 7.61 (d, J = 7.71, 2H, ArH), 7.72−7.78 (m, 3H, ArH, NH), 8.32 (s, 1H, CH). ^{13}C NMR (DMSO-d_6): 24.37, 31.88, 32.29, 35.78, 49.14, 50.24, 50.53, 55.40, 114.22, 120.95, 126.33, 126.68, 127.47, 128.36, 133.98, 136.29, 140.31, 141.96, 152.40, 155.03, 158.93.

*N^2-(4-Aminocyclohexyl)-9-cyclopentyl-N^6-[6-(3-fluorophenyl)-pyridin-3-ylmethyl]-9H-purine-2,6-diamine (**5n**).* Yield 92%; mp 121−122 °C. Elemental analysis Calcd for $C_{28}H_{33}FN_8O$ (500.61): C, 67.18; H, 6.64; N, 22.38. Found: C, 67.41; H, 6.69; N, 22.09. HPLC-MS (ESI+): 501.4 (99.5%). ^{1}H NMR ($CDCl_3$): 1.12−1.42 (m, 4H), 1.71−2.21 (m, 12H), 2.81 (sex, J = 5.87, 1H, CH), 3.12 (s(br), 2H, NH_2), 3.73 (sex, J = 7.44, 1H, CH), 4.62−4.72 (m, 2H, CH, NH), 4.81 (d, J = 5.77, 1H, CH_2), 6.33 (t, J = 5.77, 1H, NH), 7.12 (t, J = 8.25, 1H, ArH), 7.38−7.44 (m, 2H, ArH), 7.61−7.77 (m, 4H, ArH), 8.72 (s, 1H, CH).

*N^2-(4-Aminocyclohexyl)-9-cyclopentyl-N^6-(6-furan-2-yl-pyridin-3-ylmethyl)-9H-purine-2,6-diamine (**5o**).* Yield 78%; mp 184−186 °C.

*N^2-(4-Aminocyclohexyl)-9-cyclopentyl-N^6-(6-thiophen-3-yl-pyridin-3-ylmethyl)-9H-purine-2,6-diamine (**5r**).* Yield 68%; mp 139−140 °C. Elemental analysis Calcd for $C_{26}H_{34}N_8S$ (497.64): C, 63.64; H, 6.98; N, 22.84; S, 6.53. Found: C, 63.62; H, 6.78; N, 22.59; S, 6.76. HPLC-MS (ESI+): 498.4 (98.9%). ^{1}H NMR (DMSO-d_6): 1.04−1.17 (m, 4H), 1.64−2.05 (m, 12H), 3.25−3.38 (m, 3H, CH, NH_2), 3.54 (sex, J = 7.56, 1H, CH), 4.59−4.65 (m, 3H, CH_2, CH), 6.09 (d, J = 7.56, 1H, NH), 7.11 (s, J = 4.12, 1H, ArH), 7.62 (d, J = 4.05, 1H, ArH), 7.72−7.82 (m, 4H, ArH), 7.90 (s(br), 1H, NH), 8.53 (s, 1H, CH).

General Procedure E for Preparing Compounds 4c, 5s, and 5t. The mixture of compound **2a** or **3b** (4.92 mmol), 1-amino-2-methylpropan-2-ol (25.00 mmol), *N*,*N*-diisopropyl-*N*-ethylamine (10.83 mmol), and *N*-methylpyrrolidone (5.0 mL) was heated with stirring in a sealed tube under an argon atmosphere (for detailed conditions see Table 1). After cooling to room temperature, the mixture was partitioned between water (25 mL) and ethyl acetate (25 mL) and the water phase was extracted twice with ethyl acetate. The combined organic phases were washed with water and brine and concentrated in vacuo. The residue was treated with 1% hydrochloric acid (25 mL) and extracted twice with dichloromethane. The combined organic phases were dried with sodium sulfate and concentrated in vacuo. The crude product was used for further reactions without purification. An analytical sample was obtained after column chromatography on silica (chloroform−methanol 9:1, v/v).

*1-[6-(4-Bromobenzylamino)-9-cyclopentyl-9H-purin-2-ylamino]-2-methyl-propan-2-ol (**4c**).* Yield 82%; mp 108−110 °C. Elemental analysis Calcd for $C_{21}H_{29}BrN_6O$ (461.40): C, 54.67; H, 6.34; N, 18.21. Found: C, 54.59; H, 6.12; N, 18.07. HPLC-MS (ESI+): 482.3 (98.6%). ^{1}H NMR ($CDCl_3$): 1.28 (s, 6H, CH_3), 1.74−1.90 (m, 6H), 2.05−2.38 (m, 2H), 2.84 (d, J = 2.32, 2H, CH_2), 4.75−4.83 (m, 3H, CH_2, CH), 5.20 (s(br), 1H, OH), 7.28 (d, J = 7.75, 2H, ArH), 7.45 (d, J = 7.75, 2H, ArH), 7.62 (s, 1H, CH).

dx.doi.org/10.1021/jm4006884 | J. Med. Chem. 2013, 56, 6234−6247

*1-{9-Cyclopentyl-6-[(6-furan-2-yl-pyridin-3-ylmethyl)-amino]-9H-purin-2-ylamino}-2-methyl-propan-2-ol (**5t**).* Yield 37%; mp 128−129 °C. Elemental analysis Calcd for $C_{24}H_{29}N_7O_2$ (447.53): C, 64.41; H, 6.53; N, 21.91. Found: C, 64.65; H, 6.44; N, 21.58. HPLC-MS (ESI+): 448.4 (99.5%). ^{1}H NMR ($CDCl_3$): 1.27 (s, 6H, CH_3), 1.70−1.91 (m, 6H), 2.20−2.35 (m, 2H), 3.40 (d, J = 6.21, 2H, CH_2), 4.69 (qui, J = 6.42, 1H, CH), 4.79 (s(br), 2H, CH_2), 5.24 (t, J = 6.21, 1H, NH), 5.61 (s(br), 1H, OH), 6.04 (s(br), 1H, NH), 6.54 (t, J = 3.42, 1H, ArH), 7.03 (d, J = 3.42, 1H, ArH), 7.50−7.54 (m, 2H, ArH), 7.64 (d, J = 8.25, 1H, ArH), 7.74 (dd, J = 8.25, J' = 3.42, 1H, ArH), 8.63 (s, 1H, CH).

*4-{9-Cyclopentyl-6-[(6-furan-2-yl-pyridin-3-ylmethyl)-amino]-9H-purin-2-ylamino}-cyclohexanol (**5s**).* *trans*-4-Aminocyclohexan-1-ol hydrochloride (9.43 mmol) was suspended in methanol (10 mL), and to the suspension sodium methoxide (9.43 mmol) was added. The reaction mixture was stirred for 10 min at room temperature, and sodium chloride was filtered off. The filtrate was evaporated under reduced pressure, and to the residue (2-chloro-9-cyclopentyl-9*H*-purin-6-yl)-(6-furan-2-yl-pyridin-3-ylmethyl)-amine (0.25 mmol) and *N*-methylpyrrolidone (1 mL) was added. The reaction mixture was heated at 160 °C for 16 h under an argon atmosphere. After cooling to room temperature, water (10 mL) was added and resulting suspension was extracted twice with ethyl acetate (25 mL). Combined organic phases were washed with water, and brine, dried over anhydrous sodium sulfate, and evaporated under reduced pressure. The crude product was purified by column chromatography on silica, mobile phase chloroform−methanol (9:1). Yield 33%; mp 164−166 °C. Elemental analysis Calcd for $C_{26}H_{31}N_7O_2$ (473.57): C, 65.94; H, 6.60; N, 20.70. Found: C, 66.08; H, 6.48; N, 20.34. HPLC-MS (ESI+): 474.4 (99.6%). ^{1}H NMR ($CDCl_3$): 1.22 (q, J = 10.2, 2H), 1.43 (q, J = 10.2, 2H), 1.72−1.81 (m, 2H), 1.90−2.02 (m, 6H), 2.11−2.25 (m, 4H), 2.86 (s(br), 1H, OH), 3.61−3.76 (m, 2H), 4.64 (d, J = 7.68, 1H, NH), 4.69 (qui, J = 7.14, 1H, CH), 4.79 (d, J = 5.43, 2H, CH_2), 6.12 (t, J = 5.43, 1H, NH), 6.52 (dd, J = 3.39, J' = 1.77, 1H, ArH), 7.02 (d, J = 3.39, 1H, ArH), 7.48 (s, 1H, ArH), 7.52 (d, J = 3.39, 1H, ArH), 7.63 (d, J = 8.13, 1H, ArH), 7.73 (dd, J = 8.13, J' = 2.07, 1H, ArH), 8.61 (s, 1H, CH).

General Procedure F for the Preparation of Compounds 6a and 6b. To the solution of methoxyderivative (0.48 mmol) in dichloromethane (10 mL), boron tribromide (2.40 mmol) solution in dichloromethane (10 mL) was slowly added with stirring at room temperature. The mixture was stirred for further 18 h, and then methanol (20 mL) was added dropwise. The mixture was evaporated under reduced pressure, and the residue was purified by column chromatography on silica and mobile phase chloroform−methanol−ammonium hydroxide (4:1:0.025).

*N^2-(4-Aminocyclohexyl)-9-cyclopentyl-N^6-(2′-hydroxybiphenyl-4-ylmethyl)-9H-purine-2,6-diamine (**6a**).* Yield 95%; mp 168−170 °C. Elemental analysis Calcd for $C_{29}H_{35}N_7O$ (497.63): C, 69.99; H, 7.09; N, 19.70. Found: C, 69.68; H, 7.23 N, 19.57. HPLC-MS (ESI+): 498.5 (99.9%). ^{1}H NMR ($CDCl_3$): 1.16−1.40 (m, 4H), 1.71−2.22 (m, 12H), 2.52 (s(br), 2H, NH_2), 2.76 (sep, J = 5.43, 1H, CH), 3.67 (sex, J = 7.41, 1H, CH), 4.59 (d, J = 7.25, 1H, NH), 4.72 (qui, J = 7.00, 1H, CH), 4.79 (d, J = 5.63, 2H, CH_2), 6.10 (s(br), 1H, NH), 7.10 (t, J = 7.43, 1H, ArH), 7.16 (d, J = 8.04, 1H, ArH), 7.24 (t, J = 7.43, 1H, ArH), 7.48−7.66 (m, 4H, ArH), 8.63 (s, 1H, CH).

*N^2-(4-Aminocyclohexyl)-9-cyclopentyl-N^6-[6-(2-hydroxyphenyl)-pyridin-3-ylmethyl]-9H-purine-2,6-diamine (**6b**).* Yield 86%; mp 202−203 °C. Elemental analysis Calcd for $C_{28}H_{34}N_8O$ (498.62): C, 67.45; H, 6.87; N, 22.47. Found: C, 67.28; H, 7.11 N, 22.41. HPLC-MS (ESI+): 499.5 (97.8%). ^{1}H NMR ($CDCl_3$): 1.16−1.40 (m, 4H), 1.71−2.22 (m, 12H), 2.49 (s(br), 2H, NH_2), 2.80 (sep, J = 5.31, 1H, CH), 3.62 (sex, J = 7.25, 1H, CH), 4.61 (d, J = 7.77, 1H, NH), 4.69 (qui, J = 7.17, 1H, CH), 4.82 (d, J = 5.43, 2H, CH_2), 6.13 (s(br), 1H, NH), 6.91 (t, J = 7.38, 1H, ArH), 7.02 (d, J = 8.19, 1H, ArH), 7.29 (t, J = 7.38, 1H, ArH), 7.50 (s, 1H, ArH), 7.78 (d, J = 8.19, 1H, ArH), 7.82−7.86 (m, 2H, ArH), 8.54 (s, 1H, CH). ^{13}C NMR ($CDCl_3$): 24.22, 29.77, 31.86, 32.69, 34.38, 49.94, 50.31, 55.52, 114.53, 118.62, 118.84, 118.88, 118.93, 126.14, 131.41, 133.34, 135.69, 137.11, 145.10, 153.25, 154.64, 156.70, 158.78, 159.87.

Cell Maintenance and Cytotoxicity Assays. The cytotoxicity of the studied compounds was determined using cell lines of different histological origin as described earlier.[17,53] Briefly, compounds in 3-fold dilutions were added to the cells in triplicate. The treatment lasted for 72 h, after which Calcein AM solution was added, and the fluorescence of live cells at 485 nm/538 nm (excitation/emission) was measured with a Fluoroskan Ascent microplate reader (Labsystems). IC_{50} (the drug concentration that reduced the number of viable cells to 50%) values were determined from the dose−response curves. Roscovitine and CR8, used as standard drugs, were prepared according to published procedures.[4,10]

Immunoblotting and Antibodies. Immunoblotting analysis was performed as described earlier.[17,53] Briefly, cellular lysates were prepared by harvesting cells in Laemmli sample buffer. Proteins were separated on SDS-polyacrylamide gels and electroblotted onto nitrocellulose membranes. After blocking, the membranes were incubated with specific primary antibodies overnight, washed, and then incubated with peroxidase-conjugated secondary antibodies. Finally, peroxidase activity was detected with ECL+ reagents (AP Biotech) using a CCD camera LAS-4000 (Fujifilm). Specific antibodies were purchased from Sigma-Aldrich (anti-α-tubulin, clone DM1A; peroxidase-labeled secondary antibodies; anti-pRb antibody phosphorylated at S612; anti-CDK2, clone PSTAIR), Santa Cruz Biotechnology (anti-Mcl-1, clone S-19; anti-PARP, clone F-2; anti-β-actin, clone C4; anti-pCdk2 (T160); anti-pCDK1 (T161); anti-CDK1, clone B-6), Roche Applied Science (anti-5-bromo-2′-deoxyuridine-fluorescein, clone BMC 9318), Bethyl Laboratories (anti-pRNA polymerase II antibodies phosphorylated at S5 and (S2)), Millipore (anti-RNA polymerase II, clone ARNA-3), Cell Signaling (anti-pPP1α (T320); anti-PP1α; anti-pNPM (T199); anti-NPM; anticaspase-3, clone 3G2; anticaspase-7; anticleaved caspase-9 (D330); anti-pRb antibodies phosphorylated at S780 and S807/811; anti-Rb, clone 4H1) or were a generous gift from Dr. B. Vojtěšek from Masaryk Memorial Cancer Institute, Brno, Czech Republic (anti-p53, clone DO-1).

Kinase Inhibition Assays. CDK2/Cyclin E kinase was produced in Sf9 insect cells via baculoviral infection and purified on a NiNTA column (Qiagen). CDK5/p35, CDK7Cyclin H/MAT1, and CDK9/Cyclin T1 were purchased from ProQinase GmbH. The kinases were assayed with 1 mg/mL histone H1 (for CDK2 and CDK5) or (YSPTSPS)2KK peptide (for CDK7 and CDK9) in the presence of 15/0.15/1.5/1.5 μM ATP (for CDK2/CDK5/CDK7CDK9), 0.05 μCi [γ-^{33}P]ATP, and of the test compound in a final volume of 10 μL, all in a reaction buffer (60 mM HEPES-NaOH, pH 7.5, 3 mM $MgCl_2$, 3 mM $MnCl_2$, 3 μM Na-orthovanadate, 1.2 mM DTT, 2.5 μg/50 μL PEG20.000). The reactions were stopped by adding 5 μL of 3% aq H_3PO_4. Aliquots were spotted onto P-81 phosphocellulose (Whatman), washed 3× with 0.5% aq H_3PO_4, and finally air-dried. Kinase inhibition was quantified using a FLA-7000 digital image analyzer (Fujifilm). The concentration of the test compounds required to decrease the CDK activity by 50% was determined from dose−response curves and designated as IC_{50}.[17,53]

Cell Cycle Analysis. Subconfluent cells were treated with test compounds at different concentrations for 24 h. The cultures were pulse-labeled with 10 μM 5-bromo-2′-deoxyuridine (BrdU) for 30 min at 37 °C prior to harvesting. The cells were then washed in PBS, fixed with 70% ethanol, and denatured in 2 M HCl. Following neutralization, the cells were stained with anti-BrdU fluorescein-labeled antibodies, washed, stained with propidium iodide, and analyzed by flow cytometry using a 488 nm laser (Cell Lab Quanta SC, Beckman Coulter) as described previously.[17,53]

Caspases Activity Assay. The cells were homogenized in an extraction buffer (10 mM KCl, 5 mM HEPES, 1 mM EDTA, 1 mM EGTA, 0.2% CHAPS, inhibitors of proteases, pH 7.4) on ice for 20 min. The homogenates were clarified by centrifugation at 10000*g* for 30 min at 4 °C, and then the proteins were quantified and diluted to equal concentrations. Lysates were then incubated for 5 h with 100 μM Ac-DEVD-AMC as a substrate of caspases-3,7 in the assay buffer (25 mM PIPES, 2 mM EGTA, 2 mM $MgCl_2$, 5 mM DTT, pH 7.3) or for 24 h with 100 μM Ac-LEHD-AMC as a substrate of caspase-9 in the assay buffer (100 mM HEPES, pH 7.5; 0.5 mM EDTA; 20%

glycerol, 5 mM DTT). The fluorescence of the product was measured using a Fluoroskan Ascent microplate reader (Labsystems) at 355/460 nm (excitation/emission) as described previously.[17]

Molecular Modeling. 3D structures of compounds were prepared with Marvin, a software used for drawing, displaying, and characterizing chemical structures, substructures, and reactions [Marvin 5.10.3, 2012, ChemAxon (http://www.chemaxon.com)]. 3D structures were optimized and all hydrogens were added within the MarvinSketch 5.10 program. All compounds contain mostly aromatic residues, which were kept planar as well as secondary amino groups attached to C2 and C6 positions on the purine ring. The cyclohexane ring was kept in the most stable chair conformation, and the cyclopentane ring was attached in the N9 position to the equatorial position on the endo carbon as this combination poses the smallest sterical clashes with the purine central ring. Ionization of groups was considered for the range of pH 5.5−7.5. Therefore, the primary amino groups attached to the aliphatic carbons were kept charged ($pK_{a\ est.\ Marvin} < 5$), nitrogens attached to the aromatic rings were kept neutral ($pK_a > 10$). All nonaromatic and nonring bonds were set as rotatable within AutoDock Tools program.[54]

The crystal structure for CDK2 with roscovitine (PDB ID: 2A4L) was used as the protein docking template. Glu8 and His84 were set as flexible. Polar hydrogens were added to receptor or selected for all ligands with the AutoDock Tools program[54] prior to docking with the Autodock Vina program.[55] Docking grid box was set to 14 Å around the center of the ligand in the crystal structure, which was deleted prior to docking. Vina docking parameters were extended in order to increase docking accuracy and exhaustiveness with energy_range = 10 (default 3), num_modes = 500 (default 9), exhaustiveness = 20 (default 8).

As the docking results with the default setting did not correlate well with the experimental IC_{50} data ($r^2 < 0.2$, data not shown), we analyzed binding motifs of CDK2 inhibitors found in crystal structures. In all cases, the binding motif interacted with conserved hydrogen bonds of the Leu83 and Glu81 backbones as in the roscovitine crystal structure (PDB ID: 2A4L). For this reason, we applied a three-step docking procedure, taking into account the conserved binding motif: (1) after the first round of docking, the pose of the best crystal-like position was selected, (2) then the ligand was constrained by the atoms forming conserved hydrogen bonds and it was treated like a flexible side chain and the dummy atom of hydrogen was docked, (3) the final pose of the ligand stemming from the previous step was then rescored to obtain binding free energies while retaining conserved binding motif.

Dihedral scans for assessing the rigidity of two rings were calculated at the DF-PBE/6-311++g(3df,3pf) level of theory with the C-PCM implicit solvent model for water. All relaxed scans were done with the Gaussian 09 program, revision A.2.[56]

■ ASSOCIATED CONTENT

Supporting Information

CDK 5, CDK7, and CDK9 inhibitory activity of selected compounds, list of synthesized compounds with detailed reaction conditions, experimental and theoretical free energies calculated from IC_{50}s and Vina results and their comparison, induction of apoptosis and replication of compound **6b**, and dihedral scans between the two rings for compounds **5a**−**6b**. This material is available free of charge via the Internet at http://pubs.acs.org.

■ AUTHOR INFORMATION

Corresponding Author

*Phone: +420585634953. Fax: +420585634870. E-mail: akrylhydrazid@seznam.cz.

Notes

The authors declare no competing financial interest.

■ ACKNOWLEDGMENTS

This work was supported by the Czech Science Foundation (grants P305/12/0783 and 203/09/H046), the Ministry of Education, Youth and Sports, Czech Republic (grant ED0007/01/01; Centre of the Region Haná for Biotechnological and Agricultural Research), the Operational Program Research and Development for Innovations (European Regional Development Fund (CZ.1.05/2.1.00/03.0058), and European Social Fund (CZ.1.07/2.3.00/20.0017)) and by the Student Projects PrF_2013_023 and PrF_2013_028 of Palacký University.

■ REFERENCES

(1) Malumbres, M.; Barbacid, M. Mammalian cyclin-dependent kinases. *Trends Biochem. Sci.* **2005**, *30*, 630−641.

(2) Krystof, V.; Uldrijan, S. Cyclin-dependent kinase inhibitors as anticancer drugs. *Curr. Drug Targets* **2010**, *11*, 291−302.

(3) Lapenna, S.; Giordano, A. Cell cycle kinases as therapeutic targets for cancer. *Nature Rev. Drug Discovery* **2009**, *8*, 547−566.

(4) Havlicek, L.; Hanus, J.; Vesely, J.; LeClerc, S.; Meijer, L.; Shaw, G.; Strnad, M. Cytokinin-derived cyclin-dependent kinase inhibitors: synthesis and cdc2 inhibitory activity of olomoucine and related compounds. *J. Med. Chem.* **1997**, *40*, 408−412.

(5) Hsieh, W. S.; Soo, R.; Peh, B. K.; Loh, T.; Dong, D.; Soh, D.; Wong, L. S.; Green, S.; Chiao, J.; Cui, C. Y.; Lai, Y. F.; Lee, S. C.; Mow, B.; Soong, R.; Salto-Tellez, M.; Goh, B. C. Pharmacodynamic effects of seliciclib, an orally administered cell cycle modulator, in undifferentiated nasopharyngeal cancer. *Clin. Cancer Res.* **2009**, *15*, 1435−1442.

(6) Le, T. C.; Faivre, S.; Laurence, V.; Delbaldo, C.; Vera, K.; Girre, V.; Chiao, J.; Armour, S.; Frame, S.; Green, S. R.; Gianella-Borradori, A.; Dieras, V.; Raymond, E. Phase I evaluation of seliciclib (*R*-roscovitine), a novel oral cyclin-dependent kinase inhibitor, in patients with advanced malignancies. *Eur. J. Cancer* **2010**, *46*, 3243−3250.

(7) Chang, Y. T.; Gray, N. S.; Rosania, G. R.; Sutherlin, D. P.; Kwon, S.; Norman, T. C.; Sarohia, R.; Leost, M.; Meijer, L.; Schultz, P. G. Synthesis and application of functionally diverse 2,6,9-trisubstituted purine libraries as CDK inhibitors. *Chem. Biol.* **1999**, *6*, 361−375.

(8) Gray, N. S.; Wodicka, L.; Thunnissen, A. M.; Norman, T. C.; Kwon, S.; Espinoza, F. H.; Morgan, D. O.; Barnes, G.; LeClerc, S.; Meijer, L.; Kim, S. H.; Lockhart, D. J.; Schultz, P. G. Exploiting chemical libraries, structure, and genomics in the search for kinase inhibitors. *Science* **1998**, *281*, 533−538.

(9) Legraverend, M.; Ludwig, O.; Bisagni, E.; LeClerc, S.; Meijer, L.; Giocanti, N.; Sadri, R.; Favaudon, V. Synthesis and in vitro evaluation of novel 2,6,9-trisubstituted purines acting as cyclin-dependent kinase inhibitors. *Bioorg. Med. Chem.* **1999**, *7*, 1281−1293.

(10) Oumata, N.; Bettayeb, K.; Ferandin, Y.; Demange, L.; Lopez-Giral, A.; Goddard, M. L.; Myrianthopoulos, V.; Mikros, E.; Flajolet, M.; Greengard, P.; Meijer, L.; Galons, H. Roscovitine-derived, dual-specificity inhibitors of cyclin-dependent kinases and casein kinases 1. *J. Med. Chem.* **2008**, *51*, 5229−5242.

(11) Trova, M. P.; Barnes, K. D.; Alicea, L.; Benanti, T.; Bielaska, M.; Bilotta, J.; Bliss, B.; Duong, T. N.; Haydar, S.; Herr, R. J.; Hui, Y.; Johnson, M.; Lehman, J. M.; Peace, D.; Rainka, M.; Snider, P.; Salamone, S.; Tregay, S.; Zheng, X.; Friedrich, T. D. Heterobiaryl purine derivatives as potent antiproliferative agents: inhibitors of cyclin dependent kinases. Part II. *Bioorg. Med. Chem. Lett.* **2009**, *19*, 6613−6617.

(12) Trova, M. P.; Barnes, K. D.; Barford, C.; Benanti, T.; Bielaska, M.; Burry, L.; Lehman, J. M.; Murphy, C.; O'Grady, H.; Peace, D.; Salamone, S.; Smith, J.; Snider, P.; Toporowski, J.; Tregay, S.; Wilson, A.; Wyle, M.; Zheng, X.; Friedrich, T. D. Biaryl purine derivatives as potent antiproliferative agents: inhibitors of cyclin dependent kinases. Part I. *Bioorg. Med. Chem. Lett.* **2009**, *19*, 6608−6612.

(13) Zatloukal, M.; Jorda, R.; Gucky, T.; Reznickova, E.; Voller, J.; Pospisil, T.; Malinkova, V.; Adamcova, H.; Krystof, V.; Strnad, M. Synthesis and in vitro biological evaluation of 2,6,9-trisubstituted

purines targeting multiple cyclin-dependent kinases. *Eur. J. Med. Chem.* **2013**, *61*, 61−72.
(14) Jorda, R.; Paruch, K.; Krystof, V. Cyclin-dependent kinase inhibitors inspired by roscovitine: purine bioisosteres. *Curr. Pharm. Des.* **2012**, *18*, 2974−2980.
(15) Bettayeb, K.; Sallam, H.; Ferandin, Y.; Popowycz, F.; Fournet, G.; Hassan, M.; Echalier, A.; Bernard, P.; Endicott, J.; Joseph, B.; Meijer, L. N-&-N, a new class of cell death-inducing kinase inhibitors derived from the purine roscovitine. *Mol. Cancer Ther.* **2008**, *7*, 2713−2724.
(16) Popowycz, F.; Fournet, G.; Schneider, C.; Bettayeb, K.; Ferandin, Y.; Lamigeon, C.; Tirado, O. M.; Mateo-Lozano, S.; Notario, V.; Colas, P.; Bernard, P.; Meijer, L.; Joseph, B. Pyrazolo[1,5-*a*]-1,3,5-triazine as a purine bioisostere: access to potent cyclin-dependent kinase inhibitor (*R*)-roscovitine analogue. *J. Med. Chem.* **2009**, *52*, 655−663.
(17) Jorda, R.; Havlicek, L.; McNae, I. W.; Walkinshaw, M. D.; Voller, J.; Sturc, A.; Navratilova, J.; Kuzma, M.; Mistrik, M.; Bartek, J.; Strnad, M.; Krystof, V. Pyrazolo[4,3-*d*]pyrimidine bioisostere of roscovitine: evaluation of a novel selective inhibitor of cyclin-dependent kinases with antiproliferative activity. *J. Med. Chem.* **2011**, *54*, 2980−2993.
(18) Heathcote, D. A.; Patel, H.; Kroll, S. H.; Hazel, P.; Periyasamy, M.; Alikian, M.; Kanneganti, S. K.; Jogalekar, A. S.; Scheiper, B.; Barbazanges, M.; Blum, A.; Brackow, J.; Siwicka, A.; Pace, R. D.; Fuchter, M. J.; Snyder, J. P.; Liotta, D. C.; Freemont, P. S.; Aboagye, E. O.; Coombes, R. C.; Barrett, A. G.; Ali, S. A novel pyrazolo[1,5-*a*]pyrimidine is a potent inhibitor of cyclin-dependent protein kinases 1, 2, and 9, which demonstrates antitumor effects in human tumor xenografts following oral administration. *J. Med. Chem.* **2010**, *53*, 8508−8522.
(19) Paruch, K.; Dwyer, M. P.; Alvarez, C.; Brown, C.; Chan, T. Y.; Doll, R. J.; Keertikar, K.; Knutson, C.; McKittrick, B.; Rivera, J.; Rossman, R.; Tucker, G.; Fischmann, T. O.; Hruza, A.; Madison, V.; Nomeir, A. A.; Wang, Y.; Lees, E.; Parry, D.; Sgambellone, N.; Seghezzi, W.; Schultz, L.; Shanahan, F.; Wiswell, D.; Xu, X.; Zhou, Q.; James, R. A.; Paradkar, V. M.; Park, H.; Rokosz, L. R.; Stauffer, T. M.; Guzi, T. J. Pyrazolo[1,5-*a*]pyrimidines as orally available inhibitors of cyclin-dependent kinase 2. *Bioorg. Med. Chem. Lett.* **2007**, *17*, 6220−6223.
(20) Williamson, D. S.; Parratt, M. J.; Bower, J. F.; Moore, J. D.; Richardson, C. M.; Dokurno, P.; Cansfield, A. D.; Francis, G. L.; Hebdon, R. J.; Howes, R.; Jackson, P. S.; Lockie, A. M.; Murray, J. B.; Nunns, C. L.; Powles, J.; Robertson, A.; Surgenor, A. E.; Torrance, C. J. Structure-guided design of pyrazolo[1,5-*a*]pyrimidines as inhibitors of human cyclin-dependent kinase 2. *Bioorg. Med. Chem. Lett.* **2005**, *15*, 863−867.
(21) Parry, D.; Guzi, T.; Shanahan, F.; Davis, N.; Prabhavalkar, D.; Wiswell, D.; Seghezzi, W.; Paruch, K.; Dwyer, M. P.; Doll, R.; Nomeir, A.; Windsor, W.; Fischmann, T.; Wang, Y.; Oft, M.; Chen, T.; Kirschmeier, P.; Lees, E. M. Dinaciclib (SCH 727965), a novel and potent cyclin-dependent kinase inhibitor. *Mol. Cancer Ther.* **2010**, *9*, 2344−2353.
(22) Paruch, K.; Dwyer, M. P.; Alvarez, C.; Brown, C.; Chan, T. Y.; Doll, R. J.; Keertikar, K.; Knutson, C.; McKittrick, B.; Rivera, J.; Rossman, R.; Tucker, G.; Fischmann, T.; Hruza, A.; Madison, V.; Nomeir, A. A.; Wang, Y. L.; Kirschmeier, P.; Lees, E.; Parry, D.; Sgambellone, N.; Seghezzi, W.; Schultz, L.; Shanahan, F.; Wiswell, D.; Xu, X. Y.; Zhou, Q. A.; James, R. A.; Paradkar, V. M.; Park, H.; Rokosz, L. R.; Stauffer, T. M.; Guzi, T. J. Discovery of Dinaciclib (SCH 727965): A Potent and Selective Inhibitor of Cyclin-Dependent Kinases. *ACS Med. Chem. Lett.* **2010**, *1*, 204−208.
(23) Gorlick, R.; Kolb, E. A.; Houghton, P. J.; Morton, C. L.; Neale, G.; Keir, S. T.; Carol, H.; Lock, R.; Phelps, D.; Kang, M. H.; Reynolds, C. P.; Maris, J. M.; Billups, C.; Smith, M. A. Initial testing (stage 1) of the cyclin dependent kinase inhibitor SCH 727965 (dinaciclib) by the pediatric preclinical testing program. *Pediatr. Blood Cancer* **2012**, *59*, 1266−1274.
(24) Johnson, A. J.; Yeh, Y. Y.; Smith, L. L.; Wagner, A. J.; Hessler, J.; Gupta, S.; Flynn, J.; Jones, J.; Zhang, X.; Bannerji, R.; Grever, M. R.; Byrd, J. C. The novel cyclin-dependent kinase inhibitor dinaciclib (SCH727965) promotes apoptosis and abrogates microenvironmental cytokine protection in chronic lymphocytic leukemia cells. *Leukemia* **2012**, *26*, 2554−2557.
(25) Zhang, D.; Mita, M.; Shapiro, G. I.; Poon, J.; Small, K.; Tzontcheva, A.; Kantesaria, B.; Zhu, Y.; Bannerji, R.; Statkevich, P. Effect of aprepitant on the pharmacokinetics of the cyclin-dependent kinase inhibitor dinaciclib in patients with advanced malignancies. *Cancer Chemother. Pharmacol.* **2012**, *70*, 891−898.
(26) Benson, C.; White, J.; De, B. J.; O'Donnell, A.; Raynaud, F.; Cruickshank, C.; McGrath, H.; Walton, M.; Workman, P.; Kaye, S.; Cassidy, J.; Gianella-Borradori, A.; Judson, I.; Twelves, C. A phase I trial of the selective oral cyclin-dependent kinase inhibitor seliciclib (CYC202; *R*-Roscovitine), administered twice daily for 7 days every 21 days. *Br. J. Cancer* **2007**, *96*, 29−37.
(27) Chen, R.; Keating, M. J.; Gandhi, V.; Plunkett, W. Transcription inhibition by flavopiridol: mechanism of chronic lymphocytic leukemia cell death. *Blood* **2005**, *106*, 2513−2519.
(28) Massard, C.; Soria, J. C.; Anthoney, D. A.; Proctor, A.; Scaburri, A.; Pacciarini, M. A.; Laffranchi, B.; Pellizzoni, C.; Kroemer, G.; Armand, J. P.; Balheda, R.; Twelves, C. J. A first in man, phase I dose-escalation study of PHA-793887, an inhibitor of multiple cyclin-dependent kinases (CDK2, 1 and 4) reveals unexpected hepatotoxicity in patients with solid tumors. *Cell Cycle* **2011**, *10*, 963−970.
(29) Tong, W. G.; Chen, R.; Plunkett, W.; Siegel, D.; Sinha, R.; Harvey, R. D.; Badros, A. Z.; Popplewell, L.; Coutre, S.; Fox, J. A.; Mahadocon, K.; Chen, T.; Kegley, P.; Hoch, U.; Wierda, W. G. Phase I and pharmacologic study of SNS-032, a potent and selective Cdk2, 7, and 9 inhibitor, in patients with advanced chronic lymphocytic leukemia and multiple myeloma. *J. Clin. Oncol.* **2010**, *28*, 3015−3022.
(30) Bettayeb, K.; Oumata, N.; Echalier, A.; Ferandin, Y.; Endicott, J. A.; Galons, H.; Meijer, L. CR8, a potent and selective, roscovitine-derived inhibitor of cyclin-dependent kinases. *Oncogene* **2008**, *27*, 5797−5807.
(31) Liu, Y. X.; Wei, D. G.; Zhu, Y. R.; Liu, S. H.; Zhang, Y. L.; Zhao, Q. Q.; Cai, B. L.; Li, Y. H.; Song, H. B.; Liu, Y.; Wang, Y.; Huang, R. Q.; Wang, Q. M. Synthesis, herbicidal activities, and 3D-QSAR of 2-cyanoacrylates containing aromatic methylamine moieties. *J. Agric. Food Chem.* **2008**, *56*, 204−212.
(32) Dreyer, M. K.; Borcherding, D. R.; Dumont, J. A.; Peet, N. P.; Tsay, J. T.; Wright, P. S.; Bitonti, A. J.; Shen, J.; Kim, S. H. Crystal structure of human cyclin-dependent kinase 2 in complex with the adenine-derived inhibitor H717. *J. Med. Chem.* **2001**, *44*, 524−530.
(33) Zim, D.; Monteiro, A. L.; Dupont, J. $Pd(Cl)_2(SEt_2)_2$ and $Pd(OAc)_2$: simple and efficient catalyst precursors for the Suzuki cross-coupling reaction. *Tetrahedron Lett.* **2000**, *41*, 8199−8202.
(34) Payton, M.; Chung, G.; Yakowec, P.; Wong, A.; Powers, D.; Xiong, L.; Zhang, N.; Leal, J.; Bush, T. L.; Santora, V.; Askew, B.; Tasker, A.; Radinsky, R.; Kendall, R.; Coats, S. Discovery and evaluation of dual CDK1 and CDK2 inhibitors. *Cancer Res.* **2006**, *66*, 4299−4308.
(35) MacCallum, D. E.; Melville, J.; Frame, S.; Watt, K.; Anderson, S.; Gianella-Borradori, A.; Lane, D. P.; Green, S. R. Seliciclib (CYC202, *R*-Roscovitine) induces cell death in multiple myeloma cells by inhibition of RNA polymerase II-dependent transcription and down-regulation of Mcl-1. *Cancer Res.* **2005**, *65*, 5399−5407.
(36) Santo, L.; Vallet, S.; Hideshima, T.; Cirstea, D.; Ikeda, H.; Pozzi, S.; Patel, K.; Okawa, Y.; Gorgun, G.; Perrone, G.; Calabrese, E.; Yule, M.; Squires, M.; Ladetto, M.; Boccadoro, M.; Richardson, P. G.; Munshi, N. C.; Anderson, K. C.; Raje, N. AT7519, A novel small molecule multi-cyclin-dependent kinase inhibitor, induces apoptosis in multiple myeloma via GSK-3beta activation and RNA polymerase II inhibition. *Oncogene* **2010**, *29*, 2325−2336.
(37) Demidenko, Z. N.; Blagosklonny, M. V. Flavopiridol induces p53 via initial inhibition of Mdm2 and p21 and, independently of p53, sensitizes apoptosis-reluctant cells to tumor necrosis factor. *Cancer Res.* **2004**, *64*, 3653−3660.

(38) Kotala, V.; Uldrijan, S.; Horky, M.; Trbusek, M.; Strnad, M.; Vojtesek, B. Potent induction of wild-type p53-dependent transcription in tumour cells by a synthetic inhibitor of cyclin-dependent kinases. *Cell. Mol. Life Sci.* **2001**, *58*, 1333−1339.
(39) Kwon, Y. G.; Lee, S. Y.; Choi, Y.; Greengard, P.; Nairn, A. C. Cell cycle-dependent phosphorylation of mammalian protein phosphatase 1 by cdc2 kinase. *Proc. Natl. Acad. Sci. U. S. A.* **1997**, *94*, 2168−2173.
(40) Tokuyama, Y.; Horn, H. F.; Kawamura, K.; Tarapore, P.; Fukasawa, K. Specific phosphorylation of nucleophosmin on Thr(199) by cyclin-dependent kinase 2-cyclin E and its role in centrosome duplication. *J. Biol. Chem.* **2001**, *276*, 21529−21537.
(41) Larochelle, S.; Merrick, K. A.; Terret, M. E.; Wohlbold, L.; Barboza, N. M.; Zhang, C.; Shokat, K. M.; Jallepalli, P. V.; Fisher, R. P. Requirements for Cdk7 in the assembly of Cdk1/cyclin B and activation of Cdk2 revealed by chemical genetics in human cells. *Mol. Cell* **2007**, *25*, 839−850.
(42) Malumbres, M.; Barbacid, M. Cell cycle, CDKs and cancer: a changing paradigm. *Nature Rev. Cancer* **2009**, *9*, 153−166.
(43) Tetsu, O.; McCormick, F. Proliferation of cancer cells despite CDK2 inhibition. *Cancer Cell* **2003**, *3*, 233−245.
(44) Caporali, S.; Alvino, E.; Starace, G.; Ciomei, M.; Brasca, M. G.; Levati, L.; Garbin, A.; Castiglia, D.; Covaciu, C.; Bonmassar, E.; D'Atri, S. The cyclin-dependent kinase inhibitor PHA-848125 suppresses the in vitro growth of human melanomas sensitive or resistant to Temozolomide, and shows synergistic effects in combination with this triazene compound. *Pharmacol. Res.* **2010**, *61*, 437−448.
(45) Du, J.; Widlund, H. R.; Horstmann, M. A.; Ramaswamy, S.; Ross, K.; Huber, W. E.; Nishimura, E. K.; Golub, T. R.; Fisher, D. E. Critical role of CDK2 for melanoma growth linked to its melanocyte-specific transcriptional regulation by MITF. *Cancer Cell* **2004**, *6*, 565−576.
(46) Abdullah, C.; Wang, X.; Becker, D. Expression analysis and molecular targeting of cyclin-dependent kinases in advanced melanoma. *Cell Cycle* **2011**, *10*, 977−988.
(47) Blachly, J. S.; Byrd, J. C. Emerging Drug Profile: Cyclin-Dependent Kinase Inhibitors. *Leuk. Lymphoma* **2013**.
(48) Bettayeb, K.; Baunbaek, D.; Delehouze, C.; Loaec, N.; Hole, A. J.; Baumli, S.; Endicott, J. A.; Douc-Rasy, S.; Benard, J.; Oumata, N.; Galons, H.; Meijer, L. CDK Inhibitors Roscovitine and CR8 Trigger Mcl-1 Down-Regulation and Apoptotic Cell Death in Neuroblastoma Cells. *Genes Cancer* **2010**, *1*, 369−380.
(49) Wilson, S. C.; Atrash, B.; Barlow, C.; Eccles, S.; Fischer, P. M.; Hayes, A.; Kelland, L.; Jackson, W.; Jarman, M.; Mirza, A.; Moreno, J.; Nutley, B. P.; Raynaud, F. I.; Sheldrake, P.; Walton, M.; Westwood, R.; Whittaker, S.; Workman, P.; McDonald, E. Design, synthesis and biological evaluation of 6-pyridylmethylaminopurines as CDK inhibitors. *Bioorg. Med. Chem.* **2011**, *19*, 6949−6965.
(50) Meanwell, N. A. Improving drug candidates by design: a focus on physicochemical properties as a means of improving compound disposition and safety. *Chem. Res. Toxicol.* **2011**, *24*, 1420−1456.
(51) Collins, C. S.; Hong, J.; Sapinoso, L.; Zhou, Y.; Liu, Z.; Micklash, K.; Schultz, P. G.; Hampton, G. M. A small interfering RNA screen for modulators of tumor cell motility identifies MAP4K4 as a promigratory kinase. *Proc. Natl. Acad. Sci. U. S. A.* **2006**, *103*, 3775−3780.
(52) Liebl, J.; Weitensteiner, S. B.; Vereb, G.; Takacs, L.; Furst, R.; Vollmar, A. M.; Zahler, S. Cyclin-dependent kinase 5 regulates endothelial cell migration and angiogenesis. *J. Biol. Chem.* **2010**, *285*, 35932−35943.
(53) Krystof, V.; Cankar, P.; Frysova, I.; Slouka, J.; Kontopidis, G.; Dzubak, P.; Hajduch, M.; Srovnal, J.; de Azevedo, W. F. J.; Orsag, M.; Paprskarova, M.; Rolcik, J.; Latr, A.; Fischer, P. M.; Strnad, M. 4-Arylazo-3,5-diamino-1*H*-pyrazole CDK inhibitors: SAR study, crystal structure in complex with CDK2, selectivity, and cellular effects. *J. Med. Chem.* **2006**, *49*, 6500−6509.
(54) Sanner, M. F. Python: a programming language for software integration and development. *J. Mol. Graphics Modell.* **1999**, *17*, 57−61.
(55) Trott, O.; Olson, A. J. AutoDock Vina: improving the speed and accuracy of docking with a new scoring function, efficient optimization, and multithreading. *J. Comput. Chem.* **2010**, *31*, 455−461.
(56) Frisch, M. J.; Trucks, G. W.; Schlegel, H. B.; Scuseria, G. E.; Robb, M. A.; Cheeseman, J. R.; Scalmani, G.; Barone, V.; Mennucci, B.; Petersson, G. A.; Nakatsuji, H.; Caricato, M.; Li, X.; Hratchian, H. P.; Izmaylov, A. F.; Bloino, J.; Zheng, G.; Sonnenberg, J. L.; Hada, M.; Ehara, M.; Toyota, K.; Fukuda, R.; Hasegawa, J.; Ishida, M.; Nakajima, T.; Honda, Y.; Kitao, O.; Nakai, H.; Vreven, T.; Montgomery, J. A.; Peralta, J. E. Jr.; Ogliaro, F.; Bearpark, M.; Heyd, J. J.; Brothers, E.; Kudin, K. N.; Staroverov, V. N.; Kobayashi, R.; Normand, J.; Raghavachari, K.; Rendell, A.; Burant, J. C.; Iyengar, S. S.; Tomasi, J.; Cossi, M.; Rega, N.; Millam, J. M.; Klene, M.; Knox, J. E.; Cross, J. B.; Bakken, V.; Adamo, C.; Jaramillo, J.; Gomperts, R.; Stratmann, R. E.; Yazyev, O.; Austin, A. J.; Cammi, R.; Pomelli, C.; Ochterski, J. W.; Martin, R. L.; Morokuma, K.; Zakrzewski, V. G.; Voth, G. A.; Salvador, P.; Dannenberg, J. J.; Dapprich, S.; Daniels, A. D.; Farkas, O.; Foresman, J. B.; Ortiz, J. V.; Cioslowski, J.; Fox, D. J. *Gaussian 2009*, revision A.02; Gaussian, Inc.: Wallingford, CT2009.

PŘÍLOHA III

Haider C, Grubinger M, **Řezníčková E**, Weiss TS, Rotheneder H, Miklos W, Berger W, Jorda R, Zatloukal M, Gucký T, Strnad M, Kryštof V, Mikulits W (2013) Novel inhibitors of cyclin-dependent kinases combat hepatocellular carcinoma without inducing chemoresistance. Mol Cancer Ther. 12, 1947-1957.

Published OnlineFirst August 12, 2013; DOI: 10.1158/1535-7163.MCT-13-0263

Molecular Cancer Therapeutics

Novel Inhibitors of Cyclin-Dependent Kinases Combat Hepatocellular Carcinoma without Inducing Chemoresistance

Christine Haider, Markus Grubinger, Eva Reznícková, et al.

Mol Cancer Ther 2013;12:1947-1957. Published OnlineFirst August 12, 2013.

Published OnlineFirst August 12, 2013; DOI: 10.1158/1535-7163.MCT-13-0263

Small Molecule Therapeutics

Molecular Cancer Therapeutics

Novel Inhibitors of Cyclin-Dependent Kinases Combat Hepatocellular Carcinoma without Inducing Chemoresistance

Christine Haider[1], Markus Grubinger[1], Eva Řezníčková[3], Thomas S. Weiss[5], Hans Rotheneder[2], Walter Miklos[1], Walter Berger[1], Radek Jorda[3], Marek Zatloukal[4], Tomáš Gucký[4], Miroslav Strnad[3,4], Vladimír Kryštof[3], and Wolfgang Mikulits[1]

Abstract

Treatment options for hepatocellular carcinoma using chemotherapeutics at intermediate and advanced stages of disease are limited as patients most rapidly escape from therapy and succumb to disease progression. Mechanisms of the hepatic xenobiotic metabolism are mostly involved in providing chemoresistance to therapeutic compounds. Given the fact that the aberrant activation of cyclin-dependent kinases (CDK) is frequently observed in hepatocellular carcinomas, we focused on the efficacy of the novel compounds BA-12 and BP-14 that antagonize CDK1/2/5/7 and CDK9. Inhibition of those CDKs in human hepatocellular carcinoma cell lines reduced the clonogenicity by arresting cells in S–G_2 and G_2–M phase of the cell cycle and inducing apoptosis. In contrast, primary human hepatocytes failed to show cytotoxicity and apoptosis. No loss of chemosensitivity was observed in hepatocellular carcinoma cells after long-term exposure to inhibitors. *In vivo*, treatment of xenografted human hepatocellular carcinomas with BA-12 or BP-14 effectively repressed tumor formation. Moreover, BA-12 or BP-14 significantly diminished diethylnitrosamine (DEN)-induced hepatoma development in mice. These data show that BA-12 or BP-14 exhibit strong antitumorigenic effects in the absence of chemoresistance, resulting in a superior efficacy compared with currently used chemotherapeutics in hepatocellular carcinomas. *Mol Cancer Ther; 12(10); 1947–57. ©2013 AACR.*

Introduction

Hepatocellular carcinoma (HCC) represents the sixth most common cancer and the third leading cause of cancer-related deaths worldwide (1). Less than 30% to 40% of patients with hepatocellular carcinomas are eligible for potentially curative therapies, including surgical resection and orthotopic liver transplantation due to advanced stages of disease at the time of diagnosis (2). As a result, patients with advanced hepatocellular carcinoma receive systemic chemotherapy. The use of chemotherapy is often combined with transarterial chemoembolization (TACE), where the hepatic artery is obstructed (3). However, chemotherapeutic treatment of hepatocellular carcinoma most frequently associates with the increased expression of drug resistance genes, resulting in the insensitivity to available chemotherapeutic agents (4). Doxorubicin has shown inefficacy with a response rate of about 0% to 15% (5, 6), and other chemotherapy agents, such as epirubicin, cisplatin, 5-fluorouracil, etoposide, and their combinations, show even lower efficacies. For doxorubicin, one of the most important causes of chemoresistance is the increased expression of the ATP-binding cassette (ABC) transporters. Overexpression of the ABC member *ABCB1* (*MDR1*) encoding P-glycoprotein (P-gp) is associated with lower accumulation of doxorubicin in hepatocellular carcinoma cells and with a worse prognosis (7). Sorafenib represents the current treatment standard for advanced hepatocellular carcinoma by prolonging median survival of patients for about 3 months (8). These limitations in treatment modalities strongly indicate the urgent need for novel alternative treatment options.

Cyclin-dependent kinases (CDK) are fundamental for cell-cycle control and regulation of apoptosis (9, 10) and are found deregulated in most cancer cells. hepatocellular carcinoma shows frequent upregulation of CDKs through inactivation of CDK inhibitory proteins including $p16^{Ink4}$,

Authors' Affiliations: [1]Department of Medicine I, Institute of Cancer Research, Comprehensive Cancer Center Vienna; [2]Max F. Perutz Laboratories, Department of Medical Biochemistry, Medical University of Vienna, Vienna, Austria; [3]Laboratory of Growth Regulators, Faculty of Science, Palacký University & Institute of Experimental Botany; [4]Centre of the Region Haná for Biotechnological and Agricultural Research, Department of Growth Regulators, Palacký University, Olomouc, Czech Republic; and [5]Department of Pediatrics and Juvenile Medicine, Center for Liver Cell Research, University Hospital Regensburg, Regensburg, Germany

Note: Supplementary data for this article are available at Molecular Cancer Therapeutics Online (http://mct.aacrjournals.org/).

Corresponding Author: Wolfgang Mikulits, Medical University Vienna, Borschkegasse 8a, Vienna 1090, Austria. Phone: 43-1-4016057527; Fax: 43-1-40160957519; E-mail: wolfgang.mikulits@meduniwien.ac.at

doi: 10.1158/1535-7163.MCT-13-0263

Published OnlineFirst August 12, 2013; DOI: 10.1158/1535-7163.MCT-13-0263

$p21^{WAF1/CIP1}$, $p27^{KIP1}$, and $p57^{KIP2}$ as well as through increasing levels of cyclins (11, 12). In particular, CDK1 and CDK2 often show an aberrant regulation (13, 14). CDK2 provides S-phase entry by binding to cyclin E and allows S-phase progression by interacting with cyclin A (15). CDK1/cyclin A activity is essential for the initiation of prophase during the G_2–M transition (16). Interestingly, cyclin A was found to be overexpressed in 39% of hepatocellular carcinoma samples (17). Similarly, CDK1/cyclin B complexes participate and complete mitosis and cyclin B overexpression is frequently observed in hepatocellular carcinoma (18). Besides the fact that the sustained inhibition of CDK7 and CDK9 induces apoptosis (19), little is known about the deregulation of CDK5, CDK7, and CDK9 in hepatocellular carcinoma.

Thus, the targeting of CDKs has become an attractive approach in oncology (12). A multitude of small-molecule CDK inhibitors has been evaluated as promising antiproliferative agents for cancer therapy, including (R)-roscovitine (Seliciclib, CYC202). Roscovitine is known to selectively inhibit CDK1, CDK2, CDK5, CDK7, and CDK9 activities through its binding to the ATP-binding site (20). Currently, roscovitine is evaluated in a phase I clinical trial in combination with sapacitabine with patients suffering from advanced solid tumors (NCT00999401) and in a phase II trial from patients with non–small cell lung cancer (21). The effects of roscovitine and its derivatives vary according to cell type, but they are generally able to block the cell cycle at every position (22). The cell-cycle arrest is attributed to a direct inhibition of CDK1 and CDK2, whereas the induction of cell death by roscovitine is considered as a direct consequence of blocking the CDK7/CDK9-dependent transcription. CDK7 is an integral component of the transcription factor TFIIH (23), which phosphorylates the Ser5 in the C-terminal domain (CTD) of RNA polymerase II (Pol II) to facilitate transcription initiation. CDK9, a portion of the elongation factor P-TEFb (24), conducts a complementary function by phosphorylating Ser2 in the CTD of RNA Pol II, which is required for transcription elongation.

In this study, we investigated the molecular mechanisms of two novel roscovitine derivatives, designated BA-12 and BP-14, in hepatocellular carcinoma cells and further determined their anticancer activity in xenograft models and chemically induced hepatoma. We show that both compounds inhibit CDK1 and CDK2 on their own, leading to the arrest of hepatocellular carcinoma cells in S–G_2 and G_2–M. Moreover, BA-12 and BP-14 reduce the phosphorylation of RNA Pol II at Ser5 and Ser2 and selectively induce apoptosis of hepatocellular carcinoma cells rather than of primary human hepatocytes (PHH). Notably, no chemoresistance against these compounds could be observed after long-term treatment of hepatocellular carcinoma cells. *In vivo*, both BA-12 and BP-14 significantly diminished the growth of engrafted human hepatoma and were able to antagonize chemically induced liver cancer formation in mice.

Materials and Methods

Cell culture

The human hepatoma cell lines HepG2, PLC/PRF/5 (PLC), Hep3B, and 3sp (formerly described as HCC-1.1) were cultivated as described (25, 26). All cells were kept at 37°C and 5% CO_2 and were routinely screened for the absence of mycoplasma. The cell lines HepG2, PLC, and Hep3B were obtained from the American Type Culture Collection. The 3sp cells were established from a patient with hepatocellular carcinoma at the Medical University of Vienna (Vienna, Austria; ref. 26). All cell lines were verified by short-tandem repeat analysis in November 2012.

Primary human hepatocytes

Non-neoplastic tissue samples from liver resections were obtained from patients undergoing partial hepatectomy for metastatic liver tumors of colorectal cancer. Experimental procedures were conducted according to the guidelines of the charitable state controlled foundation HTCR (Human Tissue and Cell Research, Regensburg, Germany), with the informed patient's consent approved by the local ethical committee of the University of Regensburg. PHHs were isolated using a modified two-step EGTA/collagenase perfusion procedure as described previously (27). Viability of isolated PHHs was determined by trypan blue exclusion and cells with a viability of more than 85% were used for further work. Cells were plated on collagen-coated plates (BD Biosciences) at a density of 1.2×10^5 cells/cm^2. The medium consisted of Dulbeccos' modified Eagle medium (DMEM) with 10% fetal calf serum (FCS), 2 mmol/L L-glutamine, 100 mg/mL streptomycin, 100 U/mL penicillin, and supplements as follows: 125 mU/mL insulin, 7.3 ng/mL glucagon, and 0.8 μg/mL hydrocortisone. Cells were incubated at 37°C in a humidified incubator with 5% CO_2 and media were changed daily.

Therapeutic agents

BA-12 (2-[[[2-[(4-aminocyclohexyl)amino]-9-cyclopentyl-purin-6-yl]amino]methyl]-4-chloro-phenol; Supplementary Fig. S1A) and BP-14 (*N*2-(4-aminocyclohexyl)-9-cyclopentyl-*N*6-[[6-(2-furyl)-3-pyridyl]methyl]purine-2,6-diamine; Supplementary Fig. S1B) were synthesized by procedures as described (28). Compounds were dissolved in dimethyl sulfoxide (DMSO). The stock solution of 100 mmol/L was diluted in assay buffer or in medium to concentrations indicated in the text. The maximum concentration of DMSO in the assays never exceeded 0.1%.

Determination of cell viability and inhibitory concentration

Cell viability was determined using the MTT assay. Briefly, cells were seeded in triplicates at a density of 6×10^3 cells per 96 wells. After 24 hours, cells were incubated with drug-containing medium for 72 hours. Cells were incubated with MTT solution (5 mg/mL; Sigma) and medium was replaced with DMSO after 5 hours. The

Published OnlineFirst August 12, 2013; DOI: 10.1158/1535-7163.MCT-13-0263

absorbance was measured at 620 nm by using a microplate reader (Asys HiTech). MTT assays were repeated three times for each drug application. IC_{50} values were obtained by log-linear interpolation of data points and are depicted by dose–response curves using the software GraphPad Prism 5.01.

Kinase inhibition assays using cell-free extracts

Whole-cell extracts were prepared by lysing Hep3B cells with a buffer containing 20 mmol/L Tris pH 8.0, 100 mmol/L NaCl, 1 mmol/L EDTA, and 0.5% NP-40. Hundred micrograms of extract was used for immunoprecipitation at 4°C for 4 hours either with 1 μg of the anti-CDK2 antibody M2 (Santa Cruz Biotechnology) or with 1 μg of the anti-cyclin B1 antibody GNS1 (Santa Cruz Biotechnology). Precipitated protein was resuspended in 20 μL kinase buffer containing 5 μCi [γ-^{32}P]ATP (PerkinElmer), 1 μg histone 1 (New England Biolabs), and the respective concentration of inhibitor. After incubation for 60 minutes at 30°C, the supernatant was boiled in sample buffer and separated by SDS-PAGE. Proteins were transferred to nitrocellulose membranes and stained with Ponceau S before analysis by autoradiography.

Clonogenic survival assay

Five hundred cells were seeded in a 6-well plate and, either untreated or pretreated with BA-12 or BP-14 for 24 hours, incubated with standard medium for 10 days at 37°C and 5% CO_2. Colonies were fixed with methanol/acetic acid (3:1) and stained with 0.25% crystal violet. The crystal violet of fixed cells was solubilized with 1% SDS, and the absorbance was photometrically determined at 560 nm.

Cell proliferation analyzed by bromodeoxyuridine incorporation

Cultured cells were grown in medium containing 10 μmol/L bromodeoxyuridine (BrdUrd) for 1 hour. After removing labeling medium, cells were fixed and DNA denatured with a fixing/denaturing solution containing 2 mol/L HCl for 30 minutes at 37°C. To analyze BrdUrd incorporation *in vivo*, 200 μL Ringer solution containing 1 mg BrdUrd was intraperitoneally injected into xenografted mice 2 hours before sacrifice. Tumor tissue was fixed in 4% formaldehyde and processed for immunohistochemistry. BrdUrd incorporation was detected with a monoclonal anti-BrdUrd antibody (Sigma) and a peroxidase-conjugated secondary antibody (Calbiochem).

Flow cytometry

The analysis of cellular DNA content was conducted with a multicolor BD LSRFortessa cell analyzer (Becton Dickinson). Before the cytofluorometric measurement, about 5×10^5 cells were washed with PBS, fixed in 70% ethanol, washed again with PBS, and treated with 100 μg RNAse A/50 μg propidium iodide per mL for 10 minutes to stain cellular DNA. The percentage of cells in the various cell-cycle positions was calculated using a software package from the same manufacturer.

Determination of long-term chemosensitivity

Hepatoma cells were continuously cultivated in the presence of BA-12 or BP-14 at concentrations lower than the IC_{50} (1:2 IC_{50}, 1:4 IC_{50}, 1:8 IC_{50}, and 1:16 IC_{50}). The selection of chemoresistant cells was monitored every 6 weeks for 9 months by the determination of IC_{50} values using the MTT assay. Hepatocellular carcinoma cells showing higher IC_{50} values after treatment with inhibitors than untreated cells are considered as chemoresistant.

Immunoblotting

Immunoblotting was conducted as described previously (29). Primary antibodies: anti-S807/811 Rb (Cell Signaling Technology), 1:500; anti-Rb (Cell Signaling Technology), 1:1,000, anti-phospho-Ser5 RNA Pol II (CDK7; Bethyl Laboratories), 1:1,000; anti-phospho-Ser2 RNA Pol II (CDK9; Bethyl Laboratories), 1:1,000; anti-RNA Pol II (Santa Cruz Biotechnology), 1:1,000; anti-PARP (Cell Signaling Technology), 1:1,000; anti-cleaved caspase-7 (Cell Signaling Technology), 1:1,000; anti-caspase-7 (Cell Signaling Technology), 1:1,000; anti-β-actin (Sigma), 1:2,500. Horseradish peroxidase–conjugated secondary antibodies (Calbiochem) were used at dilutions of 1:10,000.

Xenografted tumor formation and drug intervention

A total of 5×10^6 human hepatoma cells were resuspended in 100 μL Ringer solution and subcutaneously injected into severe combined immunodeficient (SCID) mice (Harlan Laboratories). Tumor volume was determined as described previously (29). Pharmacologic intervention was conducted in tumor-bearing mice for 17 days by daily intraperitoneal injection of either 5 mg/kg BA-12 or 1 mg/kg BP-14 in 100 μL of 0.01% DMSO. Control tumor–bearing mice received DMSO only. The experiments were carried out using 5 mice per group and carried out according to the Austrian guidelines for animal care and protection.

Diethylnitrosamine-induced liver cancer and drug intervention

To initiate tumor development in the liver, 14-day-old male C57BL/6J mice were intraperitoneally injected with a single dose of diethylnitrosamine (DEN, 25 mg/kg). After 8 month, pharmacologic intervention was administrated in DEN-induced mice by 3 cycles of treatment with compounds for 10 days and a release from compounds for 7 days between the cycles. About 5 mg/kg BA-12 or 1 mg/kg BP-14 was intraperitoneally injected in 100 μL of 0.01% DMSO. Control mice received DMSO only. Thereafter, mice were sacrificed and livers were fixed in 4% formaldehyde. Two researchers (C. Haider and M. Grubinger) independently scored the diameters of neoplasia that could be monitored at the liver surface. Cancerous nodules with a diameter of up to 1 cm, covering more than 97% of all visible hepatomas, were included into the

Published OnlineFirst August 12, 2013; DOI: 10.1158/1535-7163.MCT-13-0263

analysis. The experiments were carried out using 20 mice per group and carried out according to the Austrian guidelines for animal care and protection.

Immunohistochemistry and TUNEL analysis

Mice were sacrificed and tumors were fixed as described (30). Four-micrometer-thick, paraffin-embedded sections were stained with anti-BrdUrd (Sigma), 1:200. Biotinylated secondary antibody was used at 1:200. The immunoperoxidase procedure was conducted using a Vectastain Elite ABC kit (Vector Laboratories) as described by the manufacturer. To detect DNA fragmentation by terminal deoxynucleotidyl transferase–mediated dUTP nick end labeling (TUNEL) analysis in tumor tissues, an *In Situ* Cell Death Detection kit (Roche) was used as recommended by the manufacturer.

Statistical analysis

Data were expressed as means ± SD or SEM. The statistical significance of differences was evaluated using an unpaired, nonparametric Student *t* test. Significant differences between experimental groups were *, $P < 0.05$; **, $P < 0.01$; or ***, $P < 0.005$.

Results

Cytotoxicity and kinase specificity of BA-12 and BP-14

Novel derivatives of roscovitine, designated BA-12 and BP-14, were synthesized on the basis of our knowledge of structure–activity relationships for roscovitine-related compounds (28, 31). Cell viability assays showed strong cytotoxic effects of BA-12 and BP-14 on human HepG2 and PLC hepatoma cells (Fig. 1A and B). Analysis of additional established hepatocellular carcinoma cell lines (Hep3B and 3sp) confirmed the cytotoxicity of BA-12 and BP-14 (Supplementary Fig. S2A and S2B). Dose–response curves revealed IC_{50} values below 1 μmol/L for both compounds in the various hepatocellular carcinoma cell lines, reaching as low as 0.02 μmol/L in PLC cells for

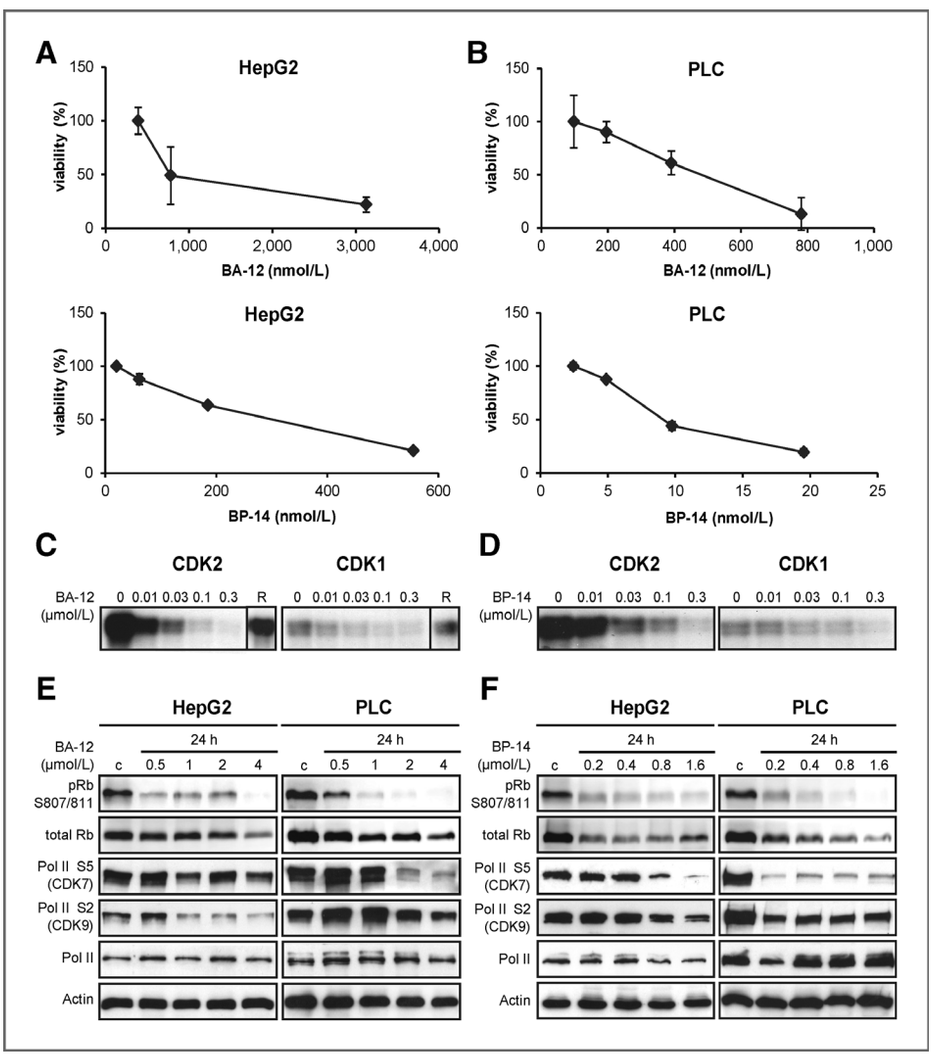

Figure 1. BA-12 and BP-14 diminish cell viability of hepatoma cells and block multiple CDKs. A and B, dose-dependent effects of BA-12 and BP-14 on the viability of human HepG2 (A) and PLC cells (B). C and D, inhibition of CDK1 and CDK2 activity by BA-12 (C) and BP-14 (D) in cell-free extracts. Roscovitine (R) was used at a concentration of 0.03 μmol/L. E and F, reduction of the CDK2-specific phosphorylation of Rb as well as suppression of CDK7 and CDK9 activity after exposure to different concentrations of BA-12 (E) and BP-14 (F) for 24 hours in HepG2 and PLC cells. As detected by immunoblotting, CDK7 and CDK9 activities correspond to serine 5 and serine 2 phosphorylation of RNA polymerase (Pol) II, respectively. The expression of actin indicates equal loading of protein samples. c, control. Error bars depict SD from at least three individual experiments.

Published OnlineFirst August 12, 2013; DOI: 10.1158/1535-7163.MCT-13-0263

BP-14 (Supplementary Table S1). Kinase assays using cell-free extracts showed that BA-12 or BP-14 significantly reduced CDK1/CDK2 activity at concentrations of 0.03 μmol/L (Fig. 1C and D). Notably, roscovitine showed no effect at this concentration which suggests less potency than BA-12 and BP-14 (Fig. 1C). Furthermore, administration of HepG2 and PLC cells with 0.5 μmol/L BA-12 or 0.2 μmol/L BP-14, respectively, caused a significant decrease in CDK2-specific phosphorylation of retinoblastoma (Rb; Fig. 1E and F). This was associated with a more moderate lowering of total Rb levels at higher drug concentrations that might be due to apoptosis. In the same line, treatment of HepG2 and PLC cells with 1 and 2 μmol/L BA-12, respectively, resulted in a more than 2.5-fold reduction of RNA polymerase II phosphorylation on serine 5 (CDK7) and serine 2 (CDK9; Fig. 1E and F), suggesting inhibition of CDK7/CDK9 activity. Administration of BP-14 below 1 μmol/L led to a strong decrease of CDK7/CDK9 activity in HepG2 and PLC cells. Quantification of CDK inhibition using recombinant CDK substrates displayed IC_{50} values of BA-12 and BP-14 between 0.01 and 0.05 μmol/L including antagonizing effects on CDK5 (Supplementary Table S2), thus corroborated the data obtained by cell-free extracts. Together, these results suggest that both BA-12 and BP-14 are highly potent cytotoxic compounds on hepatocellular carcinoma cell lines by the specific inhibition of CDK1/CDK2/CDK5/CDK7 and CDK9.

BA-12 and BP-14 abrogate clonogenicity and repress cell-cycle progression

We observed a more than 15-fold reduction of clonogenic growth behavior after treatment of HepG2 and PLC cells with 1 μmol/L BA-12 (Fig. 2A). BP-14–treated cells displayed loss of clonogenicity even at 0.2 μmol/L (Fig. 2B). Analysis of DNA synthesis revealed that treatment of HepG2 or PLC cells with 1 μmol/L of either BA-12 or BP-14 decreased BrdUrd incorporation more than 2-fold as compared with control (Fig. 2C and D), indicating inhibition of DNA synthesis. Proliferation kinetics showed a cytostatic effect of BA-12 at 2 μmol/L and of BP-14 at 0.8 μmol/L in both HepG2 and PLC cells as well as in Hep3B hepatoma cells (Supplementary Fig. S3A and S3B). Accordingly, both compounds induced an accumulation in the G_2–M and S–G_2 phase of the cell cycle (Fig. 2E and F). These data suggest that both BA-12 and BP-14 act antiproliferative by blocking DNA replication and by arresting hepatocellular carcinoma cells in the S–G_2–M phase of the cell cycle.

BA-12 and BP-14 induce apoptosis in hepatoma cells rather than in PHHs

We next examined whether apoptosis is induced by BA-12 or BP-14 in HepG2 cells that harbor wild-type p53 and in PLC cells expressing full-length but mutated p53 (32). Administration of 1 μmol/L BA-12 induced cleavage of PARP and p53 expression in HepG2 cells (Fig. 3A, left). Comparable observations were made after treatment with 2 μmol/L BA-12 in p53-mutated PLC cells (Fig. 3A, right). BP-14 was able to trigger PARP cleavage even at a concentration of 0.2 μmol/L (Fig. 3B), thus being more potent to induce apoptosis as compared with BA-12. Cleavage of caspase-7 further confirmed data of PARP processing (Fig. 3A and B). As BP-14 induced apoptosis at 0.2 μmol/L in the absence of CDK7/9 inhibition, these data suggest cytotoxic effects that are also independent of CDK7/9. Yet, both BA-12 and BP-14 failed to induce PARP processing in PHHs, which are the cellular origin of hepatoma (Fig. 3C and D). Accordingly, both BA-12 and BP-14 exhibited IC_{50} values of 26 and 20 μmol/L in PHHs, respectively, which was 35-fold (BA-12) or 160-fold (BP-14) higher than observed in HepG2 cells (Supplementary Table S1). From these data, we conclude that the novel CDK inhibitors induce apoptosis of hepatocellular carcinoma cells at low concentration in a p53-independent fashion and fail to execute cytotoxic effects in PHHs.

Long-term cytotoxicity of BA-12 and BP-14 in hepatocellular carcinoma cells

Most of the chemotherapeutic compounds that are currently available for hepatocellular carcinoma treatment show low cytotoxic efficacy presumably due to the modification and rapid removal from neoplastic hepatocytes by mechanisms of induced multiple drug resistance (33). This poses one of the major problems in combating liver cancer. Therefore, we analyzed whether BA-12 and BP-14 display changes in cytotoxicity by treating hepatoma cells at concentrations half of their IC_{50} values as well as at serial dilutions (1:2 IC_{50}, 1:4 IC_{50}, 1:8 IC_{50}, and 1:16 IC_{50}) for up to 9 months. In case, hepatocellular carcinoma cells lower their chemosensitivity by acquiring a resistance mechanism, IC_{50} values increase over time. Most notably, we observed that IC_{50} values were maintained in hepatoma cells as compared with control during sustained drug exposure (Table 1). These data provide strong evidence that the cytotoxic effects of BA-12 and BP-14 on hepatocellular carcinoma cells are maintained upon persistent drug treatment, suggesting that hepatoma cells fail to acquire chemoresistance toward BA-12 and BP-14.

In vivo application of BA-12 and BP-14: inhibition of xenografts and DEN-induced hepatoma

To examine antitumorigenic effects of BA-12 and BP-14 *in vivo*, we assessed hepatoma xenograft models derived from HepG2 and PLC cells. Tumor-bearing mice were injected either with BA-12 or BP-14 at maximum-tolerated doses (MTD). Xenografted mice well tolerated the treatment regimen of BA-12 and BP-14 as 100% of mice survived until the end of drug application. Administration of BA-12 or BP-14 resulted in reduced tumor volumes and tumor stasis of xenografts. Both were effective in the PLC as well as in the HepG2 model (Fig. 4A and B). Interestingly, BP-14 exhibited a higher potency than BA-12 in the PLC model resulting in a more pronounced reduction of the tumor volume. Evaluation of S-phase–positive cells in HepG2- and PLC-derived tumors by BrdUrd incorporation into

Published OnlineFirst August 12, 2013; DOI: 10.1158/1535-7163.MCT-13-0263

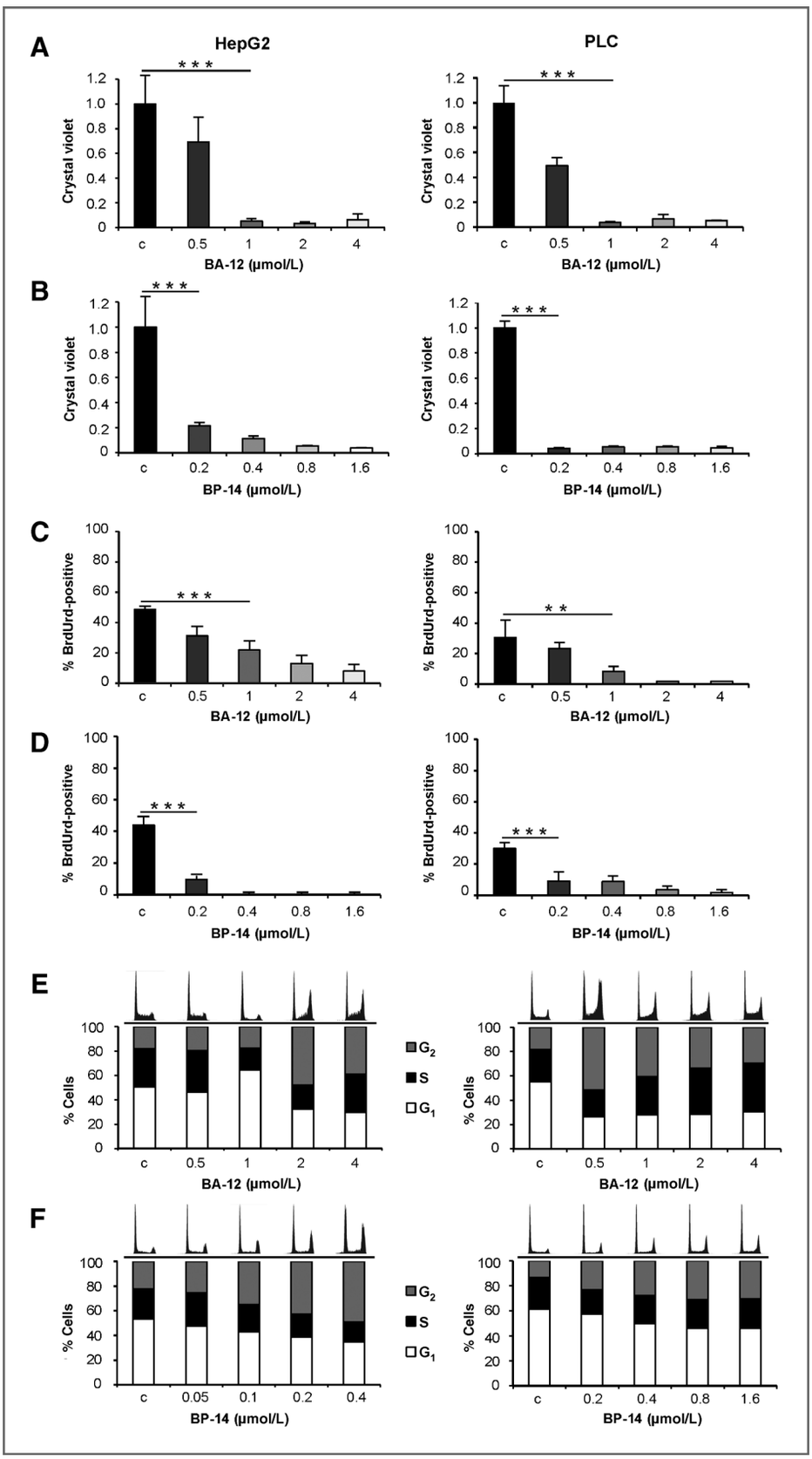

Figure 2. BA-12 and BP-14 interfere with clonogenicity and cell-cycle progression of hepatocellular carcinoma cells. A and B, quantitative evaluation of crystal violet–positive colonies generated from HepG2 (left) and PLC cells (right). Cells were pretreated with different concentrations of BA-12 (A) or BP-14 (B). C and D, HepG2 (left) and PLC cells (right) were exposed to BA-12 (C) or BP-14 (D) for 24 hours and the DNA synthesis analyzed by BrdUrd incorporation. E and F, flow cytometry showing the cell-cycle distribution of HepG2 (left) and PLC cells (right) after treatment with different concentrations of BA-12 (E) or BP-14 (F) for 24 hours. The cellular DNA content is shown in histograms (top) and the percentage of cells in G_1, S-, or G_2 phase are depicted in bars after quantification (bottom). c, control. Error bars depict SD from at least 3 individual experiments. Statistical significance is indicated with asterisks (**, $P < 0.01$; ***, $P < 0.005$).

Published OnlineFirst August 12, 2013; DOI: 10.1158/1535-7163.MCT-13-0263

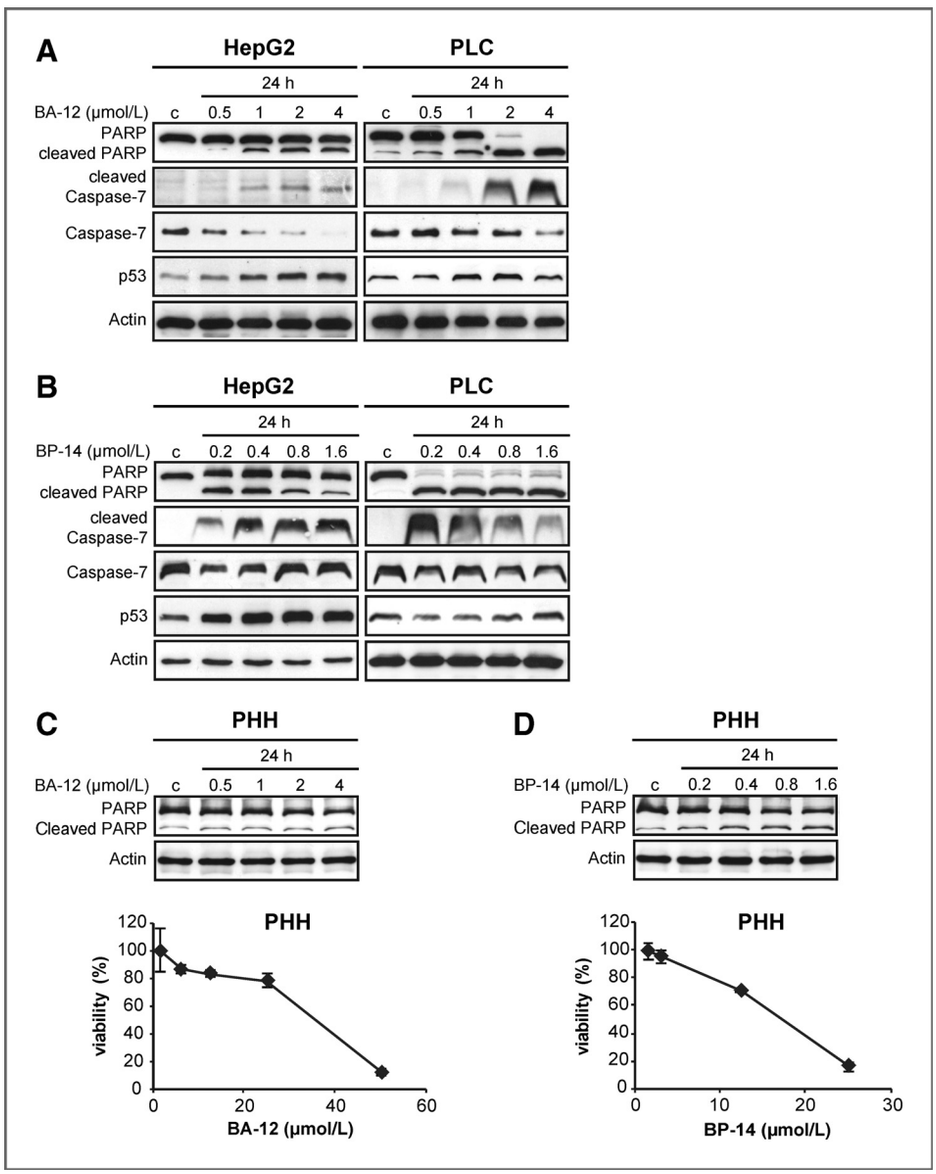

Figure 3. Apoptosis induced by BA-12 and BP-14 in hepatocellular carcinoma cells but not in PHHs. A and B, cleavage of PARP and caspase-7 after treatment of HepG2 and PLC cells with different concentrations of BA-12 (A) or BP-14 (B) for 24 hours. C, PARP cleavage (top) and determination of dose-dependent effects of BA-12 on the viability (bottom) of PHHs. D, PARP cleavage and viability of PHHs after treatment with BP-14. Actin is shown as loading control. Error bars depict SD from at least 3 individual experiments.

DNA revealed an up to 2-fold decrease after exposure to either BA-12 or BP-14 (Fig. 4C and D). Further analysis showed a 2-fold increase of TUNEL-positive cells after treatment of HepG2-derived tumors with BA-12 or BP-14, which was similar in PLC tumors, indicating that both compounds induce apoptosis in tumor tissues (Fig. 4E and F). Thus, cytostatic effects by reduced DNA synthesis and cytotoxic effects by augmented apoptosis explain the efficacy of these compounds.

Table 1. Sustained cytotoxicity in hepatocellular carcinoma cell lines after long-term exposure to BA-12 and BP-14

	BA-12		BP-14	
	HepG2	Hep3B	HepG2	Hep3B
c, μmol/L	0.81	0.64	0.11	0.12
$^1/_2$ IC_{50}, μmol/L	0.99	0.29	0.11	0.17
$^1/_4$ IC_{50}, μmol/L	0.87	0.32	0.16	0.21
$^1/_8$ IC_{50}, μmol/L	0.80	0.24	0.09	0.08
$^1/_{16}$ IC_{50}, μmol/L	0.99	0.35	0.06	0.07

We further analyzed the ability of BA-12 and BP-14 to interfere with endogenous liver cancer development that was chemically induced by the hepatotoxin DEN. Treatment modalities of DEN-induced mice included three cycles of treatment at MTDs of BA-12 and BP-14 for 10 days with interim breaks of 7 days (Fig. 5A). Evaluation of tumor nodules that are observed on the surface of cancerous livers revealed that BA-12 causes a 1.4-fold decrease of tumor nodules size as compared with control mice. Intervention with BP-14 showed comparable anticancer

Published OnlineFirst August 12, 2013; DOI: 10.1158/1535-7163.MCT-13-0263

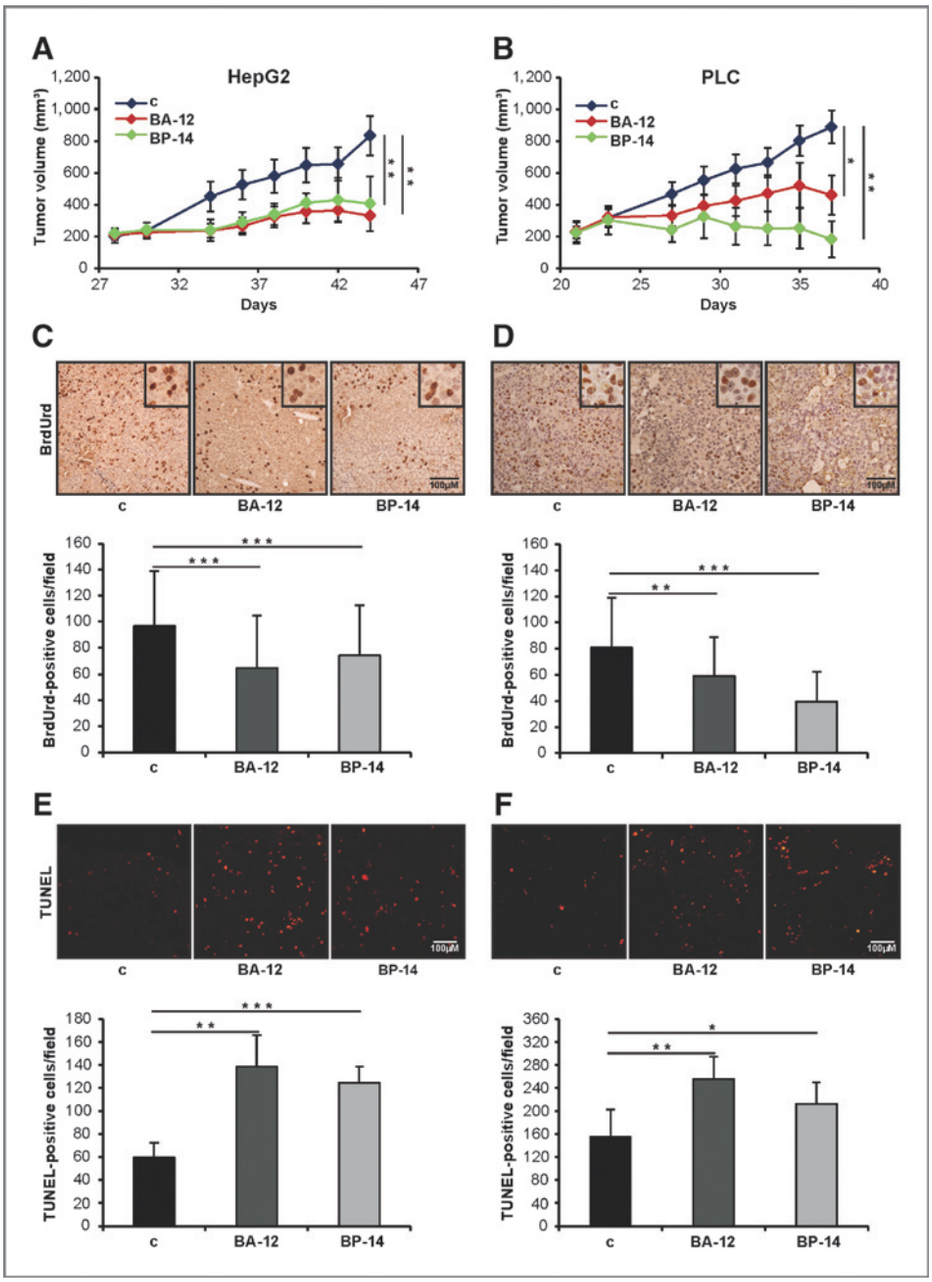

Figure 4. Intervention of xenografted hepatocellular carcinoma models with BA-12 and BP-14. Tumors were generated by subcutaneous injections of HepG2 and PLC cells into immunodeficient SCID mice. Pharmacologic intervention was conducted in tumor-bearing mice by daily intraperitoneal injection of either BA-12 or BP-14 for 17 days. A and B, volumes of HepG2- (A) and PLC-derived tumors (B) in the absence of compounds (control) and after interference with BA-12 or BP-14. C and D, immunohistochemistry showing tumor sections stained with anti-BrdUrd antibody. Insets show BrdUrd labeling at higher magnification. The panel below shows quantitative analysis of BrdUrd incorporation. c, control. E and F, TUNEL-positive cells in tumor sections and the respective quantitative analysis. Error bars depict SD and SEM from 3 individual experiments that were carried out in quadruplicates. Statistical significance is indicated with asterisks (*, $P < 0.05$; **, $P < 0.01$; ***, $P < 0.005$).

effects by a 1.3-fold decline of DEN-induced hepatoma (Fig. 5B and C). Noteworthy, mice treated with BA-12 and BP-14 did not show a decrease in body weight compared with control group (Fig. 5D), suggesting that both compounds do not show obvious side effects. In summary, these data indicate that both BA-12 and BP-14 exhibit strong antihepatoma activities *in vivo* as observed in xenograft models as well as in endogenous liver cancer.

Discussion

A considerable number of small-molecule inhibitors of CDKs have been designed to block proliferation of cancer cells (34). Inhibitors of the first generation include roscovitine, a 2,6,9-tri–substituted purine derived from studies evaluating the structure–activity relationship of this compound class (20, 35). It is a selective inhibitor of CDK1/cyclin B, CDK2/cyclin E, CDK5/p35, CDK7/cyclin H, and CDK9/cyclin T1. In this study, we assessed the anticancer activities of the novel roscovitine derivatives BA-12 and BP-14 in hepatoma. These compounds show a much higher potency than roscovitine as indicated by the inhibition of CDK1/2 in cell-free extracts (Fig. 1C) and through considerably lower IC_{50} values against recombinant CDK1, 2, 5, 7 and 9 (compare Supplementary

Published OnlineFirst August 12, 2013; DOI: 10.1158/1535-7163.MCT-13-0263

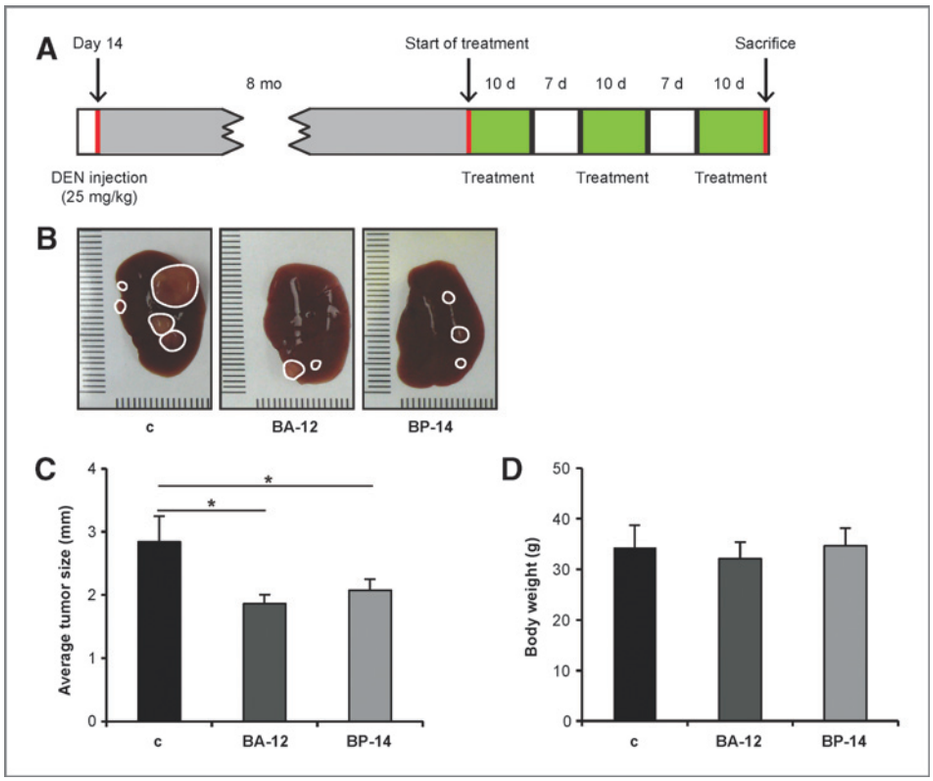

Figure 5. BA-12 or BP-14 reduce DEN-induced hepatoma formation. Endogenous liver cancer was induced by a single DEN injection in 14 day-old male C57BL/6J mice. A, scheme depicting the treatment schedule with BA-12 or BP-14. After 8 months (hatched box), DEN-induced mice were subjected to 3 cycles of drug treatment for 10 days (green boxes) and a release from compound for 7 days between the cycles. B, representative morphologies of DEN-induced hepatoma (control) and those treated with BA-12 and BP-14. White circles indicate cancerous liver nodules in the left lateral liver lobe. C, diameters of cancerous nodules were scored on the surface of livers and depicted in bars. Statistical significance is indicated with asterisks (*, $P < 0.05$). D, effect of drug treatment on mouse body weight. Groups of mice were weighed after the 3 cycles of drug treatment and mean weights are depicted in bars.

Table S2; with Table 1 in ref. 31), suggesting an ameliorated selectivity against these kinases. The kinase selectivity of both BA-12 and BP-14 to CDKs was verified on a panel of 110 human protein kinases (E. Řezníčková, manuscript in preparation). Besides CDKs, the most sensitive kinases are CK1d and ERK8. In addition, BA-12 also targets CLK2.

Nowadays the standard treatment of unresectable, intermediate stages of hepatocellular carcinoma is TACE. Several chemotherapeutics are used of which doxorubicin and cisplatin are most commonly used (36). Compared with doxorubicin, BA-12 shows a similar IC_{50} on hepatoma cell lines, whereas BP-14 shows a 10-fold higher efficacy (26). Cisplatin displays an even 10- to 20-fold lower ability of inhibition. The major problem with current chemotherapeutic drugs is that chemoresistance frequently occurs in hepatocellular carcinoma therapy. Recently, Ye and colleagues described that repeated doses of doxorubicin lead to an overexpression of P-gp and MRP1 and to a subsequent loss of doxorubicin accumulation, thus making cells less susceptible to treatment already after a short period of drug exposure (33). In contrast, our results show that BA-12 and BP-14 fail to trigger resistance mechanisms in various hepatoma cell lines. Hepatocellular carcinoma cells did not exhibit enhanced viability even after long-term treatment. In addition, both compounds were tested using a panel of chemosensitive tumor cell lines and their chemoresistant sublines overexpressing ABCB1. The P-gp–overexpressing sublines showed a lower sensitivity against BA-12 and BP-14 by showing IC_{50} values, which were 2-fold higher than in parental cells (data not shown). Thus, these data propose BA-12 and BP-14 as substrates of P-gp. In agreement, several studies showed that roscovitine represents a high-affinity substrate of P-gp as well, yet no concomitant ABCB1-mediated resistance could be observed after treatment with roscovitine (26). Noteworthy, roscovitine was also shown to induce apoptosis in a doxorubicin-resistant human myeloma cell line that overexpresses P-gp (37). Therefore, we speculate that despite being P-gp substrates, BA-12 and BP-14 do not induce resistance and are thus being promising novel therapeutic agents with persistent antihepatoma activities. BA-12 and BP-14 might be superior to currently available chemotherapeutics but should be used as first line therapy due to the frequent upregulation of P-gp in drug-treated patients with hepatocellular carcinoma.

Roscovitine is effective in antagonizing CDKs before its processing by either glucuronidation or cytochrome P450–mediated metabolism. The cytochromes P450 CYP3A4 and CYP2B6 generate the carboxylate PMF30-128 as major metabolite that lacks inhibitory function on CDKs (38). Glucuronidation takes place via the UDP-glucuronosyltransferases (UGT) 1A1, 1A3, and 2B7 (38, 39). Although not tested yet, we assume that BA-12 and BP-14 are metabolized in a similar way. Currently running experiments focus on the uptake and metabolism of these drugs and investigate whether the compound clearance via 1A1, 1A3, and 2B7 is much more reduced as compared with roscovitine. We further hypothesize that glucoronidation

Published OnlineFirst August 12, 2013; DOI: 10.1158/1535-7163.MCT-13-0263

might be the cause for the higher potency of BP-14 as compared with BA-12. BA-12 harbors a hydroxyl group that gets oxidized to glucuronic acid and is thus much more water soluble leading to a more rapid elimination from the body. The faster metabolic clearance of BA-12 might explain the 10-fold difference in IC_{50} values between BA-12 and BP-14.

HepG2 cells represent a widely used hepatocellular model in pharmacologic studies, as these malignant hepatocytes are well-differentiated and show features of normal parenchymal liver cells such as secretion of lipoproteins, biosynthesis of multiple plasma proteins, and plasma membrane polarity (40, 41). However, HepG2 cells show lower levels of CYPs and UDP-glucuronosyl-transferases (42), when compared with PHHs. Therefore, we treated PHHs with compounds and showed via determination of their IC_{50} values that BA-12 and BP-14 are cytotoxic in PHHs at about 35- and 160-fold higher levels as compared with hepatoma cell lines, respectively. Notably, both compounds are not capable to induce apoptosis of PHHs suggesting lack of obvious adverse effects of BA-12 and BP-14 due to the high xenobiotic metabolism under physiologic conditions.

BA-12 and BP-14 display further anticancer activities as pilot experiments revealed. Both compounds are able to reduce cell invasion and migration of 3-dimensional hepatospheres into the surrounding extracellular matrix (data not shown). In accordance with these findings, CDK7 was found to affect the migration of ovarian, breast, melanoma, and prostate cancer cell lines (43). In the same line, CDK9 was shown to be involved in cancer cell invasion, as miR-34a suppresses the assembly of the CDK9-c-Myc-P-TEFb complexes, leading to an inhibition of cell migration and invasion (44). CDK9 further induces TNF-α–mediated expression of MMP-9 that facilitates tumor dissemination (45). In addition, inhibition of CDK5 is suggested to be beneficial for anticancer therapy as CDK 5 stimulates Rac1-dependent migration of endothelial cells during tumor angiogenesis (46). The putative multiple inhibitory roles of BA-12 and BP-14 in hepatoma growth and migration make them promising new drugs that must be considered for clinical investigation.

Disclosure of Potential Conflicts of Interest

No potential conflicts of interest were disclosed.

Authors' Contributions

Conception and design: C. Haider, M. Grubinger, M. Strnad, V. Kryštof, W. Mikulits

Development of methodology: C. Haider, M. Grubinger

Acquisition of data (provided animals, acquired and managed patients, provided facilities, etc.): C. Haider, E. Řezníčková, T.C. Weiss, H. Rotheneder, W. Miklos, W. Berger, R. Jorda, V. Kryštof

Analysis and interpretation of data (e.g., statistical analysis, biostatistics, computational analysis): C. Haider, M. Grubinger, W. Miklos, W. Berger, W. Mikulits

Writing, review, and/or revision of the manuscript: C. Haider, M. Grubinger, R. Jorda, M. Strnad, V. Kryštof, W. Mikulits

Administrative, technical, or material support (i.e., reporting or organizing data, constructing databases): T.C. Weiss, M. Zatloukal, T. Gucký

Study supervision: M. Strnad, W. Mikulits

Other: Synthesis of CDK inhibitor BA-12, M. Zatloukal; Synthesis of studied compounds, T. Gucký

Acknowledgments

The authors thank Heidemarie Huber for excellent technical support and artwork.

Grant Support

This work was supported by the European Union, FP7 Health Research, project number HEALTH-F4-2008-202047 (to W. Mikulits), by the Austrian Science Fund, FWF, grant number P20905-B13 (to W. Mikulits), by the Herzfelder Family Foundation (to H. Rotheneder and W. Mikuilts), by the Czech Science Foundation, grants P305/12/0783 and 301/08/1649 (to V. Kryštof, M. Zatloukal, and M. Strnad), by the Ministry of Education, Youth and Sports, Czech Republic, grant Mobility 7AMB12AT011 (to V. Kryštof and E. Řezníčková), and by grant ED0007/01/01 of Centre of the Region Hana for Biotechnological and Agricultural Research (to M. Strnad, M. Zatloukal, and T. Gucký).

The costs of publication of this article were defrayed in part by the payment of page charges. This article must therefore be hereby marked *advertisement* in accordance with 18 U.S.C. Section 1734 solely to indicate this fact.

Received April 5, 2013; revised July 26, 2013; accepted August 2, 2013; published OnlineFirst August 12, 2013.

References

1. Ferlay J, Shin HR, Bray F, Forman D, Mathers C, Parkin DM. Estimates of worldwide burden of cancer in 2008: GLOBOCAN 2008. Int J Cancer 2010;127:2893–917.
2. Cao H, Phan H, Yang LX. Improved chemotherapy for hepatocellular carcinoma. Anticancer Res 2012;32:1379–86.
3. Bruix J, Sherman M. Management of hepatocellular carcinoma. Hepatology 2005;42:1208–36.
4. Voiculescu M, Winkler RE, Moscovici M, Neuman MG. Chemotherapies and targeted therapies in advanced hepatocellular carcinoma: from laboratory to clinic. J Gastrointestin Liver Dis 2008;17:315–22.
5. Sciarrino E, Simonetti RG, Le Moli S, Pagliaro L. Adriamycin treatment for hepatocellular carcinoma. Experience with 109 patients. Cancer 1985;56:2751–5.
6. Lai CL, Wu PC, Chan GC, Lok AS, Lin HJ. Doxorubicin versus no antitumor therapy in inoperable hepatocellular carcinoma. A prospective randomized trial. Cancer 1988;62:479–83.
7. Asghar U, Meyer T. Are there opportunities for chemotherapy in the treatment of hepatocellular cancer? J Hepatol 2012;56:686–95.
8. Llovet JM, Bruix J. Novel advancements in the management of hepatocellular carcinoma in 2008. J Hepatol 2008;48 Suppl 1:S20–S37.
9. Bloom J, Cross FR. Multiple levels of cyclin specificity in cell-cycle control. Nat Rev Mol Cell Biol 2007;8:149–60.
10. Rossi AG, Sawatzky DA, Walker A, Ward C, Sheldrake TA, Riley NA, et al. Cyclin-dependent kinase inhibitors enhance the resolution of inflammation by promoting inflammatory cell apoptosis. Nat Med 2006;12:1056–64.
11. Fornari F, Gramantieri L, Ferracin M, Veronese A, Sabbioni S, Calin GA, et al. MiR-221 controls CDKN1C/p57 and CDKN1B/p27 expression in human hepatocellular carcinoma. Oncogene 2008;27:5651–61.
12. Senderowicz AM. Targeting cell cycle and apoptosis for the treatment of human malignancies. Curr Opin Cell Biol 2004;16:670–8.
13. Hui AM, Makuuchi M, Li X. Cell cycle regulators and human hepatocarcinogenesis. Hepatogastroenterology 1998;45:1635–42.
14. Cho SJ, Lee SS, Kim YJ, Park BD, Choi JS, Liu L, et al. Xylocydine, a novel Cdk inhibitor, is an effective inducer of apoptosis in hepatocellular carcinoma cells in vitro and in vivo. Cancer Lett 2010;287:196–206.

Published OnlineFirst August 12, 2013; DOI: 10.1158/1535-7163.MCT-13-0263

15. Satyanarayana A, Kaldis P. Mammalian cell-cycle regulation: several Cdks, numerous cyclins and diverse compensatory mechanisms. Oncogene 2009;28:2925–39.
16. Furuno N, den Elzen N, Pines J. Human cyclin A is required for mitosis until mid prophase. J Cell Biol 1999;147:295–306.
17. Chao Y, Shih YL, Chiu JH, Chau GY, Lui WY, Yang WK, et al. Overexpression of cyclin A but not Skp 2 correlates with the tumor relapse of human hepatocellular carcinoma. Cancer Res 1998;58:985–90.
18. Ito Y, Takeda T, Sakon M, Monden M, Tsujimoto M, Matsuura N. Expression and prognostic role of cyclin-dependent kinase 1 (cdc2) in hepatocellular carcinoma. Oncology 2000;59:68–74.
19. Lam LT, Pickeral OK, Peng AC, Rosenwald A, Hurt EM, Giltnane JM, et al. Genomic-scale measurement of mRNA turnover and the mechanisms of action of the anti-cancer drug flavopiridol. Genome Biol 2001;2:RESEARCH0041.
20. Meijer L, Borgne A, Mulner O, Chong JP, Blow JJ, Inagaki N, et al. Biochemical and cellular effects of roscovitine, a potent and selective inhibitor of the cyclin-dependent kinases cdc2, cdk2 and cdk5. Eur J Biochem 1997;243:527–36.
21. Jackson RC, Barnett AL, McClue SJ, Green SR. Seliciclib, a cell-cycle modulator that acts through the inhibition of cyclin-dependent kinases. Expert Opin Drug Discov 2008;3:131–43.
22. Herv√ G, Karima B, Laurent M. (R)-Roscovitine (CYC202, Seliciclib). Inhibitors of cyclin-dependent kinases as anti-tumor agents. Boca Raton, FL: CRC Press; 2006. p. 187–225.
23. Yankulov KY, Bentley DL. Regulation of CDK7 substrate specificity by MAT1 and TFIIH. EMBO J 1997;16:1638–46.
24. Peterlin BM, Price DH. Controlling the elongation phase of transcription with P-TEFb. Mol Cell 2006;23:297–305.
25. Schneller D, Machat G, Sousek A, Proell V, van Zijl F, Zulehner G, et al. p19(ARF)/p14(ARF) controls oncogenic functions of signal transducer and activator of transcription 3 in hepatocellular carcinoma. Hepatology 2011;54:164–72.
26. van Zijl F, Mall S, Machat G, Pirker C, Zeillinger R, Weinhaeusel A, et al. A human model of epithelial to mesenchymal transition to monitor drug efficacy in hepatocellular carcinoma progression. Mol Cancer Ther 2011;10:850–60.
27. Armeanu S, Lauer UM, Smirnow I, Schenk M, Weiss TS, Gregor M, et al. Adenoviral gene transfer of tumor necrosis factor-related apoptosis-inducing ligand overcomes an impaired response of hepatoma cells but causes severe apoptosis in primary human hepatocytes. Cancer Res 2003;63:2369–72.
28. Gucky T, Jorda R, Zatloukal M, Bazgier V, Berka K, Reznickova E, et al. A novel series of highly potent 2,6,9-trisubstituted purine cyclin-dependent kinase inhibitors. J Med Chem 2013;56:6234–47.
29. Gotzmann J, Huber H, Thallinger C, Wolschek M, Jansen B, Schulte-Hermann R, et al. Hepatocytes convert to a fibroblastoid phenotype through the cooperation of TGF-beta1 and Ha-Ras: steps towards invasiveness. J Cell Sci 2002;115:1189–202.
30. Zulehner G, Mikula M, Schneller D, van Zijl F, Huber H, Sieghart W, et al. Nuclear beta-catenin induces an early liver progenitor phenotype in hepatocellular carcinoma and promotes tumor recurrence. Am J Pathol 2010;176:472–81.
31. Krystof V, McNae IW, Walkinshaw MD, Fischer PM, Muller P, Vojtesek B, et al. Antiproliferative activity of olomoucine II, a novel 2,6,9-trisubstituted purine cyclin-dependent kinase inhibitor. Cell Mol Life Sci 2005;62:1763–71.
32. Puisieux A, Galvin K, Troalen F, Bressac B, Marcais C, Galun E, et al. Retinoblastoma and p53 tumor suppressor genes in human hepatoma cell lines. FASEB J 1993;7:1407–13.
33. Ye CG, Yeung JH, Huang GL, Cui P, Wang J, Zou Y, et al. Increased glutathione and mitogen-activated protein kinase phosphorylation are involved in the induction of doxorubicin resistance in hepatocellular carcinoma cells. Hepatol Res 2013;43:289–99.
34. Krystof V, Baumli S, Furst R. Perspective of cyclin-dependent kinase 9 (CDK9) as a drug target. Curr Pharm Des 2012;18:2883–90.
35. Havlicek L, Hanus J, Vesely J, Leclerc S, Meijer L, Shaw G, et al. Cytokinin-derived cyclin-dependent kinase inhibitors: synthesis and cdc2 inhibitory activity of olomoucine and related compounds. J Med Chem 1997;40:408–12.
36. de Lope CR, Tremosini S, Forner A, Reig M, Bruix J. Management of HCC. J Hepatol 2012;56 Suppl 1:S75–87.
37. Rajnai Z, Mehn D, Beery E, Okyar A, Jani M, Toth GK, et al. ATP-binding cassette B1 transports seliciclib (R-roscovitine), a cyclin-dependent kinase inhibitor. Drug Metab Dispos 2010;38:2000–6.
38. Komina O, Nosske E, Maurer M, Wesierska-Gadek J. Roscovitine, a small molecule CDK inhibitor induces apoptosis in multidrug-resistant human multiple myeloma cells. J Exp Ther Oncol 2011; 9:27–35.
39. McClue SJ, Stuart I. Metabolism of the trisubstituted purine cyclin-dependent kinase inhibitor seliciclib (R-roscovitine) *in vitro* and *in vivo*. Drug Metab Dispos 2008;36:561–70.
40. Raynaud FI, Whittaker SR, Fischer PM, McClue S, Walton MI, Barrie SE, et al. In vitro and in vivo pharmacokinetic-pharmacodynamic relationships for the trisubstituted aminopurine cyclin-dependent kinase inhibitors olomoucine, bohemine and CYC202. Clin Cancer Res 2005;11:4875–87.
41. Altmann B, Giselbrecht S, Weibezahn KF, Welle A, Gottwald E. The three-dimensional cultivation of the carcinoma cell line HepG2 in a perfused chip system leads to a more differentiated phenotype of the cells compared to monolayer culture. Biomed Mater 2008;3: 034120.
42. Meli L, Jordan ET, Clark DS, Linhardt RJ, Dordick JS. Influence of a three-dimensional, microarray environment on human cell culture in drug screening systems. Biomaterials 2012;33:9087–96.
43. Westerink WM, Schoonen WG. Phase II enzyme levels in HepG2 cells and cryopreserved primary human hepatocytes and their induction in HepG2 cells. Toxicol In Vitro 2007;21:1592–602.
44. Collins CS, Hong J, Sapinoso L, Zhou Y, Liu Z, Micklash K, et al. A small interfering RNA screen for modulators of tumor cell motility identifies MAP4K4 as a promigratory kinase. Proc Natl Acad Sci U S A 2006; 103:3775–80.
45. Yamamura S, Saini S, Majid S, Hirata H, Ueno K, Deng G, et al. MicroRNA-34a modulates c-Myc transcriptional complexes to suppress malignancy in human prostate cancer cells. PLoS One 2012;7: e29722.
46. Shan B, Zhuo Y, Chin D, Morris CA, Morris GF, Lasky JA. Cyclin-dependent kinase 9 is required for tumor necrosis factor-alpha-stimulated matrix metalloproteinase-9 expression in human lung adenocarcinoma cells. J Biol Chem 2005;280:1103–11.

PŘÍLOHA IV

Řezníčková E, Weitensteiner S, Havlíček L, Jorda R, Gucký T, Berka K, Bazgier V, Zahler S, Kryštof V, Strnad M (2015) Characterization of a Pyrazolo[4,3-d]pyrimidine Inhibitor of Cyclin-Dependent Kinases 2 and 5 and Aurora A With Pro-Apoptotic and Anti-Angiogenic Activity In Vitro. Chem Biol Drug Des. 86, 1528-1540.

Chem Biol Drug Des 2015; **86:** 1528–1540

Research Article

Characterization of a Pyrazolo[4,3-*d*]pyrimidine Inhibitor of Cyclin-Dependent Kinases 2 and 5 and Aurora A With Pro-Apoptotic and Anti-Angiogenic Activity *In Vitro*

Eva Řezníčková[1], Sabine Weitensteiner[2], Libor Havlíček[3], Radek Jorda[1], Tomáš Gucký[1], Karel Berka[4], Václav Bazgier[1,5], Stefan Zahler[2], Vladimír Kryštof[1,*] and Miroslav Strnad[1]

[1]Laboratory of Growth Regulators & Department of Chemical Biology and Genetics, Centre of the Region Haná for Biotechnological and Agricultural Research, Palacký University and Institute of Experimental Botany AS CR, Šlechtitelů 27, 78371 Olomouc, Czech Republic
[2]Department of Pharmacy, LMU Munich – Center for Drug Research – Pharmaceutical Biology, Butenandtstr. 5-13, 81377 Munich, Germany
[3]Isotope Laboratory, Institute of Experimental Botany ASCR, Vídeňská 1083,14220 Prague, Czech Republic
[4]Regional Centre of Advanced Technologies and Materials, Department of Physical Chemistry, Faculty of Science, Palacký University, 17. listopadu 12, 77146 Olomouc, Czech Republic
[5]Department of Physical Chemistry, Faculty of Science, Palacký University, 17. listopadu 1192/12, 771 46 Olomouc, Czech Republic
**Corresponding author: Vladimír Kryštof, vladimir.krystof@upol.cz*

Selective inhibitors of kinases that regulate the cell cycle, such as cyclin-dependent kinases (CDKs) and aurora kinases, could potentially become powerful tools for the treatment of cancer. We prepared and studied a series of 3,5,7-trisubstituted pyrazolo[4,3-*d*] pyrimidines, a new CDK inhibitor scaffold, to assess their CDK2 inhibitory and antiproliferative activities. A new compound, 2i, which preferentially inhibits CDK2, CDK5, and aurora A was identified. Both biochemical and cellular assays indicated that treatment with compound 2i caused the downregulation of cyclins A and B, the dephosphorylation of histone H3 at Ser10, and the induction of mitochondrial apoptosis in the HCT-116 colon cancer cell line. It also reduced migration as well as tube and lamellipodia formation in human endothelial cells. The kinase inhibitory profile of compound 2i suggests that its anti-angiogenic activity is linked to CDK5 inhibition. This dual mode of action involving apoptosis induction in cancer cells and the blocking of angiogenesis-like activity in endothelial cells offers possible therapeutic potential.

Key words: angiogenesis, apoptosis, aurora A, cyclin-dependent kinase, inhibitor, pyrazolo[4,3-*d*]pyrimidine

Abbreviations: BrdU, 5-bromo-2′-deoxyuridine; CDK, cyclin-dependent kinase; IC_{50}, half maximum inhibitory concentration; FITC, fluorescein isothiocyanate; HMEC, human microvascular epithelial cells; HUVEC, human umbilical vein endothelial cells; PARP-1, poly-(ADP-ribose)polymerase-1; PCNA, proliferating cell nuclear antigen; PDGFR, platelet-derived growth factor receptor; Plk-1, Polo-like kinase 1; PUMA, p53 upregulated modulator of apoptosis; Rb, retinoblastoma; VEGF, vascular endothelial growth factor.

Received 9 April 2015, revised 9 July 2015 and accepted for publication 13 July 2015

Established hallmarks of cancer cells include sustained proliferative signaling and evasion of growth suppressors (1). Both of these processes have been linked to genetic and epigenetic changes in cell cycle regulating genes. The selective targeting of cyclin-dependent kinases (CDKs) was one of the first proposed approaches to cancer therapy and has been studied extensively (2). While CDK2 is not regarded as a good target for cancer drugs (3,4), several synthetic CDK inhibitors have entered clinical trials as drug candidates for oncological indications (5,6). The negative perception of CDKs as drug targets was reinforced by the discovery that several CDKs have compensatory roles in the cell cycle. For example, CDK1 can compensate for the absence or inhibition of CDK2 and vice-versa (7). On the other hand, most inhibitors that have been tested in clinical trials target multiple CDKs and so may advantageously overcome this compensation.

While some existing inhibitors target CDKs that regulate cell cycling, many also interfere with the transcriptional CDKs 7 and 9. CDK9 in particular has been identified as a target of most of the CDK inhibitors that have entered clinical trials, e.g. flavopiridol, roscovitine, SNS-032, and AT7519 (5,6,8). CDK9 inhibition causes the downregulation of short half-life proteins connected to apoptosis (notably, Mcl-1, and XIAP) that are critical for the survival of cancer cells, especially those causing multiple myeloma and chronic lymphocytic leukemia (9–12).

 doi: 10.1111/cbdd.12618

Rather surprisingly, some CDK inhibitors that have been evaluated in clinical studies (SNS-032, flavopiridol, and ZK 304709) have also been shown to exert anticancer effects *in vivo* by interfering with tumor angiogenesis (13–15). This was ascribed to the down-regulation of both the mRNA and protein of vascular endothelial growth factor (VEGF), the most potent known tumor angiogenic factor, via CDK9 inhibition. However, we have recently shown that CDK5, previously identified as a regulator of neuronal processes, also regulates two processes that are essential for angiogenesis: endothelial cell migration and tube formation (16). Moreover, we found that the anti-angiogenic activity of several CDK inhibitors with different structures, including roscovitine, is at least partially due to interference with CDK5 (16,17).

We recently prepared a pyrazolo[4,3-*d*]pyrimidine bioisostere of the well-known CDK inhibitor roscovitine (18). The bioisostere proved to be a more potent CDK inhibitor than roscovitine itself, with greater anticancer activity *in vitro*. We therefore sought to build on this finding by exploiting our knowledge of structure-activity relationships in purine CDK inhibitors to prepare a small library of potential CDK inhibitors with pyrazolo[4,3-*d*]pyrimidine skeletons. Here, we describe the synthesis of these compounds and present data on their biological activity.

Methods and Materials

Synthesis

Melting points were determined on a Kofler block and are uncorrected. NMR spectra were measured on a UNITY Inova-400 or Gemini-300 spectrometer (Varian, Yarnton, UK) using deuterated solvents at 303 K. The residual solvent signal was used as an internal standard. Chemical shifts are given in the δ-scale [p.p.m.], and coupling constants in Hz. ESI or APCI mass spectra were determined using a Micromass ZMD mass spectrometer (Waters, Milford, MA, USA) (direct inlet, coin voltage 20 V). IR spectra were recorded on a Nicolet 200 FTIR instrument (Thermo Scientific, Waltham, MA, USA). Column chromatography was performed using silica gel Kieselgel 60 (Merck, Darmstadt, Germany) (230–400 mesh). The purity of all synthesized compounds was evaluated by HPLC-PDA (200–500 nm) and was ≥95% in all cases other than compounds **1c** (82%) and **1e** (89%). Detailed information about synthesis and characterization of the compounds are described in Supporting information (Appendix S1).

Kinase inhibition

All prepared compounds were evaluated for the inhibition of CDK2/cyclin E as previously described (18,19). Briefly, CDK2/cyclin E was produced in Sf9 insect cells via baculoviral infection and purified on a NiNTA column (Qiagen, Hilden, Germany). The kinase reactions were assayed with 1 mg/mL histone H1 in the presence of 15 μM ATP, 0.05 μCi [γ^{33}P]ATP, and the tested compound in a final volume of 10 μL, all in reaction buffer (60 mM HEPES-NaOH, pH 7.5, 3 mM $MgCl_2$, 3 mM $MnCl_2$, 3 μM Na-orthovanadate, 1.2 mM DTT, 2.5 μg/50 μL $PEG_{20.000}$). The reaction was stopped by adding 3% aq. H_3PO_4; aliquots were spotted onto P-81 phosphocellulose (Whatman, Maidstone, UK), washed with 0.5% aq. H_3PO_4, and air-dried.

The protein kinase selectivity of compound **2i** was tested against a panel of CDKs and aurora A (Table 2) using the ProQinase platform according to the manufacturer's protocol. Compound **2i** was also profiled at concentrations of 1 and 10 μM by screening against 88 enzymes (Table S1) as described previously (20).

Molecular docking

All 3D structures of studied compounds were prepared using Marvin 14.9.8, 2014, ChemAxon (http://www.chemaxon.com). The crystal structures of CDK2 with Cyclin A (PDBID: 3DDQ), CDK2 with Cyclin E (PDBID: 1W98), and aurora A (PDBID: 3O50) were used as the protein docking templates. Polar hydrogens were added to all ligands and proteins with the AutoDock Tools program (21). Molecular docking was performed using the AutoDock Vina program (22) with a grid box centered on the protein's active site and a box size of 18 Å. The value of the exhaustiveness parameter was set to 30 (default 8).

Cell maintenance and cytotoxicity assay

The cells were cultured in DMEM or RPMI-1640 (supplemented with 10% fetal calf serum, 4 mM glutamine, 100 IU/mL penicillin, 100 μg/mL streptomycin) in a humidified CO_2 incubator at 37 °C and then seeded into 96-well microtiter plates at appropriate densities for their cell sizes and growth rates. After a preincubation period, the cells were treated with the test compound at six different concentrations, in triplicate, and incubated for 72 h. A solution of Calcein AM was then added and the fluorescence of the live cells was measured at 485 nm/538 nm (ex/em) with a Fluoroskan Ascent microplate reader (Labsystems, Helsinki, Finland). IC_{50} values, i.e. the compound concentrations required to reduce the number of viable cells by 50% relative to an untreated control, were determined from the dose-response curves.

Immunoblotting

Immunoblotting was performed as described previously (18,19). Total cellular protein lysates were prepared by harvesting treated cells in Laemmli sample buffer. Proteins were separated on SDS-polyacrylamide gels and electroblotted onto nitrocellulose membranes. The blotted membranes were stained with 0.2% Ponceau-S in 1% aq acetic acid to confirm equal protein loading, then destained and blocked using PBS and 0.1% Tween 20 (PBS-T) with 5% low fat milk or 3% bovine serum albumin (BSA). The membranes were then incubated with specific antibodies

overnight at 4 °C. After washing three times in PBS-T, the membranes were incubated with peroxidase-conjugated secondary antibodies. After another three washes in PBS-T, peroxidase activity was determined using ECL kit (Thermo Scientific, Waltham, MA, USA) according to the manufacturer's instructions.

Antibodies

Specific antibodies were purchased from Santa Cruz Biotechnology, Dallas, TX, USA (anti-ARK-1, clone N-20; anti-ARK-2, clone E-15; anti-Bcl-2, clone 100; anti-cyclin B1, clone GNS1; anti-cyclin E, clone HE12; anti-Mcl-1, clone S-19; anti-MDM-2, clone SMP14 and anti-PARP-1, clone F-2), Cell Signaling, Danvers, MA, USA (anti-phospho-Plk-1 Thr210; anti-PUMA; anti-phospho-Rb Ser807/811; anti-Rb, clone 4H1), DAKO Cytomation, Glostrup, Denmark (anti-caspase 3), Millipore, Billerica, MA, USA (anti-Histone H3 phosphorylated at Ser10), Beckman Coulter/Immunotech, Marseille, France (anti-cyclin A2-FITC), Roche Applied Science, Penzberg, Germany (anti-BrdU-FITC), Jackson Laboratories, West Grove, PA, USA (goat-anti-mouse FITC), Invitrogen, Carlsbad, CA, USA (goat-anti-rabbit-Alexa Fluor 488), Sigma Aldrich, St. Louis, MO, USA (peroxidase-labelled secondary antibodies) or were generously gifted by Dr. B. Vojtěšek (anti-p53, clone DO-1; anti-PCNA, clone PC-10).

Cell cycle analysis

Sub-confluent HCT-116 cells were treated with compound **2i** at different concentrations for 24 h. Cells treated with etoposide and nocodazole were analyzed simultaneously for comparative purposes. To study proliferation, the cultures were pulse-labeled with 10 μM 5-bromo-2′-deoxyuridine (BrdU) for 30 min before harvesting. The cells were then trypsinized, washed with PBS containing 1% BSA (PBS/BSA), fixed with ice-cold 70% ethanol, incubated on ice for 30 min, washed with PBS/BSA again, and resuspended in 2 M HCl containing 0.5% Triton-X100 for 30 min at room temperature to denature their DNA. After neutralization with 0.1 M $Na_2B_4O_7.10H_2O$, the cells were harvested by centrifugation and washed with PBS/BSA containing 0.5% Tween-20. They were then stained with anti-BrdU fluorescein-labeled antibody for 1 hour at room temperature in the dark. To study histone H3 phosphorylation and the expression of cyclins A and B, cells were harvested by trypsinization, washed in PBS, fixed with ice-cold 90% methanol, incubated on ice for 30 min and washed with PBS/BSA containing 0.5% Tween-20. For cyclin A analysis, cells were incubated with an anti-cyclin A2 fluorescein-labeled antibody for 1 h in dark. Cells for the analysis of cyclin B expression and histone H3 phosphorylation were initially incubated with the appropriate primary antibody for 1 h at room temperature, then washed with PBS containing 1% BSA and incubated with the appropriate fluorescent-labeled secondary antibody for 1 h in the dark. After washing with PBS/BSA, each sample was incubated with propidium iodide (final concentration 10 μg/mL) and RNAse A (final concentration 200 μg/mL) for 30 min at room temperature in the dark. The cells were then analyzed by flow cytometry using a 488 nm laser (Cell Lab Quanta SC; Beckman Coulter, Brea, CA, USA).

Caspase-3/7 activity assay

The cells were harvested by centrifugation and homogenized in an extraction buffer (20 mM TRIS pH 7.4, 100 mM NaCl, 5 mM EDTA, 2 mM EGTA, 2 mM NaF, 0.2% Nonidet p40, inhibitors of proteases, pH 7.4) on ice for 30 min. The samples were centrifuged at 17 000 $\times g$ for 25 min at 4 °C; the proteins were quantified and diluted to equal concentrations. The lysates were then incubated for 4 h with 100 μM Ac-DEVD-AMC as a substrate in the assay buffer (25 mM PIPES, 2 mM EGTA, 2 mM $MgCl_2$, 5 mM DTT, pH 7.3). The fluorescence of the product was measured using a Fluoroskan Ascent microplate reader (Labsystems, Helsinki, Finland) at 346/442 nm (ex/em).

Analysis of transcription

The cells were seeded in media containing [^{14}C]thymidine (62.5 Bq/mL in growth medium) for 36 h and then treated with various concentrations of compound **2i** in fresh cultivation medium for 24 h. During the final 30 min of the drug treatment period, nascent RNA was labeled by adding [^{3}H]uridine (0.75 MBq/mL) to the cultivation media. mRNA was isolated from cells using the Oligotex Direct mRNA kit (Qiagen, Hilden, Germany). For measurements of total RNA synthesis, cell lysates in 1% SDS were precipitated with 10% TCA after which the TCA-insoluble material was collected on spin filters (Invitek, Hayward, CA, USA) and washed. The nucleic acids were then eluted with 1 M NaOH. The ^{3}H and ^{14}C in the eluate were quantified simultaneously using an LS6500 liquid scintillation counter (Beckman Coulter, Brea, CA, USA). Relative total RNA synthesis and mRNA synthesis rates were determined by calculating the ^{3}H/^{14}C ratio for each sample and comparing it to that for an untreated control sample.

Scratch assay (Migration assay)

HUVECs were seeded into a 24-well plate. After reaching confluency, the cells were scratched using a 100 μL pipette tip. The wounded monolayers were washed twice with PBS containing Ca^{2+}/Mg^{2+}; then growth medium containing the appropriate concentration of the test compound was added. After 16 h of migration, the cells were washed and subsequently fixed with 4% paraformaldehyde. We have previously shown that under these conditions cell proliferation does not contribute substantially to scratch closure. Images were acquired using the TILLvisON system (TILL Photonics GmbH, Gräfelfing, Germany) and a CCD-camera connected to an Axiovert 200 microscope (Zeiss, Oberkochen, Germany). Quantitative image analyses of the cell-covered area were performed by Wimasis GmbH, Munich (23).

Quantification of lamellipodia and immunocytochemistry

Confluent layers of HUVECs were scratched and stimulated in eight-well μ-slides as described above. The cells were allowed to migrate for 8 h in the presence or absence of the appropriate concentrations of the tested compounds, until lamellipodia were clearly visible in the control. The actin cytoskeleton was then stained with rhodamine-phalloidin (Life Technologies, Darmstadt, Germany) and fluorescence images of the scratches were taken in 10× magnification with a Zeiss LSM 510 META instrument. For quantitative evaluation of lamellipodia formation, cells with prominent lamellipodia and ruffles were counted using IMAGEJ (Cell Counter plug-in by Kurt De Vos) in relation to the total number of cells at the scratch front. The ratio was calculated as the proportion of lamellipodia-positive cells per 100 cells at the scratch front. Immunofluorescence staining was performed using the same apparatus. Fixed cells were permeabilized for 2 min with 0.1 % Triton X-100 in PBS, after which the cells were washed and unspecific binding was blocked with 0.2% BSA in PBS for 15 min. The cells were then incubated with a primary antibody (cortactin, Cell Signaling, and Rac1, Upstate) in 0.2% BSA/PBS overnight at 4 °C. After three washing steps with PBS, the specimens were incubated with the appropriate AlexaFluor®-labeled secondary antibodies for 30 min at room temperature. Finally, the slides were again washed three times with PBS (5 min), embedded in FluorSave™ Reagent mounting medium, and covered with 8 mm × 8 mm glass cover slips (23).

Tube formation assay

Precooled BD Matrigel™ Matrix Growth Factor Reduced (GFR) (BD Biosciences, Heidelberg, Germany) was placed in the lower compartment of μ-slide Angiogenesis wells (ibidi GmbH, Martinsried, Germany) on ice. The Matrigel™ Matrix was polymerized by incubating the slides at 37 °C for 30 min. 12 000 HUVECs/well were then seeded onto the Matrigel™ and stimulated for 16 h. The level of tube formation was determined by light microscopy using the TILLvisON system. Quantitative image analysis of tube length, number of branching points, and tube number was performed with a software tool from Wimasis GmbH, Munich (23).

Results

Synthesis

The tested compounds were synthesized using previously published general procedures (18,23,24).

A first series of 7-benzylamino substituted pyrazolo[4,3-*d*]pyrimidines having various side chains at the 5 position (compounds **1b**–**n**) was prepared by the nucleophilic substitution of 5-chloro- or 5-methylsulfonyl-{7-benzylamino-3-isopropyl-1H-pyrazolo[4,3-*d*]pyrimidin-5-yl}amine with appropriate amines at 120–150 °C (Figure 1) (18,23,24).

Compounds of the second series, i.e. 7-(2-aminobenzyl) amino-substituted pyrazolo[4,3-*d*]pyrimidines **2d**–**n**, were obtained in higher yields from 5-chloro-7-(2-aminobenzyl) amino-3-isopropyl-1*H*-pyrazolo[4,3-*d*]pyrimidine (**2b**). In particular, this route was the only viable way of preparing compounds **2i** and **2j**, which have bulky side chains. When 5-methylsulfonyl-7-(2-aminobenzyl)amino-3-isopropyl-1*H*-pyrazolo[4,3-*d*]pyrimidine was used as the starting material in reactions with sterically demanding amines, an elimination reaction occurred within the (2-aminobenzyl) side chain that primarily generated the corresponding 7-aminopyrazolo[4,3-*d*]pyrimidines. Compound **2b** was prepared by reacting the highly condensed heteroaromatic system 4,9-dichloro-2,7-diisopropyl-1,3,5,5b,6,8,10,10b-octaazacyclopenta[*h,i*]aceanthrylene with (2-aminobenzyl) amine (24).

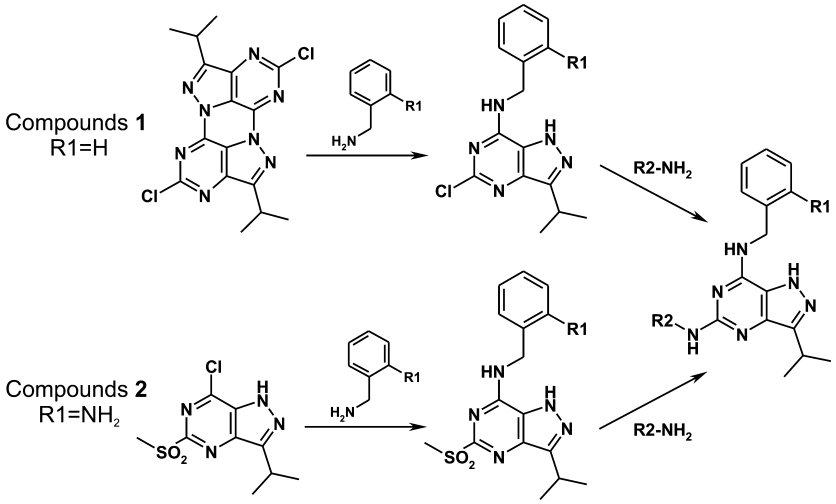

Figure 1: Synthesis of the new pyrazolo [4,3-*d*]pyrimidines. R1 and R2 substituents are listed in Table 1.

Structure-activity relationship for CDK inhibition and cytotoxicity

A series of 3,5,7-trisubstituted pyrazolo[4,3-*d*]pyrimidines was prepared based on our knowledge of the structure-activity relationships of CDK inhibitors with purine cores.

All of the prepared compounds have a common isopropyl moiety at the 3 position of the pyrazolo[4,3-*d*]pyrimidine ring system because an isopropyl group was found to be the optimal substituent at the analogous position in purine CDK inhibitors (25–29). The 5 and 7 positions were also substituted with groups that conferred high activity in purines, i.e. benzylamines at the 7 position and alkyl- or cycloalkyl- amines at position 5. Table 1 summarizes the CDK2 inhibitory activities and antiproliferative properties of the new compounds.

Table 1: Substituents and biological activities of the tested pyrazolo[4,3-*d*]pyrimidine compounds

General structure	Cmpd	Substituents		IC_{50} (nM)[a]	GI_{50} (μM)[a]	
		R1	R2	CDK2/E	MCF-7	K562
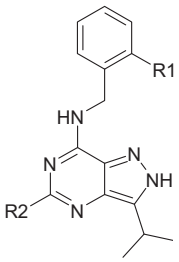	**1b**	H		130.2 ± 2.3	>100	>100
	1c	H		690.0 ± 84.9	40.9 ± 15.1	53.1 ± 13.9
	1d	H	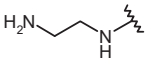	128.3 ± 62.2	4.6 ± 1.1	10.8 ± 2.1
	1e	H	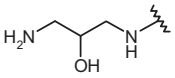	111.0 ± 51.1	23.4 ± 5.1	30.9 ± 5.6
	1f	H	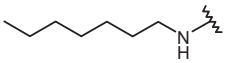	>1000	21.4 ± 8.2	17.0 ± 3.4
	1g	H	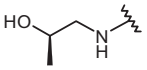	29.3 ± 9.3	19.9 ± 4.4	29.7 ± 16.1
	1i	H	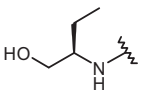	46.1 ± 26.9	5.9 ± 2.2	8.0 ± 1.7
	1k	H	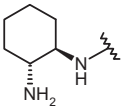	100.7 ± 8.1	6.3 ± 1.3	4.5 ± 0.4
	1l	H	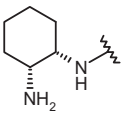	52.3 ± 6.8	2.7 ± 1.1	2.8 ± 0.8
	1n	H	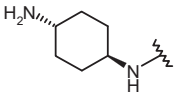	186.7 ± 70.9	22.4 ± 19.0	20.9 ± 17.2
	2a	NH_2		367.5 ± 43.5	>100	>100
	2b	NH_2		461.1 ± 72.0	>100	>100
	2d	NH_2	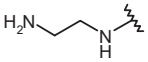	230.0 ± 88.9	47.5 ± 31.1	63.6 ± 27.9
	2g	NH_2	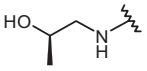	16.5 ± 8.1	4.4 ± 0.5	15.5 ± 1.0
	2h	NH_2	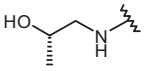	30.5 ± 19.0	12.9 ± 2.0	41.0 ± 13.2
	2i	NH_2	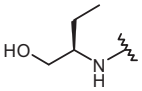	10.5 ± 3.4	2.8 ± 0.4	9.2 ± 1.4

Table 1: continued

Cmpd	Substituents R1	Substituents R2	IC_{50} (nM)[a] CDK2/E	GI_{50} (μM)[a] MCF-7	GI_{50} (μM)[a] K562
2j	NH_2	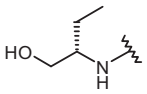	15.3 ± 1.2	10.9 ± 4.0	22.3 ± 1.7
2m	NH_2	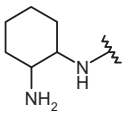	313.3 ± 102.6	23.5 ± 16.1	21.2 ± 13.2
2n	NH_2	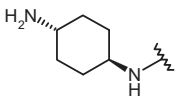	93.3 ± 37.9	47.6 ± 25.7	35.6 ± 7.6

[a]Average values from at least three determinations ± SD.

Among prepared 7-benzylamino-derivatives, three compounds possess linear side chain at 5. The weakest CDK2 inhibitory activity was observed with compound **1f** having heptylamine at 5 (IC_{50} value of 4.45 μM). Small substituents with terminal amino group increased activity of derivatives **1c** and **1d**. Interestingly, **1f** was still more potent in terms of cytotoxicity, probably due to its lower polarity and easier cellular uptake. Branched alkylderivatives **1e**, **1g** and **1i** reached nanomolar potency in CDK2 assays. Introduction of substutituted cyclohexyl at 5 further enhanced substantially not only CDK2 inhibition, but also cytotoxicity; **1k** and **1l** having (2-aminocyclohexyl)amino yielded single digit micromolar IC_{50} values. Unexpectedly, closely related **1n** with (4-aminocyclohexyl)amino functions demonstrated 10-fold drop in cellular potency.

We also prepared compounds with a 2-aminobenzylamino moiety at position 7. The effects of varying the substituent at the 5 position in this series were almost identical to those observed in the 2-benzylamino series. Because purine derivatives bearing the *R* isomers of (2-hydroxypropyl)amine and [(2-hydroxymethyl)propyl]amine at the 5 position are known to be more active than their *S* counterparts (19), we prepared the corresponding pyrazolo[4,3-*d*] pyrimidine derivatives in both optically active isoforms (compounds **2g** and **2h**, and **2i** and **2j** respectively). In both cases, the *S* isomer was less active than the *R*. However, all of these compounds had lower IC_{50} values (around 20 nM) than other members of the series. The most potent CDK2 inhibitor from the two series, compound **2i** (IC_{50} = 10 nM), was subjected to further biological profiling.

Antiproliferative effects of compound 2i

The antiproliferative activity of compound **2i** was tested against a panel of human cancer cell lines of different origins (Table 2). It exhibited strong activity in all of the tested lines, with an average IC_{50} of 5 μM. It also reduced the proliferation of normal HMEC-1 cells with an IC_{50} value of 5.4 μM. However, compound **2i** had no adverse effect on the viability of these cells (data not shown). In addition, non-proliferating (confluent) human fibroblasts, treated with different concentrations of compound **2i** for 72 hours, showed no significant reduction of the cell viability up to the concentration of 100 μM.

Table 2: Cytotoxicity of compound **2i** in human cancer cell lines

Cell line	Compound **2i** IC_{50} (μM)[a]
MCF-7	2.8 ± 0.4
MDA-MB-468	4.0 ± 0.3
HeLa	4.8 ± 1.8
HCT-116	3.5 ± 0.3
HT-29	9.8 ± 3.6
CEM	3.5 ± 0.1
K562	9.2 ± 1.4
G-361	4.2 ± 0.4
RPMI-8226	4.4 ± 0.2
U266	3.0 ± 0.3
HOS	5.5 ± 0.4

[a]Average values from three determinations ± SD.

Protein kinase selectivity

Due to the high structural similarity between roscovitine and compound **2i**, we initially explored its inhibitory potency against a panel of CDKs and other kinases. The compound proved to be selective toward CDKs, with submicromolar IC_{50} values for CDK2 and CDK5 (70 and 260 nM, respectively) and low micromolar IC_{50} values for CDK9 and CDK1 (1.91 and 3.13 μM respectively). Aside from aurora A, which it also inhibited at sub-micromolar concentrations (IC_{50} = 0.40 μM), it was not active against any of the other tested kinases (Table 3, Table S1).

Table 3: Protein kinase selectivity of compound **2i**, roscovitine, and JNJ-7706621

	IC_{50} (μM)		
Protein kinase	Compound **2i**[a]	Roscovitine[b]	JNJ-7706621[c]
CDK1/cyclin B	3.134 ± 0.021	9.900	0.009
CDK2/cyclin A	0.125 ± 0.001	3.000	0.004
CDK2/cyclin E	0.072 ± 0.003	0.500	0.003
CDK4/cyclin D1	21.730 ± 2.970	29.000	0.253
CDK5/p25NCK	0.257 ± 0.002	3.900	*n.d.*
CDK6/cyclin D1	>100	27.000	0.175
CDK7/cyclin H/Mat1	>100	1.700	*n.d.*
CDK9/cyclin T	1.914 ± 0.129	1.600	*n.d.*
Aurora A	0.395 ± 0.006	>100	0.011

[a]Average values from two determinations ± SD; [b]Data for roscovitine were previously published (50); [c]Data for JNJ-7706621 were previously published (30).

To confirm the CDK2 inhibitory properties of **2i**, we evaluated its effect on the abundance of Ser807/811-phosphorylated retinoblastoma (Rb) protein in HCT-116 cells. The commercially available dual CDK/Aurora inhibitor JNJ-7706621 (30) and the pan-selective CDK inhibitor dinaciclib (31) were used as reference compounds. All three compounds reduced the phosphorylation of Rb at Ser807/811 after 16 h treatment (Figures 2A and S1A). In addition, studies on two downstream targets of Aurora A – Thr210 of Polo-like kinase 1 (Plk-1) (32,33) and Ser10 of histone H3 (34) – revealed that this kinase is also inhibited by **2i**. HCT-116 cells were synchronized in G2/M phase by treatment with nocodazole for 16 h and subsequently treated for 2 h with **2i** or one of the reference compounds. Both **2i** and JNJ-7706621 reduced the nocodazole-induced phosphorylation of Plk-1 at Thr210 and histone H3 at Ser10 but dinaciclib did not affect the level of either phosphorylated protein (Figures 2B and S1B).

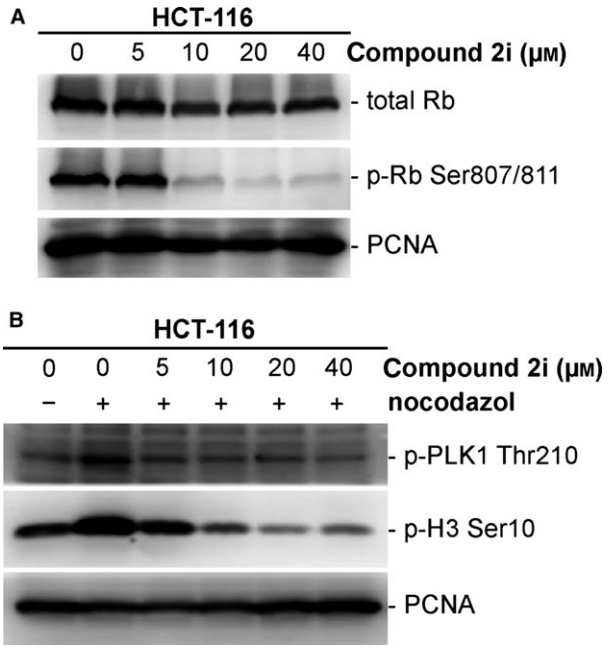

Figure 2: Compound **2i** reduces phosphorylation of Rb, Plk-1 and histone H3 proteins in HCT-116 cells. (A) Analysis of Rb phosphorylation at Ser807/811. Cells were treated with indicated concentrations of tested compound for 16 h. (B) Analysis of Plk-1 and histone H3 phosphorylation. Cells were synchronized using nocodazole (40 ng/mL) for 16 h and subsequently treated with indicated concentrations of tested compound for 2 h. Proliferating cell nuclear antigen (PCNA) levels were determined to confirm equal protein loading.

Molecular modeling

The affinity of compound **2i** for aurora A was rather surprising given that roscovitine does not inhibit this kinase. We therefore used molecular modeling to study their interaction. An initial analysis with the Autodock Vina program (22) suggested that compound **2i** binds to the ATP-binding site of CDK2/cyclin A (PDBID: 3DDQ) in an orientation similar to that adopted by roscovitine in CDK2 (PDBID: 2A4L) (35), forming two hydrogen bonds with the main chain of Leu83 and one with the main chain of Glu81. Its binding is further stabilized by additional hydrogen bonds involving its 2-aminobenzylamino moiety, one with Asp86 as a donor and the other with Lys89 as an acceptor (Figure S2). This may be why compound **2i** binds more strongly than roscovitine to CDK2: the estimated binding energies for the two compounds obtained using Autodock Vina are −9.4 and −8.9 kcal/mol respectively. We then analyzed the interactions between compound **2i** and aurora A, for which a binding energy of −7.9 kcal/mol was predicted. This revealed four hydrogen bonds that govern the binding of the compound in the kinase's active site: one between the Ala213 carbonyl group and N7, another between the Ala213 amino group and N1, a third between the Glu211 carbonyl group and N2, and a fourth between the Pro214 carbonyl group and the 2-aminobenzylamino substituent (Figure S2). The docking studies thus explained why compound **2i** binds more tightly than roscovitine to the ATP-binding site of CDK2 and suggest that it may bind to the aurora A kinase in a similar fashion.

Cell cycle analysis

The effects of compound **2i** on cell cycling were studied by using flow cytometry to determine the DNA content of asynchronously growing HCT-116 cells and their incorporation of BrdU after treatment with various concentrations of **2i** for 24 h (Figure 3A). In control experiments, cells were treated with etoposide, nocodazole and the dual CDK/aurora kinase inhibitor JNJ-7706621 (Figures S3 and S4). Treatment with **2i** reduced the population of cells in the G1 phase of the cell cycle and the number of cells undergoing active DNA replication (i.e. the number of BrdU-positive cells). While treatment with **2i** at 10 μM

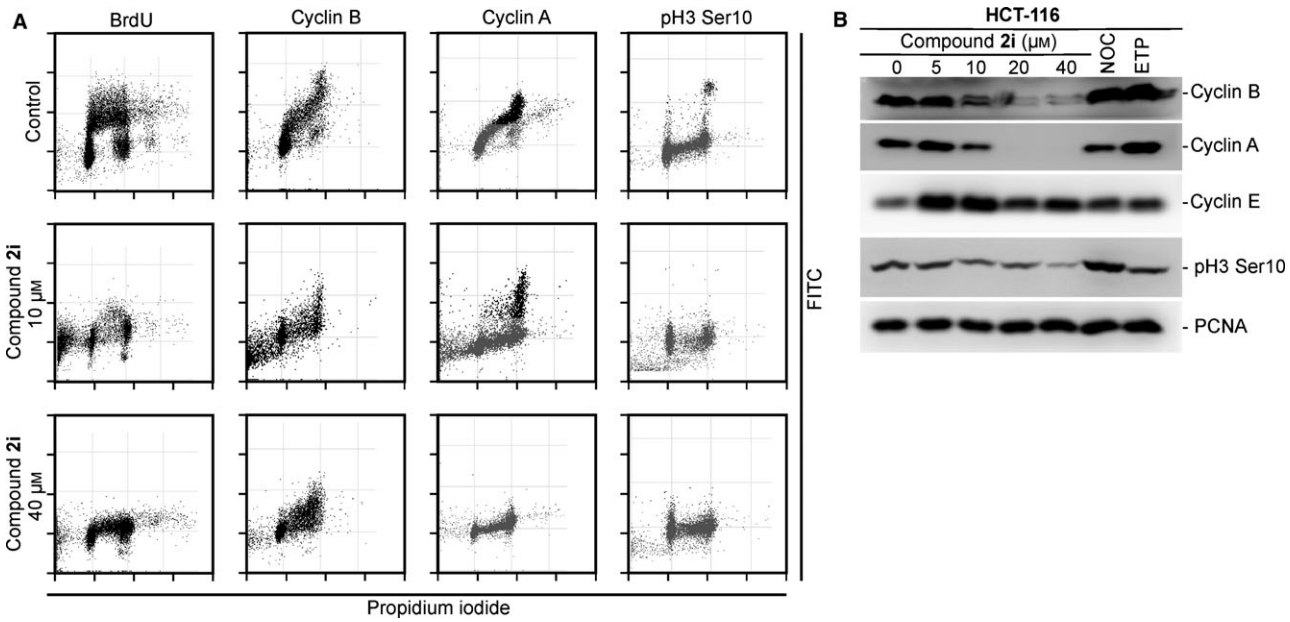

Figure 3: Cell cycle analysis of asynchronously growing HCT-116 cells treated with increasing concentrations of compound **2i** for 24 h. (A) Flow cytometric analysis of 5-bromo-2′-deoxyuridine (BrdU) incorporation, expression of cyclins B and A, and phosphorylation of histone H3 on Ser10 (pH3 Ser10). (B) Immunoblotting experiments to determine the levels of cyclins B, A, and E and the extent of phosphorylation of histone H3 at Ser10. Proliferating cell nuclear antigen (PCNA) levels were determined to confirm equal protein loading. Etoposide (ETP) and nocodazole (NOC)-treated cells were used as controls.

induced a strong increase in the sub-G1 cell population, higher concentrations had cytostatic effects and produced only a minimal number of apoptotic (sub–G1) cells. This unexpected result may be due to the parallel targeting of CDKs and Aurora kinases. The accumulation of cells in the G2 and M phases of the cell cycle is consistent with the inhibition of CDK2, CDK1, and Aurora (3,30,36,37).

Flow cytometry experiments revealed that cells treated with **2i** exhibited pronounced changes in the levels of important cell cycle regulators (cyclins A and B) and a common mitotic marker (the extent of phosphorylation of histone H3 at Ser10). Treatment with the highest tested concentration of compound **2i** (40 μM) completely suppressed cyclin expression and histone H3 phosphorylation. Similarly, treatment with **2i** at a concentration of 10 μM greatly reduced the size of the cell population expressing cyclins A and B relative to that seen in samples of untreated control cells (Figure 3A). The changes in the expression of cyclins A and B and the extent of histone H3 phosphorylation were confirmed by immunoblotting experiments and complemented with measurements of cyclin E expression (Figure 3B). The accumulation of BrdU-negative S phase cells, suppression of histone H3 phosphorylation, and reduced abundance of cyclins A and B all suggest that treatment with the higher dose of compound **2i** arrested the cell cycle of the HCT-116 cells in the S phase. Conversely, the lower dose allowed the cells to complete DNA replication and arrested them in the G2 phase.

Apoptosis and transcription

Flow cytometric analysis of HCT-116 cells treated with compound **2i** at 10 μM revealed a sub-diploid cell population, which suggested ongoing apoptosis. We therefore analyzed the levels of antiapoptotic (Bcl-2, Mcl-1) and proapoptotic (PUMA) proteins as well as the activation (fragmentation) of caspase-3 and the cleavage of its substrate, poly(ADP-ribose)polymerase-1 (PARP-1) in treated cells. Surprisingly, cells treated with **2i** at a concentration of 10 μM exhibited higher levels of cleaved caspase-3 and PARP-1 fragments than those treated with higher concentrations. The measured levels of Bcl-2 and PUMA in each case were consistent with this result. However, the expression of Mcl-1 declined in proportion to the applied concentration of compound **2i** (Figure 4A). The apoptosis-inducing effect of compound **2i** was confirmed by the results of a fluorimetric caspase-3/7 activity assay, which correlated with the immunoblotting analysis (Figure 4B). Control experiments were performed with dinaciclib and JNJ-7706621(Figure S5).

Like roscovitine and other CDK inhibitors (38–40), compound **2i** also increased the expression of p53 at concentrations above 10 μM. This increase was accompanied by decreased expression of Mdm-2, the negative regulator of p53. Such changes are usually attributed to the interference of CDK inhibitors with transcription, so we measured the effect of compound **2i** on RNA synthesis in HCT-116 cells. Incubation with **2i** for 24 h caused a dose-dependent reduction in the levels of newly synthesized mRNA

and total RNA. Treatment with **2i** at a concentration of 5 μM reduced both mRNA synthesis and global transcription by 70% relative to untreated controls. The highest tested concentrations of compound **2i** (20 and 40 μM) completely suppressed RNA synthesis (Figure 4C).

Inhibition of migration and tube formation

We have recently shown that in addition to their cytotoxicity toward cancer cells, CDK inhibitors also influence the angiogenesis-related behavior of endothelial cells, probably by targeting CDK5 (16,41). Because compound **2i** is a

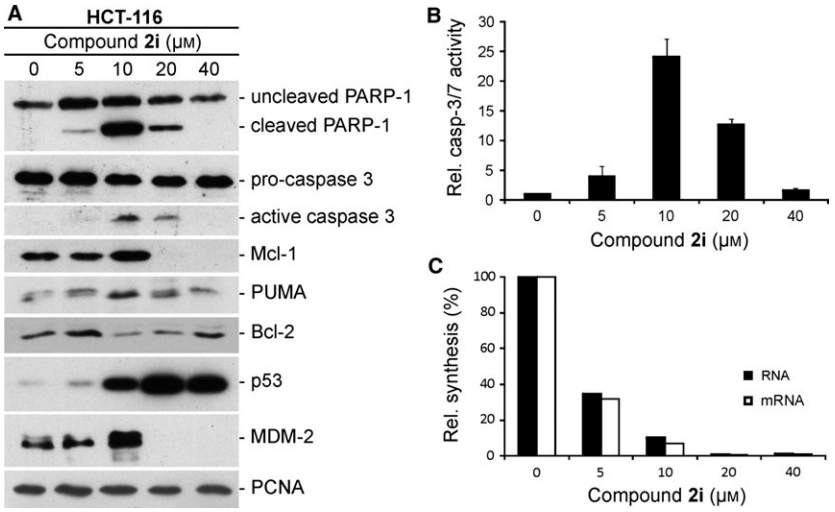

Figure 4: Compound **2i** blocks transcription and induces apoptosis in HCT-116 cells. (A) Immunoblotting of apoptotic markers; proliferating cell nuclear antigen (PCNA) levels were determined to confirm equal protein loading. (B) Results of a fluorimetric caspase-3/7 enzyme activity assay based on the cleavage of an Ac-DEVD-AMC peptide substrate. (C) The relationship between the applied concentration of compound **2i** and the mRNA and total RNA levels in HCT-116 cells.

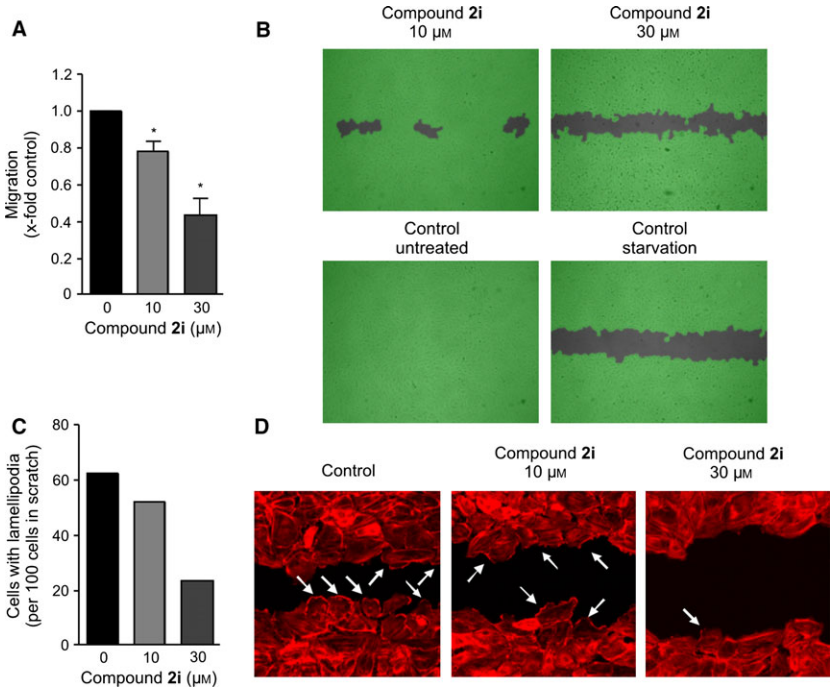

Figure 5: Compound **2i** blocks HUVEC migration and reduces the formation of lamellipodia. (A) Confluent layers of HUVECs were scratched and the cells were allowed to migrate for 16 h in the presence or absence of the specified concentrations of compound **2i**. The columns indicate the area re-covered by migrating cells (n = 3, mean ± SEM, *p < 0.05, One Way ANOVA, Dunnett). (B) Scratches at the end-point of the experiment (representative images taken from one of the three experiments conducted for each set of tested conditions). (C) Confluent layers of HUVECs were scratched and the cells were allowed to migrate for 8 h in the presence or absence of 10 or 30 μM of compound **2i**, until clear lamellipodia formation was visible in the untreated control cells. The actin cytoskeleton was stained with rhodamin-phalloidin and fluorescence images of the scratches were acquired at 10× magnification. For quantitative evaluation of lamellipodia formation, the numbers of cells with prominent lamellipodia and ruffles were counted relative to the total number of cells at the scratch front (n = 1). (D) Representative images of the scratch front (F-actin, 40× magnification).

potent inhibitor of CDK5, we examined its effects on HUVEC migration and tube formation *in vitro*. Confluent HUVECs were scratched and the cells were allowed to migrate for 16 h in the presence or absence of compound **2i**. Compared to untreated controls, the area covered by migrating cells was 20 and 60% smaller, respectively, in cultures treated with compound **2i** at concentrations of 10 and 30 μM (Figure 5A,B). The influence of compound **2i** on the actin cytoskeleton in endothelial cells was examined by analyzing the F-actin distribution in migrating cells. Untreated HUVECs formed lamellipodia with a densely packed F-actin seam at the leading edge but these structures were largely absent in treated cells (Figure 5C,D). Similar results have previously been achieved by treatment with roscovitine or CDK5-targeting siRNA (16). Compound **2i** also reduced HUVEC tube formation. Treatment with compound **2i** at a concentration of 30 μM significantly reduced the numbers of branching points and tubes as well as the total and mean tube lengths (Figure 6). Control experiments were performed with roscovitine and JNJ-7706621. Whereas roscovitine blocked migration and tube formation at sub-toxic doses as described in our previous paper (16), JNJ-7706621 showed cytotoxicity but had no effect on angiogenesis (data not shown).

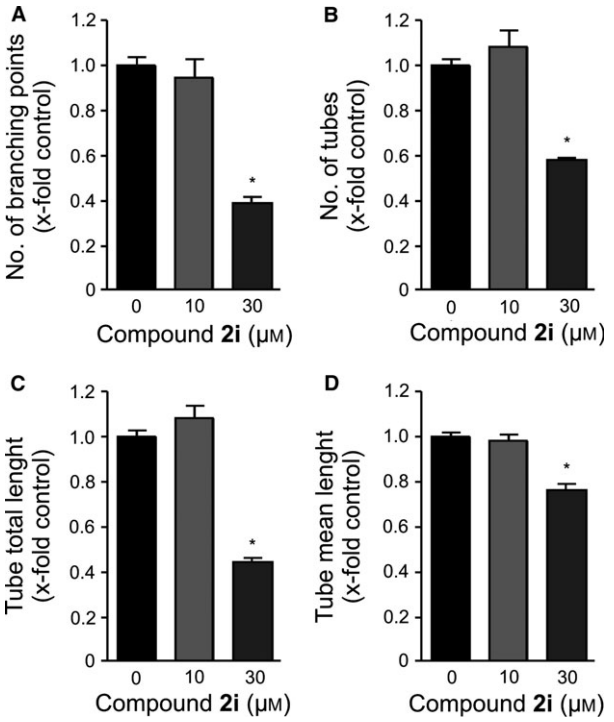

Figure 6: Compound **2i** reduces tube formation. HUVECs were seeded onto a growth factor containing matrix in the presence or absence of the indicated concentrations of compound **2i**. After 16 h of incubation, images were taken and the properties of the formed tubes were quantified ($n = 3$, mean ± SEM, *$p < 0.05$, One Way ANOVA, Dunnett). (A) Number of branching points. (B) Number of tubes. (C) Total tube length. (D) Mean tube length.

Discussion

Selectively modulating the activity of protein kinases that regulate the cell cycle, such as CDKs and aurora kinases, could potentially be useful in the treatment of cancer. In addition to the selective CDK inhibitors that are currently undergoing clinical trials, some interesting broad-spectrum kinase inhibitors such as the 3,5-diamino-1,2,4-triazole JNJ-7706621 and the indirubin-like ZK 304709 have been developed (37,42). Both compounds are potent CDK inhibitors but also target other kinases: JNJ-7706621 also inhibits aurora kinases while ZK 304709 inhibits angiogenesis-related receptor kinases such as the VEGFRs and PDGFRβ.

We unexpectedly identified a novel kinase inhibitor, compound **2i**, which targets CDK2, CDK5, and aurora A. Its structure is derived from the first-generation CDK inhibitor roscovitine. However, unlike roscovitine, **2i** has a pyrazolo[4,3-*d*]pyrimidine core; roscovitine analogs with this core structure are generally more potent than their purine-cored counterparts (18). Roscovitine inhibits the activities of CDK1/2/5/7/9 (43) but compound **2i** is a much stronger inhibitor of CDK5 and especially CDK2, which it inhibited at nanomolar concentrations. The distinctive selectivity of compound **2i** was confirmed by molecular modeling, which revealed that despite the very minor structural differences between the two compounds, it binds more tightly than roscovitine to both CDK2 and aurora A.

The *in vitro* cytotoxicity of compound **2i** was at least three times greater than that of roscovitine: the reported average IC_{50} values for roscovitine in a panel of cancer cell lines range from 15 μM to 28 μM (28,44–46), whereas the average IC_{50} for compound **2i** against the cell lines tested in this work was 5 μM. The death of HCT-116 cells treated with compound **2i** was accompanied by changes in the abundance of mitochondrial proteins (Mcl-1, Bcl-2, PUMA), the activation of caspases-3/7 and the fragmentation of PARP-1. Similar changes have been observed in cells undergoing apoptosis following treatment with roscovitine or other CDK inhibitors (11,18,47,48). Interestingly, whereas lower concentrations of compound **2i** had rather pro-apoptotic effects, higher concentrations apparently only had cytostatic effects, with little impact on markers of apoptosis – treatment with high concentrations of **2i** produced few sub-G1 cells and reduced caspase activity (Figures 3A and 4).

The greater cytotoxicity of compound **2i** relative to roscovitine was surprising because it is a less effective inhibitor of CDK7 and 9, both of which are regarded as critical targets of other potent CDK inhibitors. Inhibition of CDKs 7 and 9 blocks transcription, reduces the expression of Mcl-1, and increases the abundance and activity of p53, thereby inducing mitochondrial cell death (10,11,39,40). Cells treated with high (but not low or intermediate) doses

of compound **2i** also exhibited reduced levels of Mcl-1 level and transcription in general (Figure 4). Based on the results of the cellular assays and kinetic experiments using purified enzymes, we believe that the cytotoxicity of compound **2i** is due to the simultaneous inhibition of CDKs and aurora A. Cells treated with **2i** exhibited a pronounced downregulation of cyclins A and B along with reduced phosphorylation of histone H3 at Ser10, a site phosphorylated by aurora A (34). The suppression of histone H3 phosphorylation could be due to the direct inhibition of Aurora A or an indirect consequence of a reduction in its abundance (Figure S6). All these findings are consistent with the known anticancer activity of roscovitine, which has been found to reduce the transcription of many mitotic genes in HT29 cells including cyclin B, cdc25, and aurora A/B (49).

While the roles of CDK2 and aurora A in cancer development and the anticancer activity of their inhibitors are relatively well-explored, the link between CDK5 and tumor growth has emerged only recently. It has been shown that CDK5, a known regulator of neuronal processes, also plays a key role in the regulation of endothelial cell migration and tube formation, two essential steps in tumor-induced angiogenesis (16). Moreover, the inhibition of CDK5 by various CDK inhibitors was found to limit angiogenesis both *in vitro* and *in vivo* (17,41). We showed that compound **2i** can reduce cell migration as well as tube formation and the formation of lamellipodia in migrating HUVEC cells. Because it does not inhibit any VEGFR isoform, we assume that the molecular mechanism of its anti-angiogenic activity is linked to CDK5.

Conclusions

In conclusion, compound **2i** displays anticancer activity *in vitro* that appears to derive from the inhibition of CDKs and aurora A. This causes apoptosis in cancer cells and also suppresses angiogenesis-like activity in endothelial cells, a promising combination for therapeutic purposes. We are currently seeking to further optimize the pyrazolo [4,3-*d*]pyrimidine kinase inhibitors, particularly in terms of their selectivity and potency.

Acknowledgments

This work was supported by the Czech Science Foundation (grants P305/12/0783 and 14-19590S), the Ministry of Education, Youth and Sports of the Czech Republic (the National Program of Sustainability I, grant LO1204), Internal Grant Agency of Palacký University (projects IGA_PrF_2015_021, IGA_PrF_2014_024 and IGA_PrF_2014_023), German Research Foundation (grant DFG ZA 186/4-1), and the German Federal Ministry of Education and Research.

Conflict of Interest

The authors declare no competing financial interest.

References

1. Hanahan D., Weinberg R.A. (2011) Hallmarks of cancer: the next generation. Cell;144:646–674.
2. Malumbres M., Barbacid M. (2009) Cell cycle, CDKs and cancer: a changing paradigm. Nat Rev Cancer; 9:153–166.
3. Payton M., Chung G., Yakowec P., Wong A., Powers D., Xiong L., Zhang N., Leal J., Bush T.L., Santora V., Askew B., Tasker A., Radinsky R., Kendall R., Coats S. (2006) Discovery and evaluation of dual CDK1 and CDK2 inhibitors. Cancer Res;66:4299–4308.
4. Tetsu O., McCormick F. (2003) Proliferation of cancer cells despite CDK2 inhibition. Cancer Cell;3:233–245.
5. Krystof V., Uldrijan S. (2010) Cyclin-dependent kinase inhibitors as anticancer drugs. Curr Drug Targets;11: 291–302.
6. Lapenna S., Giordano A. (2009) Cell cycle kinases as therapeutic targets for cancer. Nat Rev Drug Discov;8:547–566.
7. Santamaria D., Barriere C., Cerqueira A., Hunt S., Tardy C., Newton K., Caceres J.F., Dubus P., Malumbres M., Barbacid M. (2007) Cdk1 is sufficient to drive the mammalian cell cycle. Nature;448:811–815.
8. Galons H., Oumata N., Meijer L. (2010) Cyclin-dependent kinase inhibitors: a survey of recent patent literature. Expert Opin Ther Pat;20:377–404.
9. Chen R., Keating M.J., Gandhi V., Plunkett W. (2005) Transcription inhibition by flavopiridol: mechanism of chronic lymphocytic leukemia cell death. Blood;106: 2513–2519.
10. MacCallum D.E., Melville J., Frame S., Watt K., Anderson S., Gianella-Borradori A., Lane D.P., Green S.R. (2005) Seliciclib (CYC202, R-Roscovitine) induces cell death in multiple myeloma cells by inhibition of RNA polymerase II-dependent transcription and down-regulation of Mcl-1. Cancer Res;65:5399–5407.
11. Manohar S.M., Rathos M.J., Sonawane V., Rao S.V., Joshi K.S. (2011) Cyclin-dependent kinase inhibitor, P276-00 induces apoptosis in multiple myeloma cells by inhibition of Cdk9-T1 and RNA polymerase II-dependent transcription. Leuk Res;35:821–830.
12. Canduri F., Peres P.C., Caceres R.A., de Azevedo W.F. (2008) CDK9 as a potential target for drug development. Med Chem;4:210–218.
13. Ali M.A., Choy H., Habib A.A., Saha D. (2007) SNS-032 prevents tumor cell-induced angiogenesis by inhibiting vascular endothelial growth factor. Neoplasia;9:370–381.
14. Melillo G., Sausville E.A., Cloud K., Lahusen T., Varesio L., Senderowicz A.M. (1999) Flavopiridol, a protein kinase inhibitor, down-regulates hypoxic induction of

vascular endothelial growth factor expression in human monocytes. Cancer Res;59:5433–5437.
15. Scholz A., Wagner K., Welzel M., Remlinger F., Wiedenmann B., Siemeister G., Rosewicz S., Detjen K.M. (2009) The oral multitarget tumour growth inhibitor, ZK 304709, inhibits growth of pancreatic neuroendocrine tumours in an orthotopic mouse model. Gut;58:261–270.
16. Liebl J., Weitensteiner S.B., Vereb G., Takacs L., Furst R., Vollmar A.M., Zahler S. (2010) Cyclin-dependent kinase 5 regulates endothelial cell migration and angiogenesis. J Biol Chem;285:35932–35943.
17. Zahler S., Liebl J., Furst R., Vollmar A.M. (2010) Anti-angiogenic potential of small molecular inhibitors of cyclin dependent kinases *in vitro*. Angiogenesis;13:239–249.
18. Jorda R., Havlíček L., McNae I.W., Walkinshaw M.D., Voller J., Šturc A., Navrátilová J., Kuzma M., Mistrík M., Bártek J., Strnad M., Kryštof V. (2011) Pyrazolo [4,3-d]pyrimidine bioisostere of roscovitine: evaluation of a novel selective inhibitor of cyclin-dependent kinases with antiproliferative activity. J Med Chem;54:2980–2993.
19. Zatloukal M., Jorda R., Gucký T., Řezníčková E., Voller J., Pospíšil T., Malínková V., Adamcová H., Kryštof V., Strnad M. (2013) Synthesis and *in vitro* biological evaluation of 2,6,9-trisubstituted purines targeting multiple cyclin-dependent kinases. Eur J Med Chem;61: 61–72.
20. Bain J., Plater L., Elliott M., Shpiro N., Hastie C.J., McLauchlan H., Klevernic I., Arthur J.S., Alessi D.R., Cohen P. (2007) The selectivity of protein kinase inhibitors: a further update. Biochem J;408:297–315.
21. Morris G.M., Huey R., Lindstrom W., Sanner M.F., Belew R.K., Goodsell D.S., Olson A.J. (2009) AutoDock4 and AutoDockTools4: automated docking with selective receptor flexibility. J Comput Chem;30:2785–2791.
22. Trott O., Olson A.J. (2010) AutoDock Vina: improving the speed and accuracy of docking with a new scoring function, efficient optimization, and multithreading. J Comput Chem;31:455–461.
23. Weitensteiner S.B., Liebl J., Kryštof V., Havlíček L., Gucký T., Strnad M., Fürst T., Vollmar A.M., Zahler S. (2013) Trisubstituted pyrazolopyrimidines as novel angiogenesis inhibitors. PLoS One;8:e54607.
24. Havlíček L., Moravcová D., Kryštof V., Strnad M. The identification of a novel highly condensed pentacyclic heteroaromatic ring system 1,3,5,5b,6,8,10,10b-octaazacyclopenta[h,i]aceanthrylene and its application in the synthesis of 5,7-substituted pyrazolo[4,3-d]pyrimidines. J Heterocycl Chem;52:669–673.
25. Gray N.S., Wodicka L., Thunnissen A.M., Norman T.C., Kwon S., Espinoza F.H., Morgan D.O., Barnes G., LeClerc S., Meijer L., Kim S.H., Lockhart D.J., Schultz P.G. (1998) Exploiting chemical libraries, structure, and genomics in the search for kinase inhibitors. Science;281:533–538.
26. Chang Y.T., Gray N.S., Rosania G.R., Sutherlin D.P., Kwon S., Norman T.C., Sarohia R., Leost M., Meijer L., Schultz P.G. (1999) Synthesis and application of functionally diverse 2,6,9-trisubstituted purine libraries as CDK inhibitors. Chem Biol;6:361–375.
27. Bettayeb K., Oumata N., Echalier A., Ferandin Y., Endicott J.A., Galons H., Meijer L. (2008) CR8, a potent and selective, roscovitine-derived inhibitor of cyclin-dependent kinases. Oncogene;27:5797–5807.
28. Bettayeb K., Sallam H., Ferandin Y., Popowycz F., Fournet G., Hassan M., Echalier A., Bernard P., Endicott J., Joseph B., Meijer L. (2008) N-&-N, a new class of cell death-inducing kinase inhibitors derived from the purine roscovitine. Mol Cancer Ther;7:2713–2724.
29. Oumata N., Bettayeb K., Ferandin Y., Demange L., Lopez-Giral A., Goddard M.L., Myrianthopoulos V., Mikros E., Flajolet M., Greengard P., Meijer L., Galons H. (2008) Roscovitine-derived, dual-specificity inhibitors of cyclin-dependent kinases and casein kinases 1. J Med Chem;51:5229–5242.
30. Emanuel S., Rugg C.A., Gruninger R.H., Lin R., Fuentes-Pesquera A., Connolly P.J., Wetter S.K., Hollister B., Kruger W.W., Napier C., Jolliffe L., Middleton S.A. (2005) The *in vitro* and *in vivo* effects of JNJ-7706621: a dual inhibitor of cyclin-dependent kinases and aurora kinases. Cancer Res;65:9038–9046.
31. Parry D., Guzi T., Shanahan F., Davis N., Prabhavalkar D., Wiswell D., Seghezzi W. *et al.* (2010) Dinaciclib (SCH 727965), a novel and potent cyclin-dependent kinase inhibitor. Mol Cancer Ther;9:2344–2353.
32. Macůrek L., Lindqvist A., Lim D., Lampson M.A., Klompmaker R., Freire R., Clouin C., Taylor S.S., Yaffe M.B., Medema R.H. (2008) Polo-like kinase-1 is activated by aurora A to promote checkpoint recovery. Nature;455:119–123.
33. Seki A., Coppinger J.A., Jang C.Y., Yates J.R., Fang G. (2008) Bora and the kinase Aurora a cooperatively activate the kinase Plk1 and control mitotic entry. Science;320:1655–1658.
34. Crosio C., Fimia G.M., Loury R., Kimura M., Okano Y., Zhou H., Sen S., Allis C.D., Sassone-Corsi P. (2002) Mitotic phosphorylation of histone H3: spatio-temporal regulation by mammalian Aurora kinases. Mol Cell Biol;22:874–885.
35. de Azevedo W.F., Leclerc S., Meijer L., Havlicek L., Strnad M., Kim S.H. (1997) Inhibition of cyclin-dependent kinases by purine analogues: crystal structure of human cdk2 complexed with roscovitine. Eur J Biochem;243:518–526.
36. Shapiro G.I. (2006) Cyclin-dependent kinase pathways as targets for cancer treatment. J Clin Oncol;24:1770–1783.
37. Seamon J.A., Rugg C.A., Emanuel S., Calcagno A.M., Ambudkar S.V., Middleton S.A., Butler J., Borowski V., Greenberger L.M. (2006) Role of the ABCG2 drug transporter in the resistance and oral bioavailability of a potent cyclin-dependent kinase/Aurora kinase inhibitor. Mol Cancer Ther;5:2459–2467.

38. David-Pfeuty T., Nouvian-Dooghe Y., Sirri V., Roussel P., Hernandez-Verdun D. (2001) Common and reversible regulation of wild-type p53 function and of ribosomal biogenesis by protein kinases in human cells. Oncogene;20:5951–5963.
39. Demidenko Z.N., Blagosklonny M.V. (2004) Flavopiridol induces p53 via initial inhibition of Mdm2 and p21 and independently of p53, sensitizes apoptosis-reluctant cells to tumor necrosis factor. Cancer Res;64:3653–3660.
40. Kotala V., Uldrijan S., Horky M., Trbusek M., Strnad M., Vojtesek B. (2001) Potent induction of wild-type p53-dependent transcription in tumour cells by a synthetic inhibitor of cyclin-dependent kinases. Cell Mol Life Sci;58:1333–1339.
41. Liebl J., Krystof V., Vereb G., Takacs L., Strnad M., Pechan P., Havlicek L., Zatloukal M., Furst R., Vollmar A.M., Zahler S. (2011) Anti-angiogenic effects of purine inhibitors of cyclin dependent kinases. Angiogenesis;14:281–291.
42. Siemeister G., Luecking U., Wagner C., Detjen K., Mc Coy C., Bosslet K. (2006) Molecular and pharmacodynamic characteristics of the novel multi-target tumor growth inhibitor ZK 304709. Biomed Pharmacother;60:269–272.
43. Bach S., Knockaert M., Reinhardt J., Lozach O., Schmitt S., Baratte B., Koken M. *et al.* (2005) Roscovitine targets, protein kinases and pyridoxal kinase. J Biol Chem;280:31208–31219.
44. Meijer L., Bettayeb K., Galons H. (2006) (R)-Roscovitine (CYC202, Seliciclib). In: Smith P.J., Yue E.W., editors. Inhibitors of Cyclin-Dependent Kinases as Anti-Tumor Agents. Boca Raton, FL, USA: CRC Press: p. 187–226.
45. Krystof V., McNae I.W., Walkinshaw M.D., Fischer P.M., Muller P., Vojtesek B., Orsag M., Havlicek L., Strnad M. (2005) Antiproliferative activity of olomoucine II, a novel 2,6,9-trisubstituted purine cyclin-dependent kinase inhibitor. Cell Mol Life Sci;62:1763–1771.
46. McClue S.J., Blake D., Clarke R., Cowan A., Cummings L., Fischer P.M., MacKenzie M., Melville J., Stewart K., Wang S., Zhelev N., Zheleva D., Lane D.P. (2002) *In vitro* and *in vivo* antitumor properties of the cyclin dependent kinase inhibitor CYC202 (R-roscovitine). Int J Cancer;102:463–468.
47. Conroy A., Stockett D.E., Walker D., Arkin M.R., Hoch U., Fox J.A., Hawtin R.E. (2009) SNS-032 is a potent and selective CDK 2, 7 and 9 inhibitor that drives target modulation in patient samples. Cancer Chemother Pharmacol;64:723–732.
48. Santo L., Vallet S., Hideshima T., Cirstea D., Ikeda H., Pozzi S., Patel K. *et al.* (2010) AT7519, A novel small molecule multi-cyclin-dependent kinase inhibitor, induces apoptosis in multiple myeloma via GSK-3beta activation and RNA polymerase II inhibition. Oncogene;29:2325–2336.
49. Whittaker S.R., Te Poele R.H., Chan F., Linardopoulos S., Walton M.I., Garrett M.D., Workman P. (2007) The cyclin-dependent kinase inhibitor seliciclib (R-roscovitine; CYC202) decreases the expression of mitotic control genes and prevents entry into mitosis. Cell Cycle;6:3114–3131.
50. Sroka I.M., Heiss E.H., Havlicek L., Totzke F., Aristei Y., Pechan P., Kubbutat M.H., Strnad M., Dirsch V.M. (2010) A novel roscovitine derivative potently induces G1-phase arrest in platelet-derived growth factor-BB-activated vascular smooth muscle cells. Mol Pharmacol;77:255–261.

Supporting Information

Additional Supporting Information may be found in the online version of this article:

Appendix S1. Synthesis and characterization of tested compounds.

Table S1. Protein kinase selectivity of compound **2i**.

Figure S1. Phosphorylation of the Rb, Plk-1, and histone H3 proteins in HCT-116 cells upon treatment with JNJ-7706621 and dinaciclib.

Figure S2. Molecular docking of compound **2i** to CDK2 (PDB ID: 3DDQ) and Aurora A (PDB ID: 3O50).

Figure S3. Cell cycle analysis of asynchronously growing HCT-116 cells treated with nocodazole (NOC) and etoposide (ETP) for 24 h.

Figure S4. Cell cycle analysis of asynchronously growing HCT-116 cells treated with JNJ-7706621 for 24 and 48 h.

Figure S5. Immunoblotting analysis of apoptotic markers in HCT-116 cells treated with dinaciclib and JNJ-7706621 for 24 h.

Figure S6. Expression of aurora A and B in HCT-116 cells treated with compound **2i** for 24 h.

PŘÍLOHA V

Řezníčková E, Popa A, Gucký T, Zatloukal M, Havlíček L, Bazgier V, Berka K, Jorda R, Popa I, Nasereddin A, Jaffe CL, Kryštof V, Strnad M (2015) 2,6,9-Trisubstituted purines as CRK3 kinase inhibitors with antileishmanial activity in vitro. Bioorg Med Chem Lett. 25, 2298-2301.

Bioorganic & Medicinal Chemistry Letters 25 (2015) 2298–2301

Contents lists available at ScienceDirect

Bioorganic & Medicinal Chemistry Letters

journal homepage: www.elsevier.com/locate/bmcl

2,6,9-Trisubstituted purines as CRK3 kinase inhibitors with antileishmanial activity in vitro

Eva Řezníčková [a], Alexandr Popa [a], Tomáš Gucký [a], Marek Zatloukal [a], Libor Havlíček [a], Václav Bazgier [a,b], Karel Berka [b,c], Radek Jorda [a,d], Igor Popa [a,e,f], Abdelmajeed Nasereddin [g], Charles L. Jaffe [g], Vladimír Kryštof [a,*], Miroslav Strnad [a]

[a] Laboratory of Growth Regulators & Department of Chemical Biology and Genetics, Centre of the Region Haná for Biotechnological and Agricultural Research, Palacký University and Institute of Experimental Botany AS CR, Šlechtitelů 11, 783 71 Olomouc, Czech Republic
[b] Department of Physical Chemistry, Faculty of Science, Palacký University, 17. listopadu 1192/12, 771 46 Olomouc, Czech Republic
[c] Regional Centre of Advanced Technologies and Materials, Faculty of Science, Palacký University, 17. listopadu 1192/12, 771 46 Olomouc, Czech Republic
[d] Regional Centre for Applied Molecular Oncology, Masaryk Memorial Cancer Institute, Žlutý kopec 7, Brno 656 53, Czech Republic
[e] Institute of Molecular and Translational Medicine, Faculty of Medicine and Dentistry, Palacký University, Hněvotínská 5, 779 00 Olomouc, Czech Republic
[f] Department of Organic Chemistry, Faculty of Science, Palacký University, 17. listopadu 12, 771 46 Olomouc, Czech Republic
[g] Department of Microbiology and Molecular Genetics, IMRIC, Hebrew University—Hadassah Medical School, 9112102 Jerusalem, Israel

ARTICLE INFO

Article history:
Received 16 February 2015
Revised 7 April 2015
Accepted 9 April 2015
Available online 16 April 2015

Keywords:
Purine
Inhibitor
Cyclin-dependent kinase
Leishmania

ABSTRACT

Here we describe the leishmanicidal activities of a library of 2,6,9-trisubstituted purines that were screened for interaction with Cdc2-related protein kinase 3 (CRK3) and subsequently for activity against parasitic *Leishmania* species. The most active compound inhibited recombinant CRK3 with an IC_{50} value of 162 nM and was active against *Leishmania major* and *Leishmania donovani* at low micromolar concentrations in vitro. Its mode of binding to CRK3 was investigated by molecular docking using a homology model.

Leishmaniasis, a diverse group of diseases caused by protozoan parasites of the genus *Leishmania*, is a threat to more than 350 million people in 98 countries worldwide.[1] *Leishmania* are transmitted to the host via the bites of sand fly vectors belonging to the genus *Phlebotomus* or *Lutzomyia,* in which they exist as motile extracellular flagellated promastigotes. After transmission to humans or other mammalian hosts, the promastigotes invade macrophages, transform into oval nonflagellated amastigotes, and multiply. This is the stage of the parasite's lifecycle that causes the symptoms of leishmaniasis.[2]

Leishmaniasis can be divided into three major forms with different clinical manifestations: cutaneous, mucocutaneous and visceral. Cutaneous leishmaniasis is the most common form of the disease and is eventually defeated by the immune system in most cases. However it sometimes progress to the mucocutaneous form where the parasite metastasizes to mucosal tissues. This form is usually refractory to therapy and can be fatal. The most serious form of the disease, visceral leishmaniasis or Kala-Azar (black fever in Hindi), is fatal if not rapidly diagnosed and treated, and is responsible for most leishmaniasis-related deaths. In visceral leishmaniasis, which is caused by *Leishmania donovani* and *Leishmania infantum* (*syn=Leishmania chagasi*), the parasite infects the liver, spleen and bone marrow causing patients to suffer symptoms including fevers, weight loss, and anaemia.[2]

Current leishmaniasis treatments are based on the administration of amphotericin B, pentavalent antimonials, paromomycin or miltefosine. Many of these drugs are expensive, highly toxic, and require long periods of hospitalization. In addition, parasite resistance to pentavalent antimonials precludes their use in a major endemic region, India.[3] It follows that there is an urgent need for the development of new leishmaniasis therapies and the identification of new drug targets that could be exploited in the treatment of this disease. To ensure that new therapies exhibit good selectivity and effectiveness, they should have targets that are absent in the mammalian host or at least different in function and structure from the host homolog. Widely studied targets that are considered

Abbreviation: CRK, Cdc2-related protein kinase.

* Corresponding author. Tel.: +420 585634854; fax: +420 585634870.
E-mail address: vladimir.krystof@upol.cz (V. Kryštof).

http://dx.doi.org/10.1016/j.bmcl.2015.04.030
0960-894X/

particularly promising for this purpose include enzymes involved in essential parasitic metabolic pathways such as sterol biosynthesis or glycolysis; peptidases, which are important for parasite-host cell interaction; and protein kinases important for leishmanial proliferation and viability such as mitogen-activated protein kinases and Cdc2-related protein kinases (CRKs).[3–5] CRKs belong to the group of serine/threonine protein kinases that play crucial roles in regulating the cell cycle and proliferation.[6] The most extensively studied CRK kinase is CRK3, a *Leishmania* enzyme essential for parasite proliferation and viability,[7] and a potential molecular target for drug development.

Several drug-like molecules have been screened for interaction with CRK3[8–10] including known CDK inhibitors such as flavopiridol, indirubines, paullones, staurosporines, substituted pyrazolo[4,3-*d*]pyrimidines and roscovitine-like purines.[7,9,11–14] Many of these compounds inhibit the parasitic CRK3, blocking the cell cycle and reducing parasite viability.

Here we report the leishmanicidal activities of a library of selected 2,6,9-trisubstituted purines that are moderate inhibitors of human CDK2, but exhibit low cytotoxicity in cancer cells.[15–17] Their low cytotoxicity means that they are unlikely to have applications in cancer therapy but may be useful in other fields of medicine where inactivity towards human cells is beneficial. The compounds were prepared using a previously reported three-step procedure[15–18] starting from 2,6-dichloropurine, which is alkylated at N9 with isopropyl alcohol under Mitsunobu conditions. This is followed by a nucleophilic substitution at the C6 purine position with a substituted benzylamine, followed by a second nucleophilic substitution at C2 with an amino alcohol or diamine. The synthesis and characterization of the novel compounds in the tested series is presented in the Supplementary material of this manuscript. We evaluated the CRK3-inhibitory and antiproliferative activities of a library of different 2,6,9-trisubstituted purines (Scheme 1). All of the compounds share an isopropyl moiety at position 9 but have different substituents at positions 2 and 6. The C2 position was modified with diverse substituents ranging from simple aliphatic chains to branched and cyclic moieties, whereas most of the C6 substituents are substituted benzylamines. Kinase inhibition assays were performed using a complex of the leishmanial CRK3 kinase and CYC6,[13] and cytotoxicity was determined against the promastigote stage of *Leishmania turanica,* an avirulent species found in the great gerbil (*Rhombomys opimus*) that is non-pathogenic towards humans. Promastigotes were treated for 72 h with tested compounds (30 μM) and the compounds' cytotoxicity was

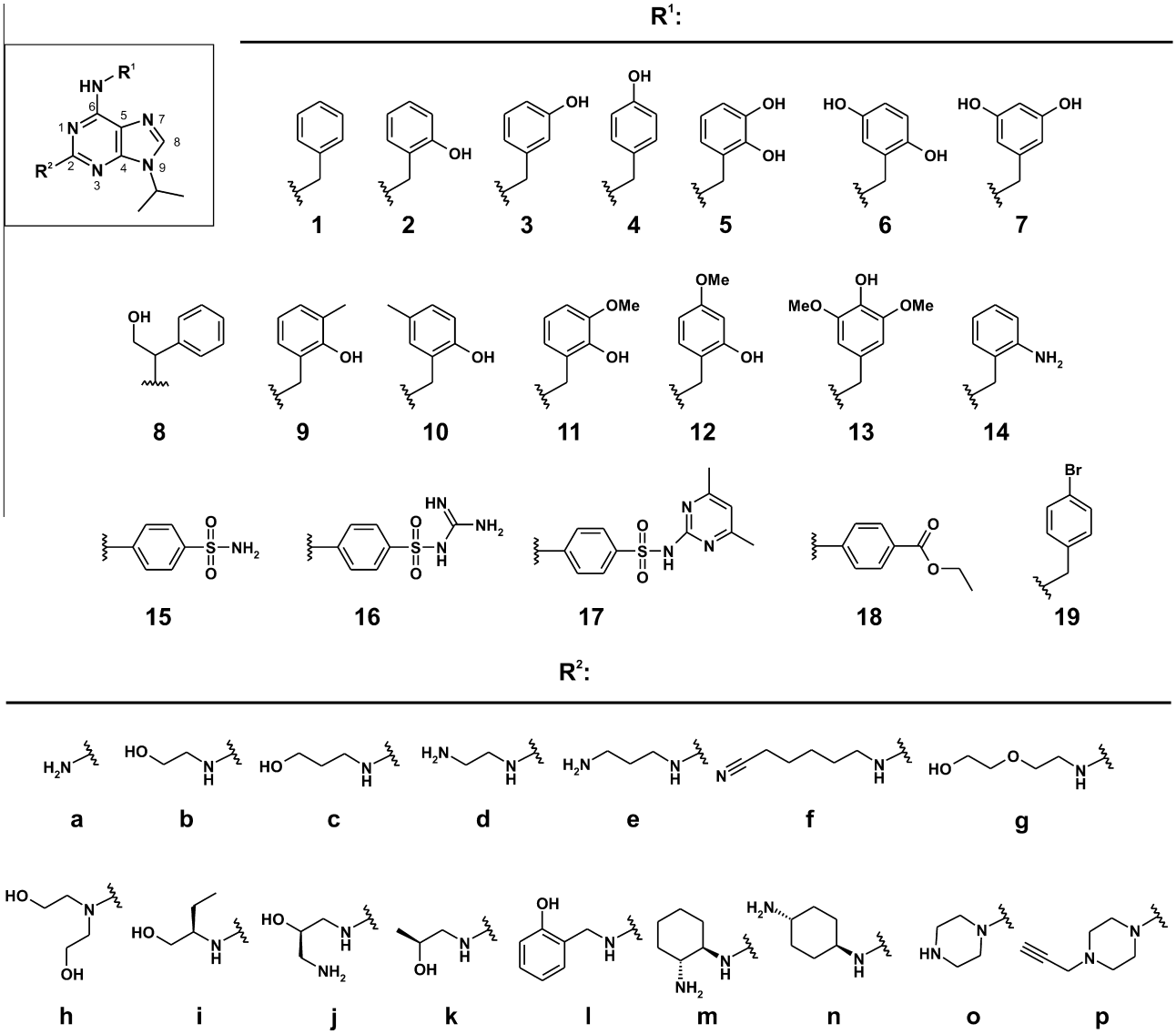

Scheme 1. Substituents of studied purines at positions 2 (substituents R^2) and 6 (substituents R^1).

expressed in terms of the percentage of viable cells relative to untreated controls.

The kinase inhibition assays showed that many of the tested compounds reduced CRK3 activity to less than 20% of the control level when applied at a concentration of 30 μM (see Supplementary data). The active compounds exhibit greater diversity at C2 position. Compounds **2c** and **11n**, which have 3-hydroxypropyl and 4-aminocyclohexylamino C2 groups, respectively, reduced the CRK3 activity to 10.5% and 10.8% of its reference level, respectively. The strongest CRK3 inhibitors had a branched 1-(hydroxymethyl)propyl substituent at C2. Compounds in this group such as **2i**, **5i**, **6i**, **9i**, **10i**, **11i**, **15i**, **16i** and **17i** reduced the CRK3 kinase activity to less than 5% of its reference level at 30 μM, suggesting that this C2 substituent is optimal for CRK3 inhibition. Dose–response curves of kinase activity were constructed to obtain more detailed information on the CRK3/CYC6 inhibitory activity of these compounds. Their half maximal inhibitory concentrations (IC_{50} values) ranged from 0.1 to 1.6 μM for compounds **16i** and **9i**, respectively (Table 1), with the lowest values being achieved by compounds having an N6-benzyl substituent bearing an *o*-hydroxyl group.

To explain these biochemical results, we investigated the binding mode of the most potent compound, **10i**, to CRK3. Since the crystal structure of CRK3 has yet to be determined, we needed to create a model of *Leishmania major* CRK3 (LmCRK3; UNIPROT O96526) based on its homology to the human CDK2 kinase (HsCDK2; PDB: 4KD1),[19] with which it exhibits 58% sequence identity. This was achieved using an approach similar to one described previously.[8,10] Interestingly, the CRK3 sequences for six human *Leishmania* pathogens show ⩾96% sequence identity over 311 amino acids, and their ATP binding pockets all have identical amino acid sequences (NCBI Blast—http://blast.ncbi.nlm.nih.gov, and TriTrypDB—http://tritrypdb.org/) (see Supplementary data).

The resulting model showed that the LmCRK3 active site is similar to that of HsCDK2 but features several amino acid changes (see the Supplementary data for a more extensive comparison). The largest difference in the shapes of the active sites is due to the replacement of $F82^{HsCDK2}$ by $Y101^{LmCRK3}$. It should be noted that while most amino acids in the LmCRK3 active site were conserved in all models, some amino acids (D105, K108) have multiple side-chain rotamers that differed between individual models. Salt bridge formation involving these two amino acids allowed the docked ligands to adopt a common pose in each case.

The common orientation of the active compounds in the LmCRK3 model is similar to that adopted by roscovitine in its complex with HsCDK2 (Fig. 1). Importantly, the hydrogen bonding D–A–D (donor–acceptor–donor) motif observed in the CDK complex is reproduced in CRK3 via the main chains of E100 and V102. However, the position occupied by the N6-benzyl ring of roscovitine in the HsCDK2 complex is blocked in the LmCRK3 model by the residue $Y101^{LmCRK3}$. Therefore, the N6 benzyl ring of the docked ligand is instead inclined towards the K108-D105 salt bridge, which interacts favorably with its *o*-hydroxyl group. Finally, the hydroxylated substituent at the ligand's C2 position forms a hydrogen bond with the main-chain carbonyl of A149. These interactions explain why an *o*-hydroxyl group on the N6 benzyl substituent and a 1-(hydroxymethyl)propylamino group at C2 are beneficial for activity against LmCRK3.

CRK3 is essential for the progression of the parasite's cell cycle[7] and several studies have shown that specific inhibitors of CRK3 can reduce parasite proliferation and viability.[9,10,12,13] We therefore tested the more active CRK3 inhibitors from the library to determine their cytotoxicity towards *L. turanica*. As expected, several of them (**2i**, **9i**, **10i**, **11i**, **19i**) strongly reduced leishmanial promastigote viability to <50% of the reference level at 30 μM. However, there was no clear correlation between CRK3 inhibitory activity and the degree of viability reduction (Fig. 2). It is possible that the differences in the compounds' leishmanicidal activity are due to different rates of membrane transport or intracellular metabolization, but interactions with other cellular targets cannot be ruled out either. IC_{50} values against three *Leishmania* species (*L.*

Table 1
CRK3/CYC6 inhibition and antileishmanial activity of the most active 2,6,9-trisubstituted purines

Compound	IC_{50}[a] (μM)			
	CRK3/CYC6	*L. turanica*	*L. major*	*L. donovani*
2i	0.590	11.9	47.2	62.4
5i	0.314	>50.0	n.d.	n.d.
6i	0.384	>50.0	n.d.	n.d.
9i	1.648	23.0	19.8	12.4
10i	0.162	11.8	2.3	2.2
11i	0.641	35.4	98.5	95.9
15i	0.214	>50.0	n.d.	n.d.
16i	0.115	>50.0	n.d.	n.d.
19i	n.d.	20.1	19.4	16.8

n.d.—not determined.
[a] All values were determined by duplicate assays.

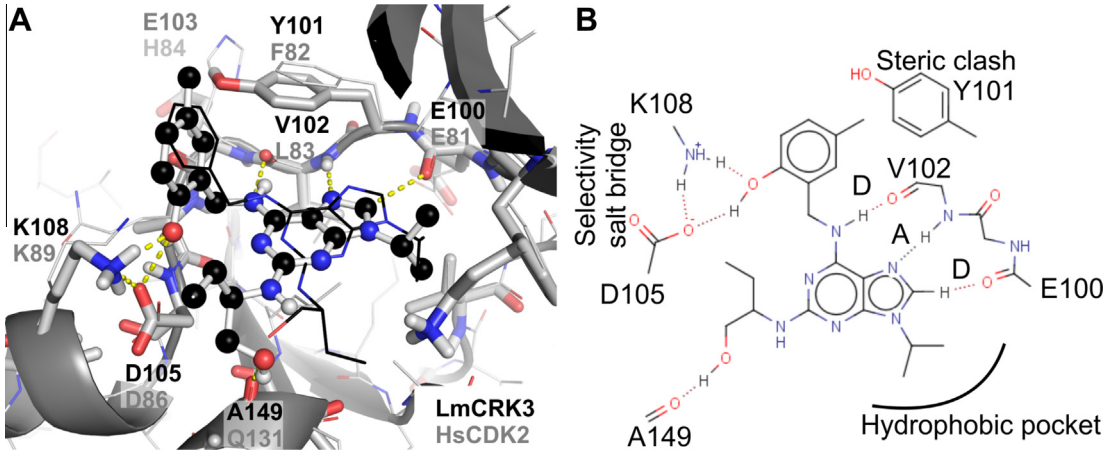

Figure 1. Docked binding pose of compound **10i** in LmCRK3 compared with that of roscovitine in HsCDK2.[20] (A) **10i** is shown with a ball-and-stick representation, LmCRK3 is shown as sticks, and the HsCDK2/roscovitine complex (PDB: 2A4L) is shown with lines. (B) **10i** interacts with the main chains of residues E100, V102 and A149 and with a salt bridge formed by K108 and D105. The N9 isopropyl group projects into the hydrophobic pocket of the binding site.

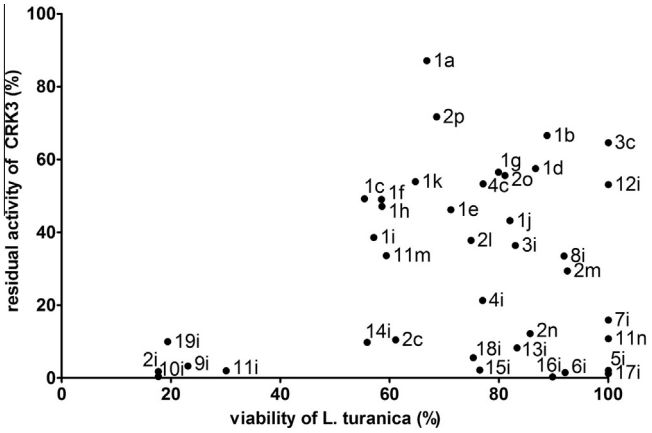

Figure 2. A plot showing the activity of selected compounds against *Leishmania turanica* and CRK3/CYC6 (expressed as percentage of inhibition). All reported measurements are based on at least duplicate experiments using the tested compounds at a concentration of 30 μM (see Supplementary data for details).

turanica, and the human parasites *L. major* and *L. donovani*) were determined for the most active compounds. While the IC_{50} values observed for most such compounds against *L. turanica* were comparable to or lower than those for *L. major* and *L. donovani*, compound **10i** was more active against the human parasites, achieving low micromolar IC_{50} values of 2.3 and 2.2 μM, respectively. We also tested the compounds' cytotoxicity towards normal human fibroblast cells (BJ). At 30 μM, the most active compounds reduced leishmanial viability to 20% of the reference level seen in control samples while maintaining the viability of non-proliferating human fibroblasts above 75% (see Supplementary data).

In conclusion, a new group of submicromolar CRK inhibitors has been identified. Their affinity for CRK3 was rationalized by examining the binding of **10i** to a homology model. The compounds also suppressed the proliferation of three different *Leishmania* promastigote species, exhibiting low micromolar activities. Interestingly, some of the compounds also showed similar activity against *Trypanosoma rhodesiense* (data not shown). As such, these compounds could potentially serve as leads for antileishmanial and antitrypanosomal drug development.

Acknowledgements

The authors gratefully acknowledge support from the Ministry of Education, Youth and Sports of the Czech Republic (via projects LO1305 and LO1204), the European Regional Development Fund and the State Budget of the Czech Republic (RECAMO, CZ.1.05/2.1.00/03.0101), the Operational Program Research and Development for Innovations (IMTM project CZ.1.05/2.1.00/01.0030), Palacký University in Olomouc (IGA_PrF_2015_027, IGA_PrF_2014_024 and IGA_PrF_2015_021) and the German Federal Ministry of Education and Research (Bio-Disc 5 project 315729). C.L.J. holds the Michael and Penny Feiwel Chair in Dermatology.

Supplementary data

Supplementary data associated with this article can be found, in the online version, at http://dx.doi.org/10.1016/j.bmcl.2015.04.030.

References and notes

1. den Boer, M.; Argaw, D.; Jannin, J.; Alvar, J. *Clin. Microbiol. Infect.* **2011**, *17*, 1471.
2. Sharlow, E. R.; Grogl, M.; Johnson, J.; Lazo, J. S. *Mol. Interventions* **2010**, *10*, 72.
3. Singh, N.; Kumar, M.; Singh, R. K. *Trop. Med.* **2012**, *5*, 485.
4. Chawla, B.; Madhubala, R. *J. Parasit. Dis.* **2010**, *34*, 1.
5. Seifert, K. *Open Med. Chem. J.* **2011**, *5*, 31.
6. Naula, C.; Parsons, M.; Mottram, J. C. *Biochim. Biophys. Acta* **2005**, *1754*, 151.
7. Hassan, P.; Fergusson, D.; Grant, K. M.; Mottram, J. C. *Mol. Biochem. Parasitol.* **2001**, *113*, 189.
8. Cleghorn, L. A.; Woodland, A.; Collie, I. T.; Torrie, L. S.; Norcross, N.; Luksch, T.; Mpamhanga, C.; Walker, R. G.; Mottram, J. C.; Brenk, R.; Frearson, J. A.; Gilbert, I. H.; Wyatt, P. G. *Chem. Med. Chem.* **2011**, *6*, 2214.
9. Grant, K. M.; Dunion, M. H.; Yardley, V.; Skaltsounis, A. L.; Marko, D.; Eisenbrand, G.; Croft, S. L.; Meijer, L.; Mottram, J. C. *Antimicrob. Agents Chemother.* **2004**, *48*, 3033.
10. Walker, R. G.; Thomson, G.; Malone, K.; Nowicki, M. W.; Brown, E.; Blake, D. G.; Turner, N. J.; Walkinshaw, M. D.; Grant, K. M.; Mottram, J. C. *PLoS Negl. Trop. Dis.* **2011**, *5*, e1033.
11. Reichwald, C.; Shimony, O.; Dunkel, U.; Sacerdoti-Sierra, N.; Jaffe, C. L.; Kunick, C. *J. Med. Chem.* **2008**, *51*, 659.
12. Xingi, E.; Smirlis, D.; Myrianthopoulos, V.; Magiatis, P.; Grant, K. M.; Meijer, L.; Mikros, E.; Skaltsounis, A. L.; Soteriadou, K. *Int. J. Parasitol.* **2009**, *39*, 1289.
13. Jorda, R.; Sacerdoti-Sierra, N.; Voller, J.; Havlicek, L.; Kracalikova, K.; Nowicki, M. W.; Nasereddin, A.; Krystof, V.; Strnad, M.; Walkinshaw, M. D.; Jaffe, C. L. *Bioorg. Med. Chem. Lett.* **2011**, *21*, 4233.
14. Houze, S.; Hoang, N. T.; Lozach, O.; Le, B. J.; Meijer, L.; Galons, H.; Demange, L. *Molecules* **2014**, *19*, 15237.
15. Havlicek, L.; Hanus, J.; Vesely, J.; LeClerc, S.; Meijer, L.; Shaw, G.; Strnad, M. *J. Med. Chem.* **1997**, *40*, 408.
16. Krystof, V.; Lenobel, R.; Havlicek, L.; Kuzma, M.; Strnad, M. *Bioorg. Med. Chem. Lett.* **2002**, *12*, 3283.
17. Otyepka, M.; Krystof, V.; Havlicek, L.; Siglerova, V.; Strnad, M.; Koca, J. *J. Med. Chem.* **2000**, *43*, 2506.
18. Zatloukal, M.; Jorda, R.; Gucky, T.; Reznickova, E.; Voller, J.; Pospisil, T.; Malinkova, V.; Adamcova, H.; Krystof, V.; Strnad, M. *Eur. J. Med. Chem.* **2013**, *61*, 61.
19. Martin, M. P.; Olesen, S. H.; Georg, G. I.; Schonbrunn, E. *ACS Chem. Biol.* **2013**, *8*, 2360.
20. de Azevedo, W. F. J.; Mueller-Dieckmann, H. J.; Schulze-Gahmen, U.; Worland, P. J.; Sausville, E.; Kim, S. H. *Proc. Natl. Acad. Sci. U.S.A.* **1996**, *93*, 2735.